U.S.NRC

United States Nuclear Regulatory Commission

Protecting People and the Environment

NUREG/CR-6976

Rod Bundle Heat Transfer Test Facility Description

Office of Nuclear Regulatory Research

AVAILABILITY OF REFERENCE MATERIALS IN NRC PUBLICATIONS

NRC Reference Material

As of November 1999, you may electronically access NUREG-series publications and other NRC records at NRC's Public Electronic Reading Room at http://www.nrc.gov/reading-rm.html. Publicly released records include, to name a few, NUREG-series publications; *Federal Register* notices; applicant, licensee, and vendor documents and correspondence; NRC correspondence and internal memoranda; bulletins and information notices; inspection and investigative reports; licensee event reports; and Commission papers and their attachments.

NRC publications in the NUREG series, NRC regulations, and *Title 10, Energy*, in the Code of *Federal Regulations* may also be purchased from one of these two sources.

1. The Superintendent of Documents
   U.S. Government Printing Office
   Mail Stop SSOP
   Washington, DC 20402–0001
   Internet: bookstore.gpo.gov
   Telephone: 202-512-1800
   Fax: 202-512-2250
2. The National Technical Information Service
   Springfield, VA 22161–0002
   www.ntis.gov
   1–800–553–6847 or, locally, 703–605–6000

A single copy of each NRC draft report for comment is available free, to the extent of supply, upon written request as follows:

Address: Office of Administration
Reproduction and Mail Services Branch
U.S. Nuclear Regulatory Commission
Washington, DC 20555-0001
E-mail: DISTRIBUTION@nrc.gov
Facsimile: 301–415–2289

Some publications in the NUREG series that are posted at NRC's Web site address http://www.nrc.gov/reading-rm/doc-collections/nuregs are updated periodically and may differ from the last printed version. Although references to material found on a Web site bear the date the material was accessed, the material available on the date cited may subsequently be removed from the site.

Non-NRC Reference Material

Documents available from public and special technical libraries include all open literature items, such as books, journal articles, and transactions, *Federal Register* notices, Federal and State legislation, and congressional reports. Such documents as theses, dissertations, foreign reports and translations, and non-NRC conference proceedings may be purchased from their sponsoring organization.

Copies of industry codes and standards used in a substantive manner in the NRC regulatory process are maintained at—

The NRC Technical Library
Two White Flint North
11545 Rockville Pike
Rockville, MD 20852–2738

These standards are available in the library for reference use by the public. Codes and standards are usually copyrighted and may be purchased from the originating organization or, if they are American National Standards, from—

American National Standards Institute
11 West 42nd Street
New York, NY 10036–8002
www.ansi.org
212–642–4900

Legally binding regulatory requirements are stated only in laws; NRC regulations; licenses, including technical specifications; or orders, not in NUREG-series publications. The views expressed in contractor-prepared publications in this series are not necessarily those of the NRC.

The NUREG series comprises (1) technical and administrative reports and books prepared by the staff (NUREG–XXXX) or agency contractors (NUREG/CR–XXXX), (2) proceedings of conferences (NUREG/CP–XXXX), (3) reports resulting from international agreements (NUREG/IA–XXXX), (4) brochures (NUREG/BR–XXXX), and (5) compilations of legal decisions and orders of the Commission and Atomic and Safety Licensing Boards and of Directors' decisions under Section 2.206 of NRC's regulations (NUREG–0750).

UNITED STATES
NUCLEAR REGULATORY COMMISSION
WASHINGTON, D.C. 20555-0001

Errata

NUREG/CR-6976 " Rod Bundle Heat Transfer Test Facility Description" , ML102290227 published July 2010

In several places of the report, the inner dimensions of the test section were incorrectly shown as 91.3 mm x 91.3 mm (3.595 in). The correct dimension should be 90.17 x 90.17 mm (3.55 in). This correction should apply to the EXECUTIVE SUMMARY on page xiii, on page 8 and, in Figure 3.2 on page 14 and Figure 3.7 on page 19.

On page 10 of Section 3.4 the descriptions should be corrected as follow:

Small Carryover Tank is 50.8 mm (2 in) sch80 pipe section 0.914 m (36 in) long.

Large Carryover Tank is 101.6 mm (4 in) sch40 pipe section 1.829 m (72 in) long.

On page 36 Table 3.1, the overall rod sheath length should be 4.369 m, not 7.36 m

U.S.NRC
United States Nuclear Regulatory Commission
Protecting People and the Environment

NUREG/CR-6976

Rod Bundle Heat Transfer Test Facility Description

Manuscript Completed: April 2008
Date Published: July 2010

Prepared by
E.R. Rosal, T.F. Lin, I.S. McClellan, R.C. Brewer

The Pennsylvania State University
University Park, PA 16802

K. Tien, NRC Project Manager

NRC Job Code W6855

Office of Nuclear Regulatory Research

ABSTRACT

This report describes the Rod Bundle Heat Transfer (RBHT) Test Facility which is designed to conduct systematic separate effects tests under well-controlled laboratory conditions in order to generate fundamental rod bundle heat transfer data from single phase cooling tests, low flow boiling tests, steam flow tests with and without droplets injection, inverted annular film boiling tests, and dispersed flow film boiling heat transfer tests in rod bundles. The facility is capable of operating in steady state forced and variable reflood modes covering a wide range of flow and heat transfer conditions at pressures from 0.134 to 0.402 MPa (20 to 60 psia). The RBHT Test Facility is a unique facility which will provide new data for the fundamental development of best-estimate computer codes to enhance our understanding of the complex two-phase phenomena, which are modeled for the reflood transient.

FOREWORD

Reflood thermal-hydraulics represents an important set of phenomena during a hypothetical loss-of-coolant-accident (LOCA). These phenomena must be accurately simulated by systems codes in determining plant response to a LOCA. In spite of significant research into reflood thermal-hydraulics, there still exists uncertainty in these calculations. As a result, the Nuclear Regulatory Commission (NRC) conducts experimental investigations of reflood thermal-hydraulics in order to provide data for model development and to validate its systems codes, which are used to provide independent confirmation of the validity of licensees' submittals.

The NRC is currently assessing and improving the TRAC/RELAP Computational Engine (TRACE) code for best estimate analysis of light water reactors. While calculation of reflood by TRACE appears to be reasonable, higher accuracy is needed as the code is applied to power uprates and new plant designs to ensure acceptable margin between expected plant performance and the regulatory limits. Accurate prediction of the consequences of a LOCA is important because it is one of the postulated accident scenarios that determine the licensed core power and several other operational parameters.

To acquire detailed, fundamental data for use in developing models for reflood during a LOCA, the NRC sponsored the design and construction of a Rod Bundle Heat Transfer (RBHT) Test Facility. Some of these detailed data have only recently become possible because of recent advances in instrumentation technology for two-phase flow measurements.

This report describes the RBHT Test Facility components and instrumentation. It also presents the results of the facility characterization tests, including pressure loss coefficients of the spacer grids, heat loss from the bundle housing, and flow areas of the bundle and other tanks as a function of height. In addition, it provides an estimate of measurement uncertainties. As such, this report will prove useful in understanding and utilizing the data to be obtained from the facility.

With improved data and code models for simulating LOCAs, we can more accurately predict the consequences of these scenarios and provide better technical bases for regulations associated with such accidents. As a result, this study will help to ensure the agency's regulations are effective and efficient.

CONTENTS

FIGURES

TABLES

EXECUTIVE SUMMARY

The NRC-sponsored Rod Bundle Heat Transfer (RBHT) Test Facility, designed to conduct systematic separate effects tests under well-controlled laboratory conditions, has been successfully developed and made operational at the Pennsylvania State University (PSU). The facility can be used to generate fundamental rod bundle heat transfer data from single phase cooling tests, low flow boiling tests, steam flow tests with and without droplets injection, inverted annular film boiling tests, and dispersed flow film boiling heat transfer tests in rod bundles.

The facility is heavily instrumented and meets all the instrumentation requirements developed in the RBHT Program. The facility includes a test section consisting of a lower plenum, a low-mass housing containing the heater rod bundle, and an upper plenum, coolant injection and steam injection systems, phase separation and liquid collection systems, a liquid droplets injection system, and a pressure fluctuation damping tank and steam exhaust piping.

The heater rod bundle in the test section of the facility simulates a small portion of a 17x17 reactor fuel assembly. The heater rods are electrically heated and have a diameter of 9.5 mm arranged in a 7x7 array with a 12.6 mm pitch. The bundle has 45 heater rods and four unheated corner rods. The latter are used to support the bundle grids and the instrumentation lines. Each rod is rated for 10 kW and designed to operate at 1.38 MPa at a maximum temperature of 1204 degrees C. Each rod is instrumented with eight 0.508 mm diameter ungrounded thermocouples. The rod bundle has seven mixing vane grids similar in design of a pressurized water reactor (PWR) 17x17 fuel assembly.

The flow housing provides the pressure and flow boundary for the heater rod bundle. It has a square geometry and is 91.3 x 91.3 mm in size, with the wall thickness of 6.35 mm. The flow housing has six pairs of windows, each providing 50.8 x 292.1 mm of viewing area. Each pair of windows is placed 180 degrees apart and located axially at elevations overlapping rod bundle spacer grids, thus providing a viewing area about 88.9 mm below and 152.4 mm above the corresponding spacer grid. The flow housing has 23 pressure taps located at various elevations. The pressure taps are connected to sensitive differential pressure cells providing measurements to calculate single-phase friction losses for determining bare rod bundle and grid loss coefficients.

The lower plenum is attached to the bottom of the flow housing. It is used as a reservoir of the coolant prior to injection into the rod bundle during reflood. The upper plenum serves as the first stage for phase separation and liquid collection of the two-phase effluent exiting the rod bundle. The de-entrained liquid is collected around the flow housing extension in the upper plenum and is subsequently drained into the top of a tube which extends inside a small carryover tank. Meanwhile, the wet steam exhausted from the upper plenum flows through a steam separator where carryover liquid droplets are further separated form the steam and collected in a small collection tank.

The dry steam from the steam separator flows into a pressure oscillation-damping tank. The latter is used to dampen pressure oscillations at the upper plenum caused by rapidly oscillating steam generation in the heater rod bundle during reflood. The steam flowing out of the pressure oscillation-damping tank is exhausted through a stainless steel pipe. The latter has a Vortex flow meter, a V-Bal pressure control valve and a muffler at the exit to minimize the noise caused by steam blowing into the atmosphere.

The injection water system consists of a water supply tank, a circulating pump and interconnecting lines to the test section lower plenum. The water injection is rated for 0.402 MPa and 154.4 degrees C. A boiler is used to provide steam for the single phase steam cooling tests with and without liquid droplet injection. The liquid droplets injection system consists of four stainless steel tubes entering through the test section at the 1.295 m elevation. The tubes run perpendicular to the heater rods and penetrate through both sides of the housing.

The test facility instrumentation is designed to measure temperatures, power, flow rates, liquid levels, pressures, void fractions, droplet sizes and distribution, and drop velocities. There are 123 instrumentation channels assigned to the collection of electrical power, fluid and wall temperatures, levels, flows, differential pressures, and static pressure measurements. The water injection line is equipped with a Coriolis flow meter that directly measures mass flow rates up to 454 kg/min. The exhaust line is equipped with a Vortex flow meter which, in conjunction with a static pressure transmitter and a fluid thermocouple measurement, is used to calculate the steam volumetric flow rates.

The test section instrumentation consists of the heater rod bundle and flow housing, the lower plenum and the upper plenum groups. Six grids have thermocouples attached to their surfaces in order to determine quenching behavior during reflood. The vapor (i.e., steam) temperatures are measured using miniature thermocouples that are attached to the spacer grids, and the traversing steam probe rakes having very small thermal time constants. A droplet imaging system known as VisiSizer has been developed in conjunction with Oxford Lasers to measure the sizes and velocities of water droplets entrained in the steam flow in various elevations along the bundle.

The control and data acquisition system employed in the facility provides control functions and data collection functions. This system consists of two parts: the computer and display terminals residing in the control room, and the VXI mainframe terminal panels residing in the test facility. The two parts are connected via an industry standard IEEE 1394 serial control and data interface. There are more than 500 channels available for scanning the data.

Various characterization tests have been performed on the RBHT facility. These characterization tests include single phase pressure drop tests, rod bundle friction factor measurements, radiation heat loss measurements, and fuel rod surface roughness, oxide thickness and emissivity measurements. Results of these characterization tests, which are presented in this report, appear to be satisfactory.

In summary, the RBHT Test Facility is capable of operating in steady-state forced and variable reflood modes covering a wide range of flow and heat transfer conditions at pressures from 0.134 - 0.402 MPa (20 - 60 psia). The facility with its robust instrumentation represents a unique experimental tool for obtaining new data for the fundamental development of best-estimate computer codes used by the NRC in review of applicants' licensing requests.

ABBREVIATIONS

BN	Boron Nitride
COBRA-TF	Coolant Boiling Rods Arrays - Two Fluids
DP	Differential Pressure
FLECHT	Full Length Emergency Cooling Heat Transfer
FM	Flow Transmitter
GR	Spacer Grid
LIDCS	Laser Illuminating Digital Camera System
NRC	Nuclear Regulatory Commission
OD	Outer Diameter
PC	Personal Computer
PSU	Pennsylvania State University
RBHT	Rod Bundle Heat Transfer
SEASET	Systems Effects and Separate Effects Tests
TC	Thermocouple

NOMENCLATURE

A	Total Surface Area of the Rod Bundle
C_v	Modified Spacer Form Loss Coefficient
D_d	Droplet Diameter
D_h	Hydraulic Diameter
D_o	Droplet Injector Hole Diameter
f	Friction Factor
g	Gravitational Acceleration
h	Heat Transfer Coefficient
k	Thermal Conductivity
k_{grid}	Grid Loss Coefficient
L	Length of the Span Over Which Frictional Losses are Measured; Insulation Thickness
L_{bare}	Bare Bundle Length
L_{grid}	Bundle Length Occupied by Each Spacer Grid
q''	Local Heat Flux
Re	Reynolds Number
T	Local Temperature
T_s	Insulation Surface Temperature
T_w	Wall Temperature
T_∞	Ambient Temperature
V_g	Gas Velocity
V	Liquid Velocity
x	Local Position in the Insulation Layer

Greek Letters

ΔP_{bare}	Pressure Drop Associated with the Bare Length of the Span
ΔP_{grids}	Pressure Drop Associated with the Grid Losses
ΔP_{Total}	Total Pressure Drop Accounting for Both the Bare Length of the Span and the Grids
ε	Ratio of the Projected Grid Cross-Sectional Area to the Undisturbed Flow Area
μ_f	Liquid Viscosity
N	Number of Grids in Span
R_o	Radius of the Orifice
ρ_f	Liquid Density
ρ_g	Gas Density
σ	Surface Tension

ACKNOWLEDGMENTS

The authors wish to acknowledge Dr. L.E. Hochreiter and Dr. F.B. Cheung, Project Principal and Co-Principal Investigators, of the Mechanical and Nuclear Engineering Department, for their technical advice and guidance. C. Jones, R. Peters, J. Bennett, and especially D. Adams, from the ARL-Test Site, for their help in the instrumentation and installation of the heater rod bundle, test section, and test facility components. J. Anderson, College of Engineering Shop Service Manager, and his staff for fabrication most of the test facility components, and especially J. Anderson for designing the steam probe rake traversing mechanism, and C. Jones and R. Peters for automating it. The authors also wish to acknowledge the continuing guidance and support of the U.S. Nuclear Regulatory Commission, Office of Research in this effort, and in particular W.A. Macon, S. Bajorek, J.M. Kelly, G. Rhee, and D. Bassette.

1. INTRODUCTION

The Rod Bundle Heat Transfer (RBHT) Test Facility is designed to conduct systematic separate-effects tests under well-controlled conditions in order to generate fundamental rod bundle heat transfer data from single phase steam cooling tests, low flow boiling tests, steam flow tests with and without injected droplets, inverted annular film boiling tests, and dispersed flow film boiling heat transfer tests. The facility is capable of operating in both forced and variable reflood modes covering wide ranges of flow and heat transfer conditions at pressures from 0.134 to 0.402 MPa (20 to 60 psia). This report provides a detailed description of the test facility design with the test components' detailed mechanical drawings given in Appendix A, the measured volume and flow areas in Appendix B, the facility photographs description in Appendix C, and the description of the droplet injection system in Appendix D.

2. GENERAL DESIGN DESCRIPTION

The test facility consists of the following major components shown schematically in Figure 2.1 and in an isometric view in Figure 2.2:

- A test section consisting of a lower plenum, a low-mass housing containing the heater rod bundle, and an upper plenum.
- Coolant injection and steam injection systems.
- Closely coupled phase separation and liquid collection systems.
- An injection system.
- A pressure fluctuation damping tank and steam exhaust piping.

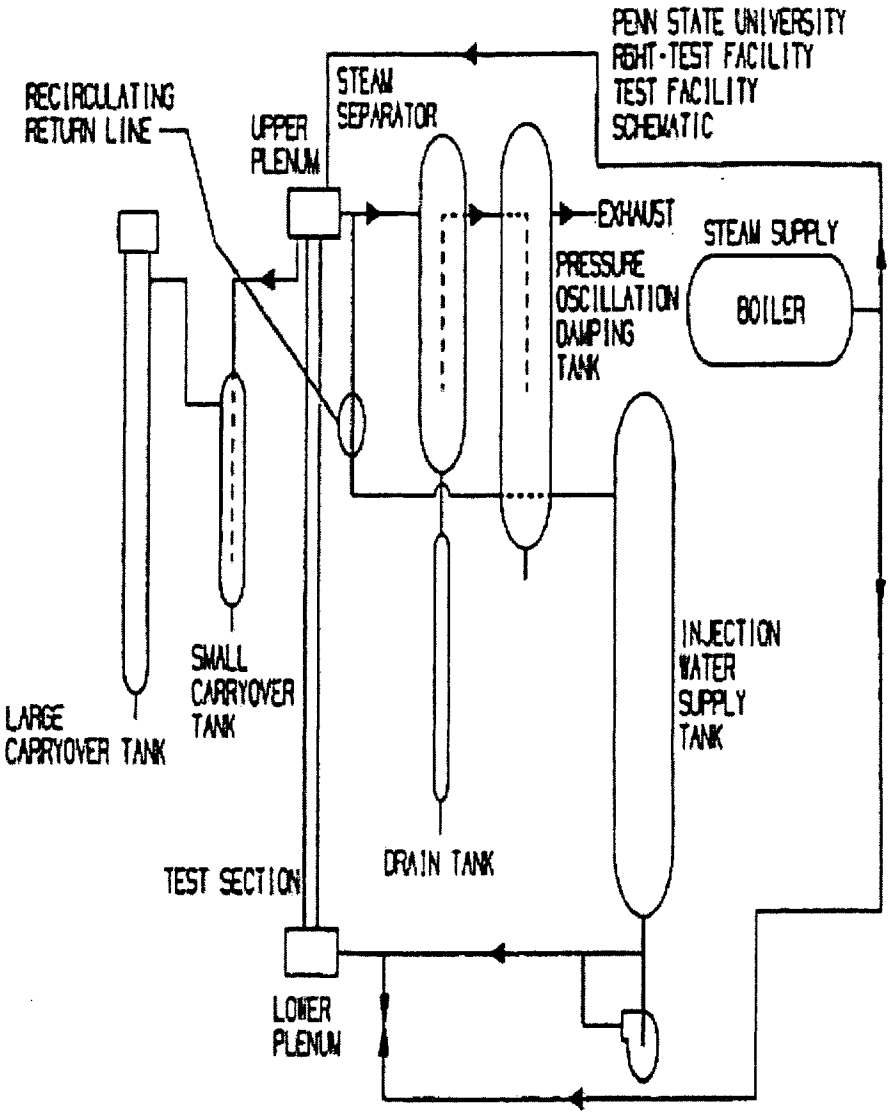

Figure 2.1 RBHT Test Facility Schematic.

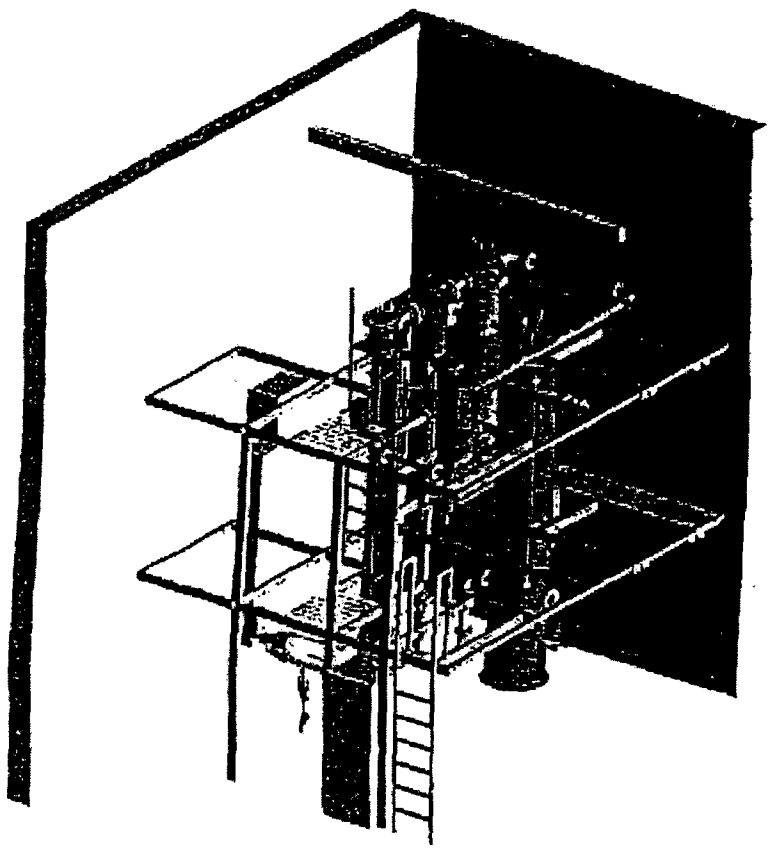

Figure 2.2 RBHT Test Facility Isometric View.

3. DETAILED COMPONENT DESIGN DESCRIPTION

The various components of the RBHT Test Facility are described in Sections 3.1 to 3.11. All components are well insulated to minimize heat losses to the environment.

Detailed mechanical drawings of the RBHT Test Facility are listed in Appendix A.

Volumes and flow areas for each component were experimentally determined by weighing the water drained from each isolated component as described in Appendix B.

3.1 Test Section

The test section consists of the heater rod bundle, the flow housing, and the lower and upper plenums, as shown in Figure 3.1. The heater rod bundle simulates a small portion of a 17x17 reactor fuel assembly. The electrically powered heater rods have a diameter of 9.5 mm (0.374 in) arranged in a 7x7 array with a 12.6 mm (0.496 in) pitch, as shown in Figure 3.2. The heater rod specifications are listed in Table 3.1. The bundle has 45 heater rods and four unheated corner rods. The corner rods are used to support the bundle grids and the grid and fluid thermocouple leads. The support rods are made from Inconel 600 tubing having a diameter of 9.525 mm (0.375 in), a wall thickness of 2.108 mm (0.083 in), and a length of 3.96 m (156 in). The heater rods are single-ended and consist of a Monel 500 electrical resistance elements filled and surrounded by hot pressed boron nitride (BN) insulation, and enclosed in an Inconel 600 cladding, as shown in Figure 3.3. This material was chosen for its high strength and low thermal expansion coefficient at high temperatures, which minimizes rod bowing and failure at high temperature operating conditions since it was desired to reuse the heater rods for a second bundle build. The heater rods have a 3.657 m (12 ft) heated length with a skewed axial power profile, as shown in Figure 3.4, with the peak power located at the 2.74 m (9 ft) elevation. The maximum-to-average power ratio (P_{max}/P_{avg}) is 1.5 and the minimum-to-average power (P_{min}/P_{avg}) is 0.5 at both ends of the heated length. The bundle has a uniform radial power distribution. Detailed engineering drawings showing the elevation information of the windows, differential pressure (DP) tap points, spacer grid instrumentation, and traversing steam probes are given in Appendix E.

Power to each rod is provided by a 60 volt, 12,600 amp, 750 kW DC power supply. Each rod is rated for 10 kW, and designed to operate at 1.38 MPa (200 psig) at a maximum temperature of 1204 degrees C (2200 degrees F), but because of its solid construction it can be operated at up to 10.34 MPa (1500 psig). Each rod is instrumented with eight 0.508 mm (20 mil) diameter ungrounded thermocouples attached to the inside surface of the Inconel sheath at various locations. All of the thermocouple leads exit at the heater rod bottom end. Thermocouple specifications are shown in Table 3.2. The Inconel 600 thermocouple sheath is compatible with the heater rod cladding and housing material to reduce thermal expansion and minimize the possibility of missing thermocouple failure during the thermocycling operations.

There were three prototype heater rod experiments performed on the final heater rod design used for the RBHT facility. The purpose of these experiments was to verify that the rod design could meet the rigorous temperature and lifetime requirements required of the rods for the high temperature tests without rod or internal thermocouple failures. The third heater rod from these experiments was cut into one-foot lengths, labeled and sent to Purdue University to measure the surface emmissivity of the Inconel cladding as well as the material properties for both the

cladding and the boron-nitride insulation. The results from the thermophysical properties tests performed by Thermophysical Properties Research Laboratories, Inc., on the heater rod and materials are given in Appendix H.

The surface of the test rod was oxidized from the high temperature tests. The same heater rod surface oxidation would occur for the heater rods put into the rod bundle since the temperature ranges were the same. Therefore, the emmissivity values measured on the test rod are applicable to the heater rods used in the RBHT Test Facility bundle build. It was observed that the Inconel oxidation was a very thin and tight oxide layer on the surface of the cladding. The roughness of the heater rod surface was also measured and was found to be between 20 - 30 μin which is consistent with smooth drawn tubing.

The rod bundle has seven mixing vane grids shown in Figure 3.5. These grids are similar in design of a PWR 17x17 fuel assembly, but instead of having dimples and springs, these grids have all dimples which provide a 0.127 mm (0.005 in) around each heater rod in order to prevent bowing when the heater rods are linearly expanding at high temperatures. The spacer grids are made out of Inconel 600 alloy sheets which are 0.508 mm (0.020 in) thick and are 44.45 mm (1.75 in) in height including the mixing vanes. The grids are located 522 mm (20.55 in) apart except for the spacing between the first and second grid, which are 588.26 mm (23.16 in) apart. The first grid is located 101.854 mm (4.01 in) above the bottom of the heater length. The grids in conjunction with the corner rods form the heater rod bundle support structure. The grid locations are similar to the ones found in a 17x17 PWR fuel assembly. The heater rod top extensions are attached to the 2.54 cm (1 in) thick nickel ground plate by means of a Morse taper that provides a good electrical contact. The heater rod bottom extension and copper electrode extend through the lower plenum O-ring pressure seal plate. The copper electrodes, which are 5.842 mm (0.230 in) in diameter and 203 mm (8 in) long, extend through holes drilled in the low-melt reservoir shown in Figure 3.6. This reservoir serves as the electrical power supply positive side connection. It contains a low temperature melting alloy at about 71.11 degrees C (160 degrees F) which is an excellent conductor, thus providing a good electrical contact and mechanical cushion allowing for rod thermal expansion to each heater rod.

The flow housing provides the pressure and flow boundary for the heater rod bundle. It has a square geometry. Its as-built inside dimensions are 91.3 x 91.3 mm (3.595 x 3.595 in), and wall thickness 6.35 mm (0.25 in), as shown in Figure 3.7. The housing is made out of Inconel 600 the same material used for the heater rod cladding and thermocouple sheaths. As pointed out previously, the high strength of Inconel 600 at elevated temperatures will minimize housing distortion during testing. The 6.35 mm (0.25 in) wall thickness is the minimum allowable for operating at 0.402 MPa (60 psig) and 537.8 degrees C (1000 degrees F), taking into consideration the cutouts to accommodate the large windows and the numerous pressure and temperature penetrations through the walls, as shown in Figure 3.8. The empty housing has a flow area of 83.4 cm^2 (12.9 in^2). With the rod bundle in place the flow area is 48.63 cm^2 (7.5 in^2). This area is 7.21 percent larger than the ideal flow area of a 7x7 rod bundle configuration. The excess flow area is due to the flow housing inside dimensional tolerance and the space needed to insert the rod bundle in the housing. The gap between the outer rods and the flow housing inner wall is 3.12 mm (0.123 in) wide. More detailed information is given in Appendix E.

The flow housing has six pairs of windows. Each window provides a 50.8 x 292.1 mm (2 x 11.5 in) viewing area as listed in Table 3.3. Each pair of windows is placed 180 degrees apart and located axially at elevations overlapping rod bundle spacer grids, thus providing a viewing area

about 88.9 mm (3.5 in) below and 152.4 mm (6 in) above the corresponding spacer grids. The windows will facilitate the measurement of droplet size and velocity using a Laser Illuminated Digital Camera System (LIDCS). The two-phase void fraction will be measured using sensitive DP cells. In addition, high speed movies using diffused back lighting can be taken during the experiments for visualization and flow regime information. The windows are made out of optical grade fused quartz and are mounted on the housing by means of a bolted flange and Kemprofile high temperature gasketing material, as shown in Figure 3.9.

The flow housing has 23 pressure taps located at various elevations, as shown schematically in Figure 3.8. The pressure taps locations are shown in the Engineering Drawings E115073 and E118338. The pressure taps are connected to sensitive DP cells providing measurements to calculate single-phase friction losses for determining bare rod bundle and grid loss coefficients. Sixteen of these pressure taps are located about 76.2 - 127 mm (3 - 5 in.) apart to provide detailed void fraction measurements in the froth region above the quench front. The DP cells connections and axial location are shown schematically in the Engineering Drawing E118338. The flow housing is supported from the nickel plate and upper plenum, allowing it to freely expand downward, thus minimizing thermal buckling and distortion.

The flow housing also has 13 stand-offs at various elevations, as shown in Figure 3.9, for the traversing steam probe rakes which measure the superheated steam temperatures in the dispersed flow regime.

3.2 Lower Plenum

The lower plenum is attached to the bottom of the flow housing. The lower plenum is made out of nominal 203.2 mm (8 in) schedule 40, 304SS pipe with an inside diameter of 201.6 mm (7.937 in), a height of 203.2 mm (8 in), and a volume of 6569.5 cm^3 (0.232 ft^3), as shown in Figure 3.10. The lower plenum is used as a reservoir for the coolant prior to injection into the rod bundle during reflood. It connects to the injection water line and steam cooling line. It has two penetrations for thermocouples monitoring the coolant temperature prior and during reflood, and pressure taps for static and differential pressure measurements.

The lower plenum also has four Conax fittings with multiple probes sealing glands for the bundle grid, steam probes, and support rod wall thermocouple extensions that are routed through the bottom of the rod bundle. It contains a flow baffle, which is attached to the flow housing bottom flange. The flow baffle has a square geometry, similar to the flow housing, as shown in Figure 3.11. The flow baffle wall has numerous small diameter holes that act as a flow distributor and flow straightener to provide an even flow distribution into the rod bundle.

3.3 Upper Plenum

The upper plenum serves as the first stage for phase separation and liquid collection of the two-phase effluent exiting the rod bundle. The liquid phase separates due to the sudden expansion from the bundle to the larger plenum flow area. The de-entrained liquid is collected around the flow housing extension in the upper plenum. The extension acts as a weir preventing the separated liquid from falling back into the heater rod bundle. The upper plenum vessel configuration is shown in Figure 3.12. The vessel is made from a 203.2 mm (8 in) 304SS pipe with an inside diameter of 201.6 mm (7.937 in) and a height of 304.8 mm (12 in). It has a volume of 9827.5 cm^3 (0.347 ft^3). The plenum has a 76.2 mm (3 in) pipe flange connection to

the steam separator and two penetrations for fluid thermocouples. It is covered with a 203.2 mm (8 in) 304SS blind flange. This flange has a 25.4 mm (1 in) penetration for steam injection, venting and connecting the safety relief valve and rupture disc assembly. It also has a pressure tap penetration for static and differential pressure measurements. In addition, the upper plenum contains an exhaust line baffle shown in Figure 3.13. The baffle is used to further de-entrain water from the steam and prevents water dripping from the upper plenum cover flange to be carried out by the exhaust steam. The baffle has a 76.2 mm (3 in) flange connection at one end. It is inserted through the upper plenum exit nozzle, and it is bolted between the nozzle flange and the flange of the pipe going to the steam separator.

3.4 Large and Small Carryover Tanks

The de-entrained liquid from the upper plenum drains into the top of a 25.6 mm (1 in) tube which extends inside a small carryover tank to detect and measure the carryover liquid as soon as possible. This tank, shown in Figure 3.15, is connected close coupled in series with a larger carryover tank, shown in Figure 3.14, which collects and measures the amount of liquid overflow from the smaller carryover tank. The small carryover tank has a volume of about 1387.8 cm^3 (0.049 ft^3) to more accurately measure the water being collected as a function of time. This tank is made from a 76.2 mm (3 in) schedule 40 pipes having an overall length of 0.9144 m (36 in) including the end caps. The large carryover tank is made from a 101.6 mm (4 in) schedule 40 pipes with a bottom end cap and top flanges having an overall length of 19.7 m (6 ft) and a capacity of 15916.9 cm^3 (0.562 ft^3). Each tank is connected with one 25.4 mm (1 in) flexible hose, one 25.4 mm (1 in) drain tube, and 9.5 mm (3/8 in) tubes with wall penetrations for installing fluid and level meters.

3.5 Steam Separator and Collection Tanks

The wet steam exhausted from the upper plenum flows through a steam separator (or dryer), shown in Figure 3.16, where carryover liquid droplets are further separated from the steam and collected in a small collection tank, shown in Figure 3.17 attached to the bottom of the steam separator. The steam separator relies on centrifugal force action to provide 99 percent dry steam. The separated liquid is drained into a collection tank where a differential pressure cell is used as a level meter to measure liquid accumulation. The steam separator is fabricated from a 355.6 mm (14 in) diameter 316SS pipes and is 914.4 mm (36 in) long. It has 50.8 mm (2 in) connecting nozzles, a 25.4 mm (1 in) drain, and a 12.7 mm (0.5 in) top vent. It also has two pressure taps for liquid level measurements and two 38.1 mm (1.5 in) side nozzle connections. The drain tank is a small vessel with a capacity of 11328.77 cm^3 (0.4 ft^3). It is made from a 101.6 mm (4 in) schedule 10, 304SS pipe with an overall length of 121.9 mm (48 in), including both end caps. It has a 25.4 mm (1 in) drain nozzle, a 25.4 mm (1 in) pipe top connection to the steam separator, pressure taps and fluid thermocouple connections.

3.6 Pressure Oscillation Damping Tank

The dry steam from the steam separator flows into a pressure oscillation-damping tank. As its name implies, it is used to dampen pressure oscillations at the upper plenum caused by rapidly oscillating steam generation in the heater rod bundle during reflood. This effect is coupled to the characteristics of the pressure control valve, which is located downstream in the steam exhaust line. It is desirable to have a smooth pressure control in order to minimize uncertainties when calculating mass balances, steam generation rates, and heat transfer coefficients in the heater

rod bundle, and avoid the pressure control valve causing oscillations in the bundle as it cycles. The tank has a volume of 0.209 cm^3 (7.38 ft^3), which is approximately equal to the total volume of the rest of the test facility. This design criterion was used successfully in the ACHILLES reflood test facility (Ref. 6). The pressure tank is fabricated from a 355.6 mm (14 in), 304SS standard schedule pipe by 2.59 m (102 in) long, as shown in Figure 3.18. Inside the tank is a 76.2 mm (3 in), schedule 40, 304SS pipe that provides a tortuous path for the steam flow to expand into a large volume, thus damping pressure oscillations. The inlet and outlet nozzles are 76.2 mm (3 in) in diameter with flanges. The vent and drain lines are made of 25.4 mm (1 in) pipe. There are 9.53 mm (3/8 in) tube penetrations for a fluid thermocouple and two static pressure taps. The tank walls are heated with clamp-on strip heaters up to about 5.55 degrees C (10 degrees F) above saturation temperatures to prevent steam condensation.

3.7 Exhaust Piping

The steam flowing out of the pressure oscillation-damping tank is exhausted through a 76.2 mm (3 in) schedule 40, 304SS pipes, shown schematically in Figure 3.19. The exhaust line has a Vortex flowmeter, a 76.2 mm (3 in) V-Ball pressure control valve, and a muffler at the exit to minimize the noise caused by steam blowing into the atmosphere. The pressure control valve is activated by a signal from a static pressure transmitter located on the upper plenum. The line is also instrumented with a static pressure transmitter, fluid thermocouples, and outer wall thermocouples. The 76.2 mm (3 in) line has flow-straightening vanes which reduce the pipe length requirements upstream of the Vortex flowmeter in order to obtain accurate flow measurements. This line has strapped-on electrical heaters to keep the wall temperature about 11.11 degrees C (20 degrees F) above saturation to insure that single-phase steam flow measurements are made by the Vortex flowmeter.

3.8 Injection Water Supply Tank

The injection water system consists of a water supply tank, a circulating pump, and interconnecting lines to the test section lower plenum. The water supply tank shown in Figure 3.20 has a capacity of 0.953 cm^3 (251.75 gal). It is designed for 0.402 MPa (60 psig) and 154.44 degrees C (310 degrees F). The tank is equipped with a submersible electrical heater to heat the injection water to specified test temperatures. The tank is pressurized by a nitrogen supply system, which regulates the over-pressure needed for the forced flooding injection tests. The tank has inlet and outlet nozzles, pressure taps for level measurements, fluid and wall thermocouples. Water from the tank can be circulated through the test section by a centrifugal pump with a capacity up to 0.946 cm^3 per minute (250 gpm) which are needed to perform liquid single-phase flow tests.

3.9 Water Injection Line

The water injection line shown schematically on Figure 3.21 consists of a 50.8 mm (2 in) diameter 304SS tubing with a 2.77 mm (0.109 in) wall. It is rated for 0.402 MPa (60 psi) and 154.4 degrees C (310 degrees F) service. This line has a Coriolis Effect type flowmeter, a V-ball control valve, a quick opening solenoid valve, and appropriate shut-off and drain valves. It also has penetrations for static pressure and fluid thermocouples, and outside wall thermocouples. The line has tracer electrical cable type heater to maintain the water being injected at the proper test inlet temperatures.

3.10 Steam Supply

A boiler with a capacity of 2613 kg/hr (5760 lbs/hr) at 1.03 MPa (150 psig) provides steam for the single phase steam cooling , pressure drop and water droplet injection tests. It also provides steam for preheating the test components prior to testing. The boiler is connected to the lower plenum by means of a 50.8 mm (2 in) 304SS tube. It is equipped with a Vortex flowmeter to measure steam flows, fluid and wall thermocouples, a V-ball control valve, and a quick acting solenoid valve. The boiler is also connected to the upper plenum to provide steam for preheating the test components prior to testing.

3.11 Droplet Injection System

A system to inject water droplets into the test section has been included in the RBHT Test Facility design. The droplet injection system consists of six 2.38 mm (3/32 in) OD stainless steel tubes entering through the test section at the 1.295 m (51 in) elevation. The tubes run perpendicular to the heater rods and penetrate through both sides of the housing as seen in Figure 3.22, and the injection flow schematic is shown in Figure 3.23. The tubes can be easily removed when not needed so they do not interfere with other types of tests. Water is supplied to the injector tubes from the injection water supply tank as described in Section 3.8 and a cluster of 0.33 mm (0.013 in) diameter holes which are drilled on the downstream side of the tubes to inject water directly into each of the 36 rod bundle sub-channels. Three injection tubes with different hole arrangements were tested as reported in Appendix D. The results showed that the triangular pitch configuration provided the desired water droplet diameter of about 0.660 mm (0.026 in).

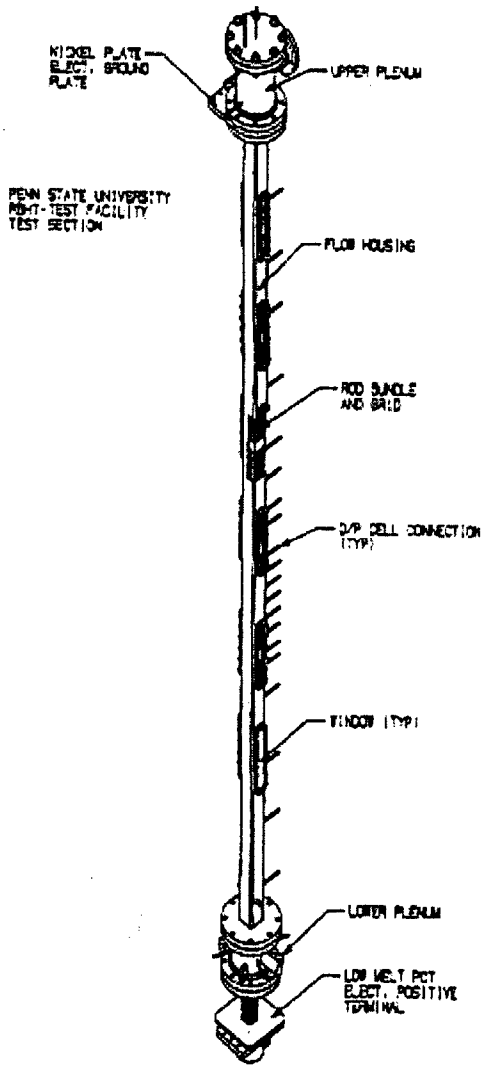

Figure 3.1 Test Section Isometric View.

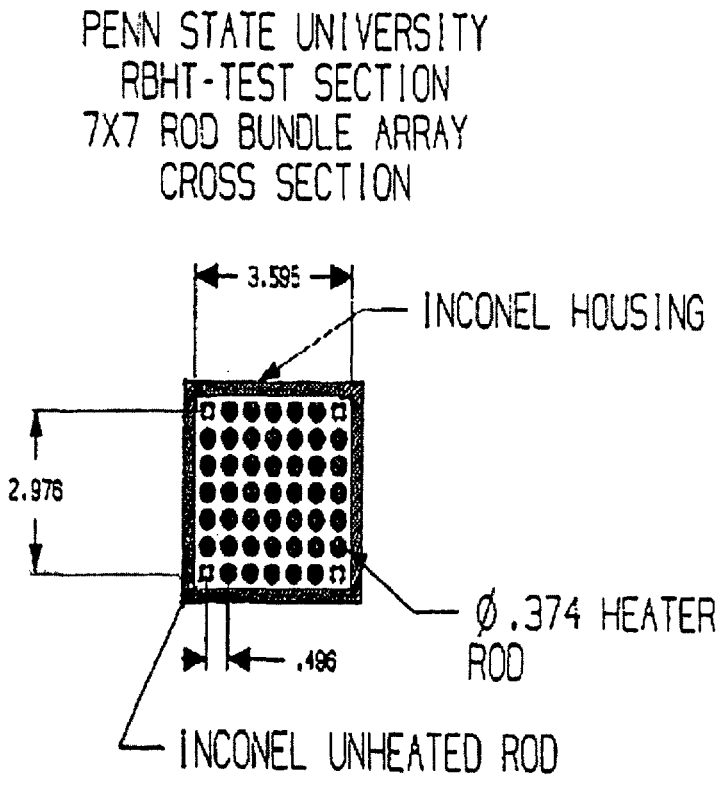

Figure 3.2 Rod Bundle Cross Section View.

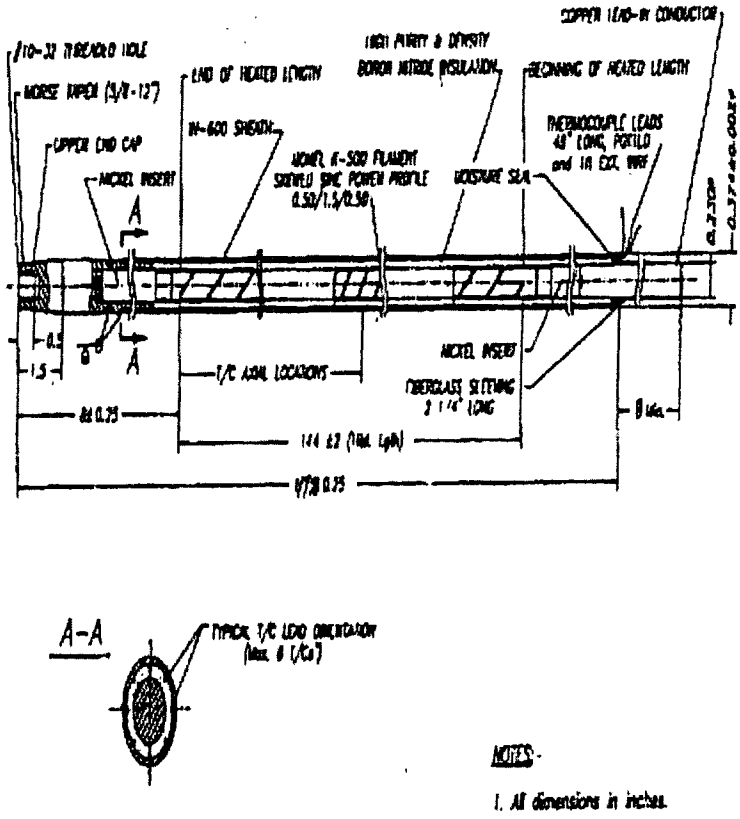

PENN STATE HEATER ROD SCHEMATIC

Figure 3.3 Heater Rod.

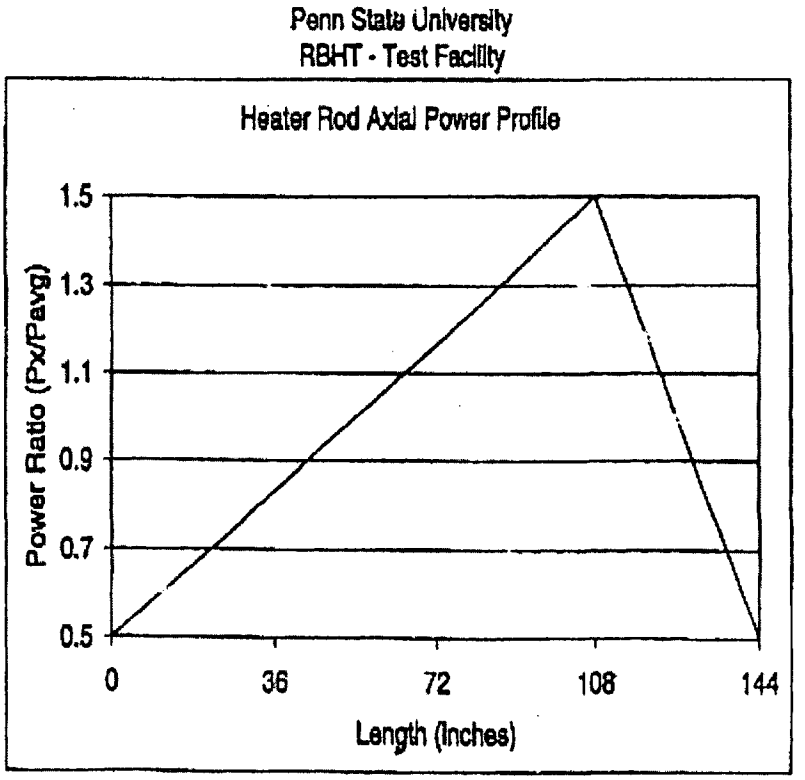

Figure 3.4 Heater Rod Axial Power Profile.

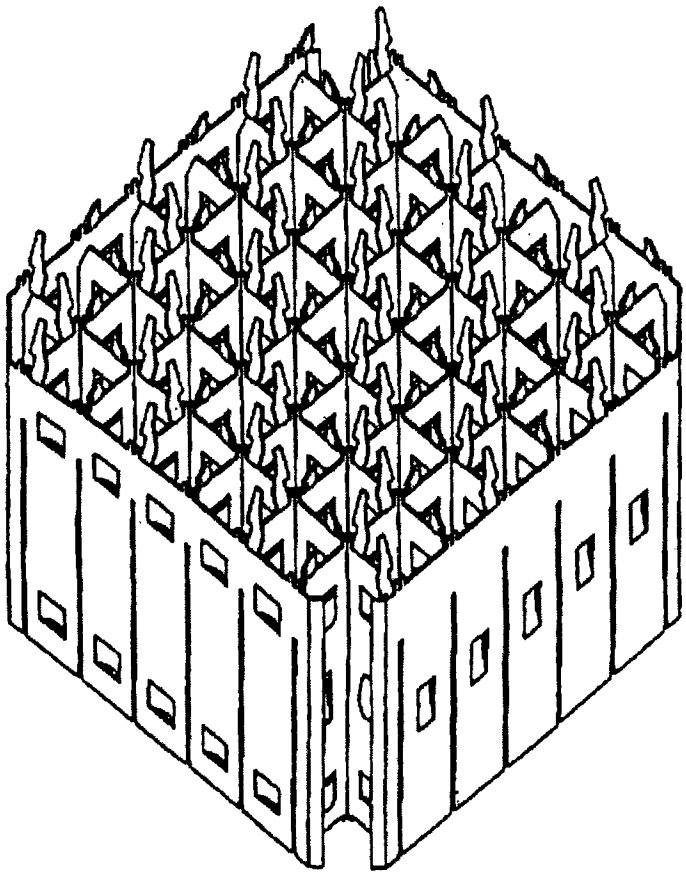

Figure 3.5 Mixing Vane Grid.

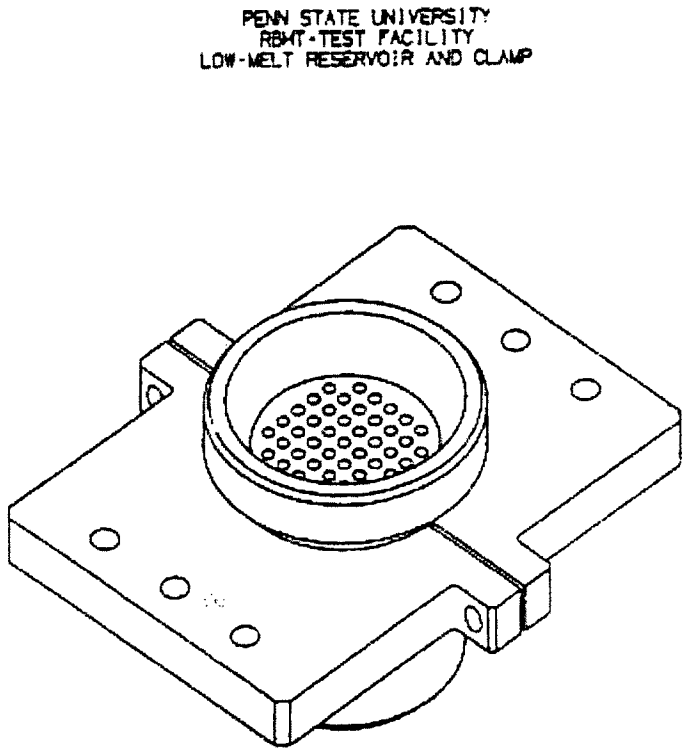

Figure 3.6 Low-Melt Reservoir.

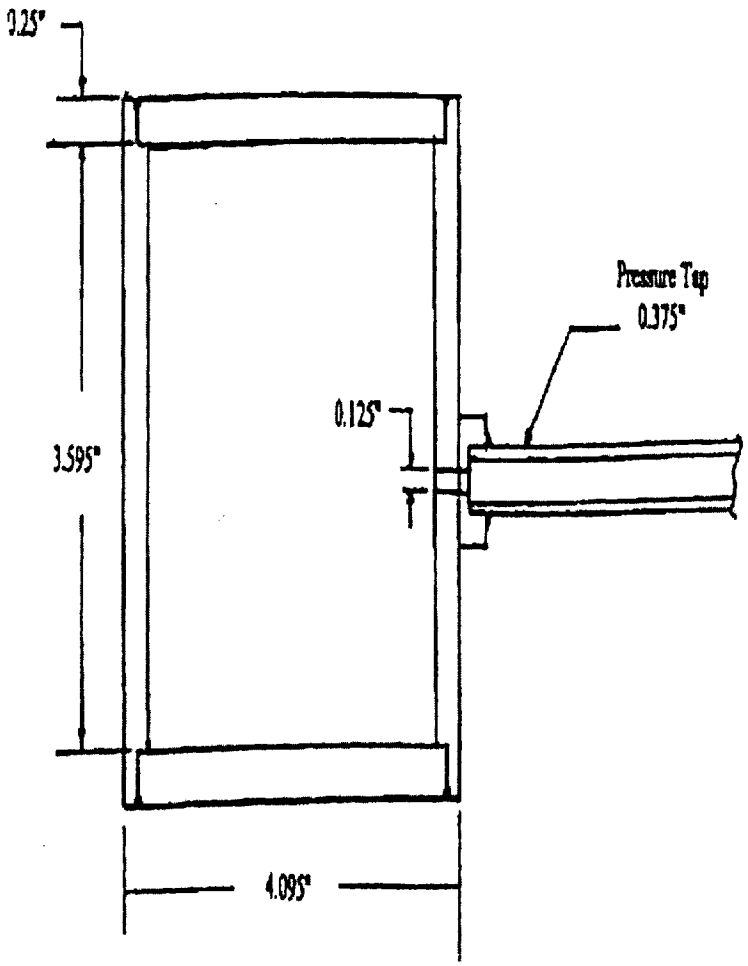

Figure 3.7 Flow Housing Cross Section View.

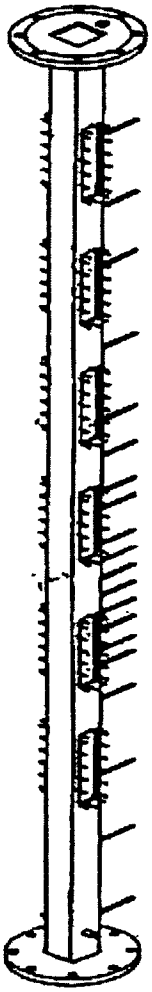

Figure 3.8 Low Mass Flow Housing.

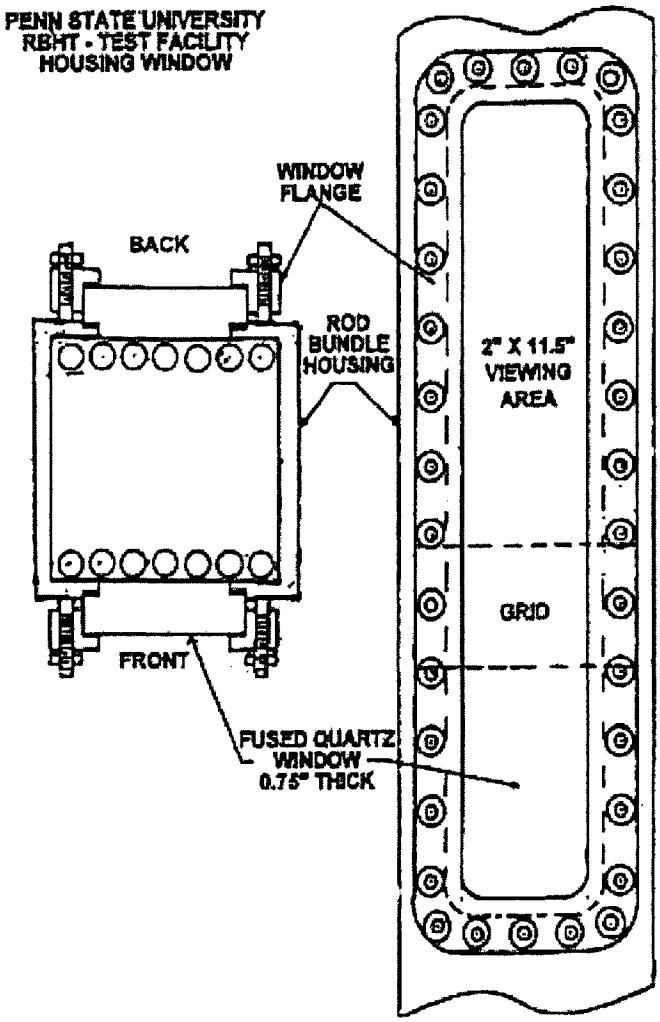

Figure 3.9 Housing Window.

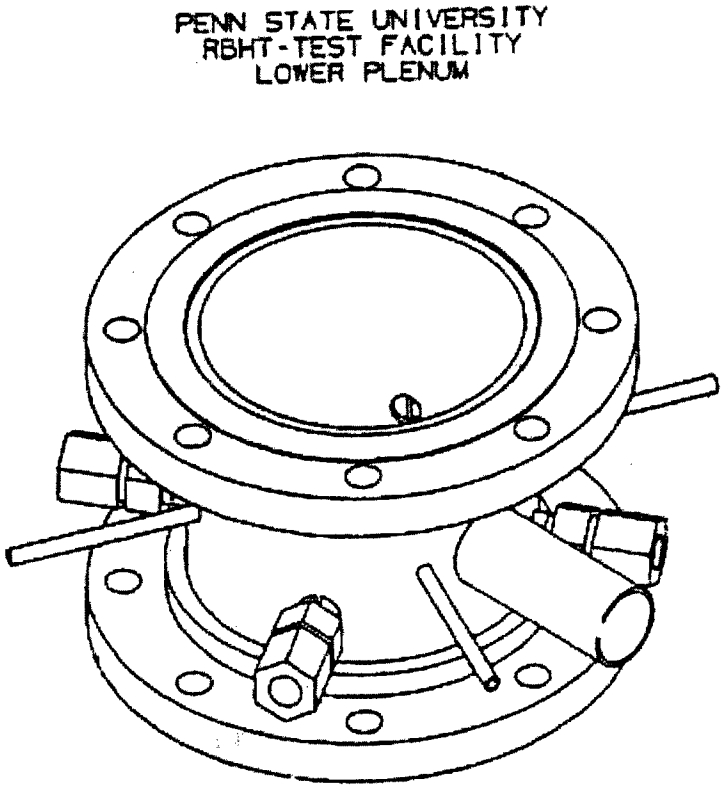

Figure 3.10 Lower Plenum.

PENN STATE UNIVERSITY
RBHT-TEST FACILITY
LOWER PLENUM FLOW BAFFLE

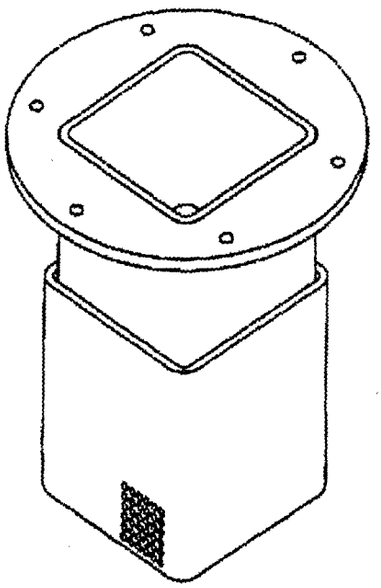

Figure 3.11 Lower Plenum Flow Baffle.

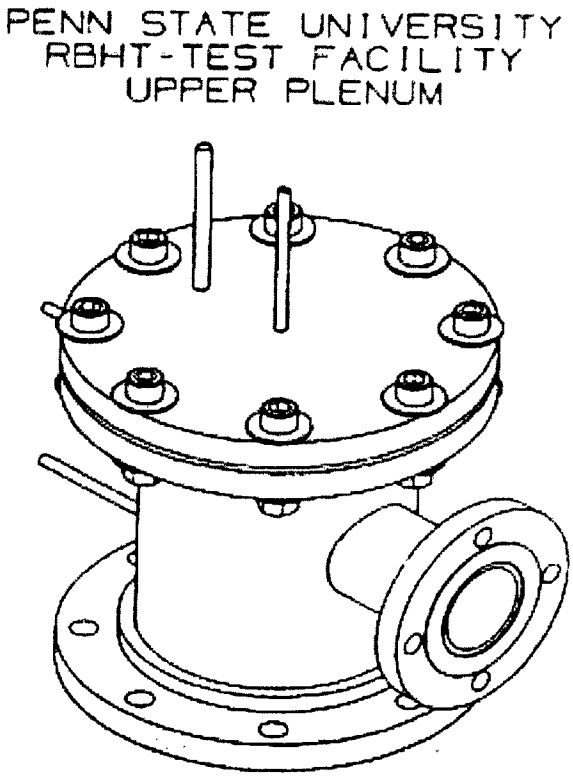

Figure 3.12 Upper Plenum.

PENN STATE UNIVERSITY
RBHT-TEST FACILITY
EXHAUST LINE BAFFLE

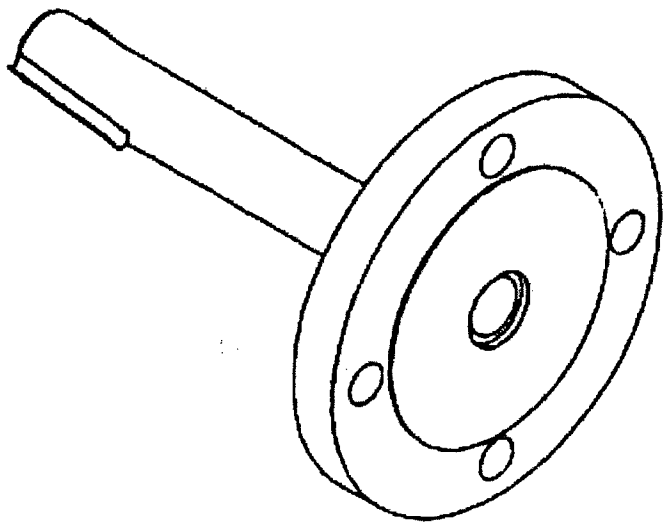

Figure 3.13 Exhaust Line Baffle.

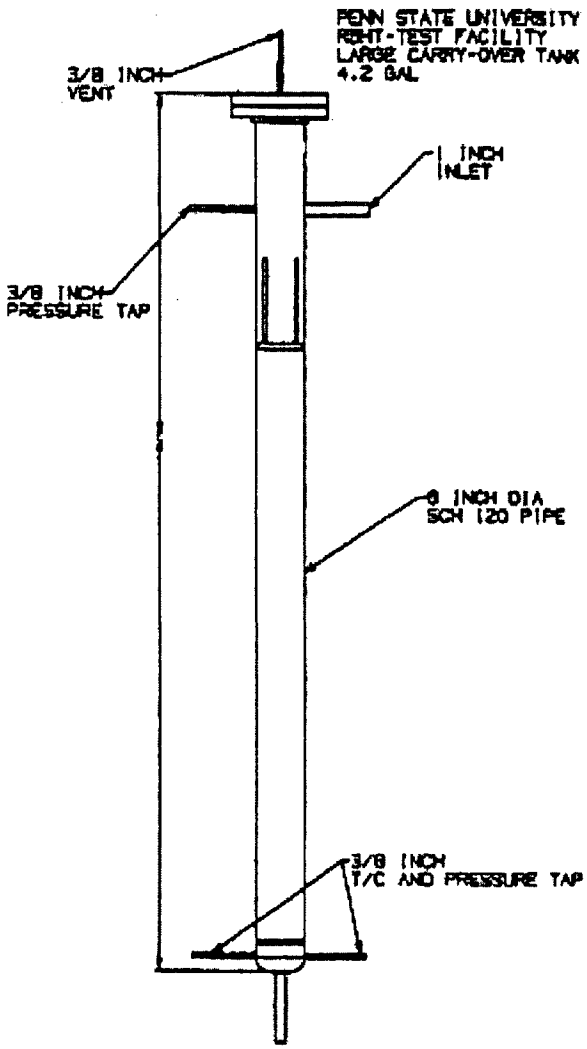

Figure 3.14 Large Carryover Tank.

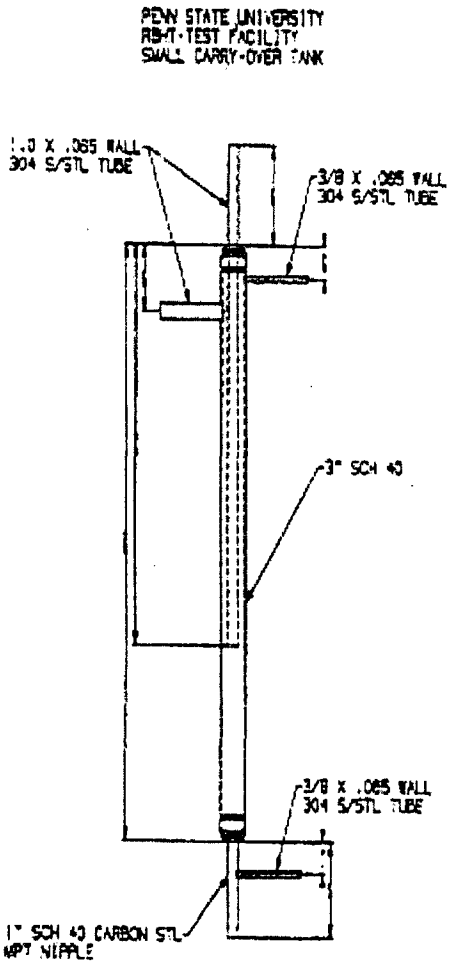

Figure 3.15 Small Carryover Tank.

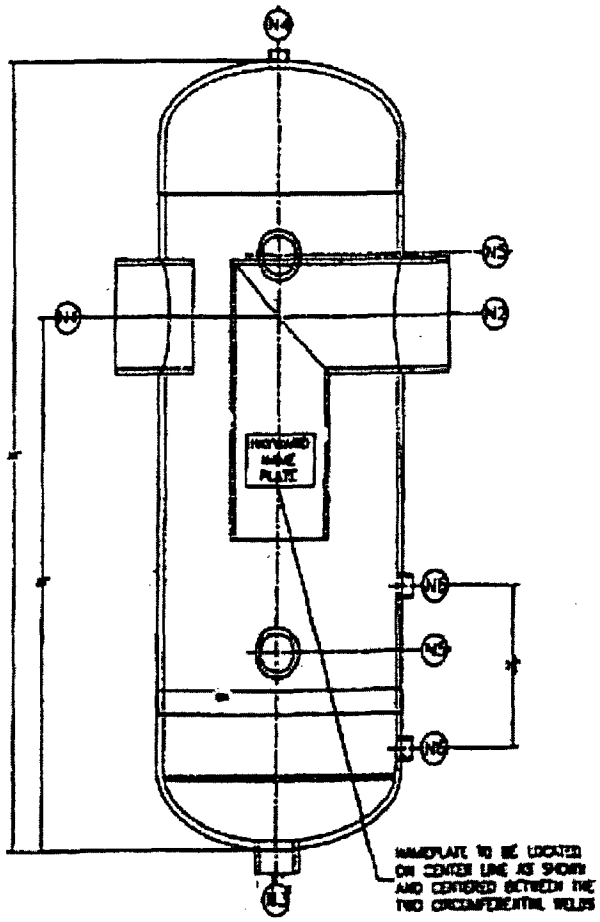

Figure 3.16 Steam Separator.

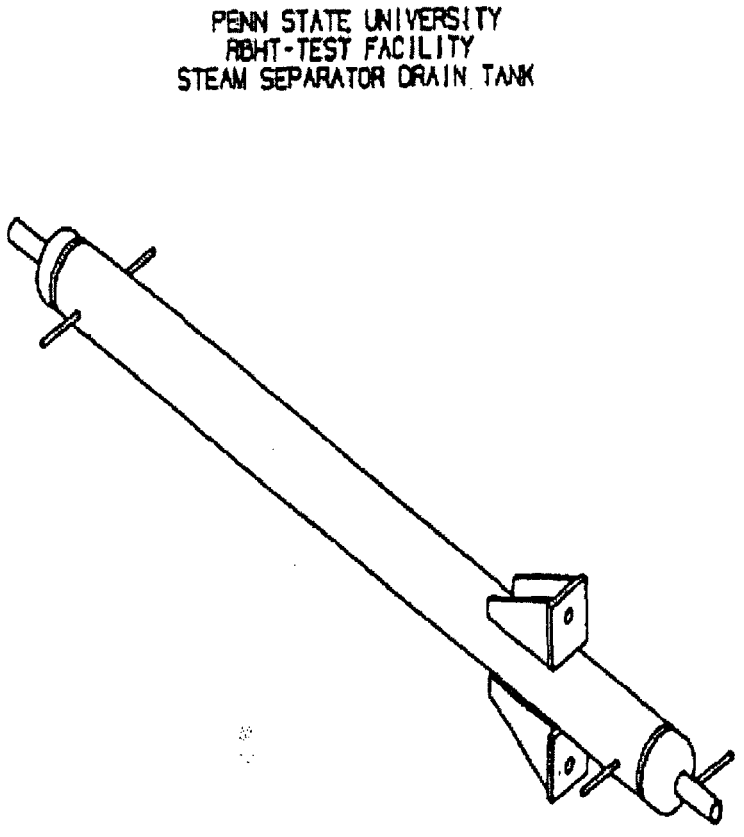

Figure 3.17 Steam Separator Drain Tank.

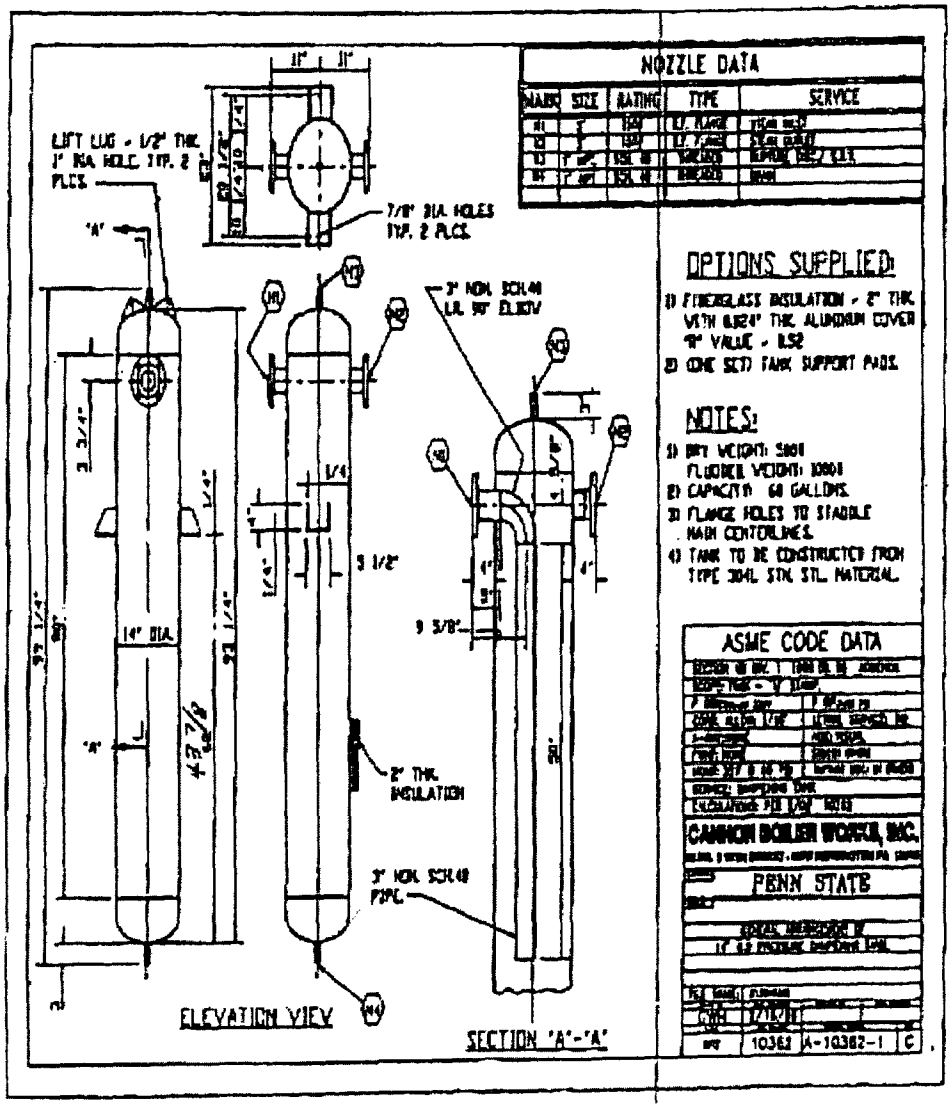

Figure 3.18 Pressure Oscillation Damping Tank.

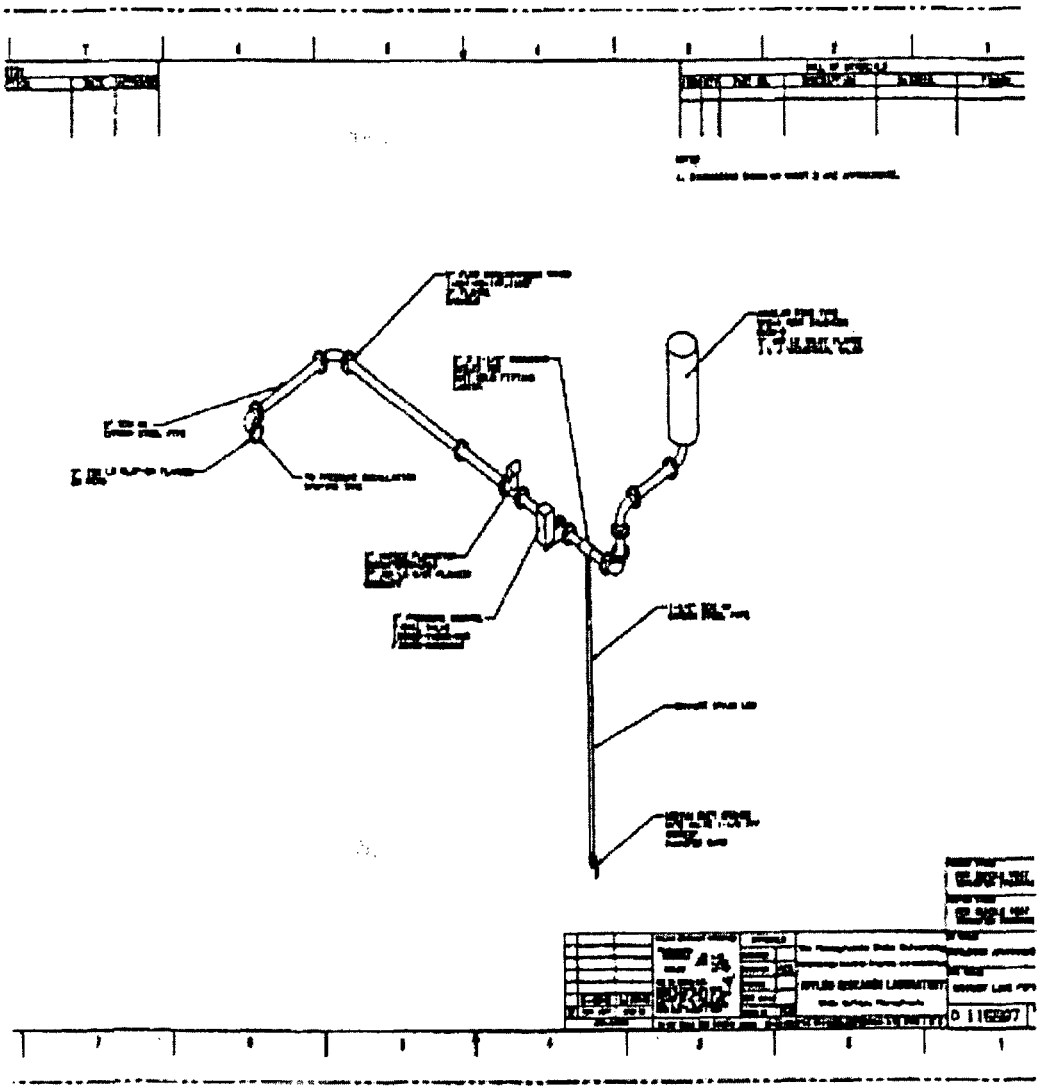

Figure 3.19 Exhaust Piping.

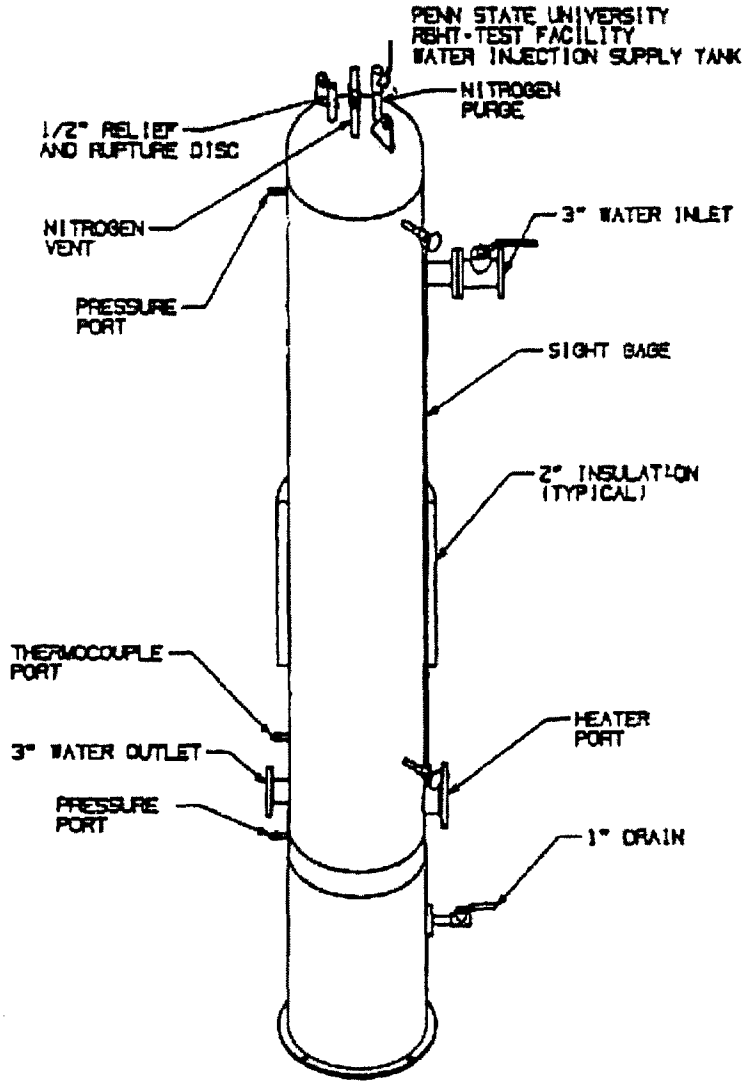

Figure 3.20 Injection Water Supply Tank.

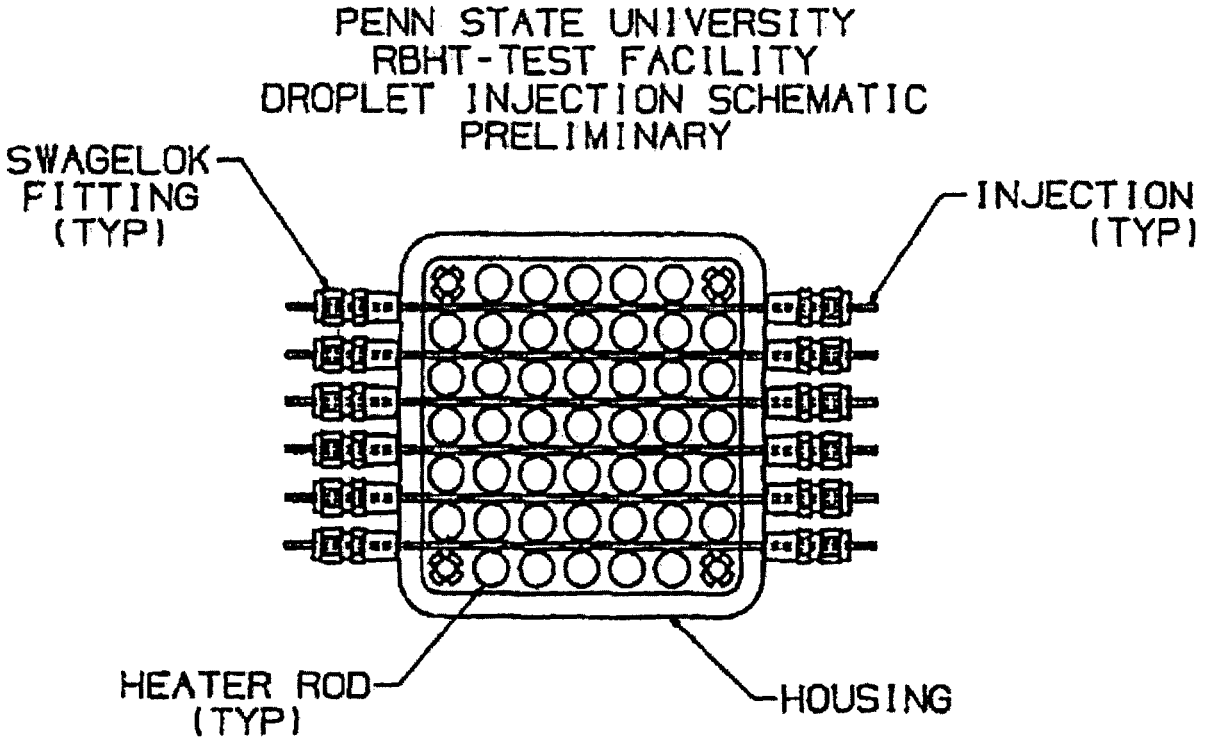

Figure 3.21 Water Injection Line.

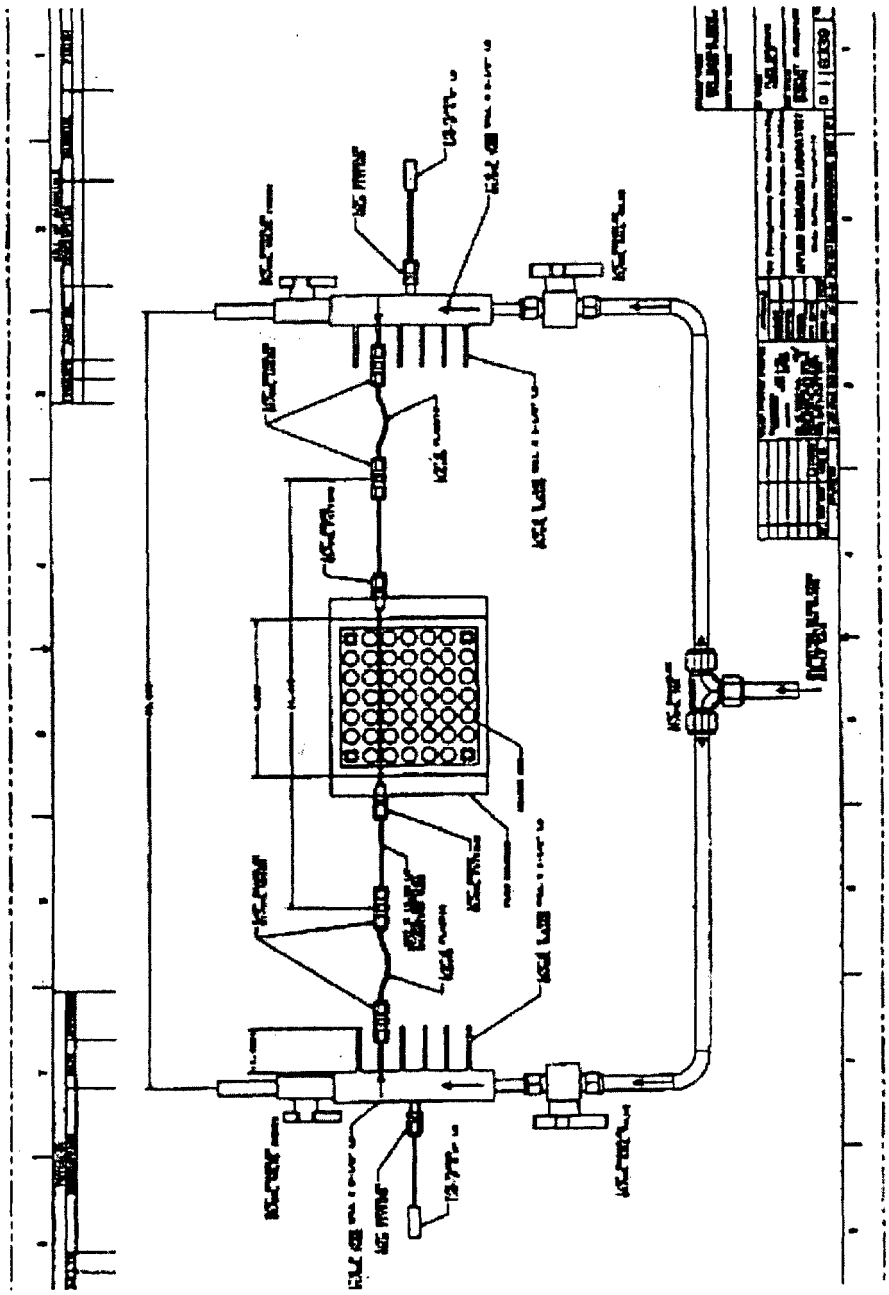

Figure 3.22 Droplet Injection Schematic.

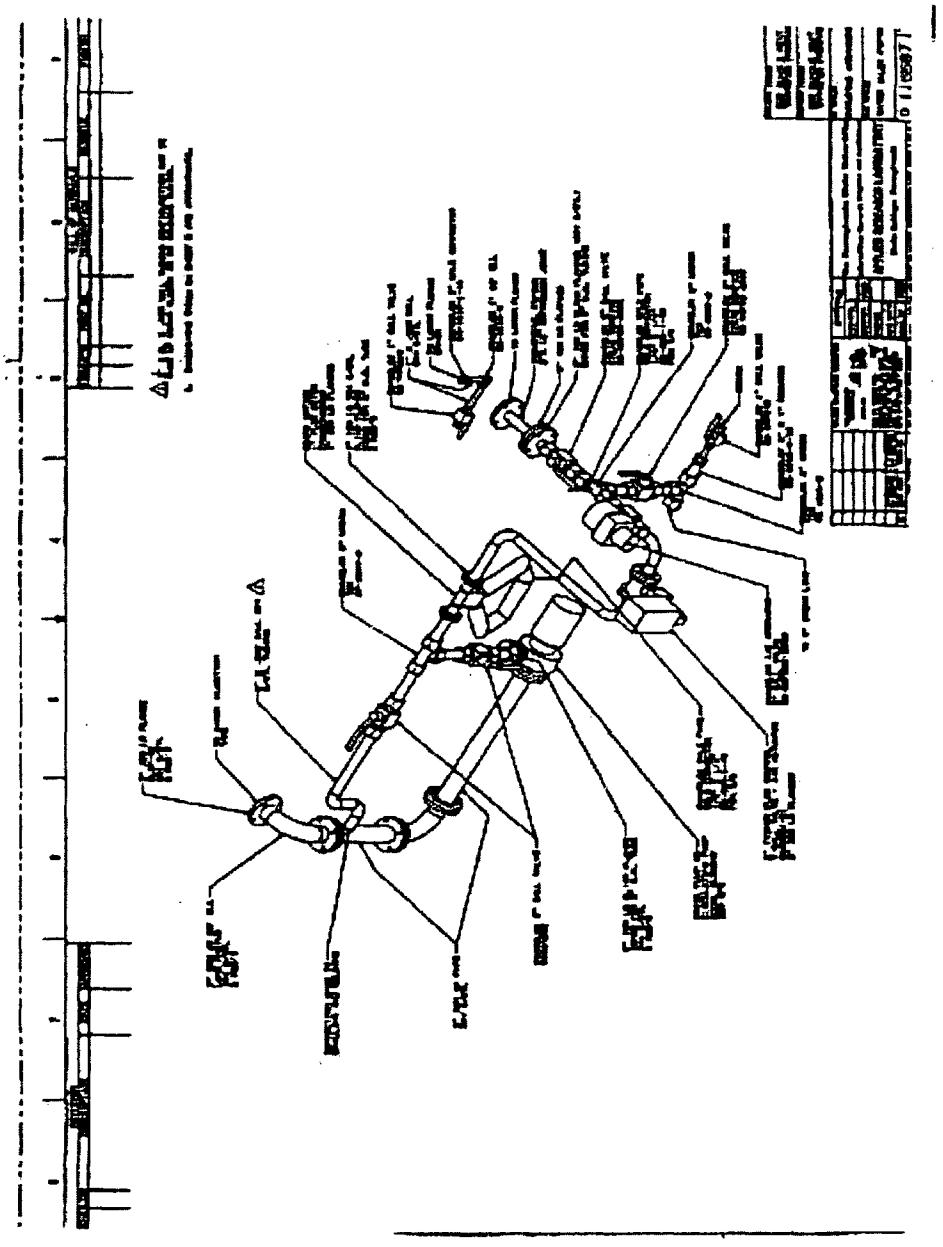

Figure 3.23 Droplet Injection System Schematic.

Table 3.1 Heater Rod General Specifications

Operating Pressure	1.38 MPa (200 psig)
Maximum Sheath Temperature	1204 degrees C (2200 degrees F)
Design Power	10.0kW
Design Voltage	57 V
Design Current	175.4 A
Design Resistance @ 537.8 degrees C	0.325 Ω
Electrical Resistance @ 31.11 degrees C	0.306 Ω ± 5%
Axial Power Profile	Linear 0.5/1.5/0.5 (See Figure 3.4)
Heated Length	3.657 m (144 in)
Average Linear Power	0.83 kW/ft
Peak Linear Power	1.25 kW/ft
Outside Diameter	9.5 mm (0.374 ± 0.002 in)
Overall Sheath Length	7.368 m (172 in)
Electrode Length	203 mm (8 in)
Electrode Diameter	5.84 mm (0.230 ± 0.002 in)
Extension Length - Top	203 mm (8 ± 0.25 in)
Sheath Surface Finish	As Swaged (63 µin or better)

Table 3.2 Thermocouple Specifications

Type	Premium grade ANSI Type K
Diameter	0.508 mm (0.020 in)
Sheath	Inconel 600
Insulation	MgO
Junction	Undergrounded, BN Backfilled
Length	Up to 5.485 m (216 in)
Resistance, Lead to Sheath	1×10^{11} Ω @ 50 volts
Length Beyond Heater Sheath	1.219 m (48 in)

Table 3.3 Flow Housing Window Viewing Areas Below and Above Mixing Vane Grids

Window	Grid No.	Height of Viewing Areas	
		Below mm (in)	Above mm (in)
A	2	101.6 (4)	152.4 (6)
B	3	108.0 (4.25)	146.1 (5.75)
C	4	108.0 (4.25)	146.1 (5.75)
D	5	108.0 (4.25)	146.1 (5.75)
E	6	98.4 (3.873)	155.6 (6.125)
F	7	108.0 (4.25)	146.1 (5.75)

4. TEST FACILITY INSTRUMENTATION

The test facility instrumentation is designed to measure temperatures, power, flows, liquid levels, pressures, void fractions, and droplet sizes, distribution, and drop velocities. The vapor velocity cannot be directly measured in a two-phase dispersed flow, but it can be calculated at different axial positions from the data. Overall and transient mass and energy balances, mass inventories, carryover liquid and steam flows as a function of time can be calculated. Heater rod power, temperature, and fluid temperature are used to calculate heat fluxes and heat transfer coefficients, quench times, rod bundle energy losses, convective and radiation heat transfer to steam, droplets, grids, support rods, and housing. Effects of grids, support rods and housing behavior during reflood can be determined. Void fraction measurements below the quench front and in the froth level above the quench front, in conjunction with the laser illuminated digital camera measurements are used to determine droplet entrainment behavior, droplet effects on heat transfer, and steam desuperheating. The Laser Illuminated Digital Camera System (LIDCS) measurements provide droplet size distribution and velocities during reflood.

4.1 Loop Instrumentation and Controls

Loop instrumentation is shown schematically in Figure 4.1, and listed in the instrumentation and data acquisition channels shown in Table 4. There are 123 instrumentation channels are assigned to the collection of electrical power, fluid and wall temperatures, levels, flows, differential pressures, and static pressure measurements. The injection water supply tank has three fluid and three wall thermocouples to monitor water and wall temperatures during heat-up prior to testing. It has a differential pressure transmitter used as a level meter to determine water mass in the tank and mass depletion during reflood testing. It also has a static pressure transmitter which monitors the nitrogen overpressure and controls the nitrogen flow needed to maintain a constant pressure during forced injection reflood tests.

The water injection line is equipped with a Coriolis Effect Micromotion flowmeter that directly measures mass flows up to 454 kg/min (1000 lbs/min) with an accuracy of plus or minus eleven hundredths of a percent (±0.11 percent) of rate. The steam line has a Rosemount Vortex shedding flowmeter to measure flow up to 7.08 m^3/min (250 ft^3/min) with an accuracy of plus or minus 65 hundredths of a percent (±0.65 percent) of rate. Each flowmeter is connected through a pneumatic controller to a V-ball flow control valve. Each line has a fluid thermocouple to measure water or steam temperature during heat-up and forced injection testing. They also have a static pressure transmitter which in conjunction with the thermocouples can determine the thermodynamic properties of the fluids. The injection line has three wall thermocouples to monitor wall temperatures during heat-up and during testing. One of these thermocouples in conjunction with a temperature controller regulates the power to an electrical heating cable wrapped around the injection line. The heating cable is used to heat-up the injection line wall and to maintain the injection water at the required injection temperature.

The small carryover tank has one fluid and two wall thermocouples. The large carryover tank instrumentation consists of one fluid thermocouple and three wall thermocouples. Both tanks have a liquid level meter which measures the amount of carryover liquid being collected during testing. In addition, a differential pressure transmitter is connected from the top of the carryover tank to the upper plenum to determine the static pressure in the carryover tank.

The steam separator is instrumented with one fluid and two wall thermocouples. The drain tank

is instrumented with two fluid and two wall thermocouples. The fluid thermocouple measures the water temperature de-entrained during testing. The wall thermocouples monitor wall temperatures during heat-up. The volume of de-entrained water is measured with a level meter connected across the drain tank.

The pressure oscillation damping tank has two fluid and three wall thermocouples which are used to monitor vessel walls during heat-up, and to insure that the vessel wall is at a temperature above saturation to prevent condensation. One wall thermocouple in conjunction with a temperature controller monitors the power applied to clamp-on heaters that heat up the tank to the desired wall temperature.

The exhaust line is equipped with a Vortex flowmeter which, in conjunction with a static pressure transmitter and fluid thermocouple measurements are used to calculate steam volumetric flows up to 7.08 m^3/min (250 ft^3/min). The flowmeter has an accuracy of plus or minus 65 hundredths of a percent (±0.65 percent) of the rate. The exhaust line also has three wall thermocouples to measure pipe wall temperatures. One wall thermocouple in conjunction with a temperature control regulates the power going to clamp-on heaters which are used for heating the pipe walls up to a temperature about 11 degrees C (20 degrees F) above saturation to prevent steam condensation and to insure accurate single phase steam flow measurements. The exhaust line has a V-ball pressure control valve. This valve is controlled by a static pressure transmitter through a pneumatic controller connected to the top of the upper plenum in order to maintain constant test section pressure during testing.

4.2 Test Section Instrumentation

The test section is heavily instrumented to obtain the data described at the beginning of this section.

The test section instrumentation consists of the heater rod bundle and flow housing, the lower plenum, and the upper plenum groups. The heater rod bundle and flow housing instrumentation is shown schematically in Figure 4.2 and listed in Table 4. A more detailed drawing is given in Figure E.5 of Appendix E. This figure shows the instrumentation axial locations in relation to heater rod heated length, heater axial power profile, grids, steam probes and steam probe rakes, housing pressure taps, and windows.

Six grids have thermocouples attached to their surfaces in order to determine quenching behavior during reflood shown in Figures 4.3 though 4.9. Grid and steam probes axial locations are shown schematically in Figure 3.8 with the detailed elevation information given in Figures E.3 and E.4 of Appendix E. Eight groups of heater rods have thermocouples at different elevations to cover, as much as possible, the entire rod bundle heated length. The radial location of each heater rod group is shown in Figure 4.10. The radial locations of instrumentation rods were chosen in order to be able to characterize heat transfer of hot rods simulated by the center rods, rod-to-rod and rod-to-housing radiation heat transfer. For this purpose, heater rod thermocouples, steam probes, and housing wall thermocouples are located at the same elevations. In addition, symmetrical location of the same group of instrumented heater rods will help in the data analysis and will determine any anomalies in the radial flow distribution through the heater rod bundle. Heater rod thermocouples are also placed at varying distances downstream from a grid to determine the decreasing heat transfer gradient between grid spans. The steam probe or fluid thermocouples are located at short distances upstream

and downstream of a grid to determine the effect of water droplets being shattered by the grids on droplet size and distribution, and the de-superheating effect on steam temperatures in the disperse flow regime.

The vapor or steam temperature will be measured using miniature thermocouples having a diameter of 0.813 mm (0.032 in) which are attached to the spacer grids, and the traversing steam probe rakes having a diameter of 0.381 mm (0.015 in). These are very small diameter thermocouples that have a fast response time such that they can follow the vapor temperature accurately in a dispersed, non-equilibrium, two-phase flow. As the froth front approaches, the number and sizes of the droplets increase which can lead to wetting of these thermocouples. Experiments performed as part of the FLECHT-SEASET program indicated that very small thermocouples would provide reliable vapor superheat ready for the longest time period until they quench as the froth region approached. While the Lehigh vapor probe was considered, it is too large and causes a flow distribution effect which is not typical of the bundle. The Lehigh probe would block 68 percent of the gap between adjacent heat rods. The effect of the probe would be to distort the data downstream of the sensing location. Such flow distribution effects were observed in the Lehigh data as well as the INEL single tube data which used these probes.

The traversing steam probe rakes are located at the spans among the grids at the upper heater rod bundle elevations, as shown schematically in Figure 4.11. The traversing steam probes rakes will measure steam temperatures in the heater rod bundle flow subchannels and the gap between the heater rods during the dispersed flow regime. The traversing steam probe rake is shown in Figure 4.12. Each rake consists of three 0.381 mm (0.015 in) diameter ungrounded thermocouples mounted on a 0.356 mm (0.014 in) thick by 6.35 mm (0.25 in) wide Inconel strip. The thermocouples are spaced 12.6 mm (0.496 in) apart which correspond to the heater rod spacing in the bundle. The thermocouple tips are located facing the steam flow. A 2.39 mm (0.094 in) diameter tube attached to the strip is used to traverse the steam probe rake across the rod bundle. This tube also carries the thermocouples leads outside the flow housing through an extension tube and a pressure seal arrangement. The tube is attached to an automated sliding mechanism shown in Figure 4.13. It consists of a sliding bar, a 24 DCV motor with a ball drive shaft, and a linear potentiometer provides a voltage input to the Data Acquisition which determines the rake thermocouple location and travel distances across the heater rod bundle.

Two fluid thermocouples are placed 24.5 mm (1 in) below the bottom of the bundle heated length such that injection water temperatures are monitored prior to and when reflood is started. There are 23 DP transmitters connected to the housing wall pressure taps providing measurements to calculate single phase flow heater rod bundle and grid friction losses, bundle mass inventory, and void fraction during reflood. Nine DP cells are connected to pressure taps located 76.2 - 127 mm (3 - 5 in) apart to provide detail mass inventory, and void fraction data in the froth region above the quench front, as shown in Figure E.2 of Appendix E. In addition, heater rod and housing wall thermocouples are placed at these pressure tap mid spans locations to determine convective and radiant heat transfer coefficients in the froth region where the differential pressure cells will give the average void fraction.

As described previously in Section 3.1, the flow housing has six pairs of windows at the following elevations: 61.39 cm (27.17 in), 113.58 cm (44.72 in),165.8 cm (65.27 in), 217.98 cm (85.82 in), 270.18 cm (106.37 in), and 322.4 cm (126.92 in). Each pair of windows is 180 degrees apart. The window lenses are made from optical grade fused quartz and provide a viewing area of about 10.16 cm (4 in) below and 15.24 cm (6 in) above grid numbers two tthrough seven. The

windows will be preheated to prevent wetting during the time when dispersed flow is occurring and LIDCS measurements are being made. The windows will be heated using infrared heaters on each window and by pulsing the heater rod bundle when preheating the flow housing walls. The infrared heaters will be removed just before a test is started. Two significant measurements above and below the grid can be made through the windows.

A droplet imaging system known as VisiSizer has been developed in conjunction with Oxford Lasers of Acton, Massachusetts, to measure the size and velocity of water droplets entrained in the steam flow of the RBHT test section shown schematically in Figure 4.14. VisiSizer uses a pulsed infrared laser to image water droplets on a 1000x1000 pixel high-resolution black and white digital camera through a set of windows in the bundle housing as shown in Figure 4.15. A digital system such as VisiSizer was chosen over conventional high-speed cameras because of issues with reliability and speed of data acquisition. A high-speed camera is capable of only a few seconds of imaging and is a tedious process that does not give instantaneous results. Each frame of a standard imaging technique would need to be analyzed by hand. The VisiSizer system is capable of analyzing 12 - 13 frames per second for an indefinite period of time. Film from the FLECHT-SEASET tests show much less image quality than images taken with VisiSizer in the experiments performed so far. However, VisiSizer is incapable of measuring anything other than complete droplets. This makes it an inadequate tool for gathering information about the entrainment front where there are ligaments and other unusual water behavior. Therefore, it is still a possibility that a high-speed camera will be used in tandem with VisiSizer for the RBHT tests.

An infrared laser is used with the system because it is capable of passing through the quartz viewing windows and being absorbed by the water droplets entrained in the steam flow. Because the infrared rays are absorbed by the water droplets, the resulting droplet shadows can be recorded by the digital camera. So far, there has been no effect of laser light scattering from rods to droplets. Pictures taken in and out of the rod bundle have the same imaging characteristics, droplet analyzing capability, and clarity. A band pass laser light filter is placed in front of the digital camera to eliminate non-infrared light from other sources and an anti-glare attachment is used to eliminate any illumination interference from outside the viewing area. In addition, rod bundle geometry has little effect in the measurement of droplet distributions and velocities.

The frames captured by the camera are fed back to a computer at approximately 12 - 13 frames per second. The software can analyze each frame for droplet size and velocity and write the recorded data to a size and velocity data array. The software program determines droplet sizes by determining the area of black vs. white pixels in each droplet image. Once the droplet area is determined, the program calculates the perimeter of the droplet image to determine the sphereosity of the droplet. The VisiSizer system is capable of determining the surface area based on diameter of any and all droplets. At any droplet concentration that is measurable with the system, an accurate measure of the total droplet surface area can be obtained. So far, number fluxes of up to six droplets per frame in velocity mode (12 droplet images) have been analyzed successfully with the droplets in a very narrow viewing area. There is the capability to increase this droplet number flux by several times using larger and multiple viewing areas.

Operating the laser in a double pulse mode enables the VisiSizer system to measure both droplet diameter and velocity for a particular probe volume. The laser pulses twice with a known pulse delay (on the order of one millisecond) while the camera shutter remains open, creating

two images in the same frame of each droplet. The distance between images is then determined and the velocity calculated. These velocity characteristics are enough to characterize the behavior of the flow despite the fact that the droplets are only captured in a single frame.

The local distribution of droplets will be determined for a known probe volume governed by the software settings. Droplets that lie out of this probe volume on either side of the line of sight will be rejected based on focus. The opposite sides of the probe volume will be set by the spacing of the rods in the bundle. Each droplet is recorded in a two-dimensional array according to size and velocity. The droplet sizes are recorded in log-normal bins while the velocity bin size is user defined. Data for the transient reflood experiments is recorded in user defined quasi-steady state time periods. At the end of each time period the data is saved and a new array is opened. Arrays characterized by similar droplets populations can then be combined for better statistical results.

The VisiSizer will enable the experimenters to collect a vast amount of information about the droplet flow in the test section. The information will be collected in an easy to handle data array and all information will be written to a CD-ROM to ensure the information will be available for later use.

The droplet injection system described in Section 3.11 has been constructed so that RBHT can collect steady-state information on droplet behavior. The injection system creates droplets of a known size and flow rate in the test section. The injection tubes are easily removed and replaced. This enables multiple injection sizes to be used as needed. The flow rate of the injection is controlled through a series of valves and flow meters. These factors should allow for the production of various droplet sizes. VisiSizer can study the droplet flow and distribution before a grid and then the system can be moved to image droplets immediately after the grid with the same conditions. In this way the effects of a spacer grid on the droplet diameter distribution can be determined.

The four corner support rods are unheated. They are used to support the bundle grids and to support grid and steam probes thermocouple leads going out of the bundle. These rods are instrumented with eight thermocouples attached at various elevations corresponding to heater rods and housing wall thermocouples. The purpose of this arrangement is to quantify radiation heat transfer losses to unheated surfaces and determine their behavior during reflood.

The DC power supply can be controlled by regulating the voltage, current, or total power output. The voltage drop across the heater rod bundle is measured by a voltmeter connected to voltage taps at the Low-Melt pot and the Nickel Ground Plate. The electrical current is measured by a copper shunt calibrated for 15,000 amps proportional to an output signal of 0-50 mV.

The Lower Plenum is instrumented with two fluid and two wall thermocouples. The fluid thermocouples monitor the injection water temperature prior and during testing. The wall thermocouples measure the vessel wall during heat-up and testing. One of the wall thermocouples in conjunction with a temperature controller regulates electrical power to clamp-on heater rods to maintain the vessel wall at inlet temperatures.

The Upper Plenum is also instrumented with two fluid thermocouples and two wall thermocouples. The fluid thermocouples measure steam and carryover liquid during testing.

The wall thermocouples monitor vessel wall temperatures during heat-up and testing. The Upper Plenum is also instrumented with a static pressure transmitter which measures and controls the test section pressure during testing.

4.3 Data Acquisition System

The control and data acquisition system provides control functions and data collection functions for the RBHT Test Facility. This system consists of two parts, the computer and display terminals residing in the control room, and the VXI mainframe and terminal panels residing in the test facility. The two parts are connected via an industry standard IEEE 1394 (Firewire) serial control and data interface.

The computer provides the display, control, and data storage functions. It has the capability of displaying control function setpoints and process variables, and critical operating parameters during tests, along with selected variables such as various rod temperatures displayed in real-time during the experiment. This system will provide dial, meter, and strip-chart functions as required. The computer collects and saves data from the various instruments, such as voltage, current, pressure, level, flow, and temperature. This provides control functions such as heater rod power, injection water pressure, upper and lower plenum temperature, etc.

The instrumentation part of this system, residing in the test facility, consists of an industry standard VXI mainframe (Vme bus with extensions for instrumentation) from Hewlett-Packard (HP E8401A), and a set of terminal panels (HP E1586A). The VXI mainframe contains a Firewire controller card (HP E8491A) and several (currently seven) state-of-the-art data acquisition and control cards (HP E1419A). The terminal panels provide the isothermal reference junctions needed for the thermocouples, as well as the voltage and current-loop input/output (I/O) interface to the RBHT facility. These terminal panels are connected to the HP E1419A cards with SCSI cables. Seven cards yield a capability of 448 I/0. The VXI mainframe can hold up to twelve cards, and the Firewire interface can support up to 16 mainframes. Each E1419A card can support up to eight signal conditioning plug-ons (scp's), conditioning eight channels each. Each E1509A scp contains low-pass anti-aliasing filters, fixed at 7 Hz. Because of this, the scan rate for each channel must be greater than or equal to the Nyquist rate of 14 Hz. The maximum a/d conversion rate on each HP E1419A card is nominally 100kHz, but is controlled to the rate the user requires. The seven cards can be synchronized to perform the scans simultaneously. The theoretical maximum scan rate for each channel (on any individual card) is 100,000/64 = 1,562.5 Hz, if all 64 channels are scanned. (Note that the actual scan rate would be less because of multiplexer switching, amplifier settling times due to gain changes, etc. There are different scp's available from HP providing different filter values to scan at these rates.) The normal data-scanning rate will be 2 Hz during the majority of the tests, but this rate can be increased to 10 Hz for specific times during testing.

An instrumentation error analysis showing the instrument uncertanity based essentially of FLECHT SEASET tests is given in Appendix F at the end of this report.

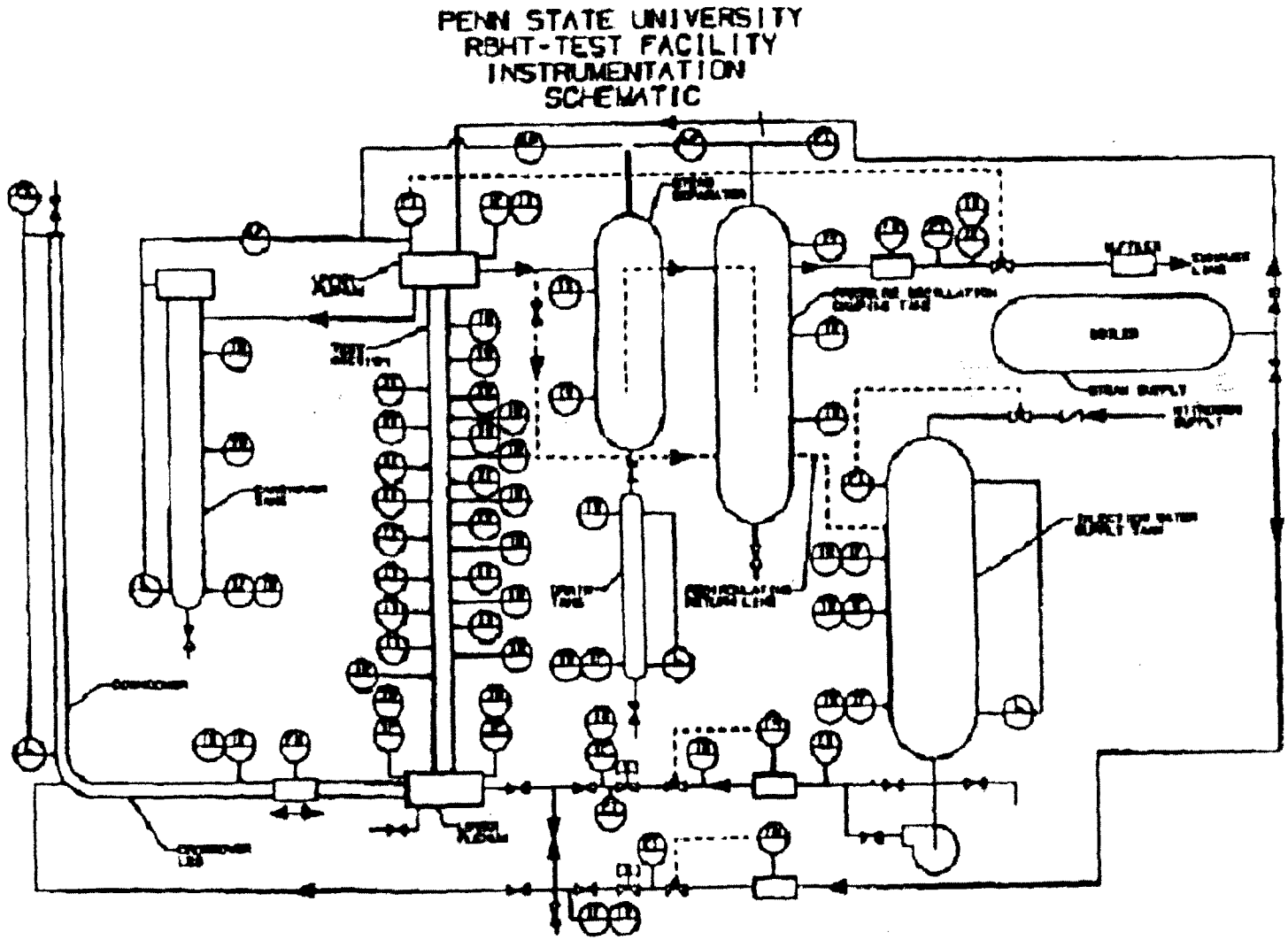

Figure 4.1 Loop Instrumentation Schematic.

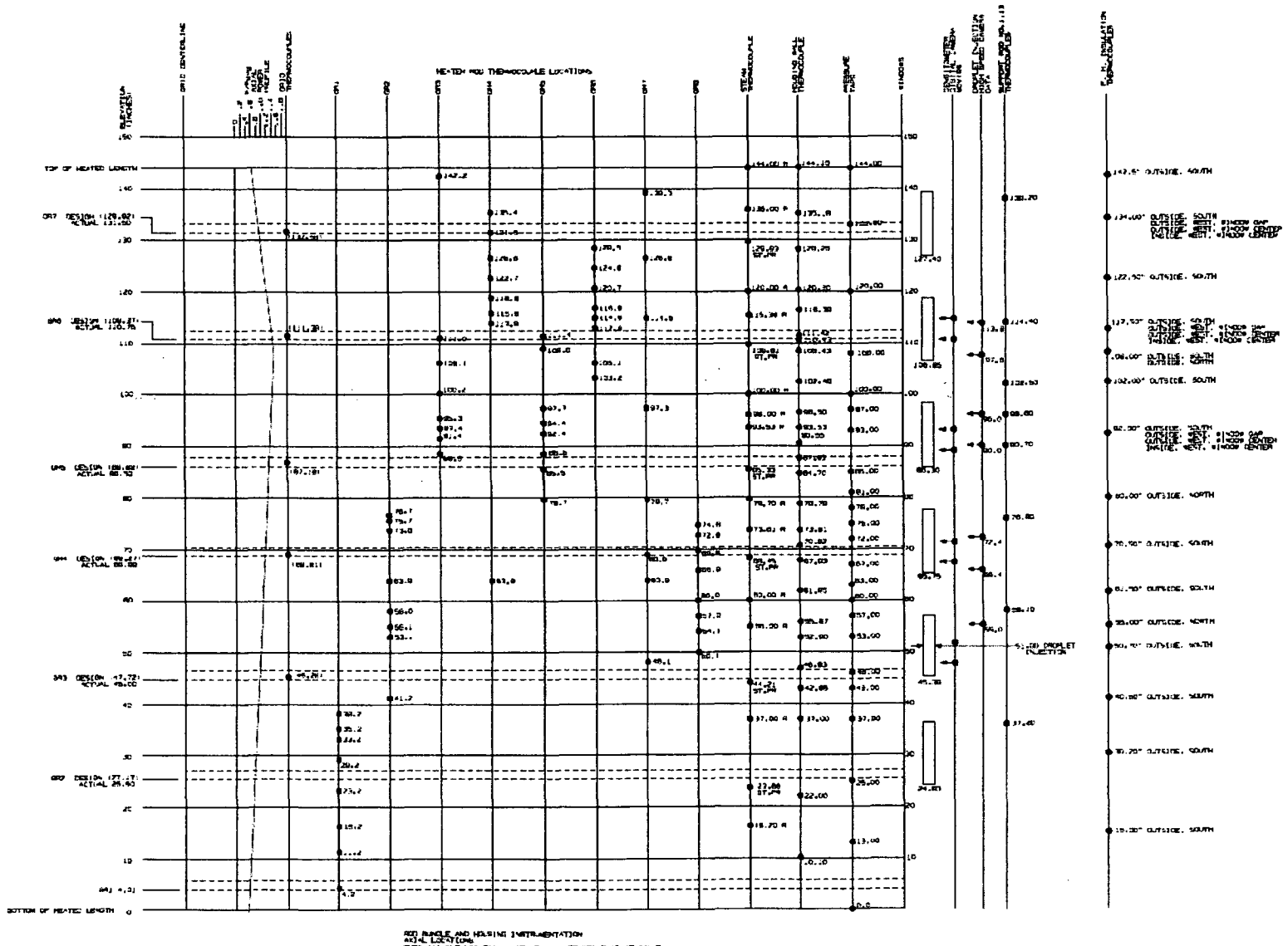

Figure 4.2 Rod Bundle and Housing Instrumentation Axial Locations.

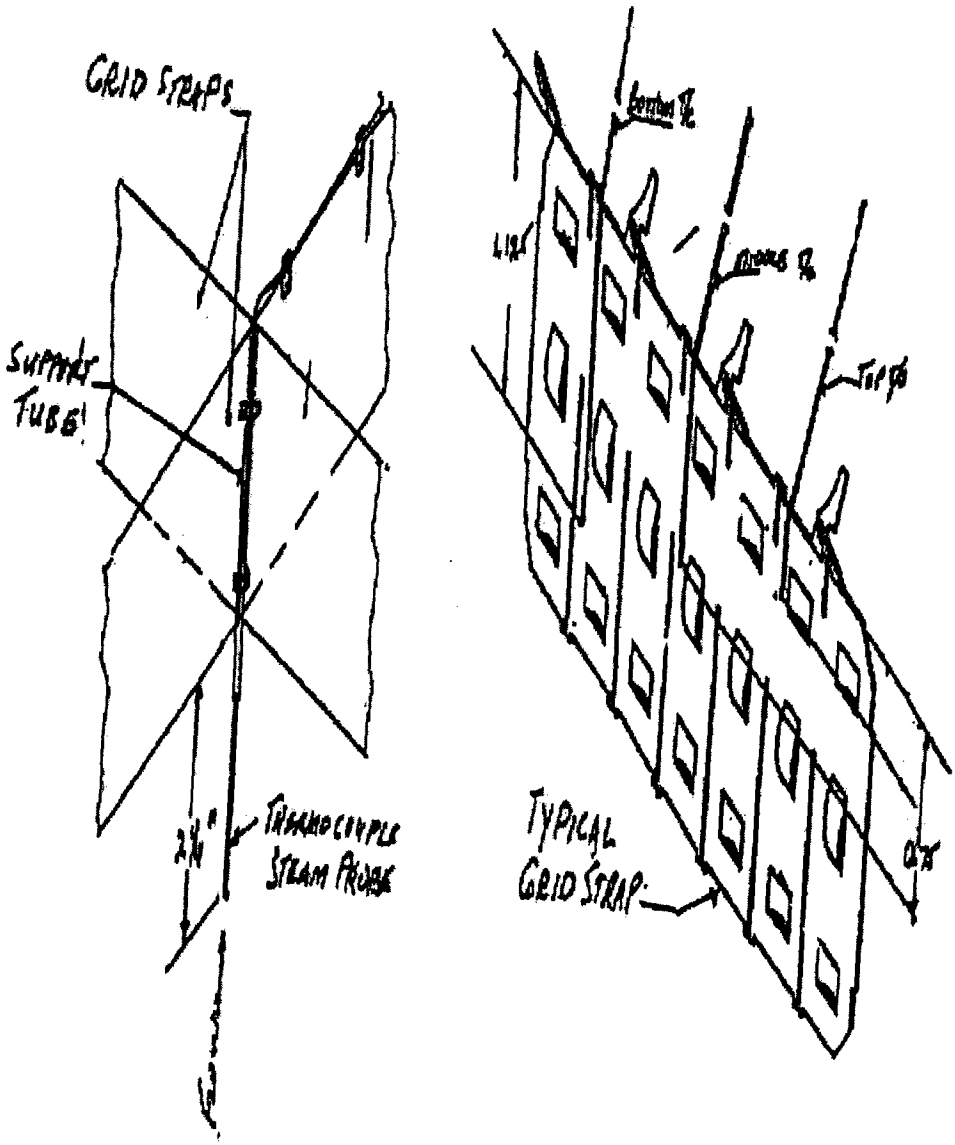

Figure 4.3 Mixing Vane Grid Instrumentation.

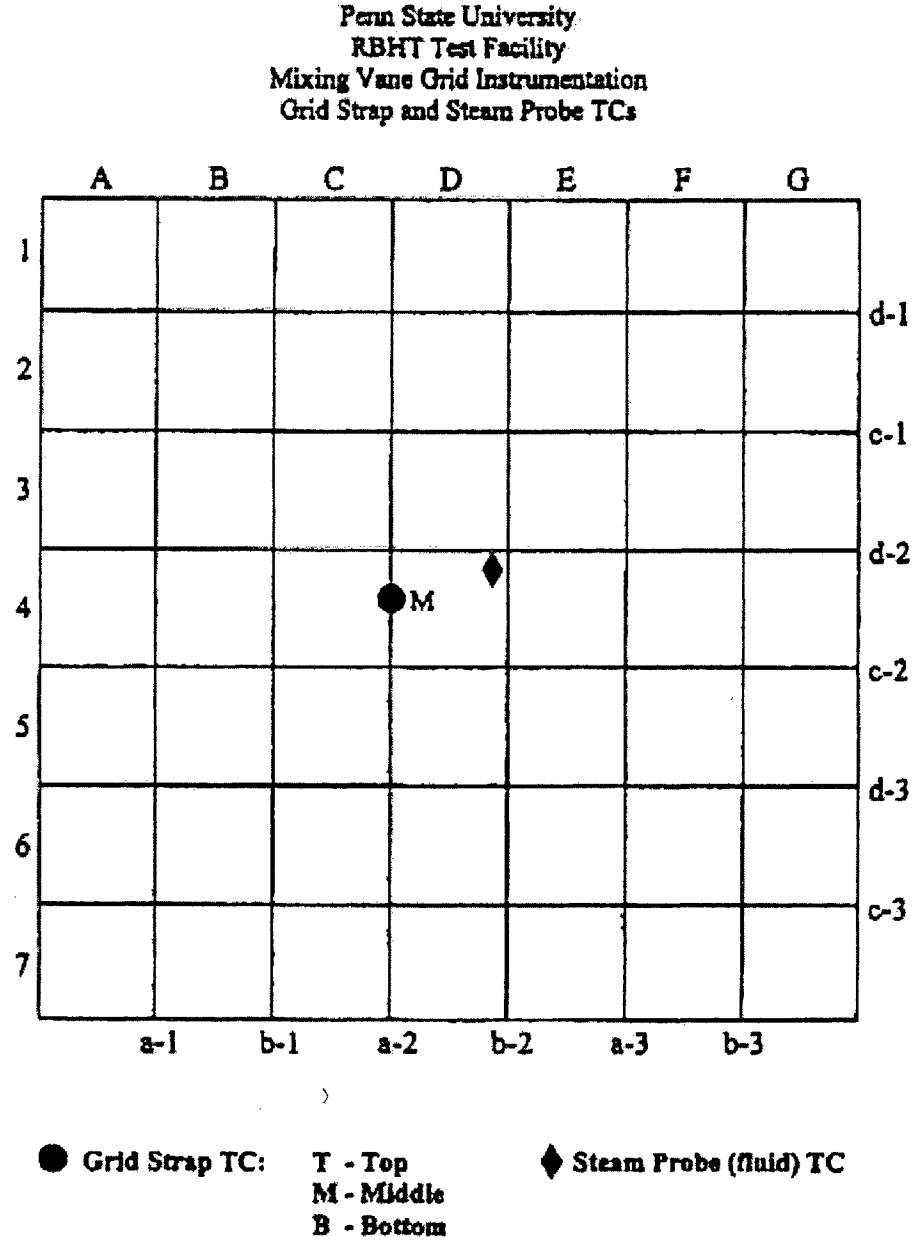

Figure 4.4 Grid No. 2 Instrumentation.

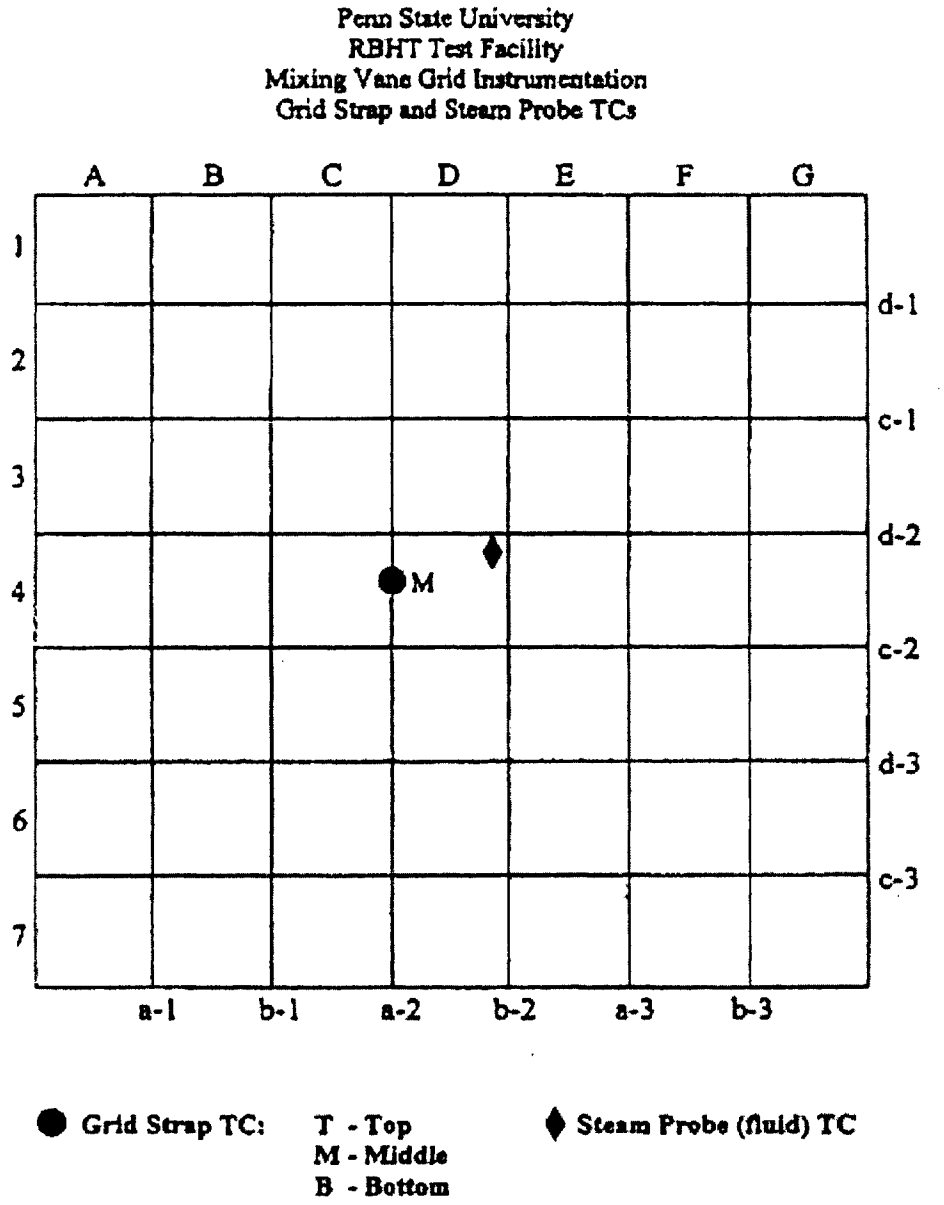

Figure 4.5 Grid No.3 Instrumentation.

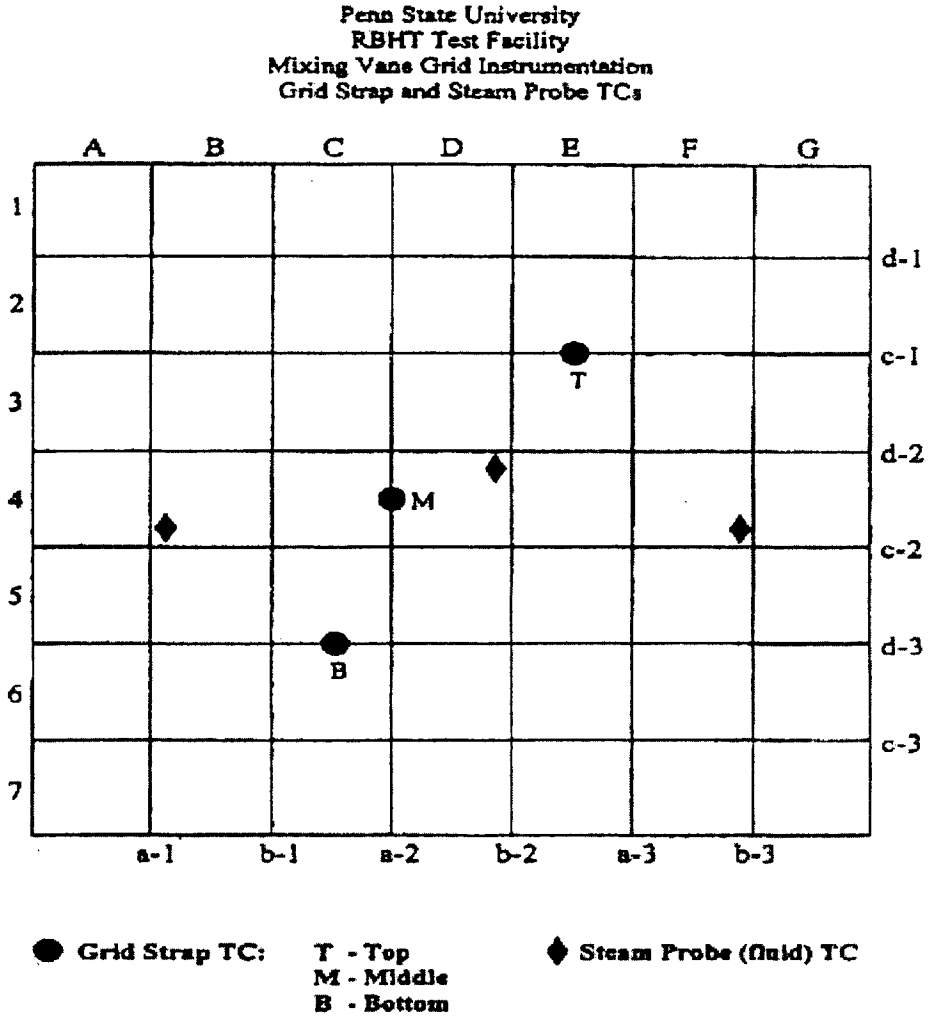

Figure 4.6 Grid No.4 Instrumentation.

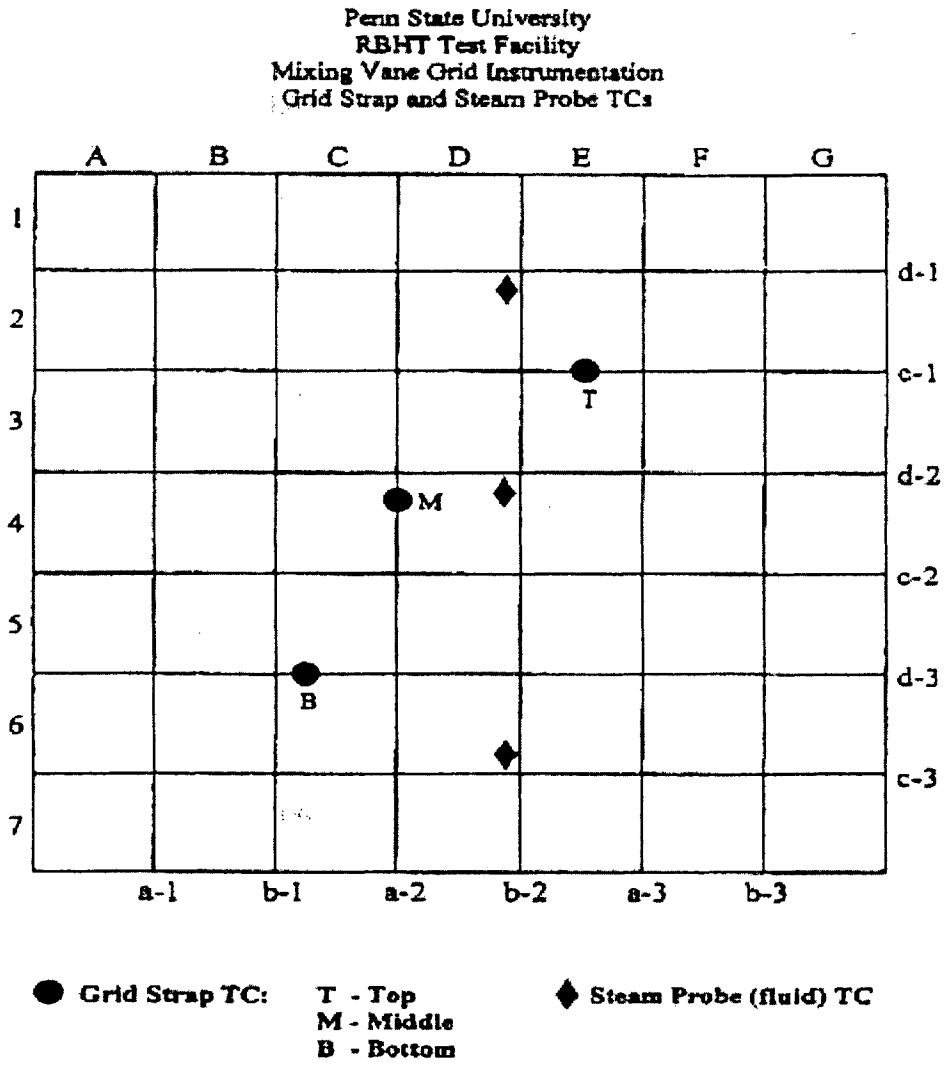

Figure 4.7 Grid No.5 Instrumentation.

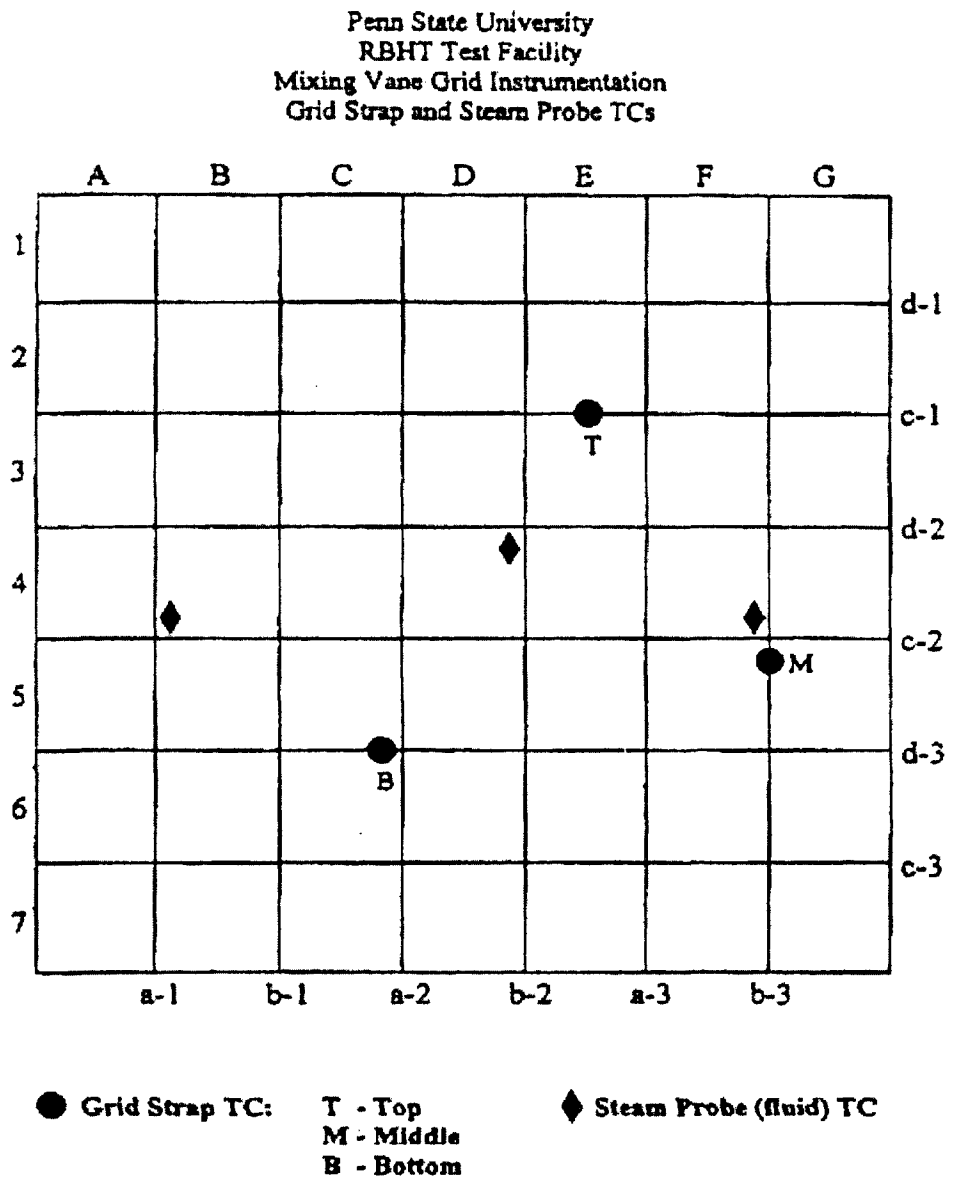

Figure 4.8 Grid No. 6 Instrumentation.

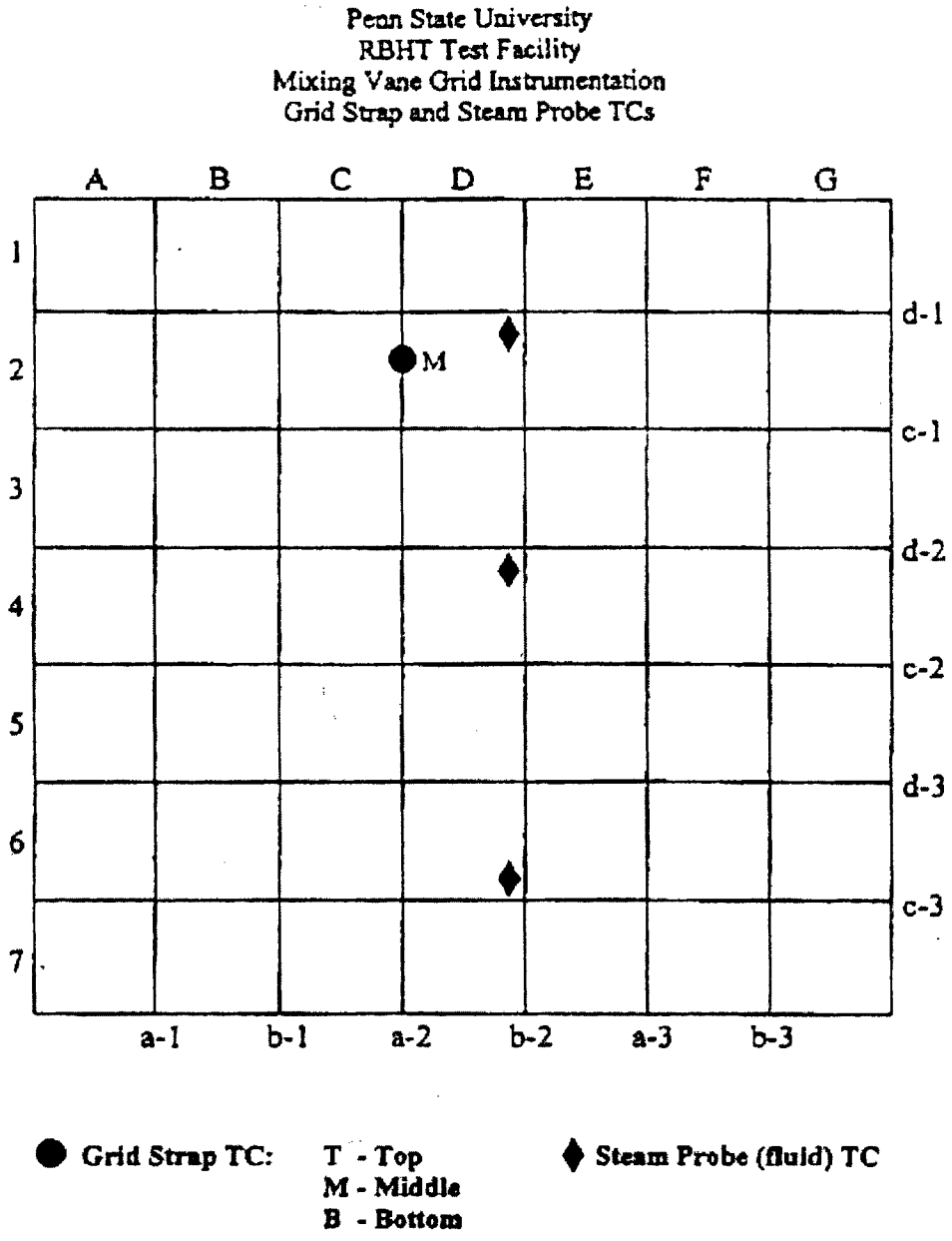

Figure 4.9 Grid No.7 Instrumentation.

PENN STATE UNIVERSITY
RBHT-TEST FACILITY
INSTRUMENTED HEATER ROD LOCATIONS

GROUP NO.	QUANTITY HEATER RODS
0	14
1	4
2	4
3	4
4	4
5	4
6	4
7	4
8	4
TOTAL:	45

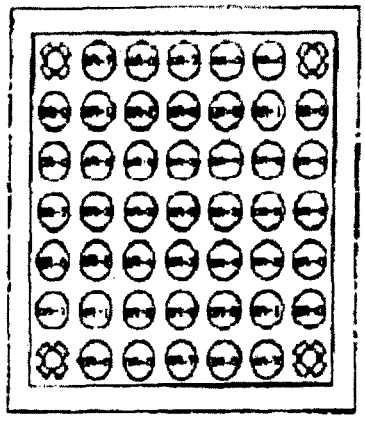

GR-0 UNINSTRUMENTED
GR-1 THRU 8 INSTRUMENTED

Figure 4.10 Instrumentation Heater Rod Radial Locations.

RBHT - Test Facility
Instrumented Heater Rod Locations

EAST

	A	B	C	D	E	F	G
1	A1 Gr-9	B1 Gr-7	C1 Gr-0	D1 Gr-7	E1 Gr-0	F1 Gr-9	G1
2	A2 Gr-0	B2 Gr-1	C2 Gr-2	D2 Gr-6	E2 Gr-8	F2 Gr-1	G2 Gr-0
3	A3 Gr-0	B3 Gr-8	C3 Gr-5	D3 Gr-3	E3 Gr-4	F3 Gr-8	G3 Gr-0
4	A4 Gr-7	B4 Gr-3	C4 Gr-3	D4 Gr-3	E4 Gr-3	F4 Gr-5	G4 Gr-0
5	A5 Gr 0	B5 Gr-2	C5 Gr-4	D5 Gr-8	E5 Gr-4	F5 Gr-2	G5 Gr-0
6	A6 Gr-7	B6 Gr-1	C6 Gr-2	D6 Gr-6	E6 Gr-8	F6 Gr-1	G6 Gr-0
7	A7	B7 Gr-0	C7 Gr-0	D7 Gr-7	E7 Gr-0	F7 Gr-7	G7 Gr-9

NORTH

SOUTH

WEST

Figure 4.11 Grid and Steam Probe Thermocouple Axial Location Schematic.

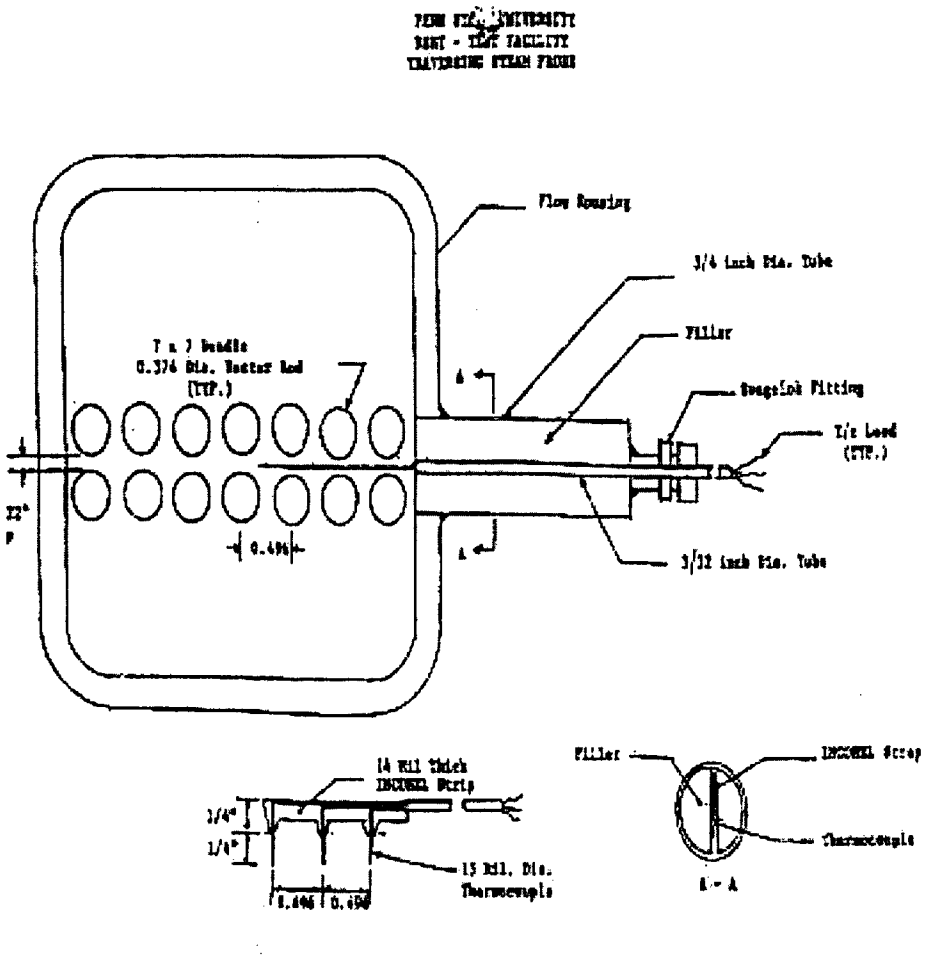

Figure 4.12 Traversing Steam Probe Rake Schematic.

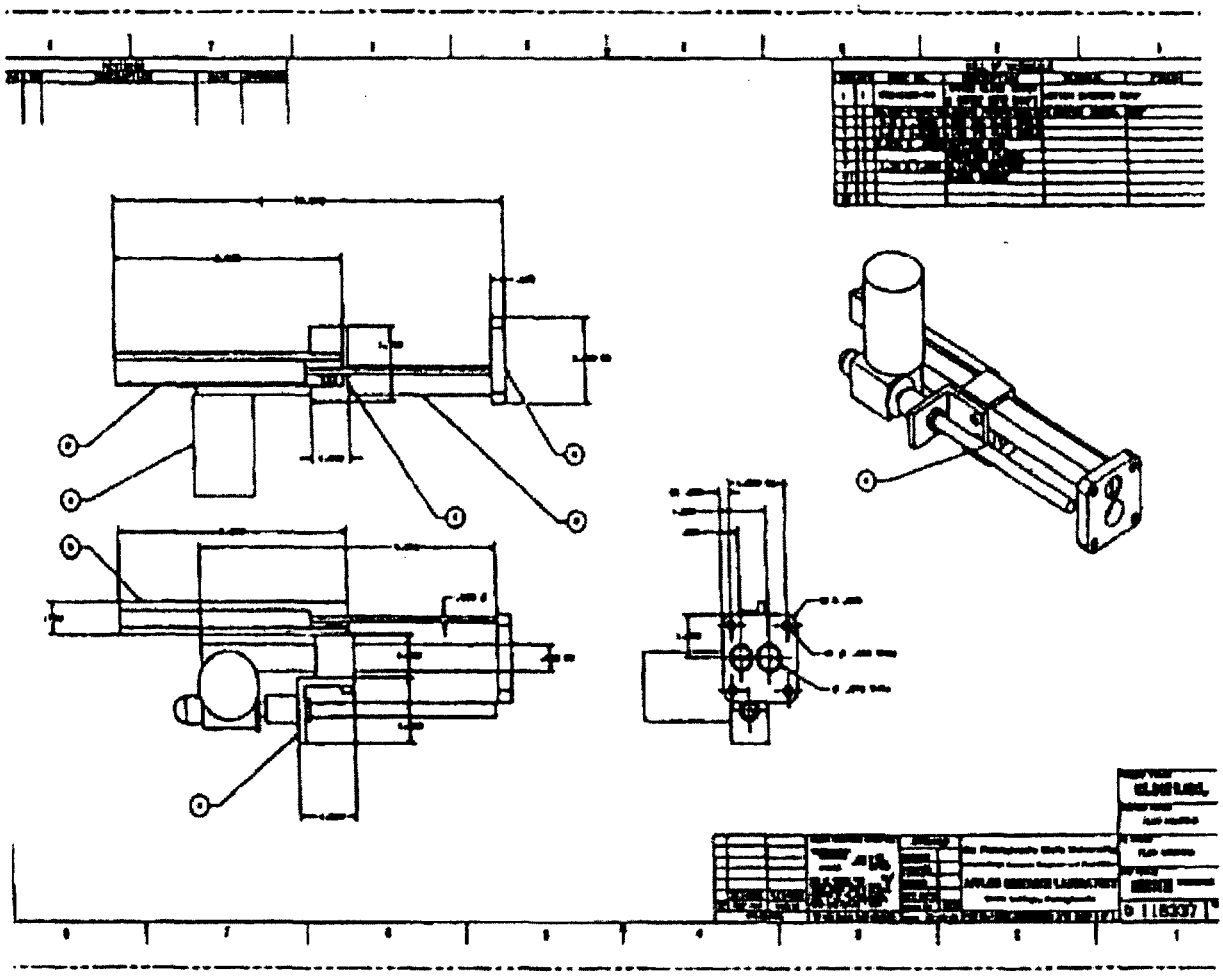

Figure 4.13 Steam Probe Rake Automatic Traversing Mechanism.

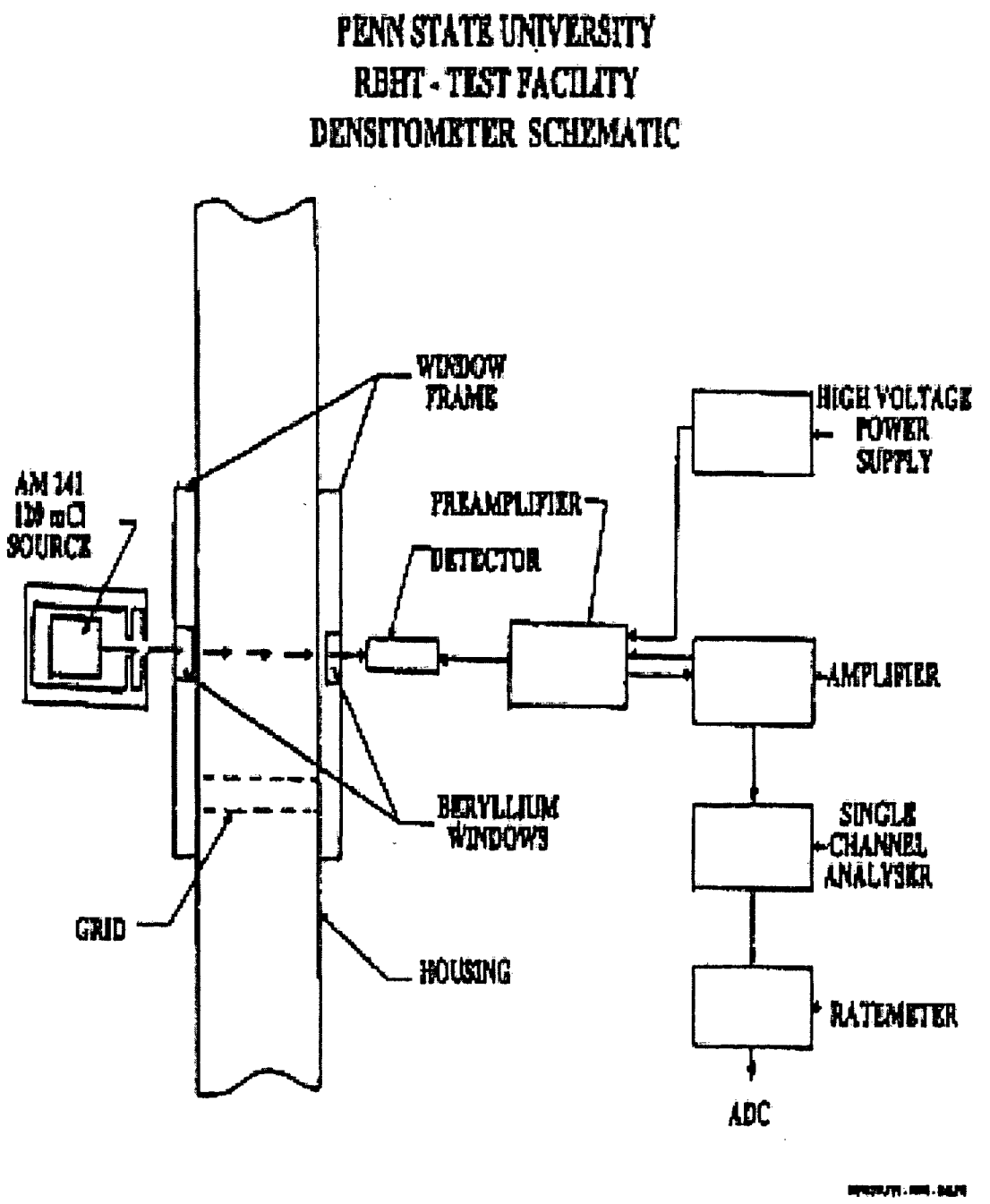

Figure 4.14 Densitometer Schematic.

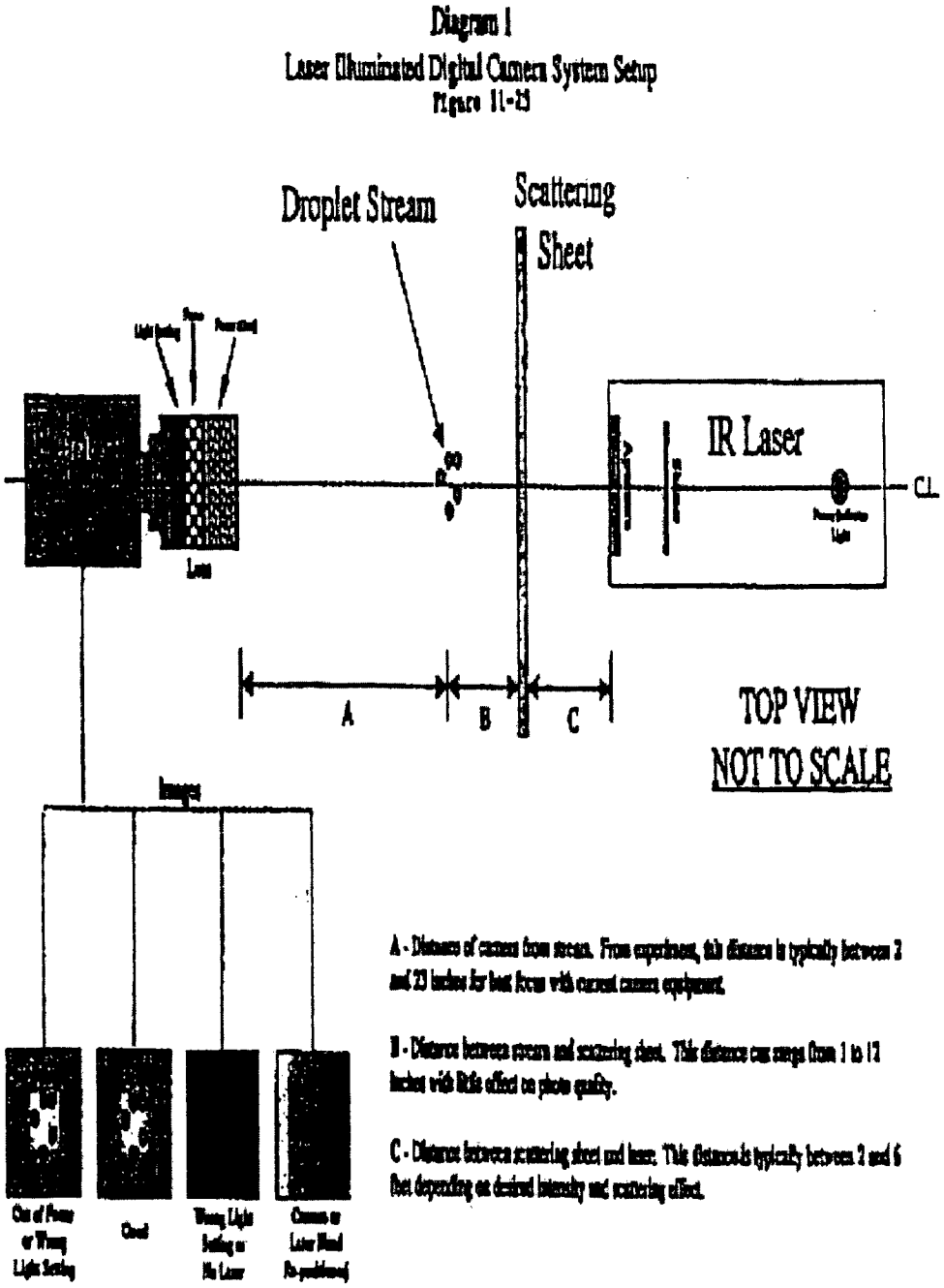

Figure 4.15 Laser Illuminated Digital Camera System.

Table 4.1 Instrumentation and Data Acquisition Channel List

NRC Table 4a, Version 7.0 ISM
Updated 4/19/02 3:22 PM
Printed 5/23/02 5:18 PM

Penn State University
RBHT - Test Facility
Instrumentation and Data Acquisition Channel List

Channel No.	Name	Location @ 295K	HR Name	Group No	Data Range (low)	Data Range (high)	Data Units	Vendor	Instrument
A1	Heater Rods								
1	HR_B1-47.9	1216.7	B1	7	283	1644	K	Stern Lab	TC Type K
2	HR_B1-83.8	1615.4	B1	7	283	1644	K	Stern Lab	TC Type K
3	HR_B1-88.8	1742.4	B1	7	283	1644	K	Stern Lab	TC Type K
4	HR_B1-79.7	2024.4	B1	7	283	1644	K	Stern Lab	TC Type K
5	HR_B1-97.1	2466.3	B1	7	283	1644	K	Stern Lab	TC Type K
6	HR_B1-114.8	2915.9	B1	7	283	1644	K	Stern Lab	TC Type K
7	HR_B1-126.7	3218.2	B1	7	283	1644	K	Stern Lab	TC Type K
8	HR_B1-139.4	3540.9	B1	7	283	1644	K	Stern Lab	TC Type K
9	HR_D1-47.9	1216.7	D1	7	283	1644	K	Stern Lab	TC Type K
10	HR_D1-83.8	1628.5	D1	7	283	1644	K	Stern Lab	TC Type K
11	HR_D1-88.8	1747.5	D1	7	283	1644	K	Stern Lab	TC Type K
12	HR_D1-79.9	2029.5	D1	7	283	1644	K	Stern Lab	TC Type K
13	HR_D1-97.3	2471.4	D1	7	283	1644	K	Stern Lab	TC Type K
14	HR_D1-115	2921.0	D1	7	283	1644	K	Stern Lab	TC Type K
15	HR_D1-126.8	3215.6	D1	7	283	1644	K	Stern Lab	TC Type K
16	HR_D1-139.4	3540.8	D1	7	283	1644	K	Stern Lab	TC Type K
17	HR_F7-47.9	1216.7	F7	7	283	1644	K	Stern Lab	TC Type K
18	HR_F7-83.8	1620.9	F7	7	283	1644	K	Stern Lab	TC Type K
19	HR_F7-88.8	1750.1	F7	7	283	1644	K	Stern Lab	TC Type K
20	HR_F7-79.9	2029.5	F7	7	283	1644	K	Stern Lab	TC Type K
21	HR_F7-97.2	2468.9	F7	7	283	1644	K	Stern Lab	TC Type K
22	HR_F7-114.9	2918.6	F7	7	283	1644	K	Stern Lab	TC Type K
23	HR_F7-126.8	3220.7	F7	7	283	1644	K	Stern Lab	TC Type K
24	HR_F7-139.4	3540.8	F7	7	283	1644	K	Stern Lab	TC Type K
25	HR_D7-47.9	1216.7	D7	7	283	1644	K	Stern Lab	TC Type K
26	HR_D7-83.8	1615.4	D7	7	283	1644	K	Stern Lab	TC Type K
27	HR_D7-88.8	1747.5	D7	7	283	1644	K	Stern Lab	TC Type K
28	HR_D7-79.8	2028.9	D7	7	283	1644	K	Stern Lab	TC Type K
29	HR_D7-97.1	2466.3	D7	7	283	1644	K	Stern Lab	TC Type K
30	HR_D7-114.8	2916.5	D7	7	283	1644	K	Stern Lab	TC Type K
31	HR_D7-126.7	3218.2	D7	7	283	1644	K	Stern Lab	TC Type K
32	HR_D7-139.4	3540.8	D7	7	283	1644	K	Stern Lab	TC Type K
311	HR_C7-112.8	2860.0	C7	6	283	1644	K	Stern Lab	TC Type K
312	HR_C7-116.8	2961.6	C7	6	283	1644	K	Stern Lab	TC Type K
313	HR_C7-124.4	3159.8	C7	6	283	1644	K	Stern Lab	TC Type K
228	HR_C7-128.4	3261.4	C7	6	283	1644	K	Stern Lab	TC Type K
33	HR_A8-47.7	1211.6	A8	7	283	1644	K	Stern Lab	TC Type K
34	HR_A8-83.8	1615.4	A8	7	283	1644	K	Stern Lab	TC Type K
35	HR_A8-88.5	1739.9	A8	7	283	1644	K	Stern Lab	TC Type K
36	HR_A8-79.8	2028.9	A8	7	283	1644	K	Stern Lab	TC Type K
37	HR_A8-97.4	2474.0	A8	7	283	1644	K	Stern Lab	TC Type K
38	HR_A8-115.1	2921.5	A8	7	283	1644	K	Stern Lab	TC Type K
39	HR_A8-126.8	3215.6	A8	7	283	1644	K	Stern Lab	TC Type K
40	HR_A8-139.8	3553.3	A8	7	283	1644	K	Stern Lab	TC Type K
41	HR_A4-48	1219.2	A4	7	283	1644	K	Stern Lab	TC Type K
42	HR_A4-83.8	1620.5	A4	7	283	1644	K	Stern Lab	TC Type K
43	HR_A4-88.8	1747.5	A4	7	283	1644	K	Stern Lab	TC Type K
44	HR_A4-79.9	2029.5	A4	7	283	1644	K	Stern Lab	TC Type K
45	HR_A4-97.1	2466.3	A4	7	283	1644	K	Stern Lab	TC Type K
46	HR_A4-115	2921.0	A4	7	283	1644	K	Stern Lab	TC Type K
47	HR_A4-126.8	3220.7	A4	7	283	1644	K	Stern Lab	TC Type K
48	HR_A4-139.4	3540.8	A4	7	283	1644	K	Stern Lab	TC Type K
49	HR_B2-4.1	104.1	B2	1	283	1644	K	Stern Lab	TC Type K
50	HR_B2-11.2	284.5	B2	1	283	1644	K	Stern Lab	TC Type K
51	HR_B2-16.2	411.5	B2	1	283	1644	K	Stern Lab	TC Type K
52	HR_B2-23.3	591.8	B2	1	283	1644	K	Stern Lab	TC Type K
53	HR_B2-29.3	744.2	B2	1	283	1644	K	Stern Lab	TC Type K
54	HR_B2-33.3	845.8	B2	1	283	1644	K	Stern Lab	TC Type K
55	HR_B2-35.3	896.6	B2	1	283	1644	K	Stern Lab	TC Type K
56	HR_B2-38.4	975.4	B2	1	283	1644	K	Stern Lab	TC Type K

Table 4.1 Instrumentation and Data Acquisition Channel List (Continued)

57	HR_C2-41	1041.4	C2	2	283	1644	K	Stern Lab	TC Type K
58	HR_C2-53.1	1348.7	C2	2	283	1644	K	Stern Lab	TC Type K
59	HR_C2-55	1397.0	C2	2	283	1644	K	Stern Lab	TC Type K
60	HR_C2-57.8	1468.1	C2	2	283	1644	K	Stern Lab	TC Type K
61	HR_C2-63.9	1623.1	C2	2	283	1644	K	Stern Lab	TC Type K
62	HR_C2-73.8	1874.5	C2	2	283	1644	K	Stern Lab	TC Type K
63	HR_C2-75.8	1925.3	C2	2	283	1644	K	Stern Lab	TC Type K
64	HR_C2-76.8	1950.7	C2	2	283	1644	K	Stern Lab	TC Type K
65	HR_D2-103.2	2621.3	D2	6	283	1644	K	Stern Lab	TC Type K
66	HR_D2-106	2692.4	D2	6	283	1644	K	Stern Lab	TC Type K
67	HR_D2-112.8	2860.0	D2	6	283	1644	K	Stern Lab	TC Type K
68	HR_D2-114.9	2918.5	D2	6	283	1644	K	Stern Lab	TC Type K
69	HR_D2-117.4	2982.0	D2	6	283	1644	K	Stern Lab	TC Type K
70	HR_D2-120.8	3068.3	D2	6	283	1644	K	Stern Lab	TC Type K
71	HR_D2-124.8	3169.9	D2	6	283	1644	K	Stern Lab	TC Type K
72	HR_D2-126.8	3268.4	D2	6	283	1644	K	Stern Lab	TC Type K
73	HR_E2-50.1	1272.5	E2	8	283	1644	K	Stern Lab	TC Type K
74	HR_E2-54	1371.6	E2	8	283	1644	K	Stern Lab	TC Type K
75	HR_E2-56.9	1445.3	E2	8	283	1644	K	Stern Lab	TC Type K
76	HR_E2-59.9	1521.5	E2	8	283	1644	K	Stern Lab	TC Type K
77	HR_E2-66	1676.4	E2	8	283	1644	K	Stern Lab	TC Type K
78	HR_E2-69.8	1772.9	E2	8	283	1644	K	Stern Lab	TC Type K
79	HR_E2-72.9	1851.7	E2	8	283	1644	K	Stern Lab	TC Type K
80	HR_E2-74.9	1902.5	E2	8	283	1644	K	Stern Lab	TC Type K
81	HR_F2-4.1	104.1	F2	1	283	1644	K	Stern Lab	TC Type K
82	HR_F2-11.2	284.5	F2	1	283	1644	K	Stern Lab	TC Type K
83	HR_F2-16.2	411.5	F2	1	283	1644	K	Stern Lab	TC Type K
84	HR_F2-23.3	591.8	F2	1	283	1644	K	Stern Lab	TC Type K
85	HR_F2-29.2	741.7	F2	1	283	1644	K	Stern Lab	TC Type K
86	HR_F2-33.3	845.8	F2	1	283	1644	K	Stern Lab	TC Type K
87	HR_F2-35.3	896.6	F2	1	283	1644	K	Stern Lab	TC Type K
88	HR_F2-38.3	972.8	F2	1	283	1644	K	Stern Lab	TC Type K
89	HR_F3-50.1	1272.5	F3	8	283	1644	K	Stern Lab	TC Type K
90	HR_F3-54	1371.6	F3	8	283	1644	K	Stern Lab	TC Type K
91	HR_F3-57	1447.8	F3	8	283	1644	K	Stern Lab	TC Type K
92	HR_F3-60	1524.0	F3	8	283	1644	K	Stern Lab	TC Type K
93	HR_F3-66.1	1678.9	F3	8	283	1644	K	Stern Lab	TC Type K
94	HR_F3-70	1778.0	F3	8	283	1644	K	Stern Lab	TC Type K
95	HR_F3-73	1854.2	F3	8	283	1644	K	Stern Lab	TC Type K
96	HR_F3-75	1905.0	F3	8	283	1644	K	Stern Lab	TC Type K
98	HR_F4-85.8	2174.2	F4	5	283	1644	K	Stern Lab	TC Type K
99	HR_F4-88.4	2245.4	F4	5	283	1644	K	Stern Lab	TC Type K
100	HR_F4-92.4	2347.0	F4	5	283	1644	K	Stern Lab	TC Type K
101	HR_F4-94.3	2395.2	F4	5	283	1644	K	Stern Lab	TC Type K
102	HR_F4-97.2	2468.9	F4	5	283	1644	K	Stern Lab	TC Type K
103	HR_F4-108.8	2763.5	F4	5	283	1644	K	Stern Lab	TC Type K
104	HR_F4-111	2818.4	F4	5	283	1644	K	Stern Lab	TC Type K
105	HR_F5-41	1041.4	F5	2	283	1644	K	Stern Lab	TC Type K
106	HR_F5-53.1	1348.7	F5	2	283	1644	K	Stern Lab	TC Type K
107	HR_F5-55	1397.0	F5	2	283	1644	K	Stern Lab	TC Type K
108	HR_F5-57.8	1468.1	F5	2	283	1644	K	Stern Lab	TC Type K
109	HR_F5-64	1625.6	F5	2	283	1644	K	Stern Lab	TC Type K
110	HR_F5-73.8	1874.5	F5	2	283	1644	K	Stern Lab	TC Type K
111	HR_F5-75.8	1925.3	F5	2	283	1644	K	Stern Lab	TC Type K
112	HR_F5-76.8	1950.7	F5	2	283	1644	K	Stern Lab	TC Type K
113	HR_F6-4.1	104.1	F6	1	283	1644	K	Stern Lab	TC Type K
114	HR_F6-11.2	284.5	F6	1	283	1644	K	Stern Lab	TC Type K
115	HR_F6-16.3	414.0	F6	1	283	1644	K	Stern Lab	TC Type K
116	HR_F6-23.3	591.8	F6	1	283	1644	K	Stern Lab	TC Type K
117	HR_F6-29.3	744.2	F6	1	283	1644	K	Stern Lab	TC Type K
118	HR_F6-33.3	845.8	F6	1	283	1644	K	Stern Lab	TC Type K
119	HR_F6-35.3	896.6	F6	1	283	1644	K	Stern Lab	TC Type K
120	HR_F6-38.3	972.8	F6	1	283	1644	K	Stern Lab	TC Type K

Table 4.1 Instrumentation and Data Acquisition Channel List (Continued)

121	HR_E6-50.2	1275.1	E6	8	283	1644	K	Stern Lab	TC Type K
122	HR_E6-54.1	1374.1	E6	8	283	1644	K	Stern Lab	TC Type K
123	HR_E6-57	1447.8	E6	8	283	1644	K	Stern Lab	TC Type K
124	HR_E6-60.2	1529.1	E6	8	283	1644	K	Stern Lab	TC Type K
125	HR_E6-66.1	1678.9	E6	8	283	1644	K	Stern Lab	TC Type K
126	HR_E6-70	1778.0	E6	8	283	1644	K	Stern Lab	TC Type K
127	HR_E6-73.1	1856.7	E6	8	283	1644	K	Stern Lab	TC Type K
128	HR_E6-75	1905.0	E6	8	283	1644	K	Stern Lab	TC Type K
129	HR_D6-103.1	2618.7	D6	6	283	1644	K	Stern Lab	TC Type K
130	HR_D6-106	2692.4	D6	6	283	1644	K	Stern Lab	TC Type K
131	HR_D6-112.9	2867.7	D6	6	283	1644	K	Stern Lab	TC Type K
132	HR_D6-114.9	2918.5	D6	6	283	1644	K	Stern Lab	TC Type K
133	HR_D6-116.8	2966.7	D6	6	283	1644	K	Stern Lab	TC Type K
134	HR_D6-120.8	3070.9	D6	6	283	1644	K	Stern Lab	TC Type K
135	HR_D6-124.8	3169.9	D6	6	283	1644	K	Stern Lab	TC Type K
136	HR_D6-128.7	3269.0	D6	6	283	1644	K	Stern Lab	TC Type K
137	HR_C6-40.9	1038.9	C6	2	283	1644	K	Stern Lab	TC Type K
138	HR_C6-52.8	1341.1	C6	2	283	1644	K	Stern Lab	TC Type K
139	HR_C6-54.8	1391.9	C6	2	283	1644	K	Stern Lab	TC Type K
140	HR_C6-57.8	1466.1	C6	2	283	1644	K	Stern Lab	TC Type K
141	HR_C6-63.8	1620.5	C6	2	283	1644	K	Stern Lab	TC Type K
142	HR_C6-73.7	1872.0	C6	2	283	1644	K	Stern Lab	TC Type K
143	HR_C6-75.8	1925.3	C6	2	283	1644	K	Stern Lab	TC Type K
144	HR_C6-76.8	1950.7	C6	2	283	1644	K	Stern Lab	TC Type K
145	HR_B6-4.1	104.1	B6	1	283	1644	K	Stern Lab	TC Type K
146	HR_B6-11.2	284.5	B6	1	283	1644	K	Stern Lab	TC Type K
147	HR_B6-16.2	411.5	B6	1	283	1644	K	Stern Lab	TC Type K
148	HR_B6-23.3	591.8	B6	1	283	1644	K	Stern Lab	TC Type K
149	HR_B6-29.3	744.2	B6	1	283	1644	K	Stern Lab	TC Type K
150	HR_B6-33.3	845.8	B6	1	283	1644	K	Stern Lab	TC Type K
151	HR_B6-35.3	896.6	B6	1	283	1644	K	Stern Lab	TC Type K
152	HR_B6-39.4	975.4	B6	1	283	1644	K	Stern Lab	TC Type K
153	HR_B5-41	1041.4	B5	2	283	1644	K	Stern Lab	TC Type K
154	HR_B5-52.9	1343.7	B5	2	283	1644	K	Stern Lab	TC Type K
155	HR_B5-55	1397.0	B5	2	283	1644	K	Stern Lab	TC Type K
156	HR_B5-57.8	1468.1	B5	2	283	1644	K	Stern Lab	TC Type K
157	HR_B5-64	1625.6	B5	2	283	1644	K	Stern Lab	TC Type K
158	HR_B5-73.9	1877.1	B5	2	283	1644	K	Stern Lab	TC Type K
159	HR_B5-75.9	1927.9	B5	2	283	1644	K	Stern Lab	TC Type K
160	HR_B5-76.9	1953.3	B5	2	283	1644	K	Stern Lab	TC Type K
161	HR_B4-88.4	2245.4	B4	3	283	1644	K	Stern Lab	TC Type K
162	HR_B4-91.3	2319.0	B4	3	283	1644	K	Stern Lab	TC Type K
163	HR_B4-93.3	2369.8	B4	3	283	1644	K	Stern Lab	TC Type K
164	HR_B4-95.1	2415.5	B4	3	283	1644	K	Stern Lab	TC Type K
165	HR_B4-100	2540.0	B4	3	283	1644	K	Stern Lab	TC Type K
166	HR_B4-106	2692.4	B4	3	283	1644	K	Stern Lab	TC Type K
167	HR_B4-109.9	2791.5	B4	3	283	1644	K	Stern Lab	TC Type K
168	HR_B4-142.3	3614.4	B4	3	283	1644	K	Stern Lab	TC Type K
169	HR_B3-50.2	1275.1	B3	8	283	1644	K	Stern Lab	TC Type K
170	HR_B3-54.1	1374.1	B3	8	283	1644	K	Stern Lab	TC Type K
171	HR_B3-56.9	1445.3	B3	8	283	1644	K	Stern Lab	TC Type K
172	HR_B3-60.1	1526.5	B3	8	283	1644	K	Stern Lab	TC Type K
173	HR_B3-66.1	1678.9	B3	8	283	1644	K	Stern Lab	TC Type K
174	HR_B3-69.9	1775.5	B3	8	283	1644	K	Stern Lab	TC Type K
175	HR_B3-73	1854.2	B3	8	283	1644	K	Stern Lab	TC Type K
176	HR_B3-75	1905.0	B3	8	283	1644	K	Stern Lab	TC Type K
177	HR_C3-79.8	2026.9	C3	5	283	1644	K	Stern Lab	TC**Type K
178	HR_C3-85.6	2174.2	C3	5	283	1644	K	Stern Lab	TC Type K
179	HR_C3-88.5	2247.9	C3	5	283	1644	K	Stern Lab	TC Type K
180	HR_C3-92.4	2347.0	C3	5	283	1644	K	Stern Lab	TC**Type K
181	HR_C3-94.4	2397.8	C3	5	283	1644	K	Stern Lab	TC**Type K
182	HR_C3-97.2	2469.9	C3	5	283	1644	K	Stern Lab	TC**Type K
183	HR_C3-108.8	2763.5	C3	5	283	1644	K	Stern Lab	TC**Type K

Table 4.1 Instrumentation and Data Acquisition Channel List (Continued)

NRC Table.xls, Version 7.0, ISM
Updated 4/19/02 3:22 PM
Printed 5/23/02 5:18 PM

Penn State University
RBHT - Test Facility
Instrumentation and Data Acquisition Channel List

185	HR_D3-88.3	2242.8	D3	3	283	1644	K	Stern Lab	TC Type K
186	HR_D3-91.3	2319.0	D3	3	283	1644	K	Stern Lab	TC Type K
187	HR_D3-93.1	2364.7	D3	3	283	1644	K	Stern Lab	TC Type K
188	HR_D3-95.3	2420.6	D3	3	283	1644	K	Stern Lab	TC Type K
189	HR_D3-100.1	2542.5	D3	3	283	1644	K	Stern Lab	TC Type K
190	HR_D3-106.1	2694.9	D3	3	283	1644	K	Stern Lab	TC Type K
191	HR_D3-110	2794.0	D3	3	283	1644	K	Stern Lab	TC Type K
192	HR_D3-142.1	3609.3	D3	3	283	1644	K	Stern Lab	TC Type K
193	HR_E3-83.4	1810.4	E3	4	283	1644	K	Stern Lab	TC Type K
194	HR_E3-113.6	2885.4	E3	4	283	1644	K	Stern Lab	TC Type K
195	HR_E3-115.5	2933.7	E3	4	283	1644	K	Stern Lab	TC Type K
196	HR_E3-118.5	3009.9	E3	4	283	1644	K	Stern Lab	TC Type K
197	HR_E3-122.7	3116.6	E3	4	283	1644	K	Stern Lab	TC Type K
198	HR_E3-126.5	3213.1	E3	4	283	1644	K	Stern Lab	TC Type K
199	HR_E3-131.7	3345.2	E3	4	283	1644	K	Stern Lab	TC Type K
200	HR_E3-135.6	3444.2	E3	4	283	1644	K	Stern Lab	TC Type K
201	HR_E4-88.4	2245.4	E4	3	283	1644	K	Stern Lab	TC Type K
202	HR_E4-91.2	2316.5	E4	3	283	1644	K	Stern Lab	TC Type K
203	HR_E4-93.2	2367.3	E4	3	283	1644	K	Stern Lab	TC Type K
204	HR_E4-95.3	2420.6	E4	3	283	1644	K	Stern Lab	TC Type K
205	HR_E4-100.9	2562.9	E4	3	283	1644	K	Stern Lab	TC Type K
206	HR_E4-106.1	2694.9	E4	3	283	1644	K	Stern Lab	TC Type K
207	HR_E4-110	2794.0	E4	3	283	1644	K	Stern Lab	TC Type K
208	HR_E4-142.3	3614.4	E4	3	283	1644	K	Stern Lab	TC Type K
209	HR_E5-83.6	1615.4	E5	4	283	1644	K	Stern Lab	TC Type K
210	HR_E5-113.6	2885.4	E5	4	283	1644	K	Stern Lab	TC Type K
211	HR_E5-115.4	2931.2	E5	4	283	1644	K	Stern Lab	TC Type K
212	HR_E5-118.7	3015.0	E5	4	283	1644	K	Stern Lab	TC Type K
213	HR_E5-122.6	3114.0	E5	4	283	1644	K	Stern Lab	TC Type K
214	HR_E5-126.6	3215.6	E5	4	283	1644	K	Stern Lab	TC Type K
215	HR_E5-131.6	3342.6	E5	4	283	1644	K	Stern Lab	TC Type K
216	HR_E5-135.6	3444.2	E5	4	283	1644	K	Stern Lab	TC Type K
217	HR_D5-50	1270.0	D5	8	283	1644	K	Stern Lab	TC Type K
218	HR_D5-54.1	1374.1	D5	8	283	1644	K	Stern Lab	TC Type K
219	HR_D5-56.9	1445.3	D5	8	283	1644	K	Stern Lab	TC Type K
220	HR_D5-60	1524.0	D5	8	283	1644	K	Stern Lab	TC Type K
221	HR_D5-66.1	1678.9	D5	8	283	1644	K	Stern Lab	TC Type K
222	HR_D5-69.9	1775.5	D5	8	283	1644	K	Stern Lab	TC Type K
223	HR_D5-72.9	1851.7	D5	8	283	1644	K	Stern Lab	TC Type K
224	HR_D5-74.9	1902.5	D5	8	283	1644	K	Stern Lab	TC Type K
225	HR_C5-63.7	1618.0	C5	4	283	1644	K	Stern Lab	TC Type K
226	HR_C5-113.6	2885.4	C5	4	283	1644	K	Stern Lab	TC Type K
227	HR_C5-115.7	2938.8	C5	4	283	1644	K	Stern Lab	TC Type K
228	HR_C5-122.7	3116.6	C5	4	283	1644	K	Stern Lab	TC Type K
230	HR_C5-126.7	3218.2	C5	4	283	1644	K	Stern Lab	TC Type K
231	HR_C5-131.6	3342.6	C5	4	283	1644	K	Stern Lab	TC Type K
232	HR_C5-135.7	3446.8	C5	4	283	1644	K	Stern Lab	TC Type K
233	HR_C4-88.4	2245.4	C4	3	283	1644	K	Stern Lab	TC Type K
234	HR_C4-91.1	2313.9	C4	3	283	1644	K	Stern Lab	TC Type K
235	HR_C4-93.4	2372.4	C4	3	283	1644	K	Stern Lab	TC Type K
236	HR_C4-95.3	2420.6	C4	3	283	1644	K	Stern Lab	TC Type K
237	HR_C4-100.1	2542.5	C4	3	283	1644	K	Stern Lab	TC Type K
238	HR_C4-106.1	2694.9	C4	3	283	1644	K	Stern Lab	TC Type K
239	HR_C4-110	2794.0	C4	3	283	1644	K	Stern Lab	TC Type K
240	HR_C4-142.2	3611.9	C4	3	283	1644	K	Stern Lab	TC Type K
241	HR_D4-88.3	2242.8	D4	3	283	1644	K	Stern Lab	TC Type K
242	HR_D4-91.3	2319.0	D4	3	283	1644	K	Stern Lab	TC Type K
243	HR_D4-93.2	2367.3	D4	3	283	1644	K	Stern Lab	TC Type K
244	HR_D4-95.2	2418.1	D4	3	283	1644	K	Stern Lab	TC Type K
245	HR_D4-100.1	2542.5	D4	3	283	1644	K	Stern Lab	TC Type K
246	HR_D4-106.1	2694.9	D4	3	283	1644	K	Stern Lab	TC Type K
247	HR_D4-110	2794.0	D4	3	283	1644	K	Stern Lab	TC Type K
248	HR_D4-142.1	3609.3	D4	3	283	1644	K	Stern Lab	TC Type K

Table 4.1 Instrumentation and Data Acquisition Channel List (Continued)

A2	Grids	@ 295K	Num	Type					
249	GRD2-fl-D-4/d2-b2	639.3	2	fl	283	1644	K	Delta M	TC Type K
250	GRD2-wall-D-4/a-2	715.5	2	wall	283	1644	K	Delta M	TC Type K
251	GRD3-fl-D-4/d2-b2	1158.7	3	fl	283	1644	K	Delta M	TC Type K
252	GRD3-fl-D-2/d1-b2	1158.7	3	fl	283	1644	K	Delta M	TC Type K
253	GRD3-fl-D-6/c3-b2	1158.7	3	fl	283	1644	K	Delta M	TC Type K
254	GRD3-wall-E-3/c-1	1244.5	3	wall	283	1644	K	Delta M	TC Type K
255	GRD3-wall-D-4/a-2	1234.9	3	wall	283	1644	K	Delta M	TC Type K
256	GRD3-wall-C-5/d-3	1225.4	3	wall	283	1644	K	Delta M	TC Type K
257	GRD4-fl-D-4/c2-b2	1682.8	4	fl	283	1644	K	Delta M	TC Type K
258	GRD4-fl-F-4/c2-b3	1682.8	4	fl	283	1644	K	Delta M	TC Type K
259	GRD4-fl-B-4/c2-a1	1682.8	4	fl	283	1644	K	Delta M	TC Type K
260	GRD4-wall-E-3/c-1	1768.5	4	wall	283	1644	K	Delta M	TC Type K
261	GRD4-wall-D-4/a-2	1759.0	4	wall	283	1644	K	Delta M	TC Type K
262	Spare3	1225.4	3	wall			none	Delta M	TC Type K
263	GRD5-fl-D-4/d2-b2	2202.7	5	fl	283	1644	K	Delta M	TC Type K
264	GRD5-fl-D-2/d1-b2	2202.7	5	fl	283	1644	K	Delta M	TC Type K
265	GRD5-fl-D-6/c3-b2	2202.7	5	fl	283	1644	K	Delta M	TC Type K
266	GRD5-wall-E-3/c-1	2268.4	5	wall	283	1644	K	Delta M	TC Type K
267	GRD5-wall-D-4/a-2	2278.9	5	wall	283	1644	K	Delta M	TC Type K
268	Spare4	1749.4	4	wall			none	Delta M	TC Type K
269	GRD6-fl-D-4/c2-b2	2724.7	6	fl	283	1644	K	Delta M	TC Type K
270	GRD6-fl-B-4/c2-a1	2724.7	6	fl	283	1644	K	Delta M	TC Type K
271	GRD6-fl-F-4/c2-b3	2724.7	6	fl	283	1644	K	Delta M	TC Type K
272	GRD6-wall-E-3/c-1	2810.4	6	wall	283	1644	K	Delta M	TC Type K
273	GRD6-wall-D-4/a-2	2800.9	6	wall	283	1644	K	Delta M	TC Type K
274	GRD6-wall-G-5/b-3	2800.9	6	wall	283	1644	K	Delta M	TC Type K
275	GRD6-wall-B-5/d-3	2791.3	6	wall	283	1644	K	Delta M	TC Type K
276	GRD7-fl-D-4/d2-b2	3247.6	7	fl	283	1644	K	Delta M	TC Type K
278	GRD7-fl-D-6/c3-b2	3247.6	7	fl	283	1644	K	Delta M	TC Type K
279	GRD7-wall-D-4/a-2	3323.8	7	wall	283	1644	K	Delta M	TC Type K
	Support Rods	@ 295K	Num	Group					
280	SPR_A1-37.2	944.9	A1	9	283	1644	K	Delta M	TC Type K
281	SPR_A1-58.1	1501.1	A1	9	283	1644	K	Delta M	TC Type K
282	SPR_A1-78.8	1950.7	A1	9	283	1644	K	Delta M	TC Type K
283	SPR_A1-90.7	2303.8	A1	9	283	1644	K	Delta M	TC Type K
284	SPR_A1-98.6	2453.6	A1	9	283	1644	K	Delta M	TC Type K
285	SPR_A1-102.5	2603.5	A1	9	283	1644	K	Delta M	TC Type K
286	SPR_A1-114.4	2905.8	A1	9	283	1644	K	Delta M	TC Type K
287	SPR_A1-138.2	3510.3	A1	9	283	1644	K	Delta M	TC Type K
288	SPR_G7-37.2	944.9	G7	9	283	1644	K	Delta M	TC Type K
289	SPR_G7-58.1	1501.1	G7	9	283	1644	K	Delta M	TC Type K
290	SPR_G7-78.8	1950.7	G7	9	283	1644	K	Delta M	TC Type K
291	SPR_G7-90.7	2303.8	G7	9	283	1644	K	Delta M	TC Type K
292	SPR_G7-98.6	2453.6	G7	9	283	1644	K	Delta M	TC Type K
293	SPR_G7-102.5	2603.5	G7	9	283	1644	K	Delta M	TC Type K
294	SPR_G7-114.4	2905.8	G7	9	283	1644	K	Delta M	TC Type K
295	SPR_G7-138.2	3510.3	G7	9	283	1644	K	Delta M	TC Type K
A3	Flow Housing	@ 295K	Rake #						
296	ST. PR-R1-18.2-A	411.5	1		283	1644	K	Delta M	TC Type K
297	ST. PR-R1-18.2-B	411.5	1		283	1644	K	Delta M	TC Type K
298	ST. PR-R1-18.2-C	411.5	1		283	1644	K	Delta M	TC Type K
299	ST. PR-R2-37-A	939.8	2		283	1644	K	Delta M	TC Type K
300	ST. PR-R2-37-B	939.8	2		283	1644	K	Delta M	TC Type K
301	ST. PR-R2-37-C	939.8	2		283	1644	K	Delta M	TC Type K
302	ST. PR-R3-55-A	1397.0	3		283	1644	K	Delta M	TC Type K
303	ST. PR-R3-55-B	1397.0	3		283	1644	K	Delta M	TC Type K
304	ST. PR-R3-55-C	1397.0	3		283	1644	K	Delta M	TC Type K
305	ST. PR-R4-60-A	1524.0	4		283	1644	K	Delta M	TC Type K
306	ST. PR-R4-60-B	1524.0	4		283	1644	K	Delta M	TC Type K
307	ST. PR-R4-60-C	1524.0	4		283	1644	K	Delta M	TC Type K
308	ST. PR-R5-73.81-A	1874.8	5		283	1644	K	Delta M	TC Type K
309	ST. PR-R5-73.81-B	1874.8	5		283	1644	K	Delta M	TC Type K

Table 4.1 Instrumentation and Data Acquisition Channel List (Continued)

310	ST_PR-R5-73.81-C	1874.8	5		283	1644	K	Delta M	TC Type K
314	ST_PR-R6-79.7-A	2024.4	6		283	1644	K	Delta M	TC Type K
315	ST_PR-R6-79.7-B	2024.4	6		283	1644	K	Delta M	TC Type K
316	ST_PR-R6-79.7-C	2024.4	6		283	1644	K	Delta M	TC Type K
317	ST_PR-R7-93.53-A	2375.7	7		283	1644	K	Delta M	TC Type K
318	ST_PR-R7-93.53-B	2375.7	7		283	1644	K	Delta M	TC Type K
319	ST_PR-R7-93.53-C	2375.7	7		283	1644	K	Delta M	TC Type K
320	ST_PR-R8-96-A	2438.4	8		283	1644	K	Delta M	TC Type K
321	ST_PR-R8-96-B	2438.4	8		283	1644	K	Delta M	TC Type K
322	ST_PR-R8-96-C	2438.4	8		283	1644	K	Delta M	TC Type K
323	ST_PR-R9-100-A	2540.0	9		283	1644	K	Delta M	TC Type K
324	ST_PR-R9-100-B	2540.0	9		283	1644	K	Delta M	TC Type K
325	ST_PR-R9-100-C	2540.0	9		283	1644	K	Delta M	TC Type K
326	ST_PR-R10-115.39-A	2930.9	10		283	1644	K	Delta M	TC Type K
327	ST_PR-R10-115.39-B	2930.9	10		283	1644	K	Delta M	TC Type K
328	ST_PR-R10-115.39-C	2930.9	10		283	1644	K	Delta M	TC Type K
329	ST_PR-R11-120-A	3048.0	11		283	1644	K	Delta M	TC Type K
330	ST_PR-R11-120-B	3048.0	11		283	1644	K	Delta M	TC Type K
331	ST_PR-R11-120-C	3048.0	11		283	1644	K	Delta M	TC Type K
332	ST_PR-R12-136-A	3454.4	12		283	1644	K	Delta M	TC Type K
333	ST_PR-R12-136-B	3454.4	12		283	1644	K	Delta M	TC Type K
334	ST_PR-R12-136-C	3454.4	12		283	1644	K	Delta M	TC Type K
493	ST_PR-R13-144-A	3657.6	13		283	1644	K	Delta M	TC Type K
494	ST_PR-R13-144-B	3657.6	13		283	1644	K	Delta M	TC Type K
495	ST_PR-R13-144-C	3657.6	13		283	1644	K	Delta M	TC Type K
335	FH1-wall-10.1	256.5	1	wall	283	1644	K	Delta M	TC Type K
336	FH2-wall-22	558.8	2	wall	283	1644	K	Delta M	TC Type K
337	FH3-wall-37	939.8	3	wall	283	1644	K	Delta M	TC Type K
338	FH4-wall-42.95	1090.9	4	wall	283	1644	K	Delta M	TC Type K
339	FH5-wall-46.93	1192.0	5	wall	283	1644	K	Delta M	TC Type K
340	FH6-wall-52.9	1343.7	6	wall	283	1644	K	Delta M	TC Type K
341	FH7-wall-55.87	1419.1	7	wall	283	1644	K	Delta M	TC Type K
342	FH8-wall-61.85	1571.0	8	wall	283	1644	K	Delta M	TC Type K
343	FH9-wall-67.83	1722.9	9	wall	283	1644	K	Delta M	TC Type K
344	FH10-wall-70.82	1798.8	10	wall	283	1644	K	Delta M	TC Type K
345	FH11-wall-73.81	1874.8	11	wall	283	1644	K	Delta M	TC Type K
346	FH12-wall-78.78	2001.0	12	wall	283	1644	K	Delta M	TC Type K
347	FH13-wall-84.7	2151.4	13	wall	283	1644	K	Delta M	TC Type K
348	FH14-wall-87.65	2226.3	14	wall	283	1644	K	Delta M	TC Type K
349	FH15-wall-90.55	2300.0	15	wall	283	1644	K	Delta M	TC Type K
350	FH16-wall-93.53	2375.7	16	wall	283	1644	K	Delta M	TC Type K
351	FH17-wall-96.5	2451.1	17	wall	283	1644	K	Delta M	TC Type K
352	FH18-wall-102.48	2603.0	18	wall	283	1644	K	Delta M	TC Type K
353	FH19-wall-108.43	2754.1	19	wall	283	1644	K	Delta M	TC Type K
354	FH20-wall-110.43	2804.9	20	wall	283	1644	K	Delta M	TC Type K
355	FH21-wall-111.42	2830.1	21	wall	283	1644	K	Delta M	TC Type K
356	FH22-wall-116.38	2956.1	22	wall	283	1644	K	Delta M	TC Type K
357	FH23-wall-120.3	3055.6	23	wall	283	1644	K	Delta M	TC Type K
358	FH24-wall-129.25	3283.0	24	wall	283	1644	K	Delta M	TC Type K
359	FH25-wall-135.18	3433.6	25	wall	283	1644	K	Delta M	TC Type K
496	FH26-wall-144.1	3660.1	26	wall	283	1644	K	Delta M	TC Type K
360	RB-IF1-8-(-1)-W	-25.4	1	fl	283	1644	K	Delta M	TC Type K
361	RB-IF2-8-(-1)-E	-25.4	2	fl	283	1644	K	Delta M	TC Type K
362	FH DP (0-144)		1	DP	0	3657.6	mm H2O	Rosemou	DP
363	FH DP (0-13)		2	DP	0	330.2	mm H2O	Rosemou	DP
364	FH DP (13-25)		3	DP	0	304.8	mm H2O	Rosemou	DP
365	FH DP (25-37)		4	DP	0	304.8	mm H2O	Rosemou	DP
366	FH DP (37-43)		5	DP	0	152.4	mm H2O	Rosemou	DP
367	FH DP (43-46)		6	DP	0	76.2	mm H2O	Rosemou	DP
368	FH DP (46-53)		7	DP	0	177.8	mm H2O	Rosemou	DP
369	FH DP (53-57)		8	DP	0	101.6	mm H2O	Rosemou	DP
370	FH DP (57-60)		9	DP	0	76.2	mm H2O	Rosemou	DP
371	FH DP (60-63)		10	DP	0	76.2	mm H2O	Rosemou	DP

Table 4.1 Instrumentation and Data Acquisition Channel List (Continued)

372	FH DP (63-67)	11	DP	0	101.6	mm H2O	Rosemou	DP
373	FH DP (67-72)	12	DP	0	127.0	mm H2O	Rosemou	DP
374	FH DP (72-75)	13	DP	0	76.2	mm H2O	Rosemou	DP
375	FH DP (75-78)	14	DP	0	76.2	mm H2O	Rosemou	DP
376	FH DP (78-81)	15	DP	0	76.2	mm H2O	Rosemou	DP
377	FH DP (81-85)	16	DP	0	101.6	mm H2O	Rosemou	DP
378	FH DP (85-93)	17	DP	0	203.2	mm H2O	Rosemou	DP
379	FH DP (93-97)	18	DP	0	101.6	mm H2O	Rosemou	DP
380	FH DP (97-100)	19	DP	0	76.2	mm H2O	Rosemou	DP
381	FH DP (100-108)	20	DP	0	203.2	mm H2O	Rosemou	DP
382	FH DP (108-120)	21	DP	0	304.8	mm H2O	Rosemou	DP
383	FH DP (120-133)	22	DP	0	330.2	mm H2O	Rosemou	DP
384	FH DP (133-144)	23	DP	0	279.4	mm H2O	Rosemou	DP
A4	Lower Plenum							
386	L Plen fl-b	fl		283	1644	K	Delta M	TC Type K
387	L Plen wall-t	wall		283	1644	K	Delta M	TC Type K
388 •	L Plen wall-b	wall		283	1644	K	Delta M	TC* Type K
A5	Upper Plenum							
389	U Plen fl-m	fl		283	1644	K	Delta M	TC Type K
390	FH DP (144-156.25)	DP		0	311.2	mm H2O	Rosemou	DP
425	U Plen Acc DP	DP		0	34.5	kPa	0	0
391	U Plen wall-t	wall		283	1644	K	Delta M	TC Type K
392	U Plen wall-b	wall		283	1644	K	Delta M	TC Type K
393 •	UP Exit Pr	Pr		0	413.7	kPa	Rosemou	PT*
A6	Electrical System							
394	Pwr Sup W	W		0	500000	W	Lem	Voltage Isolator
395	Pwr Sup V	V		0	60	VDC	Lem	Voltage Isolator
396	Pwr Sup Cur	Cur		0	12600	ADC	Lem	Voltage Isolator
397	Test Sect V	V		0	60	VDC	Lem	Voltage Isolator
398	Test Sect Cur	Cur		0	15000	ADC	Empro	Voltage Isolator
B1	Water Supply Tank							
399 •	Sup Tnk fl-t	fl		283	1644	K	Delta M	TC* Type K
401	Sup Tnk fl-b	fl		283	1644	K	Delta M	TC Type K
402	UP DP (156.25-162.38)	DP		0	155.7	mm H2O	Rosemou	DP
433 •	UP-EX PIPE DP	DP		0	34.5	kPa	Rosemou	PT*
405	Sup Tnk Lvl	Lvl		0	3022.6	mm H2O	Rosemou	L
406 •	Sup Tnk Pr	Pr		0	413.7	kPa	Rosemou	PT*
B3	Supply Line							
407 ••	Sup Ln fl	fl		283	1644	K	Delta M	TC* Type K
408	Sup Ln wall	wall		283	1644	K	Delta M	TC Type K
409	Sup Ln wall	wall		283	1644	K	Delta M	TC Type K
410	Sup Ln wall	wall		283	1644	K	Delta M	TC Type K
411 •	Sup Ln Pr	Pr		0	344.7	kPa	Rosemou	PT*
412 ••	Sup Ln FM	FM		0	4.9	kg/sec	Micromoti	FM*
B4	Droplet Injection							
413	Drop Inj FM	FM		0	0.0454	kg/sec	0	FM
C	Steam Supply Sys.							
414	St Sup fl	fl		283	1644	K	Delta M	TC Type K
415	St Sup wall	wall		283	1644	K	Delta M	TC Type K
416 •	St Sup Pr	Pr		0	413.7	kPa	Rosemou	PT*
417 •	St Sup FM	FM		0	7.1	m³/min	Rosemou	FM*
D1	Carryover Tanks							
418	Lg CT fl-b	fl		283	1644	K	Delta M	TC Type K
419	Lg CT wall-t	wall		283	1644	K	Delta M	TC Type K
420	Lg CT fl-t	fl		283	1644	K	Delta M	TC Type K
421	Lg CT wall-b	wall		283	1644	K	Delta M	TC Type K
422	Sm CT fl-	fl		283	1644	K	Delta M	TC Type K
423	Sm CT wall-t	wall		283	1644	K	Delta M	TC Type K
424	Sm CT wall-b	wall		283	1644	K	Delta M	TC Type K
426	Lg CT Lvl	Lvl		0	1574.8	mm H2O	Rosemou	L
427	Sm CT Lvl	Lvl		0	895.4	mm H2O	Rosemou	L
D2	Steam Separator							
428	St Sep fl	fl		283	1644	K	Delta M	TC Type K

Table 4.1 Instrumentation and Data Acquisition Channel List (Continued)

429	St Sep wall-t			wall	283	1644	K	Delta M	TC Type K
430	St Sep wall-b			wall	283	1644	K	Delta M	TC Type K
431	St Sep Dr fl-t			fl	283	1644	K	Delta M	TC Type K
432	St Sep Dr fl-b			fl	283	1644	K	Delta M	TC Type K
433	St Sep Dr Tnk wall			wall	283	1644	K	Delta M	TC Type K
434	St Sep Dr Tnk Lvl			Lvl	0	1663.7	mm H2O	Rosemou	L
D3	Pressure Oscillation Damping Tank (Accumulator)								
434	Acc wall-t			wall	283	1644	K	Delta M	TC Type K
437	Acc wall-m			wall	283	1644	K	Delta M	TC Type K
385	Acc wall-b			wall	283	1644	K	Delta M	TC Type K
435	Acc fl-t			fl	283	1644	K	Delta M	TC Type K
436	Acc fl-b			fl	283	1644	K	Delta M	TC Type K
438	St Sup-Acc DP			DP	0	34.5	kPa	Rosemou	PT
439	Acc Pr			Pr	0	413.7	kPa	Rosemou	PT
D4	Exhaust Line								
440	Ex Pipe fl			fl	283	1644	K	Delta M	TC Type K
441	Ex Pipe wall			wall	283	1644	K	Delta M	TC Type K
442	Ex Pipe wall			wall	283	1644	K	Delta M	TC Type K
443	Ex Pipe wall			wall	283	1644	K	Delta M	TC Type K
444	Ex Pipe Pr			Pr	0	413.7	kPa	Rosemou	PT
445	Ex Pipe FM			FM	0	12.7	m^/min	Rosemou	FM
	Quartz Windows								
446	Qtz Win_24.17-E	613.9	1		0	283	1644	K	Delta M	TC Type K
447	Qtz Win_24.17-W	613.9	1		0	283	1644	K	Delta M	TC Type K
448	Qtz Win_44.72-E	1135.9	2		0	283	1644	K	Delta M	TC Type K
449	Qtz Win_44.72-W	1135.9	2		0	283	1644	K	Delta M	TC Type K
450	Qtz Win_65.27-E	1657.9	3		0	283	1644	K	Delta M	TC Type K
451	Qtz Win_65.27-W	1657.9	3		0	283	1644	K	Delta M	TC Type K
452	Qtz Win_85.82-E	2179.8	4		0	283	1644	K	Delta M	TC Type K
453	Qtz Win_85.82-W	2179.8	4		0	283	1644	K	Delta M	TC Type K
454	Qtz Win_106.37-E	2701.8	5		0	283	1644	K	Delta M	TC Type K
455	Qtz Win_106.37-W	2701.8	5		0	283	1644	K	Delta M	TC Type K
456	Qtz Win_126.92-E	3223.8	6		0	283	1644	K	Delta M	TC Type K
457	Qtz Win_126.92-W	3223.8	6		0	283	1644	K	Delta M	TC Type K
	Control Outputs								
458	Rem Close					0	1	State		Relay
459	Rem Start/Stop					0	1	State		Relay
460	IF Fast Valve					0	1	State		Relay
461	RELAY 3 - NO					0	1	State		Relay
462	I/O Disc							State		Relay
463	Pull-Up+I/O Disc							State		Relay
464	Not Available							none		Relay
465	Not Available							none		Relay
466	PS-PWR OUTA		A			0	125000	W		Current output
467	PS-PWR OUTB		B			0	125000	W		Current output
468	IF RATEA		A			0	2.5	kg/sec		Current output
469	IF RATEB		B			0	2.5	kg/sec		Current output
470	UP PressA		A			0	206.8	kPa		Current output
471	UP PressB		B			0	206.8	kPa		Current output
472	CNTL4A		A					none		Current output
473	CNTL4B		B					none		Current output
474	Rake_CntlA		A			0	88.9	mm		Current output
475	Rake_CntlB		B			0	88.9	mm		Current output
476	Rake_CntlC		C			0	88.9	mm		Current output
477	Rake_CntlD		D			0	88.9	mm		Current output
478	CNTL7A		A					none		Current output
479	CNTL7B		B					none		Current output
480	CNTL8A		A					none		Current output
481	CNTL8B		B					none		Current output
	Rake Position								
482	Rake_PosA		A			0	88.9	mm		Linear Pot
483	Rake_NumA		A			0	13	num		Resistor Ratio
484	Rake_PosB		B			0	88.9	mm		Linear Pot

Table 4.1 Instrumentation and Data Acquisition Channel List (Continued)

485	Rake_Num8	B	0	13	num	Resistor Ratio
486	Rake_PosC	C	0	88.9	mm	Linear Pot
487	Rake_NumC	C	0	13	num	Resistor Ratio
488	Rake_PosD	D	0	88.9	mm	Linear Pot
489	Rake_NumD	D	0	13	num	Resistor Ratio
	SPARES					
490	Spare1	1			none	unused
491	Spare2	2			none	unused
492	Bad SCP2	2			none	unused
400	FH Insul-108N	-108N	283	1644	K	TC Type K
97	FH Insul-55N	-55N	283	1644	K	TC Type K
184	FH Insul-108S	-108S	283	1644	K	TC Type K
277	FH Insul-80N	-80N	283	1644	K	TC Type K
	Terminal Panel Reference Thermistors					
497	Pnl1-Therm2S		278	322	K	Thermistor
498	Pnl2-Therm2S		278	322	K	Thermistor
499	Pnl3-Therm2S		278	322	K	Thermistor
500	Pnl4-Therm2S		278	322	K	Thermistor
501	Pnl5-Therm2S		278	322	K	Thermistor
502	Pnl6-Therm2S		278	322	K	Thermistor
503	Pnl7-Therm2S		278	322	K	Thermistor
504	Pnl8-Therm2S		278	322	K	Thermistor
505	Pnl9-Therm2S		278	322	K	Thermistor
506	Pnl10-Therm2S		278	322	K	Thermistor
507	Pnl11-Therm2S		278	322	K	Thermistor
508	Pnl12-Therm2S		278	322	K	Thermistor
509	Pnl13-Therm2S		278	322	K	Thermistor
510	Pnl14-Therm2S		278	322	K	Thermistor
511	Pnl15-Therm2S		278	322	K	Thermistor
512	Pnl16-Therm2S		278	322	K	Thermistor

5. TEST FACILITY IMPROVEMENTS

Significant improvements related to other heater rod bundle testing programs, listed in Section 3, Literature Review, of the RBHT Test Plan and Design Report have been incorporated into the RBHT Test Facility. These improvements are:

- A low mass square flow housing design which better fits a square rod bundle array and minimizes the housing mass and the excess rod bundle flow area.
- The six pairs of windows which provide large viewing areas below and above grid locations, making it possible to observe and make void fraction and droplet measurements during reflood testing.
- The use of a Laser illuminated Digital Camera System to measure entrained water droplets sizes, distribution, and velocities in the transition and disperse flow regions.
- The use of a traversing steam probe rake to measure simultaneously steam temperatures in the flow subchannel and in the rod-to-rod gap.
- Differential pressure transmitter axially located 76.2-127 mm (3-5 in) apart in conjunction with heater rod and flow housing wall thermocouples to obtain detailed void fraction and heat transfer information.
- Addition of a water droplets injection system in conjunction with steam injection to study the droplet-steam cooling effects on heat transfer and grids.
- Addition of a large pressure oscillation-damping tank to minimize test section oscillations observed in the FLECHT and FLECHT-SEASET tests.
- The incorporation of closely coupled entrained liquid collection tanks and piping to reduce delay times for liquid collection.

6. SUMMARY OF CHARACTERIZATION TESTS

6.1 Single Phase Pressure Drop Tests

The data from the single phase pressure drop tests performed under the RBHT Program were analyzed to calculate the grid loss coefficient that are needed to characterize the spacer grids used in the RBHT test bundle.

Figure 6.1 shows the schematic layout of the rod bundle for the RBHT Test Facility with the location of the DP cells used for the single-phase pressure drop tests.

Following are the specifications of the rod bundle:

Number of rods: 49
Diameter of rods: 9.4996 mm (0.374 in)
Housing dimension: 91.313 mm (3.595 in) square
Flow area: 4863.73 mm^2 (7.5388 in^2)
Hydraulic diameter: 10.6426 mm (0.419 in)
Length (width or thickness) of spacer grid: 57.15 mm (2.25 in)

The experiments recorded volumetric flow rate (channel 412) as well as DP cell readings. Table 6.1 gives the detail of the DP cell location, channel number corresponding to the DP cell data, and number of grids within the DP cell span. The maximum Reynolds number achieved in the tests is about 30000.

As seen from Table 6.1, the experiments were designed such that the there were many DP cell measurements (six channels, except channels 369 and 379) that included spacer grids in their span. In other words, the pressure drop measured by such DP cells spanning spacer grid(s) would be composed of two components: frictional loss for the bare portion of the bundle, and the loss associated with the spacer grid(s) in the span. DP cells for channels 369 and 379 measure bare bundle pressure drop; i.e., they measure the single-phase frictional pressure drop within the span within the spacer grids. It should be noted that this frictional pressure drop will include the developing flow and the increased mixing effects which occur downstream of a spacer grid.

6.1.1 Procedure for Calculation of Grid Loss Coefficient, k_{grid}

The following are the steps used to calculate the grid loss coefficient.

1. Based on the volumetric flow rate measurement (channel 412) and the flow area of the bundle, the fluid velocity in the rod bundle is calculated.

2. Reynolds number of flow is calculated using fluid properties, evaluated at 2.758 bar (40 psia) and 23.88 degrees C (75 degrees F).

ρ_f = 997.27 kg/m^3 (62.258 lbm/ft^3)

μ_f = 9.1377 x 10^{-4} Pa-s (6.133 x 10^{-4} lbm/ft -sec)

3. The pressure drop measured by any DP cell is the sum of the single-phase frictional pressure

drop associated with the bare length of the span and the grid losses.

$$\Delta P_{Total} = \Delta P_{bare} + \Delta P_{grid}$$

4. Knowing the grid length and the number of grids in the span, the bare bundle length is calculated as L_{span} - N (number of grids in span) x L_{grid} = L_{bare}. Using the bare bundle pressure drop data from channel 369 or 379, the frictional pressure drop for the bar portion of the span under consideration is obtained as:

$$\Delta P_{bare} = \frac{L_{bare} in span consideration}{Span length for channel 369 or 379} \; x \; \Delta P\,(from channel 369 or 379) \qquad (6\text{-}1)$$

5. The pressure drop due to the grids is then obtained by subtracting the frictional pressure drop for the bare portion of the span from the measured DP value.

6. The grid loss is given by:

$$\Delta P_{grids} = N \frac{k \rho_f V^2}{2g} \qquad (6\text{-}2)$$

where
N number of grids in the DP cell span under consideration,
V velocity
k_{grid} grid loss coefficient, which is to be calculated.

From the above equation the grid loss coefficient k_{grid} can be determined. Figure 6.2 shows the plot of grid loss coefficient as a function of Reynolds number for all the DP cells with spacer grids in their span. As expected, the grid loss coefficient decreases with Reynolds number. The scatter in the data is minimal.

This data is consistent with other experimental work, where a grid loss coefficient of about 1 is obtained for Reynolds number of about 100,000.

6.1.2 Comparison of Data With Prediction Using Rehme's Method

Pressure drop at a spacer grid is given as:

$$\Delta P = C_v \varepsilon^2 \frac{\rho_f V^2}{2} \qquad (6\text{-}3)$$

where
C_v modified spacer form loss coefficient (a function of Reynolds number)
ε ratio of the projected grid cross-section area in the rod bundle to the undisturbed flow area (equal to 0.362 for the RBHT Test Facility)
ρ_f fluid density
V average fluid velocity in the rod bundle

The modified spacer form loss coefficient is obtained from Rehme's paper (Ref. 7) as a function of Reynolds number. For the Reynolds number range of interest, the C_v value is between 6 and 11.

The pressure drop is calculated from the Rehme's equation. The grid loss coefficient is obtained from:

$$\Delta P_{grid} = N \frac{k_{grid} \rho V^2}{2} \qquad (6\text{-}4)$$

where
N number of grids in the DP cell span under consideration
V velocity
k_{grid} grid loss coefficient, which is to be calculated

Figure 6.3 shows the comparison of grid loss coefficient from experiment with that calculated by Rehme's method. It is seen that Rehme's method underpredicts the coefficient significantly by almost a factor of 2. This is similar to what was obtained in the FLECHT-SEASET experiments.

6.2 Calculation of Friction Factor for the Rod Bundle

The data from the single-phase pressure drop tests performed under the RBHT Program was analyzed to calculate the friction factor, needed to characterize the rod bundle.

Following are the specifications of the rod bundle:

Number of rods: 49
Diameter of rods: 9.4996 mm (0.374 in)
Housing dimension: 91.313 mm (3.595 in) square
Flow area: 4863.73 mm^2 (7.5388 in^2)
Hydraulic diameter: 10.6426 mm (0.419 in)
Length (width or thickness of spacer grid: 57.15 mm (2.25 in)

The experiments recorded volumetric flow rate (channel 412) as well as DP cell readings. Channel 369 records the DP cells for a span of 14 inches (between 53 and 67 in elevation) without any spacer grids. Hence, all the pressure losses over this span are due to friction only. The maximum Reynolds number achieved in the test is about 30000.

In addition to this, a second experiment was performed to measure the pressure drop over a short span of eight in (between 100 and 108 in elevation). A schematic of the layout along with the DP cells is shown in Figure 6.4.

6.2.1 Procedure for Calculating Friction Factor, f

1. Based on the volumetric flow rate measurement (channel 412) and the flow area of the bundle, the fluid velocity in the rod bundle is calculated.

2. The Reynolds number of flow is calculated using fluid properties, evaluated at 2.758 bar (40

psia) and 23.88 degrees C (75 degrees F):

ρ_f = 997.27 kg/m^3 (62.258 lbm/ft^3)

μ_f = 9.1377 x 10^{-4} Pa-s (6.133 x 10^{-4} lbm/ft-sec)

3. The head equation for pressure drop is given by:

$$\Delta P = \frac{fL\rho_f V^2}{2g_c D_h} \qquad (6\text{-}5)$$

where

f	friction factor, which is to be calculated
L	length of the span over which frictional losses are measured (e.g., for channel 369, this is 14 in)
D_h	hydraulic diameter
V	velocity

Using equation 6-5 and the data from channel 369 for the pressure drop, the unknown friction factor is calculated. A plot of friction factor as a function of Reynolds number is shown in Figure 6.5.

Figure 6.6 shows the comparison of friction factors calculated during the three experiments. The value of the friction factor calculated for the short span experiment is lower than the value for the other two tests. This is because of the increased turbulence downstream of the spacer grid. The spacer grid acts to disrupt the boundary layer on the heater rods such that the flow must redevelop downstream of the grid, resulting in higher effective frictional losses. As seen from Figure 6.4, the short span test DP cell was located far away from the downstream of the nearest spacer grid (grid no. 5), while the DP cell for the other experiments was much closer to the downstream of the spacer grid (grid no. 3).

Based on Figure 6.5, the friction factor can be correlated to the Reynolds number by the following equation:

$$f = \frac{0.279}{\mathrm{Re}^{0.198}} \qquad (6\text{-}6)$$

The values of friction factor obtained from the experiments are higher than the values from Moody chart for the same Reynolds number.

6.3 Radiation Heat Loss Measurements

Radiation only experiments were conducted as apart of the RBHT Program to characterize the radiation heat loss, as a part of the separate effect tests. These experiments were conducted under vacuum. The following tests were conducted:

- Experiment #605: Heat up rod bundle to 426.66 degrees C (800 degrees F), to help

remove all water vapor. Manual control was used and 650.24 mm (25.6 in) vacuum was maintained.

- Experiment #606: Two hours heating, manual power control. Peak temperature of 426.66 - 454.44 degrees C (800 - 850 degrees F) was achieved.
- Experiment #607: Little over one hour, manual power control, peak temperature of 537.77 - 565.55 degrees C (1000 - 1050 degrees F) was achieved. Some cooling down was done.
- Experiment #608: Cooling down of the bundle.

For conducting this experiment, the outside of the insulation was instrumented with thermocouples, to record the temperature and hence calculate the heat loss. The locations (elevation, slot number, etc.) are given below:

- Channel 97S2-33, FH Insulation 55 N
- Channel 277S4-62, FH Insulation 80 N
- Channel 400S6-40 FH Insulation 108 N
- Channel 438S7-48 FH Insulation 108 S (not functional)

Thickness of the WR-1200 Modeled Perlite Insulation was 101.6 mm (4 in). The outer dimension of the housing was 102.87 mm (4.05 in) square.

Temperature measurements on the flow housing, at approximately the same elevation as the housing insulation thermocouples were used to calculate the temperature difference driving the heat transfer. The following housing thermocouples were used:

- Channel 341 S6-4, at 1.419 m (55.87 in) elevation
- Channel 346 S6-9, at 2.0 m (78.78 in) elevation
- Channel 353 S6-16, at 2.754 m (108.43 in) elevation

Table 6.2 summarizes the calculations for Experiment #607.

To calculate the heat loss as a fraction of the total power, the power supplied needs to be calculated. This is the product of the test section voltage and the test section current readings. Table 6.3 summarizes the current and voltage readings and the offsets.

At steady-state, the power supplied was 3345.69 W. All the power supplied corresponds to heat loss by radiation, since the facility was operated at steady-state. Based on a total power of 114 kW, the heat loss during a typical reflood test would be around 2.32 percent of the total value. This is a small fraction of the total power supplied to the RBHT facility.

6.4 Calculation of Insulation Thickness for the RBHT Test Bundle

In order to quantify the heat loss from the RBHT test bundle, it was necessary to do a heat transfer analysis using various thickness of insulation. With this analysis it will be possible to decide on the appropriate amount of insulation for the bundle. The analysis consists of a simple 1-D conduction and convection problem and is as follows:

Beginning with the most simple conduction equation:

$$q'' = k\frac{dT}{dx} \tag{6-7}$$

And considering the basic convection equation:

$$q'' = h(Ts - T_\infty) \tag{6-8}$$

The heat flux will be the same at all locations, so the two equations can be combined:

$$k\frac{dr}{dx} = h(T_s - T_\infty) \tag{6-9}$$

Now, the equation can be simplified and integrated over the width of the insulation:

$$-dT = \frac{h}{k}(T_s - T_\infty)\,dx \tag{6-10}$$

$$-\int_{T_w}^{T_s} dT = \frac{h}{k}(T_s - T_\infty)\int_0^L dx \tag{6-11}$$

$$T_w - T_s = \frac{hL}{k}(T_s - T_\infty) \tag{6-12}$$

where

T_W	bundle wall temperature
T_S	insulation surface temperature
T_∞	bulk air temperature
L	insulation thickness

Now the equation can be solved for the insulation surface temperature and this result can be used to find the heat flux using the convection equation. Note that from this point forward, the temperatures must be in **absolute** units.

$$T_s = \frac{T_w + \frac{hL}{k}T\infty}{1 + \frac{hL}{k}} \tag{6-13}$$

$$q'' = h\left[\left(\frac{T_w + \frac{hL}{k}T_\infty}{1 + \frac{hL}{k}}\right) - T_\infty\right] \tag{6-14}$$

The next issue is how to deal with the convective heat transfer coefficient and the thermal conductivity of the insulation. The convective heat transfer coefficient must be calculated using

a natural convection correlation, based on the dimensions of the bundle. The thermal conductivity of the insulation will be assumed constant and equal to the thermal conductivity of the material at about 343.33 degrees C (650 degrees F). For this analysis, a range of convective heat transfer coefficients were used, but the calculated value was about 3.69 W/m^2-K (0.65 Btu/hr-ft^2-F) and this value will be used in the sample calculation that follows. The value of the thermal conductivity of the insulation was taken from the manufacturer's specification sheet to be about 0.1003 W/m-K (0.058 Btu/hr-ft-F).

In addition to the thermal constants, the temperatures of the bundle wall and the bulk air must be estimated. Values of 537.77 degrees C (1000 degrees F) and 23.88 degrees C (75 degrees F) were used respectively. An example calculation using 50.8 mm (2 in) of insulation is as follows:

Insulation surface temperature:

$$T = \frac{T + \frac{hL}{k}T}{1 + \frac{hL}{k}} = \frac{1460R + \frac{\left(0.65\frac{Btu}{hr \cdot ft \cdot R}\right)\left(\frac{2}{12}ft\right)}{0.058\frac{Btu}{hr \cdot ft \cdot R}}(535R)}{1 + \frac{\left(0.65\frac{Btu}{hr \cdot ft \cdot R}\right)\left(\frac{2}{12}ft\right)}{0.058\frac{Btu}{hr \cdot ft \cdot R}}} = 857.5R = 397.5F \quad (6\text{-}15)$$

where
T_s = 203.05 degrees C (397.5 degrees F)

Heat Flux:

$$q'' = h[T_s - T_\infty] = 0.65\frac{Btu}{hr \cdot ft^2 \cdot R}(397.5F - 75F) = 209.6\frac{Btu}{hr \cdot ft^2} = 0.061\frac{kW}{ft^2} \quad (6\text{-}16)$$

Multiplying this result by the surface area of the rod bundle (19.5 ft^2) will yield the total power loss from the bundle:

$$q = q''A = 0.061\frac{kW}{ft^2} \cdot 19.5ft^2 = 1.2kW \quad (6\text{-}17)$$

Based on a total bundle power of 144kW, this gives a power loss of about 0.8 percent.

Tables 6.4 through 6,6 show a summary of these calculations for an insulation thickness of 4 in and housing temperatures corresponding to three axial locations.

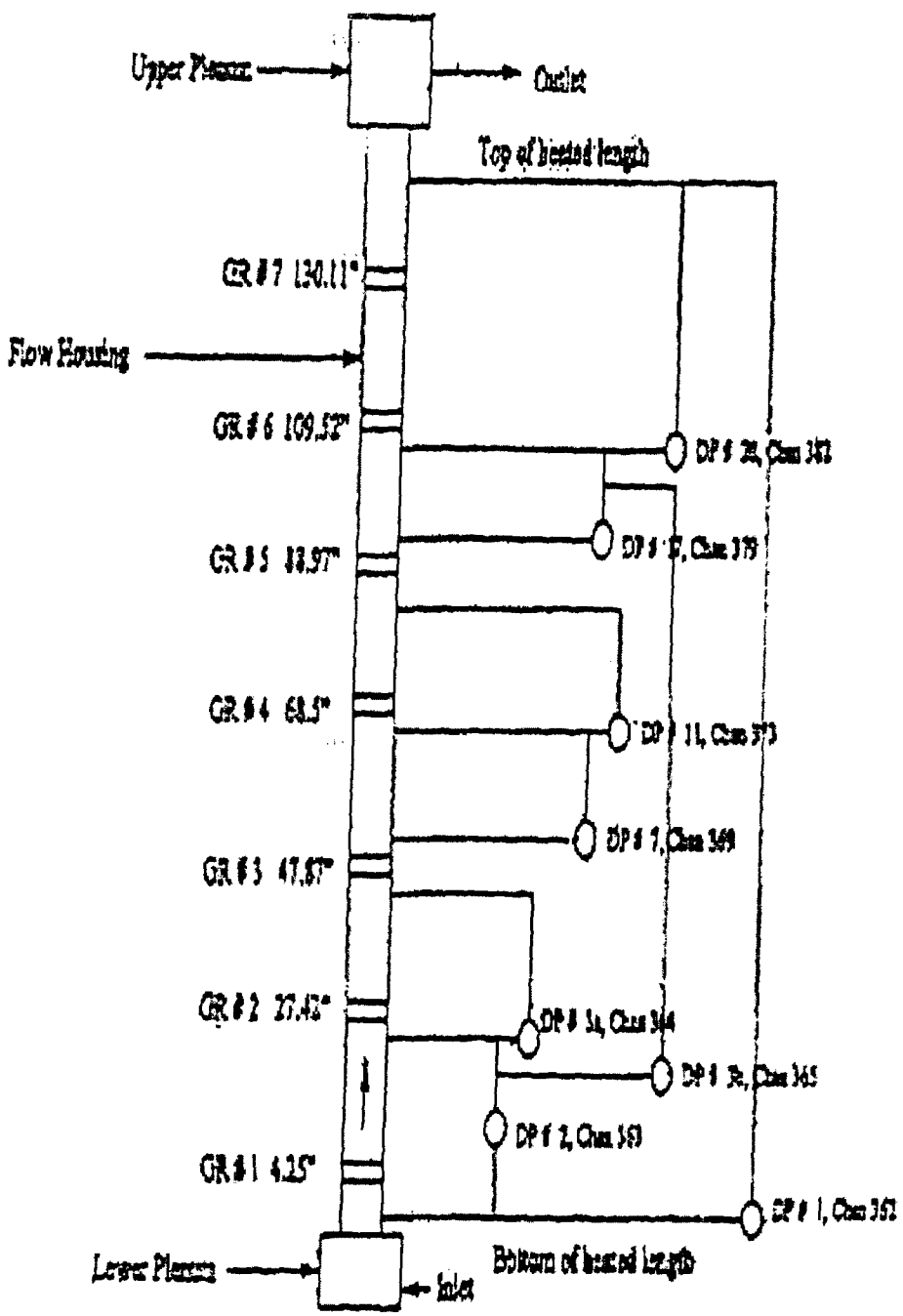

Figure 6.1 RBHT Differential Pressure Cell Layout, Single Phase Flow.

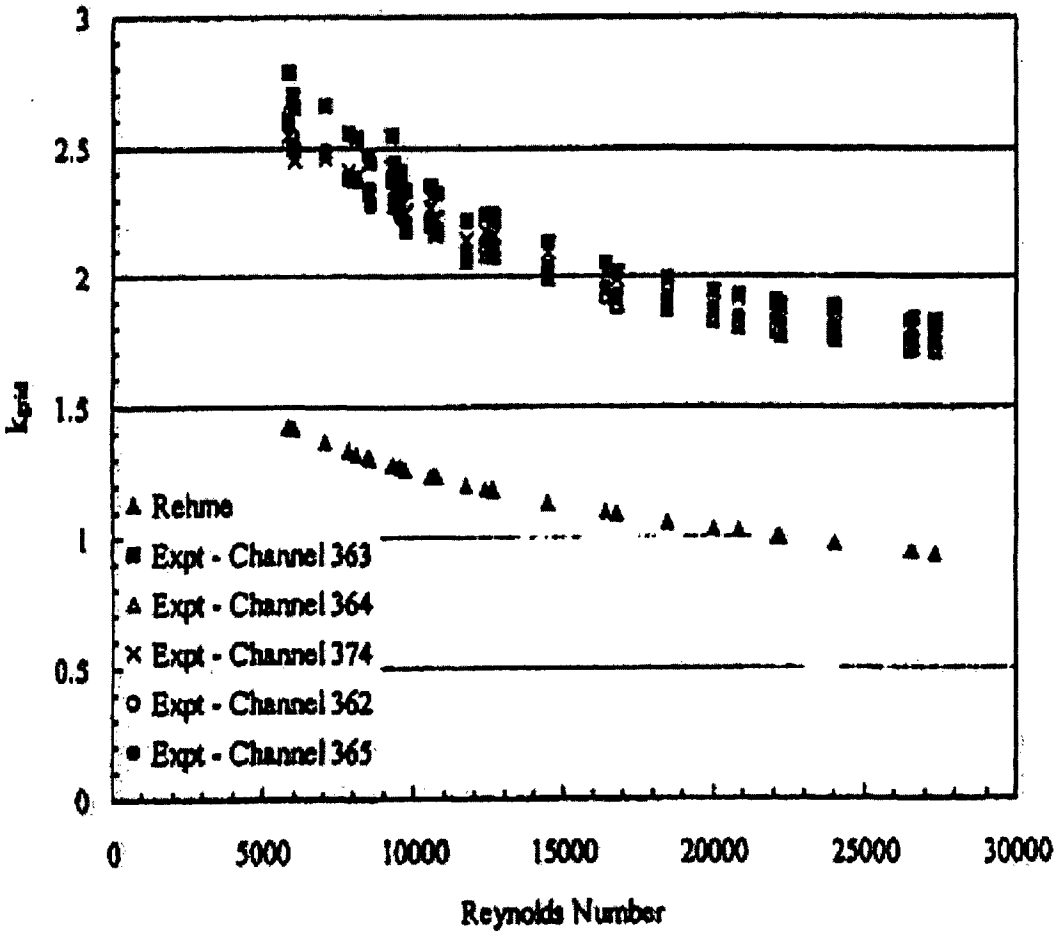

Figure 6.2 Grid Loss Coefficients vs. Reynolds Number - Experiment 276.

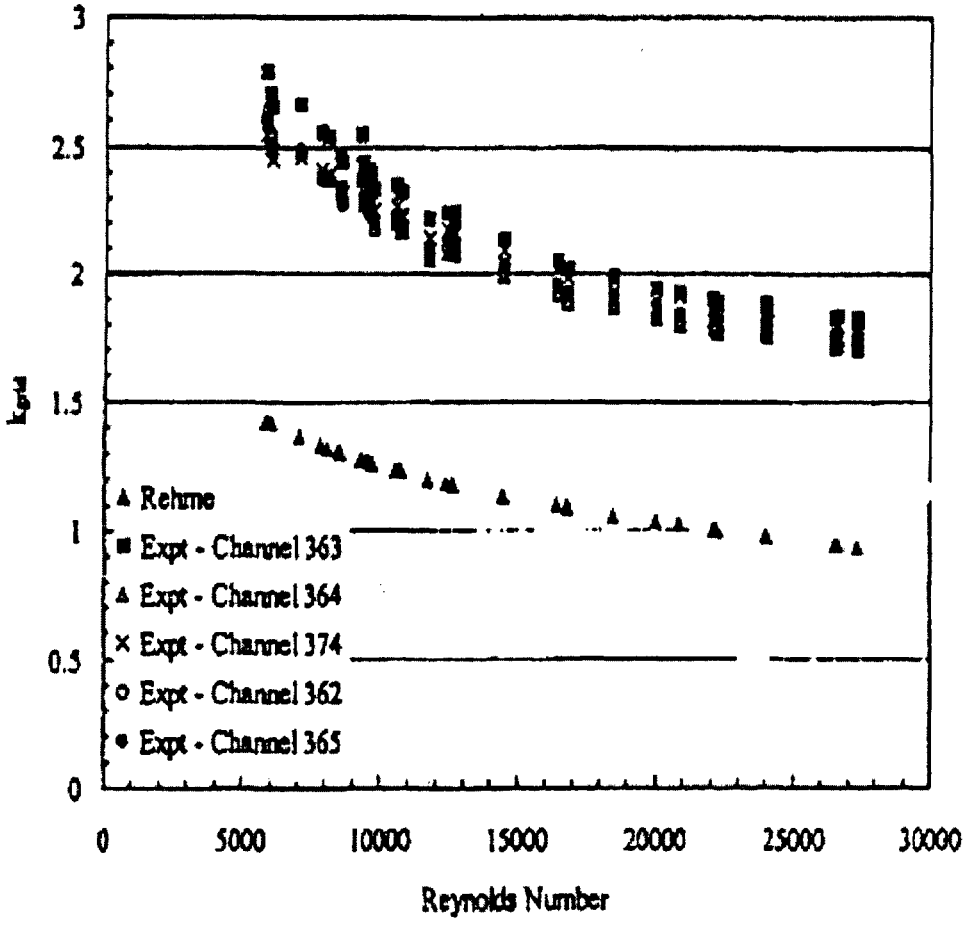

Figure 6.3 Comparison of Experimental Data With Rehme's Method.

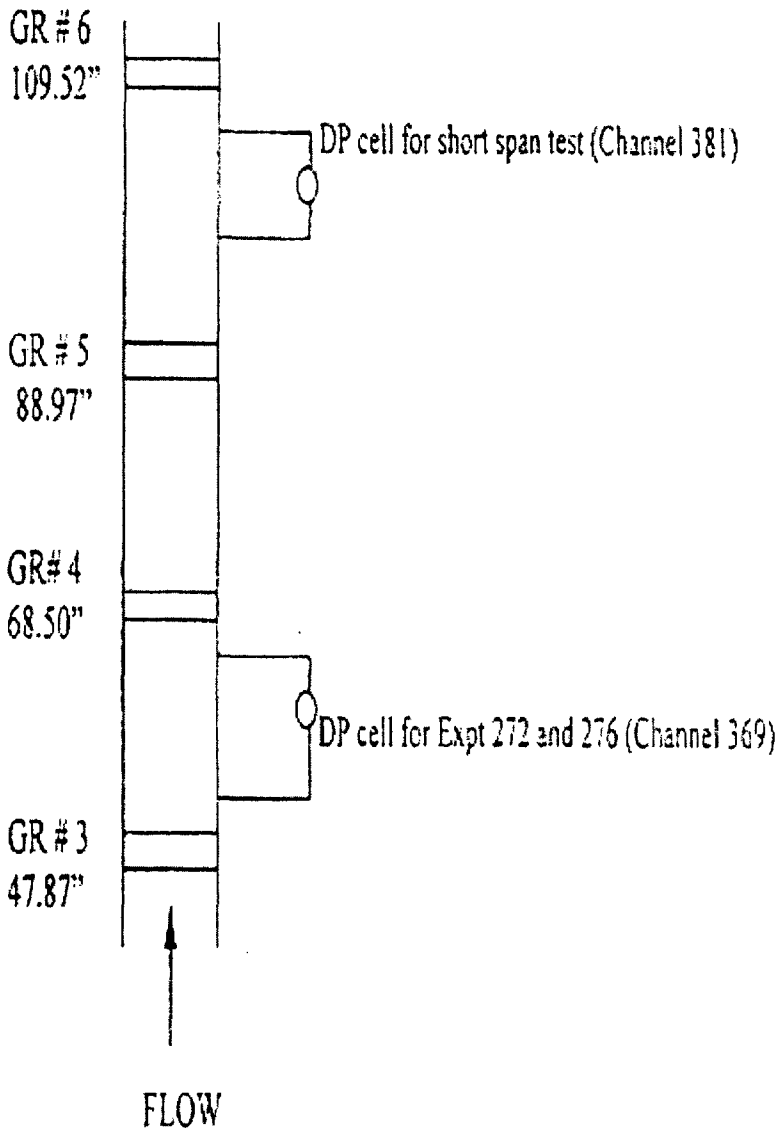

Figure 6.4 Differential Pressure Cell Layout for Pressure Drop Tests.

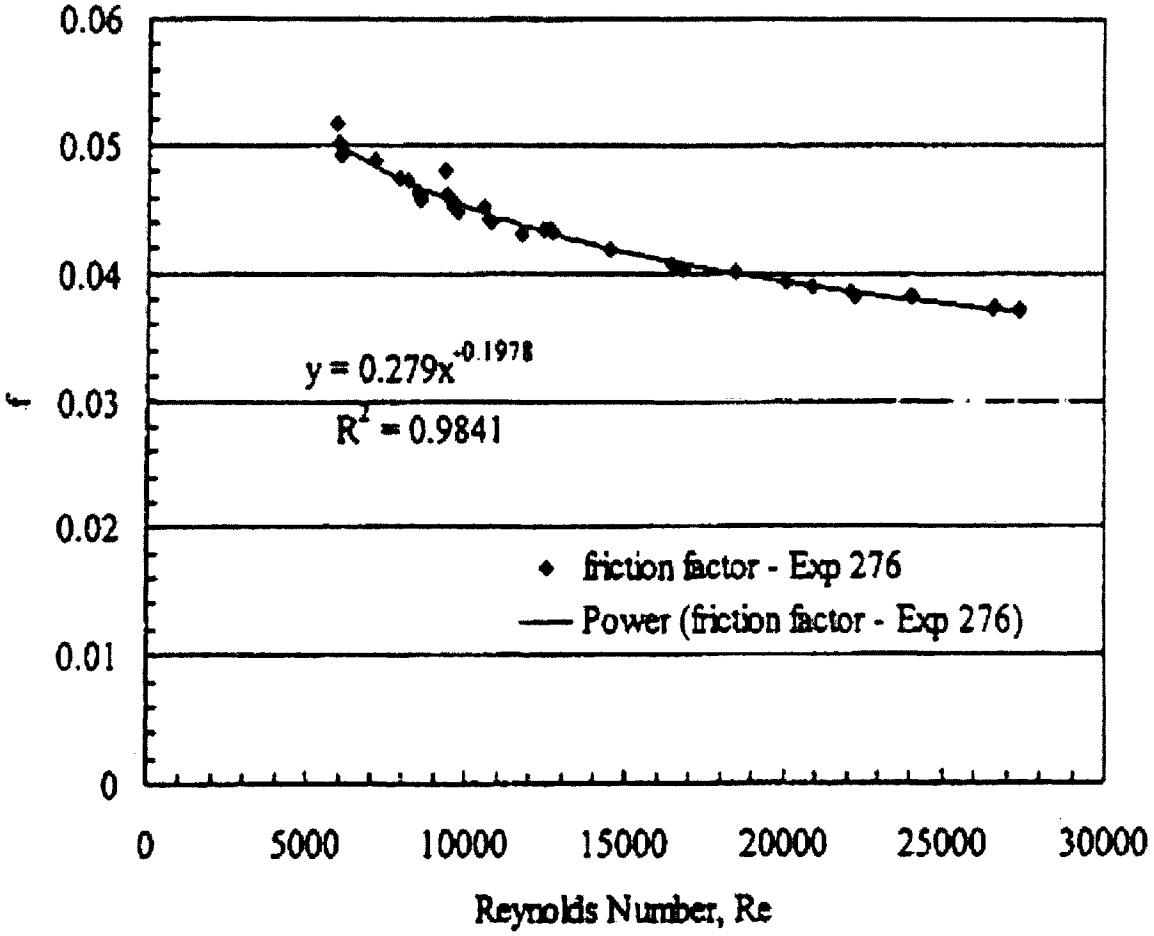

Figure 6.5 Friction Factor as a Function of the Reynolds Number.

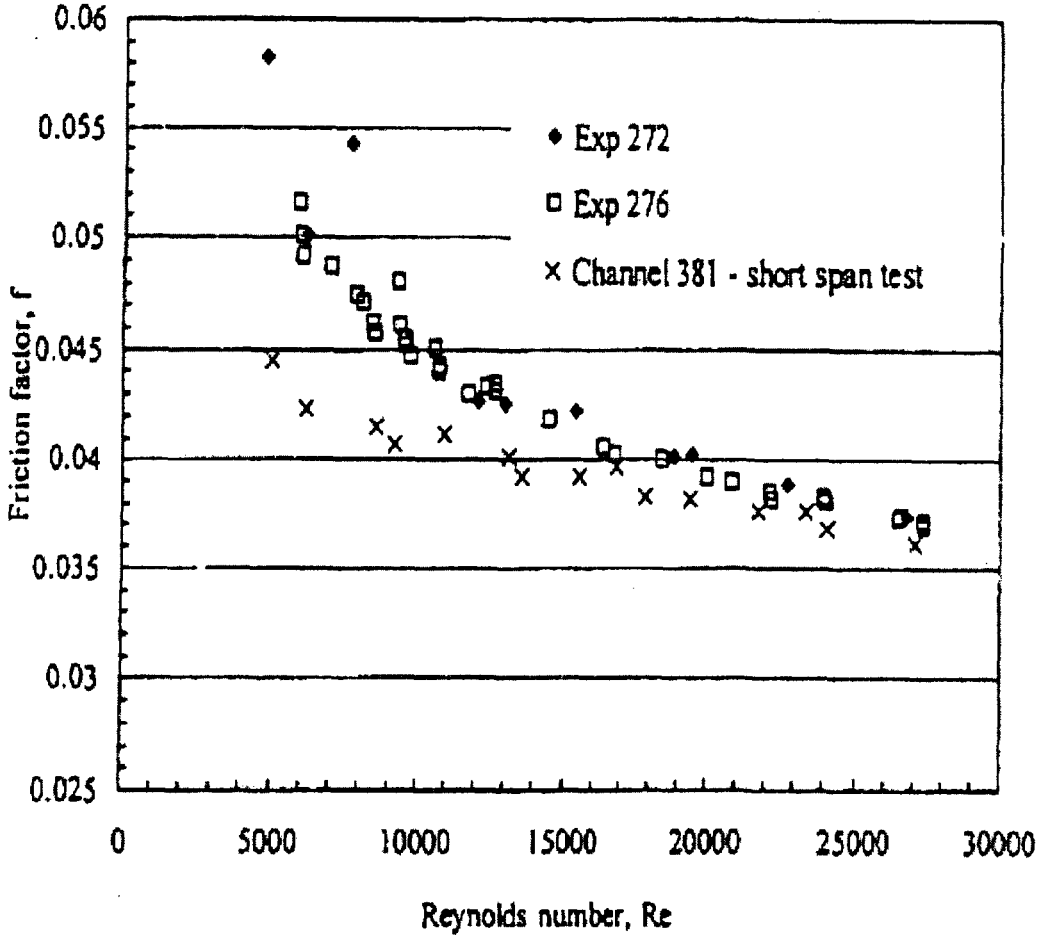

Figure 6.6 Comparison of the Friction Factors for Various Experiments.

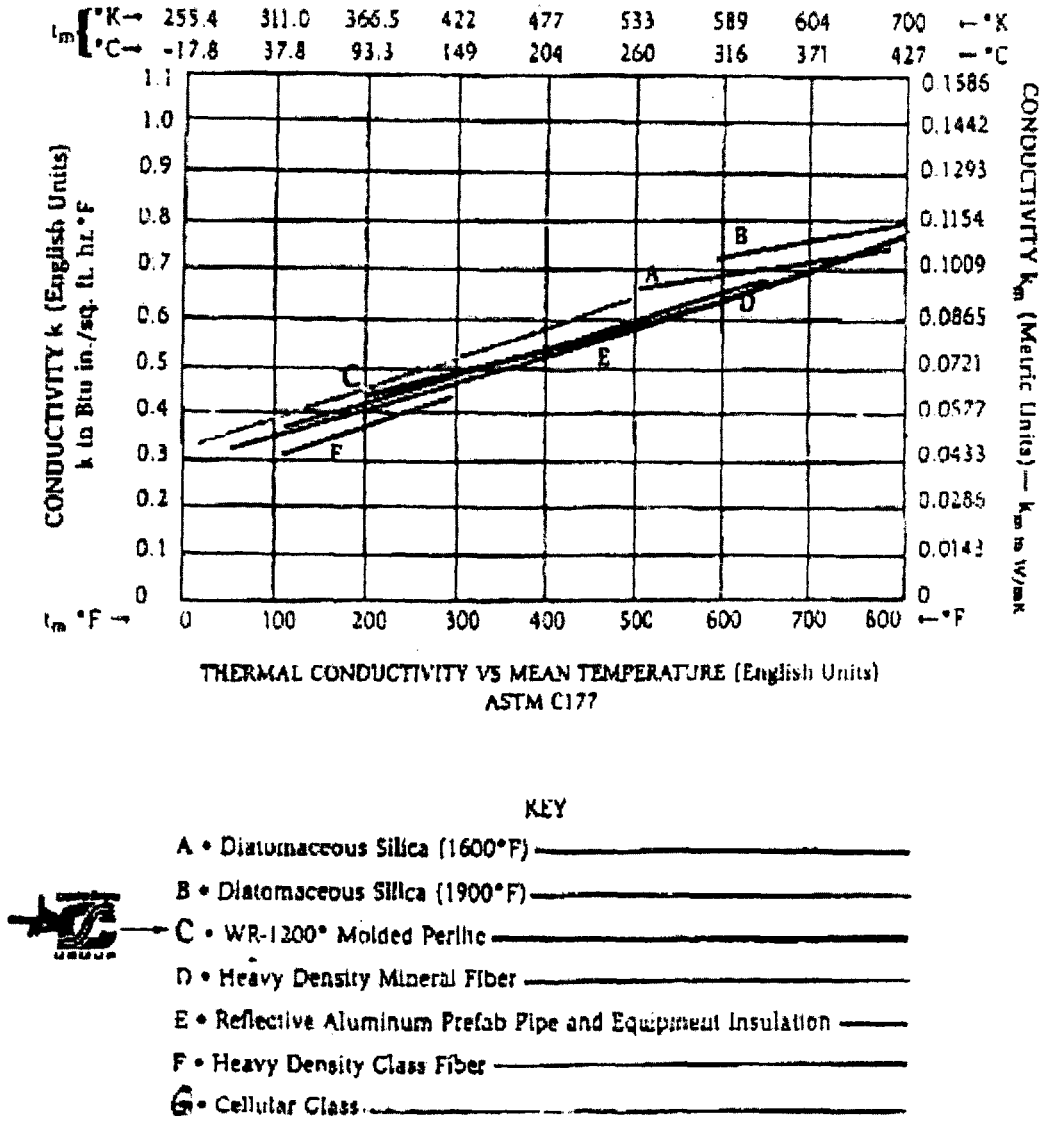

Figure 6.7 Thermal Conductivity of Insulation Materials as a Function of Temperature.

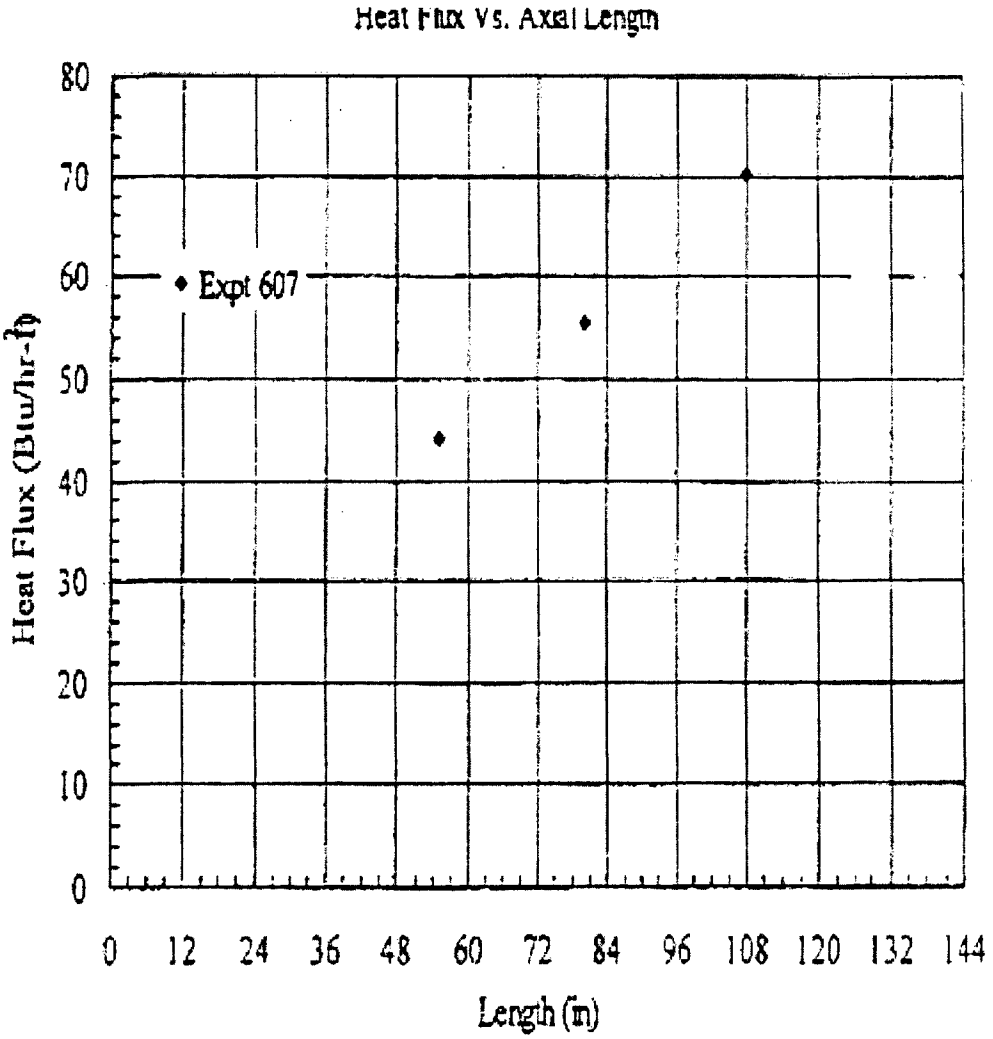

Figure 6.8 Heat Flux vs. Axial Length for Experiment 607.

Table 6.1 Differential Pressure Cell Layout Description

DP/Channel Number	Taps connection	Number of grids	Span		Calibration DP range	
			inch	mm	inch H_2O	mm H_2O
362	1-23	7	144	3657.6	0-250	0-6350
363	1-3	1	25	635	0-35	0-889
364	3-6	1	21	533.4	0-35	0-889
365	3-20	4	83	2018.2	0-120	0-3048
369	7-11	0 (Bare bundle)	14	355.6	0-25	0-635
373	11-16	1	18	457.2	0-30	0-762
379	17-20	0 (Bare bundle)	15	381	0-25	0-635
382	20-23	2	36	914.4	0-60	0-1524

Table 6.2 Calculation for Experiment 607

Elevation		Housing Temperature		Insulation Temperature		$k_{insulation}$		Heat Flux	
in	m	°F	°C	°F	°C	Btu/hr-ft-F	W/m-K	Btu/hr-ft^2	W/m^2
55	1.397	658	347.77	138	58.88	0.045	0.07788	70.2	221.43
78.78	2	566	296.66	139	59.44	0.0433	0.0749	55.47	17.585
108.43	2.754	463	239.44	103	39.44	0.0408	0.0706	44.063	13.968

Table 6.3 Current and Voltage Readings for Power Calculations

Test Section Voltage (V)	Offset (mV)	Actual Voltage (V)	Test Section Current (A)	Offset (A)	Actual Current (A)
3.84	48	3.792	650.6	118.7	531.9
4.92	50	4.87	792.6	118.2	674.4
5.01	40	4.97	804.12	118.9	685.22

Table 6.4 Elevation 1.419 m (55 in) - Heating Surface Temperature 348 degrees C (659 degrees F)

h (Btu/(hr-ft²-R))	h [W/(m²-K)]	Surface Temperature (F)	Surface Temperature [C]	Heat Flux (kW/ft²)	Heat Flux [kW/m²]	Percent Heat Loss (%)
0.1	[0.6]	446.0	[230.0]	0.0109	[0.1169]	6.34
0.2	[1.1]	347.1	[175.0]	0.0159	[0.1715]	9.29
0.3	[1.7]	289.8	[143.2]	0.0189	[0.2031]	11.00
0.4	[2.3]	252.4	[122.5]	0.0208	[0.2237]	12.12
0.5	[2.8]	226.1	[107.9]	0.0221	[0.2382]	12.91
0.6	[3.4]	206.6	[97.0]	0.0231	[0.2490]	13.49
0.7	[4.0]	191.6	[88.7]	0.0239	[0.2573]	13.94
0.8	[4.5]	179.6	[82.0]	0.0245	[0.2639]	14.30
0.9	[5.1]	169.9	[76.6]	0.0250	[0.2693]	14.59
1.0	[5.7]	161.8	[72.1]	0.0254	[0.2737]	14.83
1.1	[6.2]	155.0	[68.3]	0.0258	[0.2775]	15.03
1.2	[6.8]	149.2	[65.1]	0.0261	[0.2807]	15.21
1.3	[7.4]	144.2	[62.3]	0.0263	[0.2834]	15.36
1.4	[7.9]	139.8	[59.9]	0.0266	[0.2859]	15.49
1.5	[8.5]	135.9	[57.7]	0.0268	[0.2880]	15.60
1.6	[9.1]	132.5	[55.8]	0.0269	[0.2899]	15.71
1.7	[9.7]	129.4	[54.1]	0.0271	[0.2916]	15.80
1.8	[10.2]	126.7	[52.6]	0.0272	[0.2931]	15.88
1.9	[10.8]	124.2	[51.2]	0.0274	[0.2945]	15.95
2.0	[11.4]	121.9	[49.9]	0.0275	[0.2957]	16.02

Table 6.5 Elevation 2.0 m (78.78 in) - Housing Surface Temperature 297 degrees C (566 degrees F)

h (Btu/(hr-ft²-R))	h [W/(m²-K)]	Surface Temperature (F)	Surface Temperature [C]	Heat Flux (kW/ft²)	Heat Flux [kW/m²]	Percent Heat Loss (%)
0.1	[0.6]	387.5	[197.5]	0.0092	[0.0985]	5.34
0.2	[1.1]	304.1	[151.2]	0.0134	[0.1445]	7.83
0.3	[1.7]	255.9	[124.4]	0.0159	[0.1711]	9.27
0.4	[2.3]	224.4	[106.9]	0.0175	[0.1884]	10.21
0.5	[2.8]	202.3	[94.6]	0.0186	[0.2006]	10.87
0.6	[3.4]	185.9	[85.5]	0.0195	[0.2097]	11.36
0.7	[4.0]	173.2	[78.4]	0.0201	[0.2167]	11.74
0.8	[4.5]	163.1	[72.8]	0.0207	[0.2222]	12.04
0.9	[5.1]	154.9	[68.3]	0.0211	[0.2268]	12.28
1.0	[5.7]	148.1	[64.5]	0.0214	[0.2305]	12.49
1.1	[6.2]	142.4	[61.3]	0.0217	[0.2337]	12.66
1.2	[6.8]	137.5	[58.6]	0.0220	[0.2364]	12.81
1.3	[7.4]	133.3	[56.3]	0.0222	[0.2387]	12.93
1.4	[7.9]	129.6	[54.2]	0.0224	[0.2408]	13.04
1.5	[8.5]	126.3	[52.4]	0.0225	[0.2426]	13.14
1.6	[9.1]	123.4	[50.8]	0.0227	[0.2441]	13.23
1.7	[9.7]	120.8	[49.3]	0.0228	[0.2456]	13.30
1.8	[10.2]	118.5	[48.1]	0.0229	[0.2469]	13.37
1.9	[10.8]	116.4	[46.9]	0.0231	[0.2480]	13.44
2.0	[11.4]	114.5	[45.8]	0.0232	[0.2491]	13.49

Table 6.6 Elevation 2.75 m (108.43 in) - Housing Surfaces Temperature 239 degrees C (463 degrees F)

h (Btu/(hr-ft²-R))	h [W/(m²-K)]	Surface Temperature (F)	Surface Temperature [C]	Heat Flux (kW/ft²)	Heat Flux [kW/m²]	Percent Heat Loss (%)
0.1	[0.6]	321.9	[161.1]	0.0072	[0.0778]	4.22
0.2	[1.1]	256.1	[124.5]	0.0106	[0.1142]	6.18
0.3	[1.7]	217.9	[103.3]	0.0126	[0.1352]	7.32
0.4	[2.3]	193.1	[89.5]	0.0138	[0.1489]	8.07
0.5	[2.8]	175.6	[79.8]	0.0147	[0.1585]	8.59
0.6	[3.4]	162.6	[72.6]	0.0154	[0.1657]	8.98
0.7	[4.0]	152.6	[67.0]	0.0159	[0.1712]	9.28
0.8	[4.5]	144.6	[62.6]	0.0163	[0.1756]	9.51
0.9	[5.1]	138.2	[59.0]	0.0167	[0.1792]	9.71
1.0	[5.7]	132.8	[56.0]	0.0169	[0.1822]	9.87
1.1	[6.2]	128.3	[53.5]	0.0172	[0.1847]	10.00
1.2	[6.8]	124.4	[51.3]	0.0174	[0.1868]	10.12
1.3	[7.4]	121.0	[49.5]	0.0175	[0.1886]	10.22
1.4	[7.9]	118.1	[47.8]	0.0177	[0.1903]	10.31
1.5	[8.5]	115.5	[46.4]	0.0178	[0.1917]	10.38
1.6	[9.1]	113.3	[45.1]	0.0179	[0.1929]	10.45
1.7	[9.7]	111.2	[44.0]	0.0180	[0.1941]	10.51
1.8	[10.2]	109.4	[43.0]	0.0181	[0.1951]	10.57
1.9	[10.8]	107.7	[42.1]	0.0182	[0.1960]	10.62
2.0	[11.4]	106.2	[41.2]	0.0183	[0.1968]	10.66

7. CONCLUSIONS

The RBHT Test Facility has been designed as a flexible rod bundle separate-effects test facility which can be used to perform single-phase and two-phase experiments under well-controlled laboratory conditions to generate fundamental reflood heat transfer data. The facility is capable of operating in both forced and variable reflood modes covering wide ranges of flow and heat transfer conditions at pressures up to 0.402 MPa (60 psia). It is heavily instrumented that meets all the instrumentation requirements developed in the RBHT Program. It can be used to conduct all types of the planned experiments according to the test matrix developed under Task 9 of the RBHT Test Plan and Design Report. It is considered that the RBHT Test Facility with its robust instrumentation represents a unique NRC facility for the in-depth studies of the highly ranked reflood phenomena identified in the RBHT Program's Phenomena Identification and Ranking Table (PIRT) and will produce the data and analysis needed to refine reflood heat transfer models in the current safety analysis computer codes.

8. REFERENCES

1. Denham, M.K., D. Jowitt, and K.G. Pearson, "ACHILLES Unballooned Cluster Experiments, Part 1: Description of the ACHILLES Rig, Test Section, and Experimental Procedures," AEEW- R2336, Winfrith Technology Centre (Commercial in Confidence), Nov. 1989.

2. Denham, M.K. and K.G. Pearson, "ACHILLES Unballooned Cluster Experiments, Part 2: Single Phase Flow Experiments," AEEW-R2337, Winfrith Technology Centre (Commercial in Confidence), May 1989.

3. Pearson, K.G. and M.K. Denham, "ACHILLES Unballooned Cluster Experiments, Part 3: Low Flooding Rate Reflood Experiments," AEEW- R2339, Winfrith Technology Centre (Commercial in Confidence), June 1989.

4. Pearson, K.G. and M.K. Denham, "ACHILLES Unballooned Cluster Experiments, Part 4: Low Pressure Level Swell Experiments," AEEW- R2339, Winfrith Technology Centre Commercial in Confidence), July 1989.

5. Dore, P. and M.K. Denham, "ACHILLES Unballooned Cluster Experiments, Part 5: Best Estimate Experiments," AEEW-R2412, Winfrith Technology Centre (Commercial in Confidence), July 1990.

6. Dore, P. and D.S. Dhuga, "ACHILLES Unballooned ClusterExperiments, Part 6: Flow Distribution Experiments," AEA-RS-1064, Winfrith Technology Centre (Commercial in Confidence), December 1991.

7. Rehme, K., "Pressure Drop Correlations for Fuel Element Spacers", Nuclear Technology, Vol. 17, pp 15-23, January 1973.

APPENDIX A. RBHT TEST FACILITY COMPONENTS DETAILED MECHANICAL DRAWINGS

NOTE: Electronic copies of these drawings are included in a CD listed in Appendix G.

DRAWING NUMBER (CD File No.)	TITLE
B114306	Bellvile Washer
C114245	Pressure Gasket
C114246	Window Flange
C114247	Window
C114248	Window Stud Fixture
C114255	Cushion Gasket
C114282	Flange Modification - Upper Plenum
C114295	Lower Plenum Seal Sleeve Retaining Plate
C114296	Heater Rod Seal Sleeve
C114298	Low Melt Reservoir
C114318	Grip Strap -A-
C114319	Grid Strap -B-
C115077	Steam Probe Rake Mounting Flange
C115132	Drain Tube
C118336	Traversing Steam Probe
D114249	Flange Modification Bottom - Housing Assembly
D114279	Flange Modification Top - Housing Assembly
D114290	Housing Extension
D114291	Exhaust Baffle
D114293	Lower Plenum Flow Baffle

D114294	Seal Plate Lower Plenum
D114297	G-10 Isolation Plate
D114299	Reservoir Connector Assembly
D114301	Unheated Rod (Support Rod)
D114320	Grid Matrix
D114345	Schematic Test Facility
D114366	Seal Sleeve Extractor
D114369	Stem Separator Drain Tank
D114371	Small Carry-over Tank
D115075	Steam Probe Rake Assembly
D115076	Steam Probe Rake Tube
D1150261, L115260	Grid Assembly, List of Drawings and Parts
D115262	Outer Grid -A-
D115263	Outer Grid - B-
D115264	Outer Grid - C-
D115265	Outer Grid - D-
D115266	Inner Grid - A-
D115267	Inner Grid - B-
D115268	Inner Grid - C-
D115269	Inner Grid - D-
D115346	Drawing Tree
D115347	Skirt Steam Separator
D115587	Water Inlet Piping - sht. 1
D115587 - sht. 2	Water Inlet Piping - sht. 2
D115597	Exhaust Line Piping - sht. 1

D115597 - sht. 2	Exhaust Lint Piping - sht. 1
D115640	Steam By-pass Line Piping - sht. 1
D115640 - sht. 2	Steam By-pass Line Piping - sht. 2
D118337	Automatic Traverse Mechanism (Steam Probe Rake)
D118339	Droplet Injection System
E114243, L114242	Assembly (Housing), List of Drawings and Parts
E114244	Weldment Test Section - sht. 1
E114244 - sht. 2	Weldment Test Section - sht. 2
E114281	Upper Plenum Assembly
E114278	Nickel Ground Plate
E114292	Lower Plenum Assembly
E114302	Heater Rod
E114343	Pressure Oscillation Damping Tank
E114346	Window Test Fixture
E114370	Large Carryover Tank
E114372	Strong back Assembly
E115002	Water Supply Tank
E115016	Steam Separator Tank
E115073	Test Section Instrumentation
E115348, L115345	Building Arrangement - sht. 1, List of Drawings and Parts
E115348 - sht. 2	Building Arrangement - sht. 2
E115615	Mezzanine Frame Work - sht. 1
E115615 - sht. 2	Mezzanine Frame Work - sht. 2
E115615 - sht. 3	Mezzanine Frame Work - sht. 3

E115615 - sht. 4	Mezzanine Frame Work - sht. 4
E118338	Flow Housing Differential Pressure Instrumentation
E118340	Heater Road Bundle Grip Temperature Instrumentation
E114287, L114280	Upper Plenum, List of Drawings and Parts
L114287	Flow Housing, List of Drawings and Parts
L115260	Rod Grid Assembly, List of Drawings and Parts
R114288	Flow Housing Assembly, Reference Drawing
E118341	Heater Rod Bundle Temperature Instrumentation

APPENDIX B. RBHT TEST FACILITY COMPONENTS MEASURED VOLUMES AND FLOW AREAS

The volumes and flow areas were measured for the following components and summarized in Table B.1:

1. Water Supply Tank
2. Flow Housing
3. Upper Plenum
4. Lower Plenum
5. Large Carryover Tank
6. Small Carryover Tank
7. Pressure Oscillation Damping Tank
8. Steam Separator Drain Tank
9. Grids and Bare Heater Rod Bundle

The Steam Separator volume measurements are not reported because the results were not reliable and should be repeated.

The components volumes and flow areas are essential for calculating the Mass and Energy Balances around each component and consequently the validation of the test results.

The volumes and flow areas were determined by weighing the water drained from each component at various elevation increments into a weight tank placed on a weighing scale platform as shown schematically in Figure B.1.

Each water weight was converted into a water volume as follows:

$$V_i = W_i \times v_i \text{ @ } T_i \times 1728 \text{ in}^3/\text{ft}^3$$

where

V_i water volume, in^3
W_i water weight, lbs
v_i specific volume at T_i
T_i water temperature, degrees F

The corresponding flow areas were calculated as follows:

$$A_i = V_i \times 1/\Delta L_i$$

where

A_i flow area, in^2
V_i water volume, in^3
ΔL_i change in elevation, in

The results are presented in table and graphic forms as listed in Table B.1.

Except for the Flow Housing all the components are cylindrical and should have uniform flow area. However, most of them have internal parts and inlet/outlet nozzles which contribute to less or additional water volumes resulting in Flow Areas variations.

Table B.1 Component Volumes and Flow Areas

Component	Table No.	Figure No.
Water Supply Tank	B.2	B.2, B.3
Flow Housing	B.3	B.4, B.5
Upper Plenum	B.4	B.6, B.7
Lower Plenum	B.5	B.8, B.9
Large Carryover Tank	B.6	B.10, B.11
Small Carryover Tank	B.7	B.12, B.13
Pressure Oscillation Damping Tank	B.8	B.14, B.15
Steam Separator Drain Tank	B.9	--
Grids and Bare Heater Rod Bundle	B.10	--

Table B.2 Water Supply Tank Volumes and Flow Areas

Elevation m	ΔL m	Water Volume m^3	Cumulative Volumes m^3	Flow Area m^2
0	0	0	0	0
0.149352	0.149352	0.00931	0.00930671	0.062368
0.255778	0.106426	0.0286	0.03790787	0.268903
0.484378	0.2286	0.02134	0.05924399	0.093342
0.67818	0.18542	0.05448	0.10635418	0.281316
0.87503	0.19685	0.05446	0.16819109	0.27667
1.068832	0.193802	0.05448	0.22266956	0.28129
1.262634	0.193802	0.05448	0.27714802	0.28129
1.45796	0.195326	0.05448	0.33162649	0.278999
1.653286	0.195326	0.05448	0.3861102	0.278999
1.843786	0.1905	0.05443	0.4405418	0.285728
2.039112	0.195326	0.05443	0.4949734	0.278761
2.232914	0.193802	0.05447	0.549444	0.281245
2.426716	0.193802	0.05447	0.6039146	0.281245
2.61874	0.192024	0.05447	0.6583852	0.283574
2.812542	0.193802	0.05447	0.7128558	0.281245
2.909316	0.096774	0.02724	0.7400911	0.276709
3.00609	0.096774	0.02724	0.7673264	0.276709
3.102864	0.096774	0.02724	0.7945617	0.281432
3.198114	0.09525	0.02724	0.821797	0.285935
3.293364	0.096774	0.02724	0.8490323	0.281245
3.390138	0.096774	0.02724	0.8762676	0.281245
3.486912	0.096774	0.02724	0.9035029	0.281245
3.586988	0.100076	0.02724	0.9307382	0.270206
3.696462	0.109474	0.02224	0.95297545	0.203187

Total Volume = 251.75 Gallons ($0.95297545 m^3$)

Table B.3 Flow Housing Volumes and Flow Areas Among Pressure Taps

Span Press Tap – Press Tap	Height (m)	Volume (m^3)	Flow Area (m^2)	Cumulative Volumes (m^3)	Elevation (m)	Grid Location
Bottom Flange-No.1	0.1588	0.000729978	0.459741	0.0007292	0.15875	
1-2	0.3302	0.001600951	0.484838	0.0023302	0.48895	No. 1
2-3	0.3048	0.00150235	0.492902	0.0038329	0.79375	
3-4	0.3048	0.001431902	0.469935	0.0052652	1.09855	No. 2
4-5	0.1524	0.000746955	0.490128	0.0060124	1.25095	
5-6	0.0762	0.00039891	0.523483	0.0064106	1.32715	
6-7	0.1778	0.000910056	0.51187	0.0073201	1.50495	No. 3
7-8	0.0953	0.000441549	0.463547	0.0077609	1.6002	
8-9	0.0826	0.000404302	0.489741	0.0081657	1.68275	
9-10	0.0762	0.000370298	0.485935	0.008536	1.75895	
10-11	0.1016	0.000517864	0.509676	0.0090539	1.86055	
11-12	0.127	0.000563289	0.443548	0.0096176	1.98755	No. 4
12-13	0.0762	0.000340703	0.447096	0.0099584	2.06375	
13-14	0.0762	0.000342064	0.448902	0.0103009	2.13995	
14-15	0.0762	0.000392945	0.515676	0.0106942	2.21615	
15-16	0.1016	0.000532285	0.52387	0.0112268	2.31775	
16-17	0.2032	0.001012786	0.498451	0.0122395	2.52095	No. 5
17-18	0.108	0.000511047	0.473418	0.0127508	2.6289	
18-19	0.0635	0.000250296	0.394193	0.0130015	2.7051	
19-20	0.2271	0.001254676	0.552709	0.0142567	2.91998	
20-21	0.3096	0.001362339	0.440064	0.0156185	3.2291	No. 6
21-22	0.3145	0.001583564	0.503805	0.0172015	3.54355	No. 7
22-23	0.2111	0.000915349	0.433418	0.0181175	3.75463	
23-TopFlange	0.2002	0.000983945	0.491935	0.0191008	3.95478	

Total Volume = 5.05 gallons (0.0191008 m^3)

* The elevation was measured from the bottom of the rod bundle corresponding to a lower tap location. An elevation where a grid is placed in the table does not mean that the grid is located at that elevation. It means that a grid is located within that DP span.

Table B.4 Upper Plenum Volumes and Flow Areas

Elevation (m)	ΔL (m)	Volume (m^3)	Cumulative Volumes (m^3)	Flow Area (m^2)
0.0826	0.083	1.728	1.7281798	2.0935
0.1323	0.05	0.888	2.6165225	1.0761
0.1483	0.016	0.834	3.4607879	5.2555
0.1626	0.014	0.996	4.4467937	6.971
0.2055	0.043	1.017	5.463611	2.3723
0.2372	0.032	1.08	5.5604586	3.4019
0.2832	0.046	1.005	7.5483733	2.1819
0.3449	0.062	1.016	8.5648629	1.6472
0.38	0.035	1.001	9.5662764	2.8677

Table B.5 Lower Plenum Volumes and Flow Areas

Elevation (m)	ΔL (m)	Volume (m^3)	Cumulative Volumes (m^3)	Flow Area (m^2)
0	0	0	0	0
0.0508	0.508	0	0.001	0.01957
0.22225	0.17145	0.005	0.0058	0.02823
0.381	0.15875	0	0.0066	0.0046

Table B.6 Large Carryover Tank Volumes and Flow Areas

Elevation (m)	ΔL (m)	Volume (m^3)	Cumulative Volumes (m^3)	Flow Area (m^2)
0	0	0	0	0
0.2159	0.2159	0.002	0.0023	0.0036
0.47777	0.26187	0.002	0.0045	0.0085
0.74778	0.27026	0.002	0.0068	0.0083
1.02235	0.27457	0.002	0.0091	0.0083
1.2954	0.2771	0.002	0.01137	0.0084
1.56362	0.26822	0.002	0.01365	0.0087
2.19227	0.62865	0.002	0.01592	0.01053

Water Temperature 24.44 degrees C (76 degrees F)
Total Volume = 0.0159213 m^3 (4.206 gallons) (0.562 ft^3)

Table B.7 Small Carryover Tank Volumes and Flow Areas

Elevation (m)	ΔL (m)	Volume (m^3)	Cumulative Volumes (m^3)	Flow Area (m^2)
0	0	0	0	0
0.20955	0.20955	0	0	0.00041(*)
0.28423	0.0747	0.0002	0.0002	0.00152
0.40005	0.11582	0.0002	0.0004	0.00161
0.49682	0.0968	0.0002	0.0006	0.00178
0.59995	0.10312	0.0001	0.0007	0.00167
0.72847	0.12852	0.0003	0.001	0.00169
0.8476	0.11913	0.00015	0.00115	0.00168
0.97155	0.12395	0.00023	0.00138	0.00183(**)

Water Temperature 24.44 degrees C (76 degrees F)
Total Volume = 0.001379 m^3 (0.364 gallons), (0.049 ft^3)

* includes 1 in drain and shut-off valve
** includes water drain from 1 in inlet tube

Table B.8 Pressure Oscillation Damping Tank Volumes and Flow Areas

Elevation (m)	ΔL (m)	Volume (m^3)	Cumulative Volumes (m^3)	Flow Area (m^2)
0	0	0	0	0
0.1651	0.1651	0.0136	0.01364	0.08587
0.42393	0.25883	0.025	0.03864	0.09432
0.7112	0.45237	0.0273	0.06589	0.09484
0.79223	0.33985	0.007	0.07316	0.08981
1.09703	0.32283	0.0273	0.400422	0.08942
1.40818	0.31115	0.0273	0.12768	0.08761
1.70358	0.2954	0.0272	0.154914	0.09226
2.0193	0.31572	0.0272	0.182147	0.08619
2.0955	0.0762	0.009	0.191452	0.12213
2.1369	0.0414	0.004	0.195309	0.09348
2.2098	0.0729	0.007	0.202118	0.09323
2.302	0.0922	0.007	0.208925	0.04468

Water Temperature 17.77 degrees C (64 degrees F) Average
Room Temperature 18.33 degrees C (65 degrees F)
Total Volume = 0.289252 m^3 (55.2 gallons) (7.38 ft^3)

Table B.9 Grid and Bare Heater Rod Bundle Volumes and Flow Areas

Location	ΔL* (m)	Volume (m^3)	Cumulative Volumes (m^3)	Flow Area** (m^2)
Grid No. 4	0.04775	0.0002	0.0002	0.00419
Bare Rod Bundle	0.48108	0.00234	0.00254	0.00487
Grid No. 3	0.04775	0.00019	0.00273	0.00408
Bare Rod Bundle	0.47142	0.00233	0.00506	0.00495
Grid No. 2	0.04445	0.0002	0.00526	0.00451
Bare Rod Bundle	0.55575	0.00265	0.00821	0.00477

Water Temperature 17.22 degrees C (63 degrees F)
Average Grid Flow Area+ = 4264.5 mm^2 (6.61 in^2) (including the mixing vanes)
Average Bundle Flow Area = 4864.5 mm^2 (7.54 in^2)

* This is the width of each grid.

** This refers to the cross-sectional flow area through the bundle.

+ Grids No. 5 to 7 are identical to Grids No. 2 to 4, respectively, whereas Grid No. 1 has a flow area very close to the average grid flow area. Grids No. 2 to 4 were used as an example to show the average grid flow area as compared to the average bundle flow area.

Table B.10 Steam Separator Drain Tank Volumes and Flow Areas

Elevation (m)	ΔL (m)	Volume (m^3)	Cumulative Volumes (m^3)	Flow Area (m^2)
0	0	0	0	0
0.61925	0.61925	0.00182(1)	0.00182	0.0029
1.21107	0.59182	0.0045	0.00635	0.0077
1.80645	0.59538	0.0045	0.010888	0.0076
2.10007	0.29362	0.0023	0.013156	0.0077

Room Temperature 22.77 degrees C (73 degrees F)
Water Temperature 23.88 degrees C (75 degrees F)

(1) includes the drain line

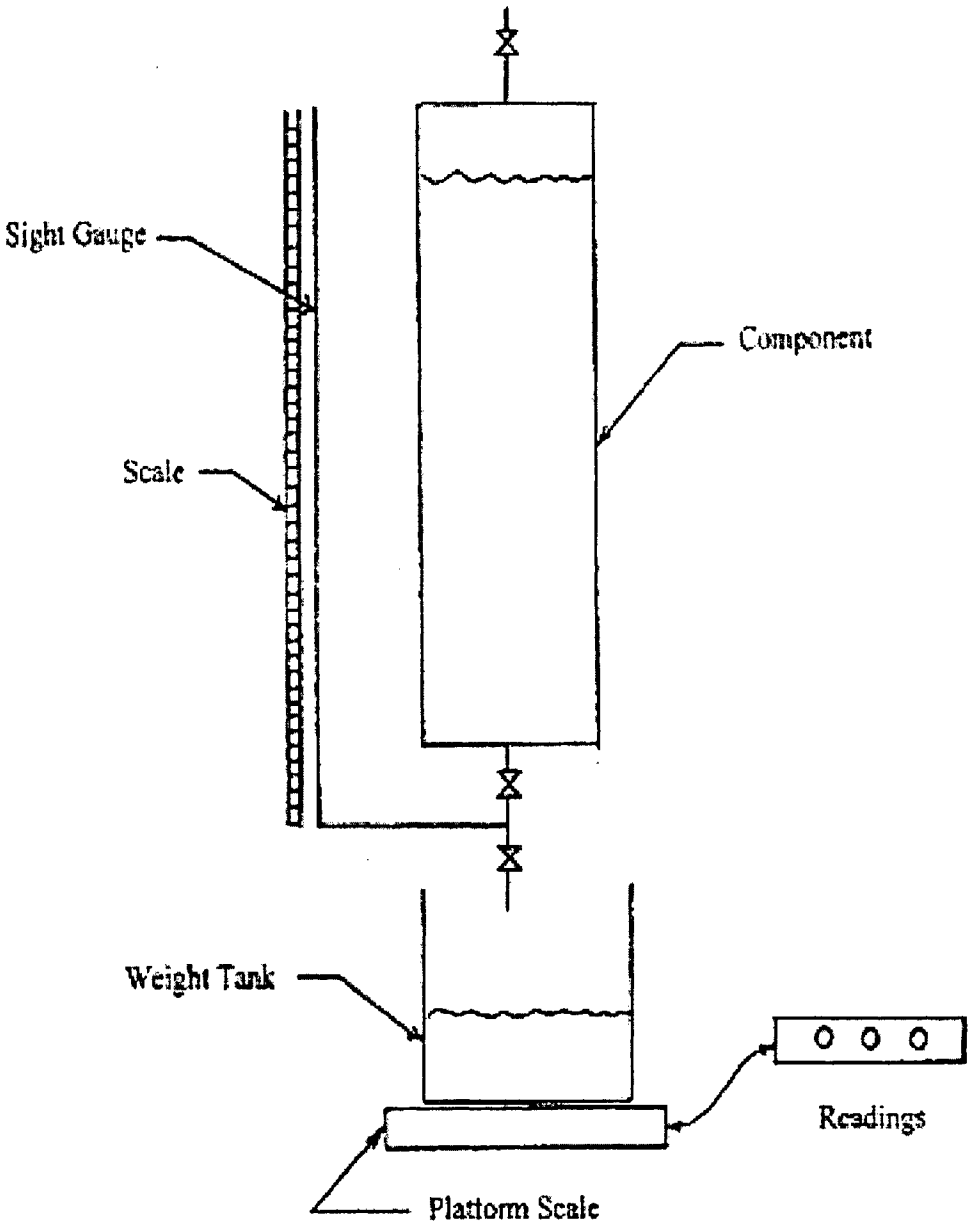

Figure B.1. Volume and Flow Area Measuring Test Schedule.

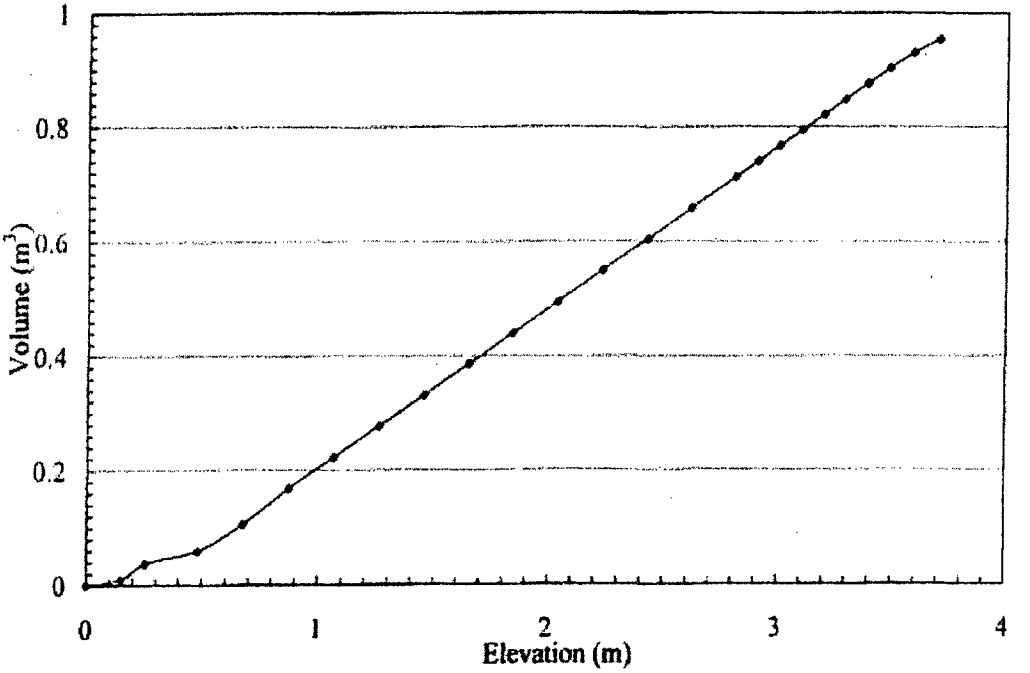

Figure B.2. Water Supply Tank Volume Measurements.

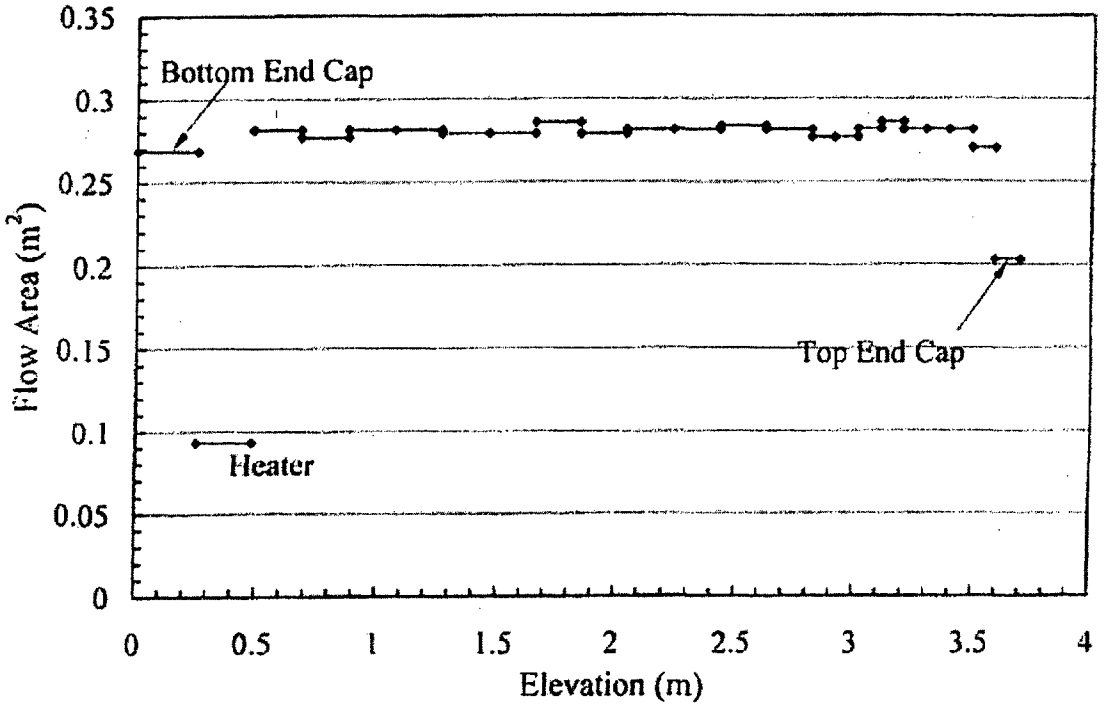

Figure B.3. Water Supply Tank Flow Areas.

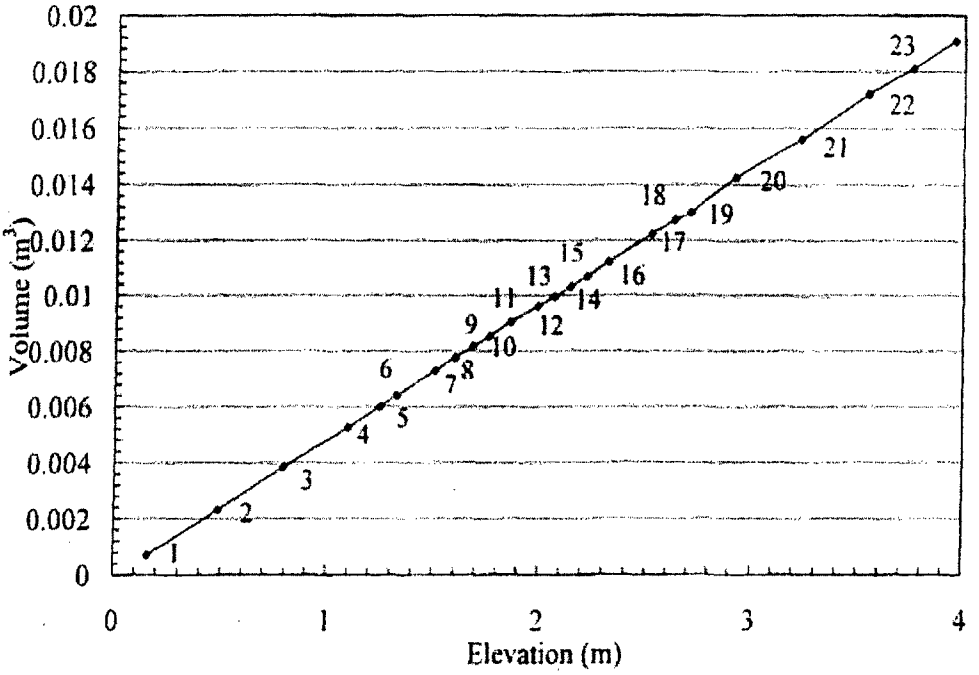

Figure B.4. Flow Housing Volumes Between Pressure Taps.

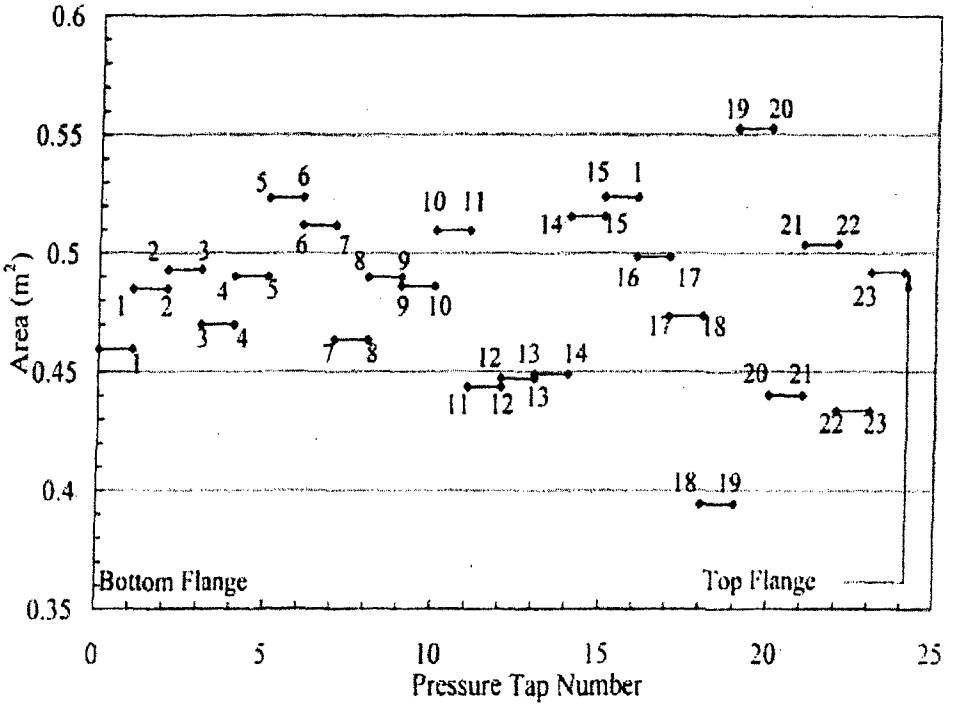

Figure B.5. Flow Housing Areas Between Pressure Taps.

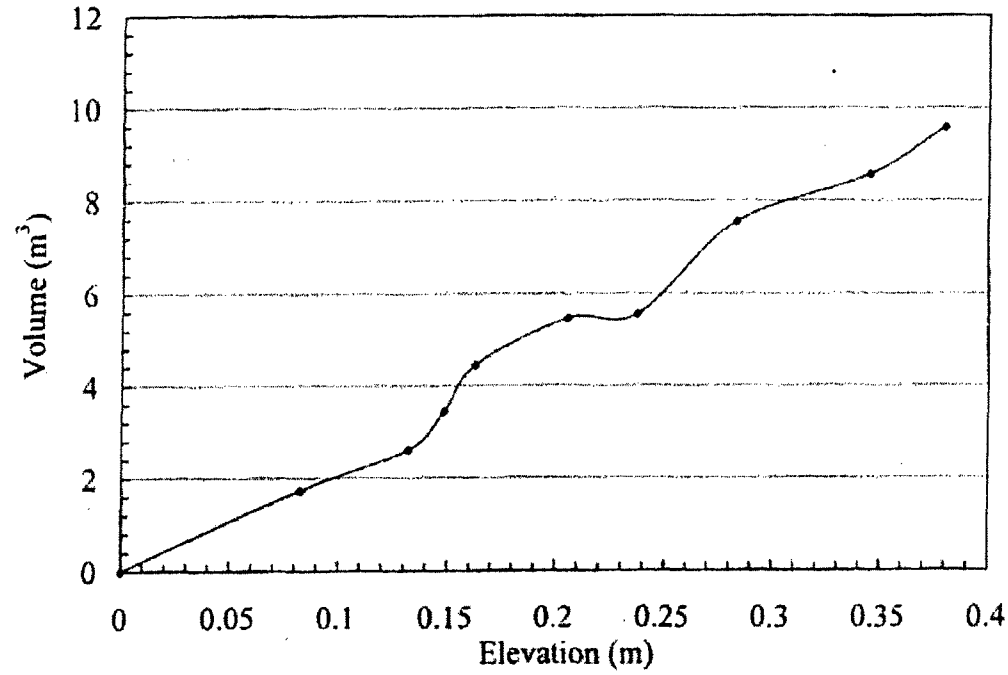

Figure B.6. Upper Plenum Volume Measurements.

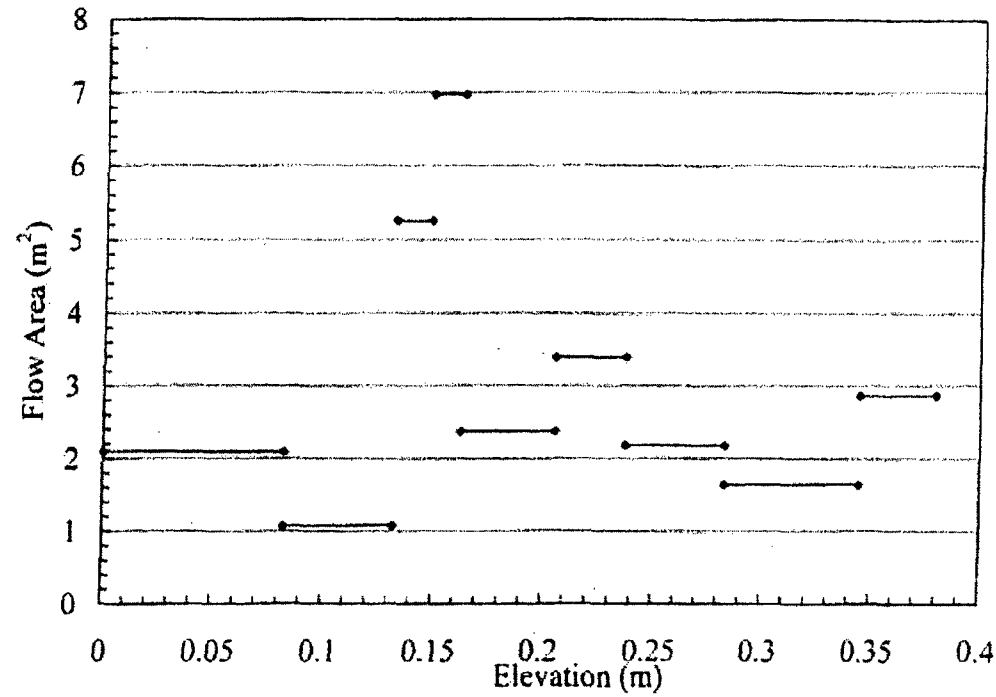

Figure B.7. Upper Plenum Flow Areas.

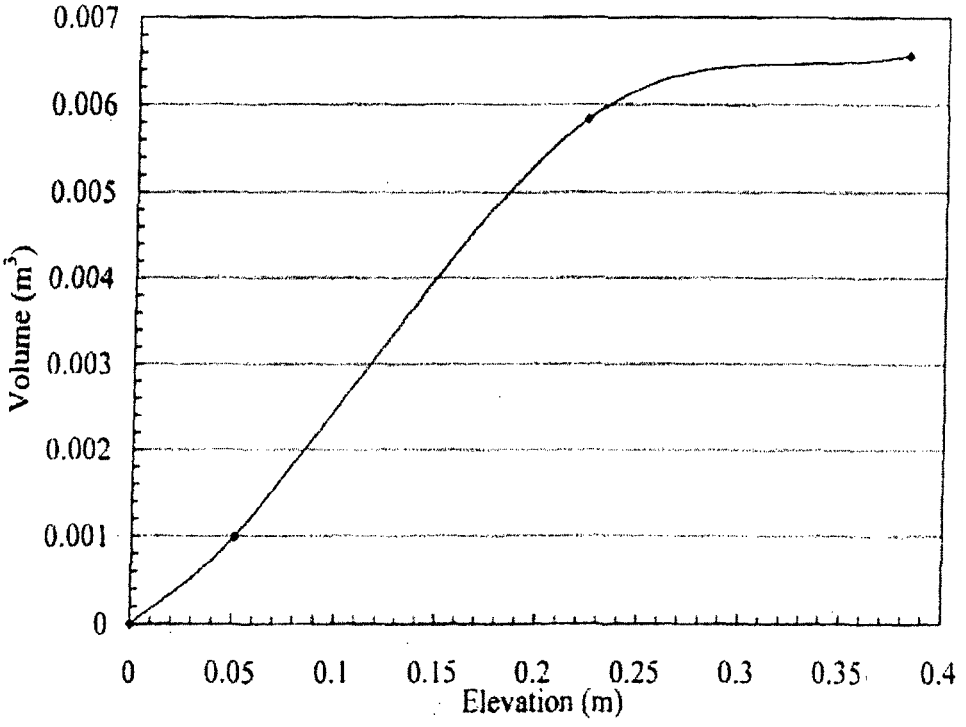

Figure B.8. Lower Plenum Volume Measurements.

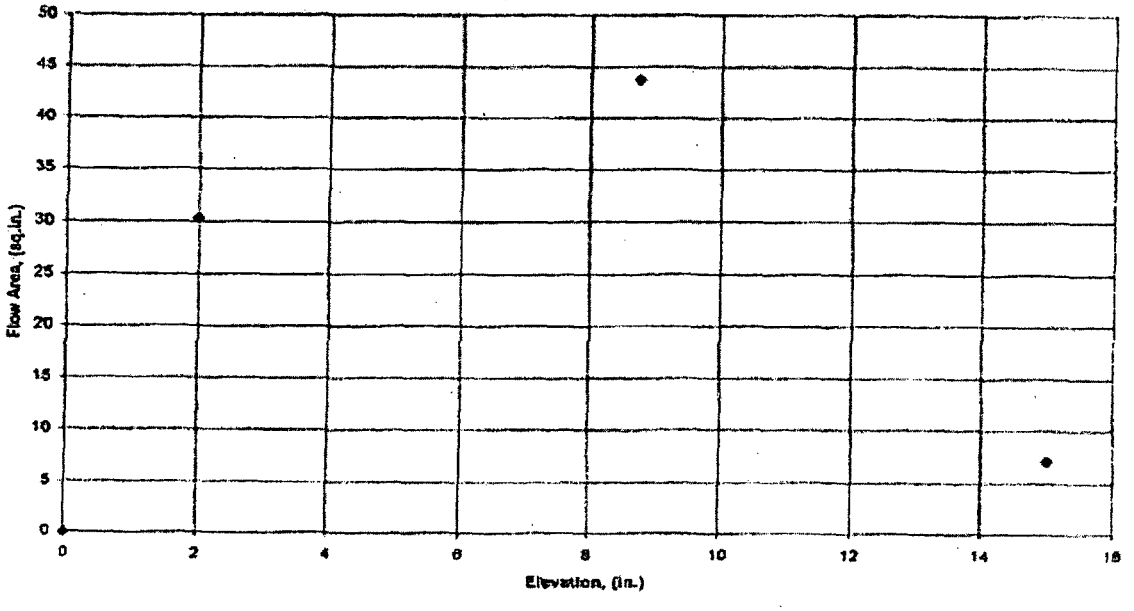

Figure B.9. Lower Plenum Flow Areas.

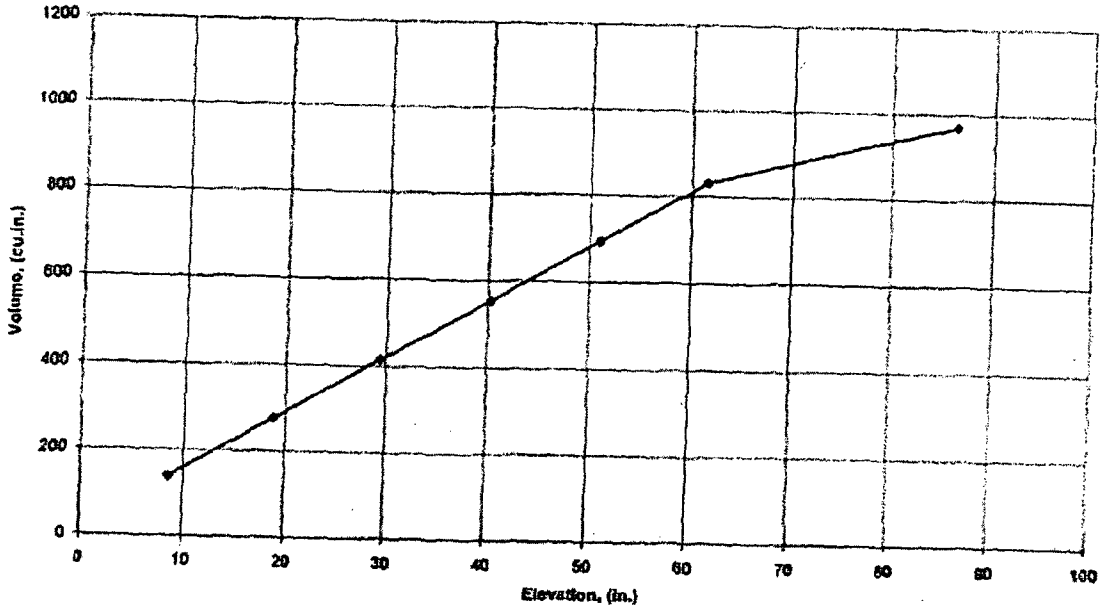

Figure B.10. Large Carryover Tank Volume Measurements.

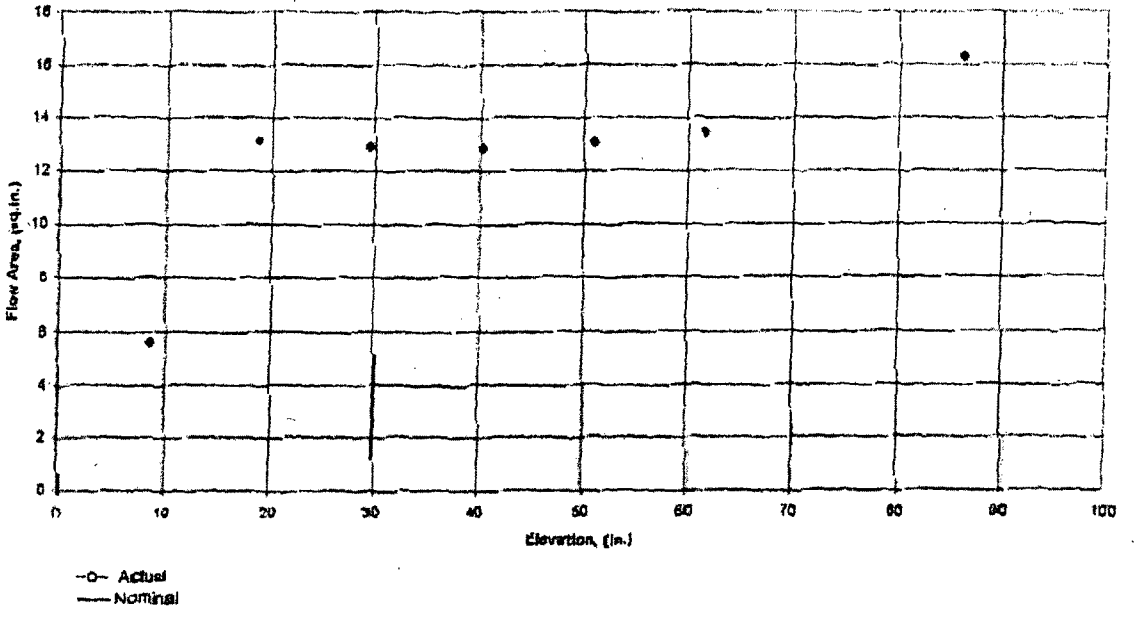

Figure B.11. Large Carryover Tank Flow Areas.

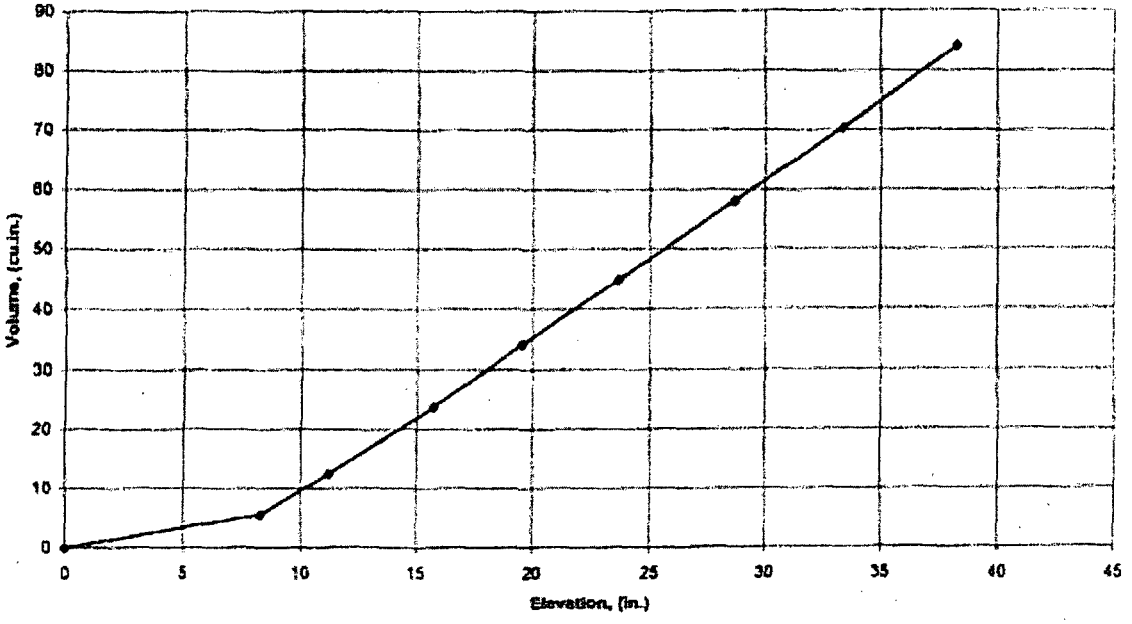

Figure B.12. Small Carryover Tank Volume Measurements.

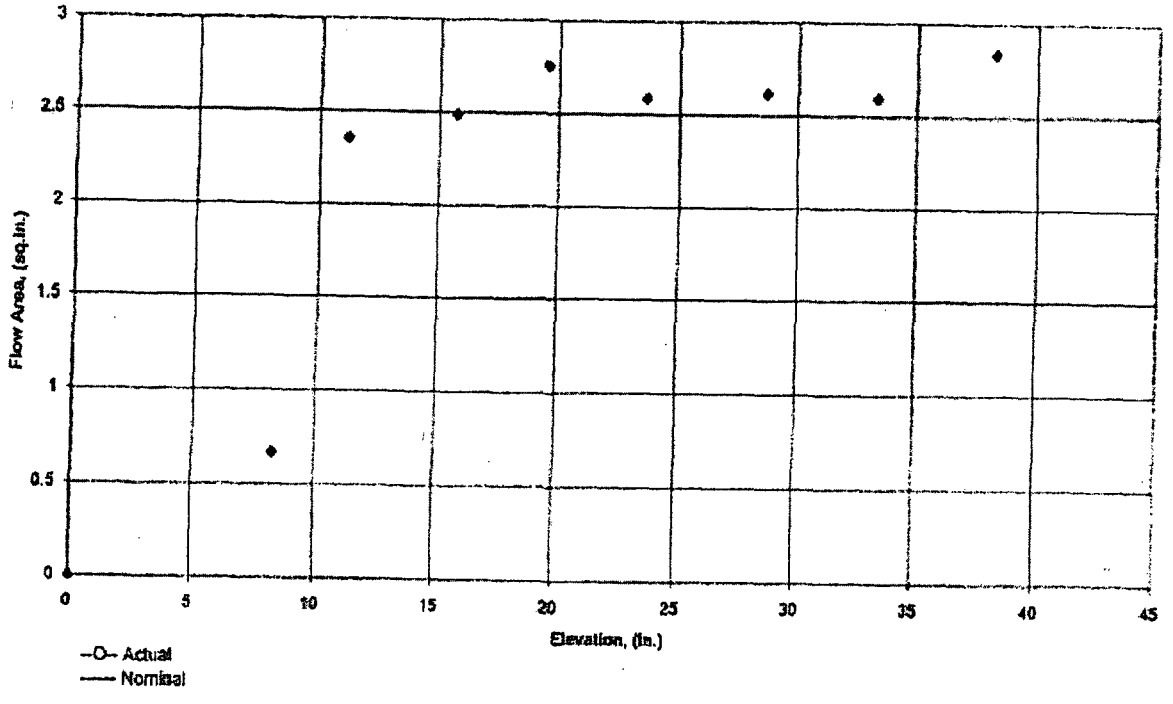

Figure B.13. Small Carryover Tank Flow Areas.

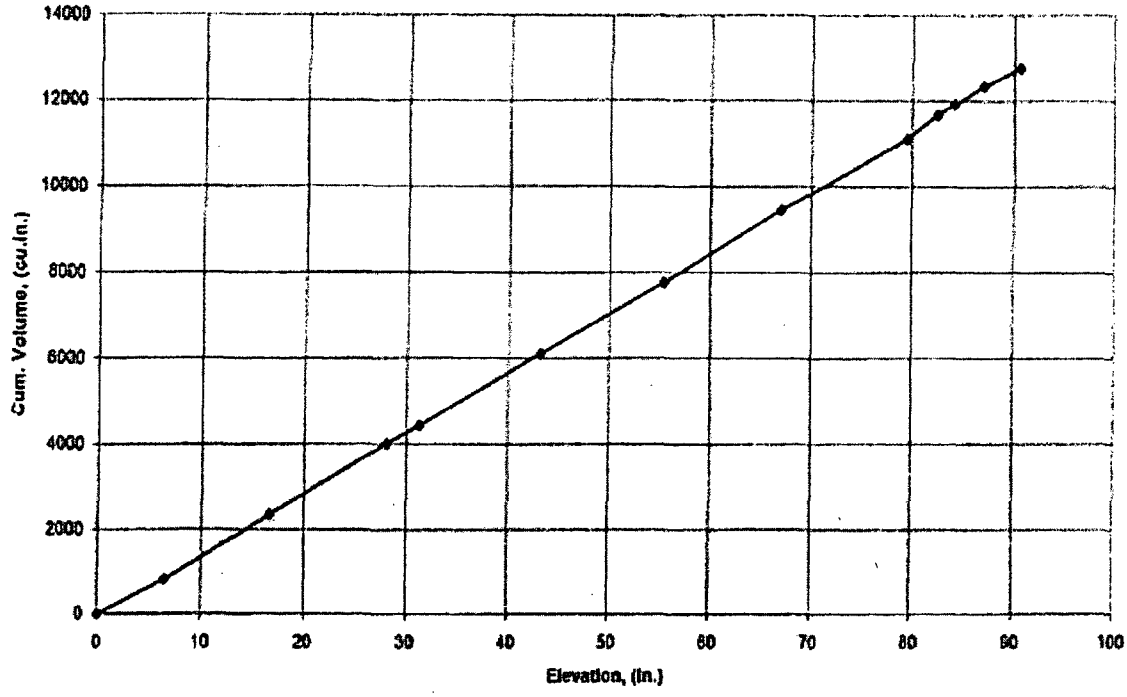

Figure B.14. Pressure Oscillation Damping Tank Volume Measurements.

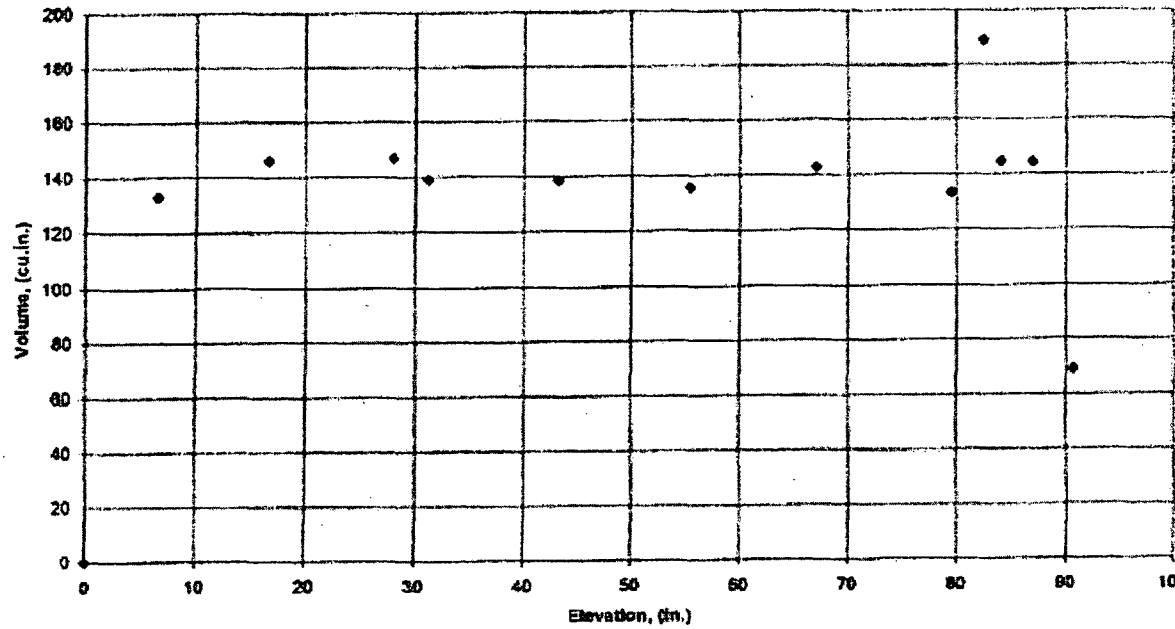

Figure B.15. Pressure Oscillation Damping Tank Flow Areas.

APPENDIX C. RBHT TEST FACILITY PHOTOGRAPHS

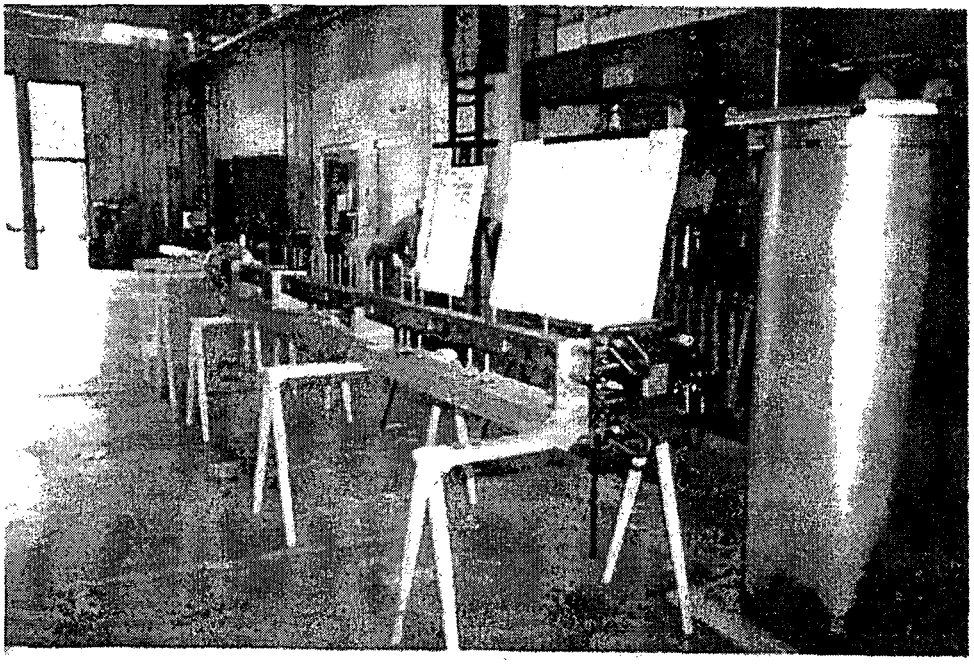

Photograph C.1 Flow Housing with the Heater Rod Bundle and the Ground Nickel Plate.

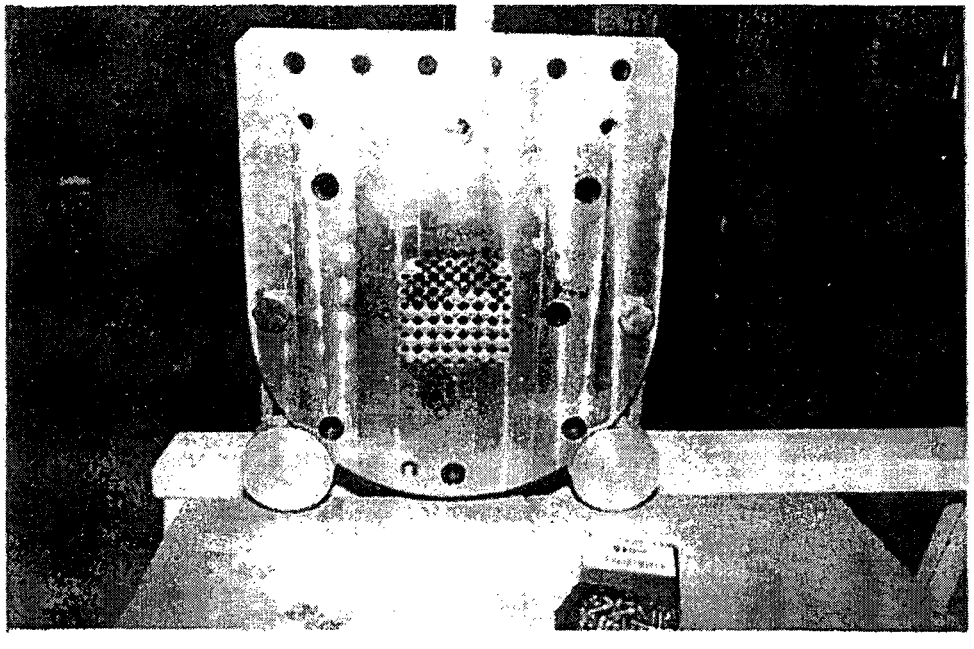

Photograph C.2 Ground Nickel Plate and Heater Rods Connection.

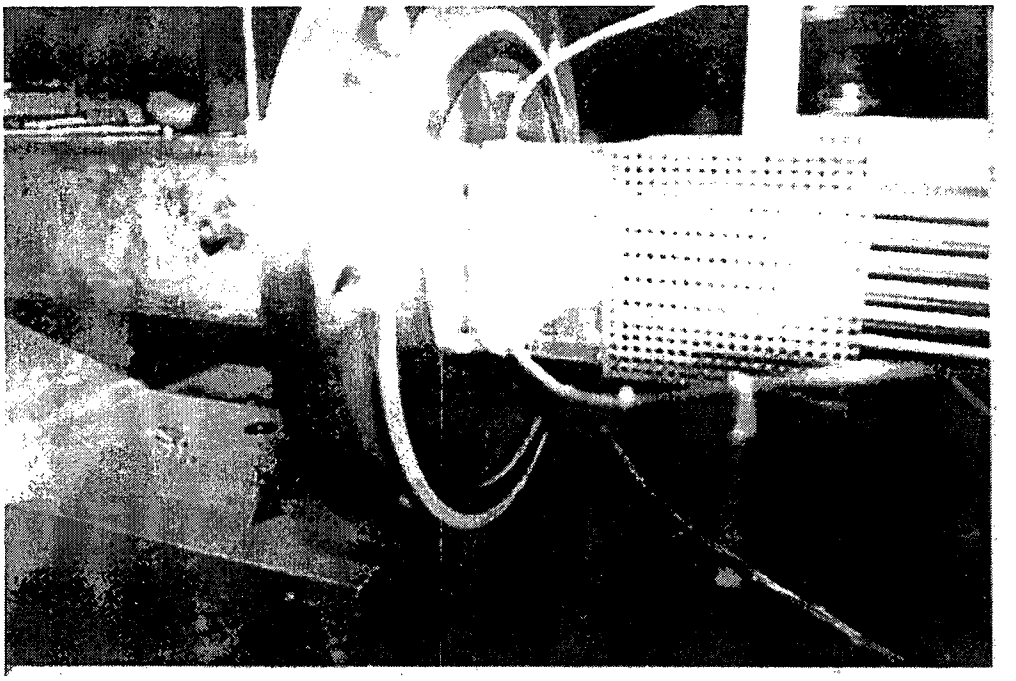

Photograph C.3 Flow Housing Bottom Extension Flow Baffle, Heater Rod Bottom Extensions, and Grid and Support Rod Thermocouple Extensions.

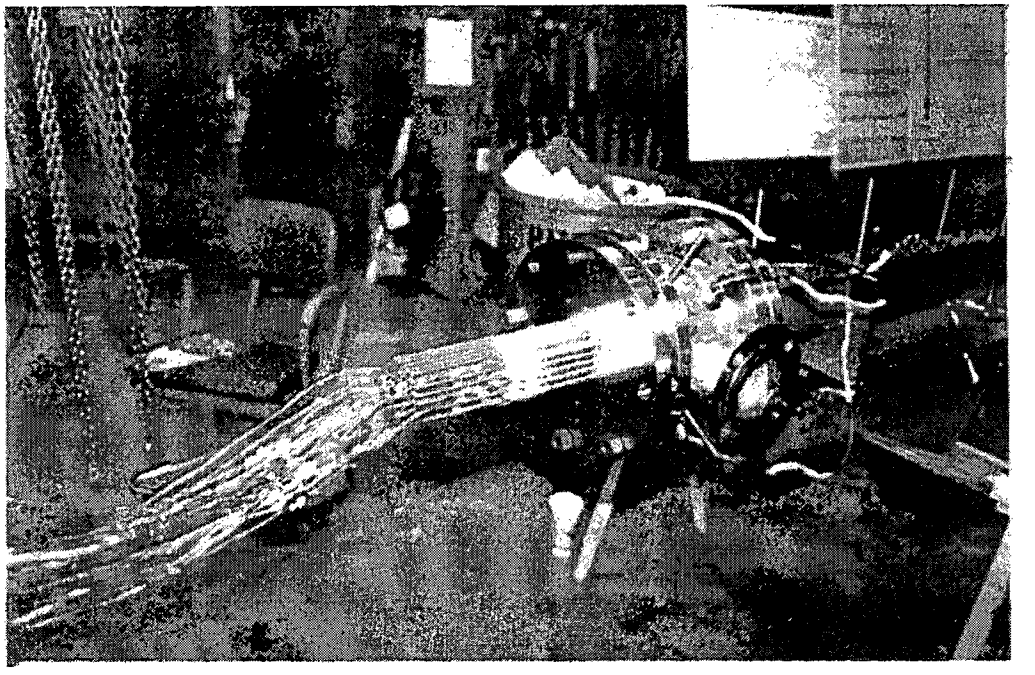

Photograph C.4 Lower Plenum Heater Rod Sealing Plate, Heater Rod Bottom Extensions and Thermocouples Extension Wires.

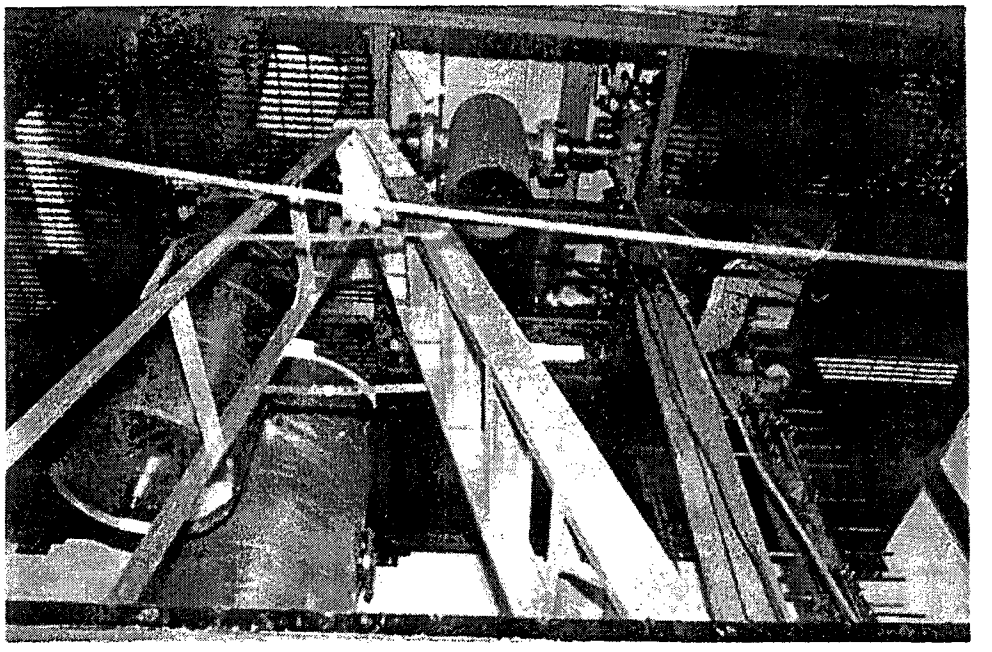

Photograph C.5 Installation of the Test Facility Components from Right to Left: Flow Housing and Support Fixture, Steam Separator, Pressure Oscillation Damping Tank, Water Injection Supply Tank, and the Mezzanine Structure.

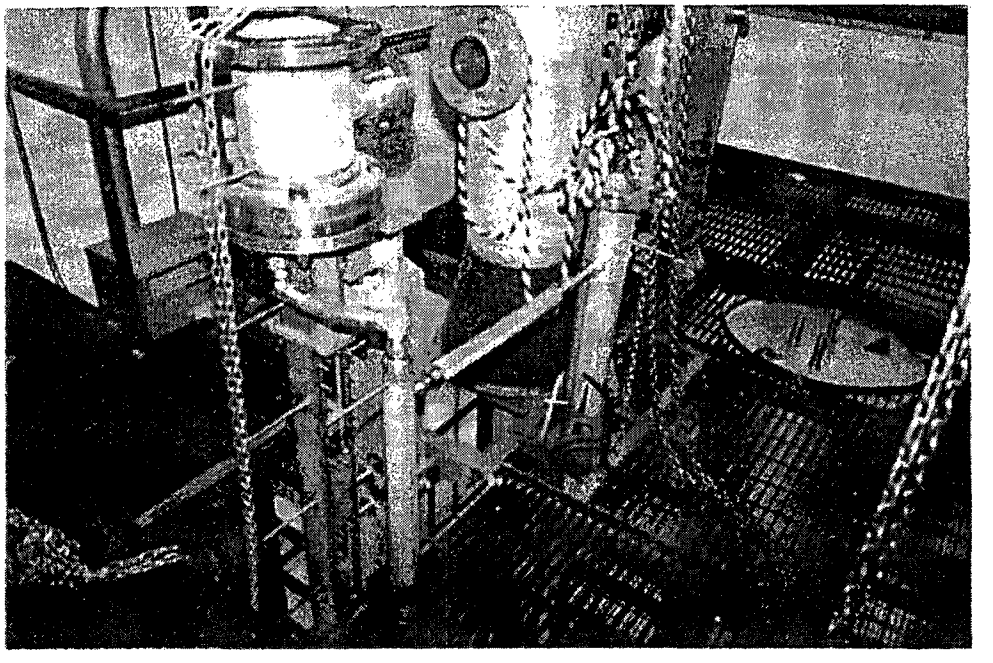

Photograph C.6 Top View of the Flow Housing, Upper Plenum, Small and Large Carryover Tanks, Steam Separator, Pressure Oscillation Damping Tank, and the Top of the Water Injection Tank.

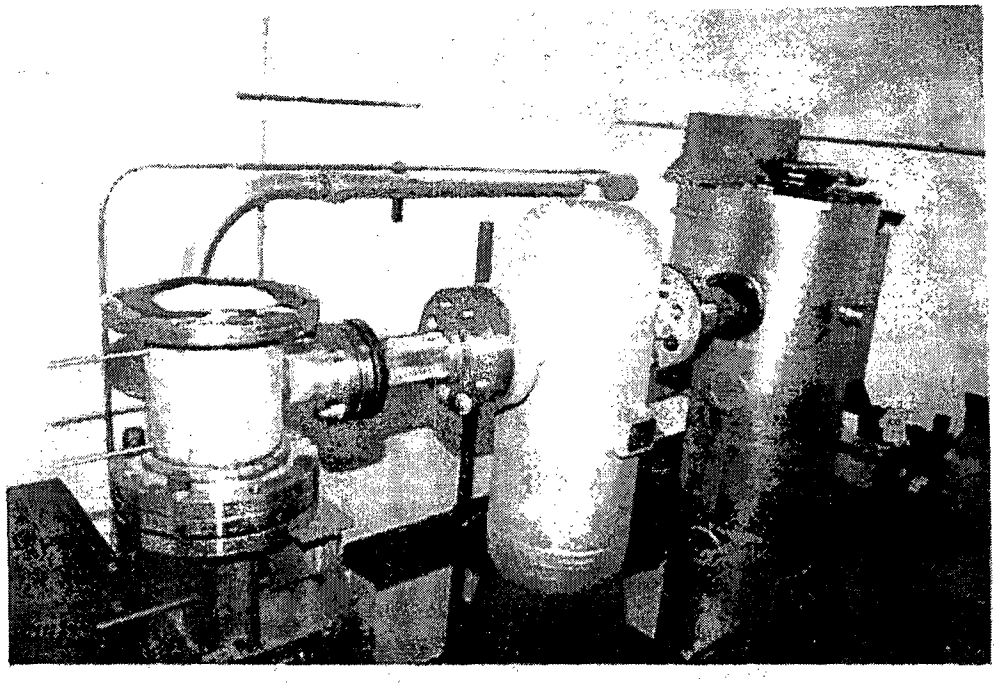

Photograph C.7 Upper Plenum, Steam Separator, and Pressure Oscillation Damping Tank Installation.

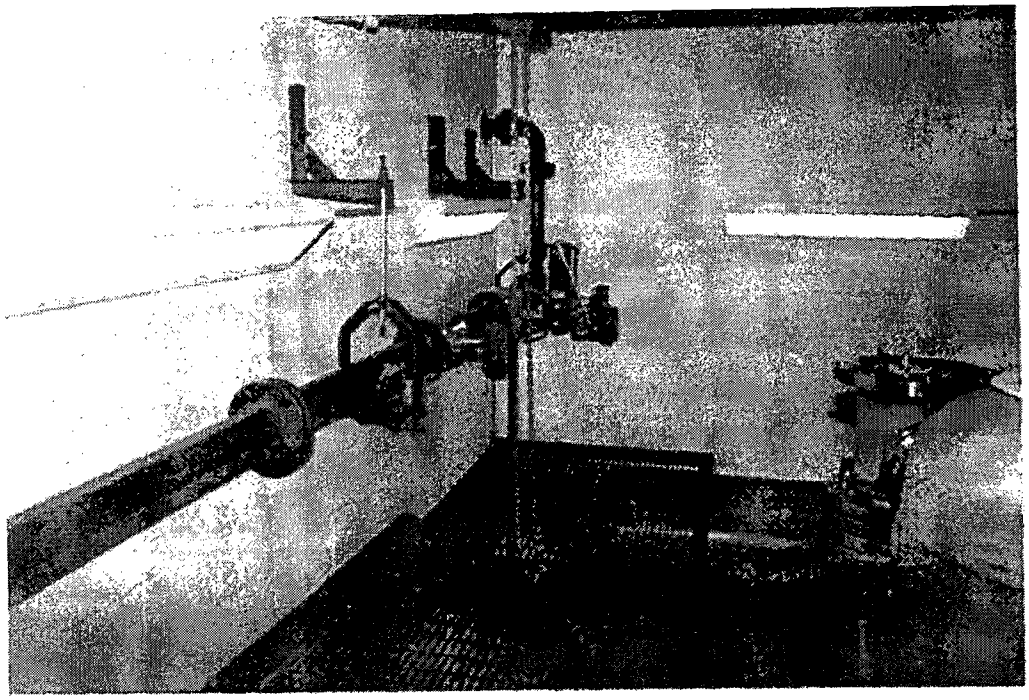

Photograph C.8 Steam Exhaust Piping with the Vortex Flowmeter and the Pressure Control V-Ball Valve.

Photograph C.9 Test Section Flow Housing Showing the Heater Rods and Grids Through the Window Openings.

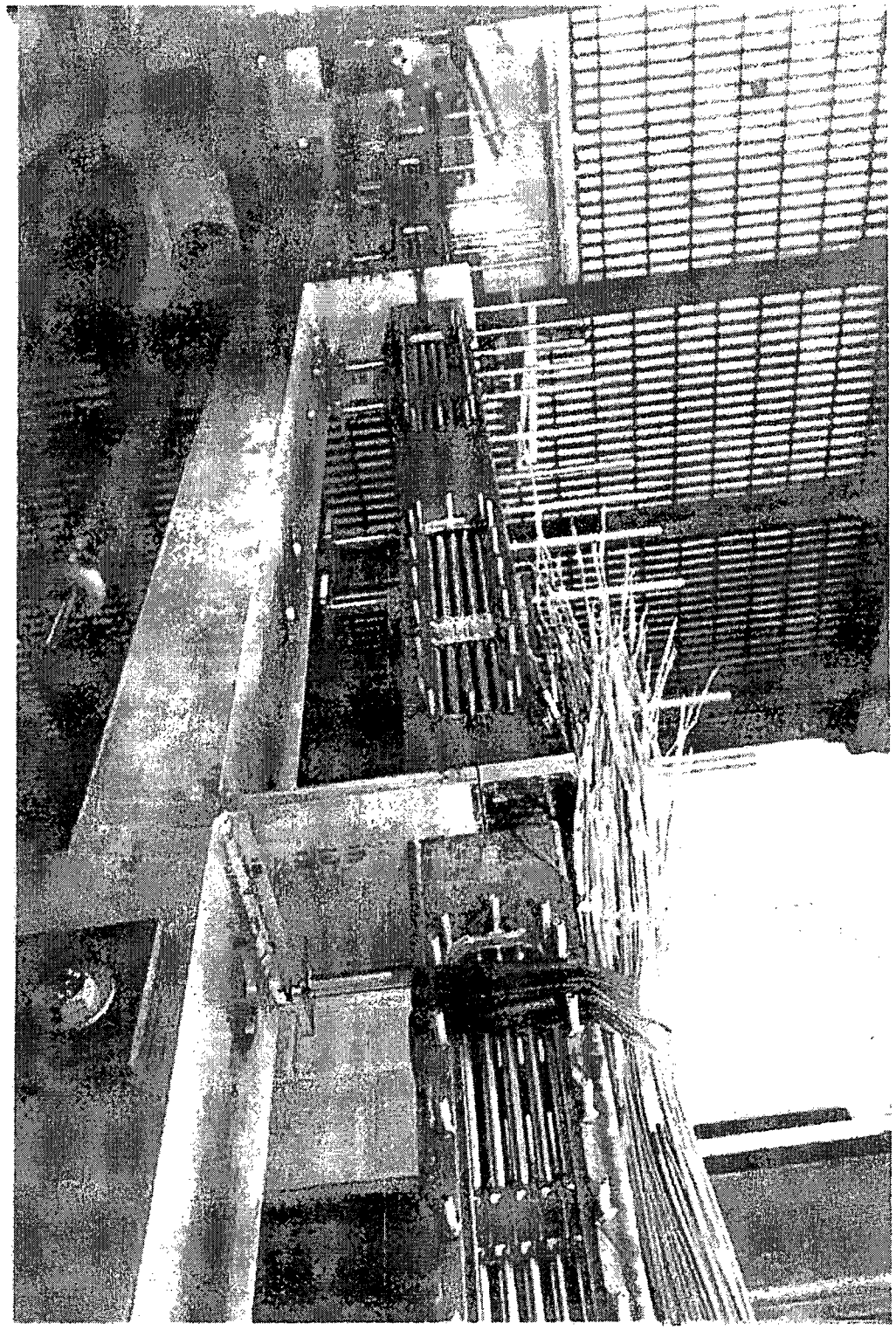

Photograph C.10 Bottom of the Flow Housing with the Lower Plenum and the Water Injection Tank.

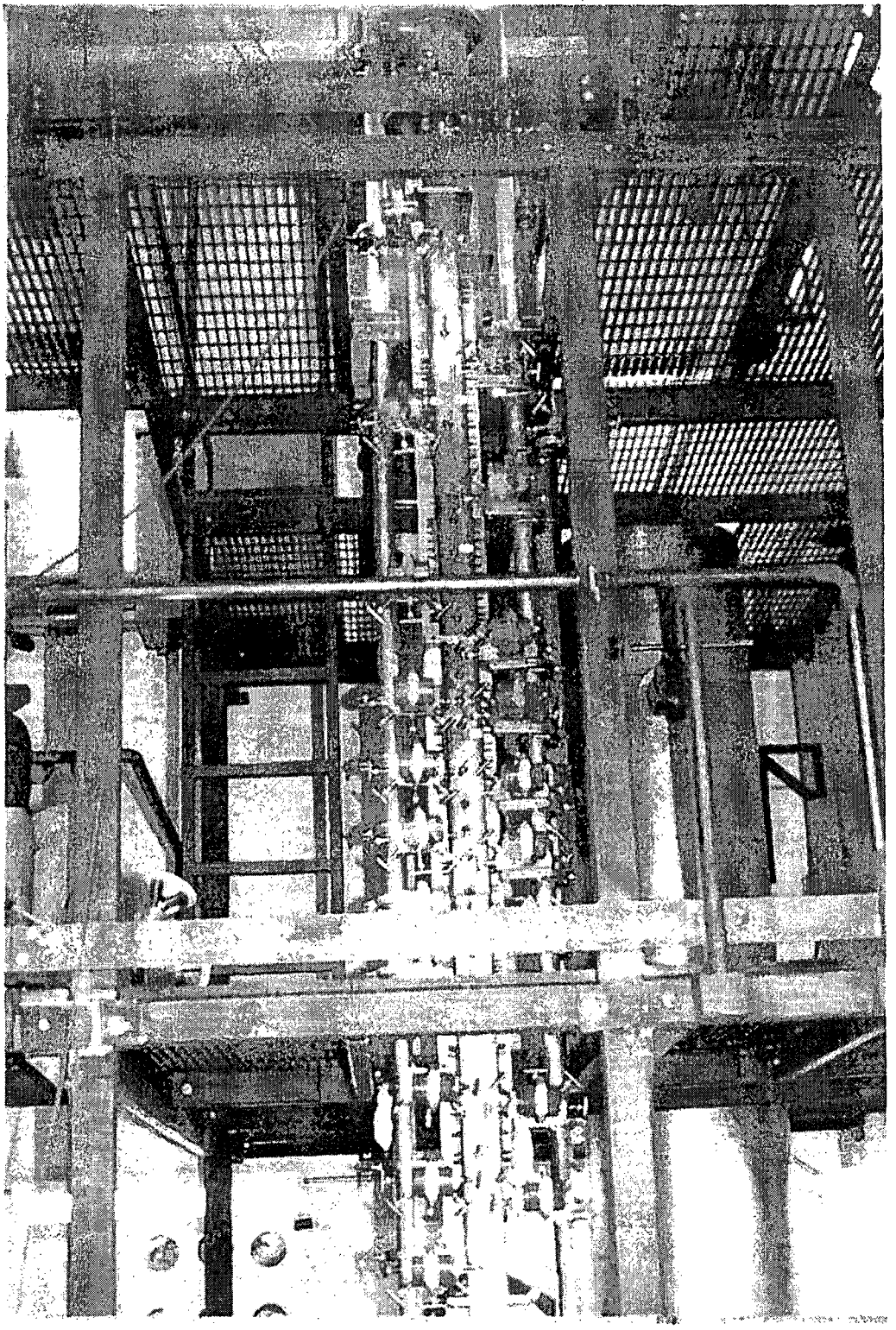

Photograph C.11 Installation of the Test Section.

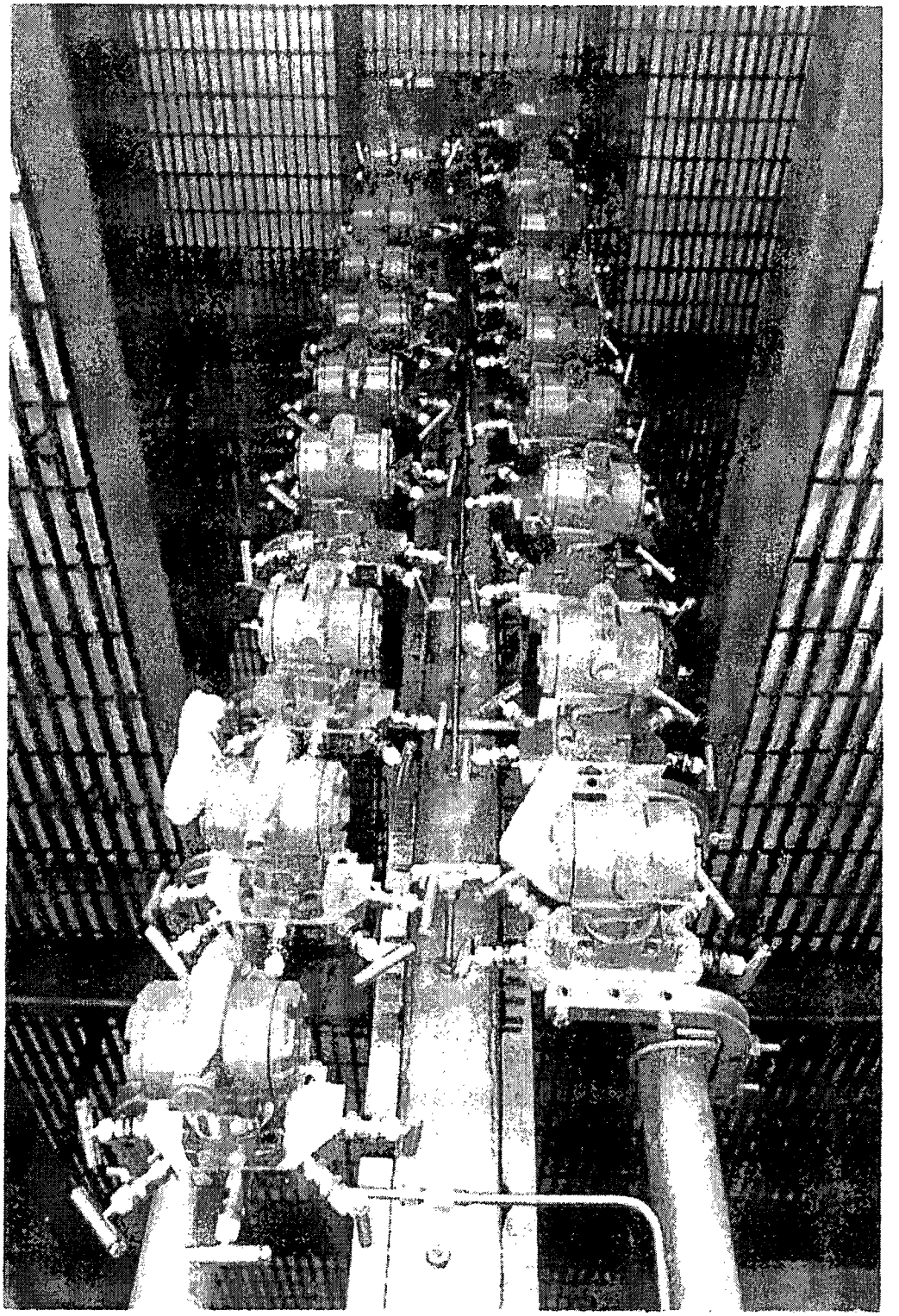

Photograph C.12 Differential Pressure Cells Installation on the Flow Housing.

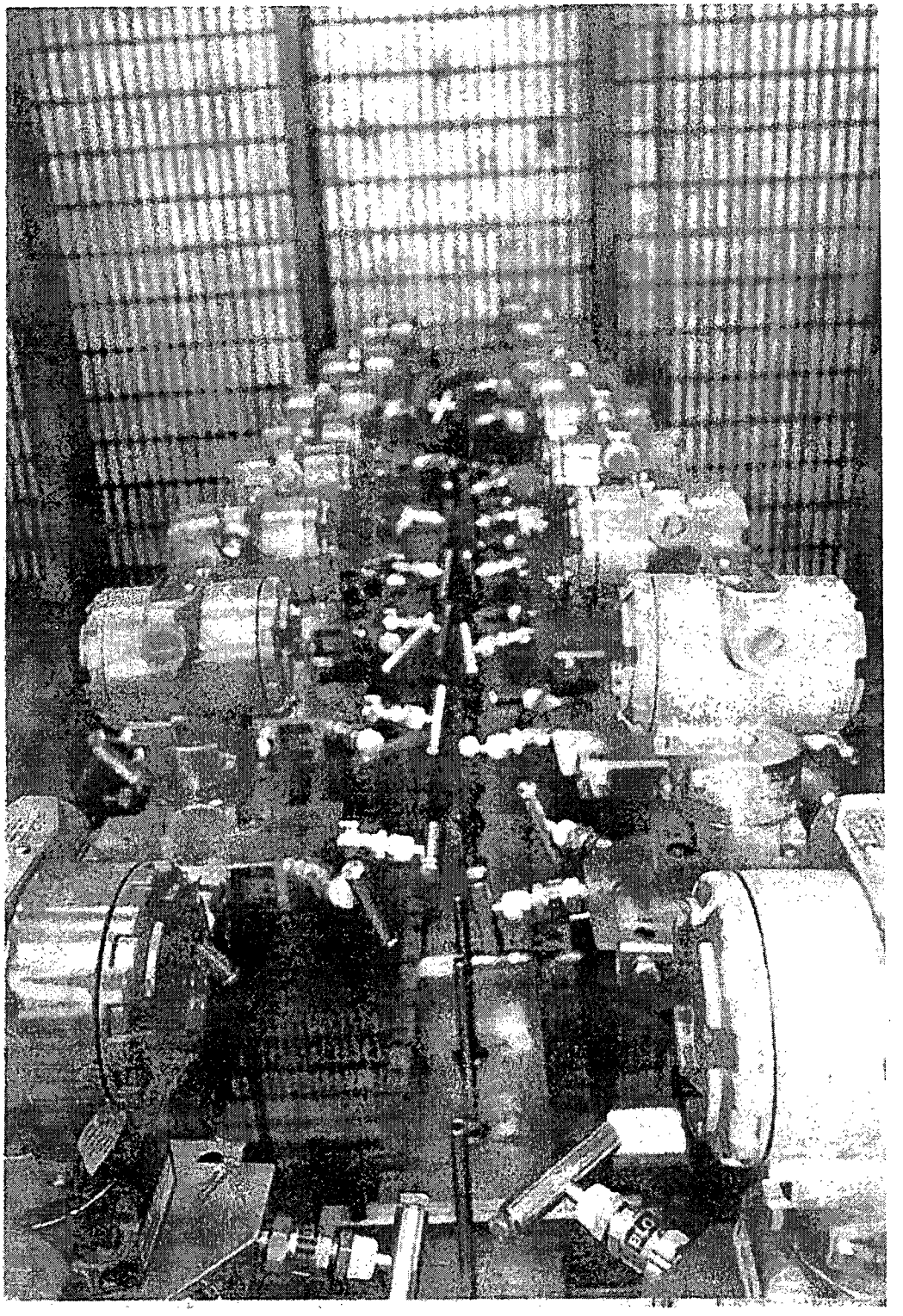

Photograph C.13 Differential Pressure Cells Installation Showing Connections of the Pressure Tap Lines to the Differential Pressure Cell Manifolds.

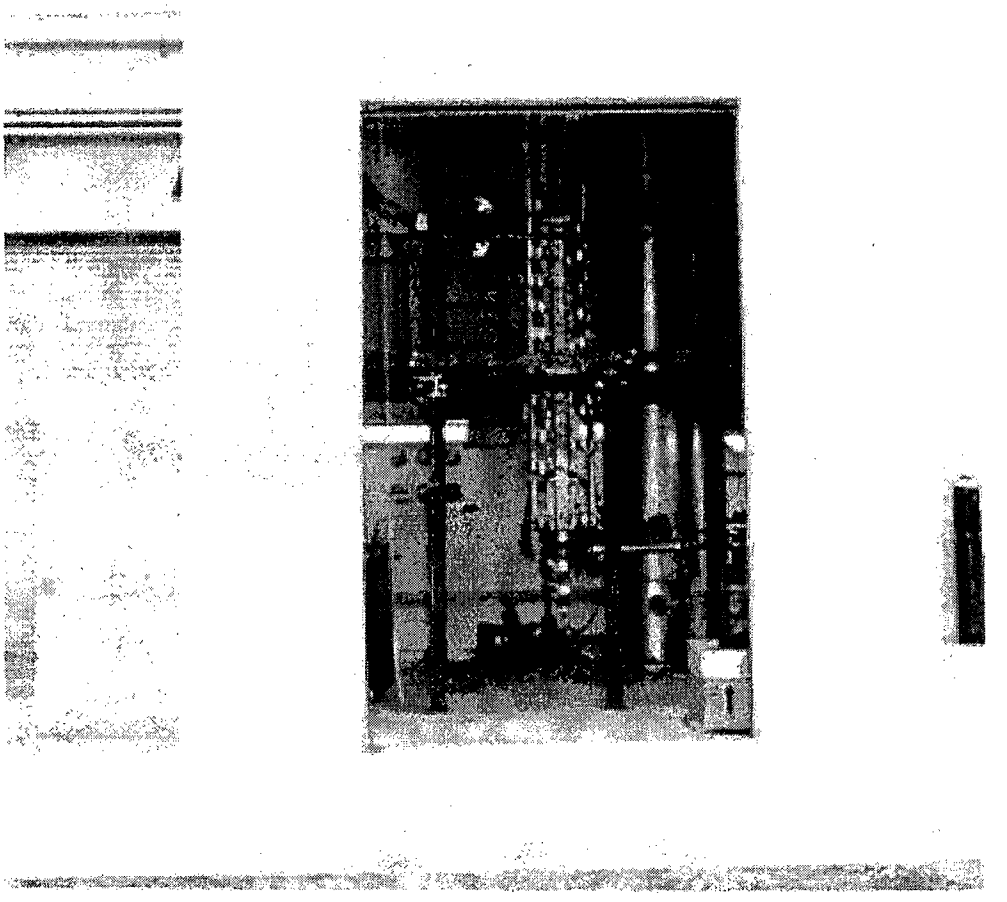

Photograph C.14 RBHT Test Facility Building View Through the Roll-up Door Showing the Test Section, Water Injection Tank, Circulating Pump, and the Mezzanine Structure.

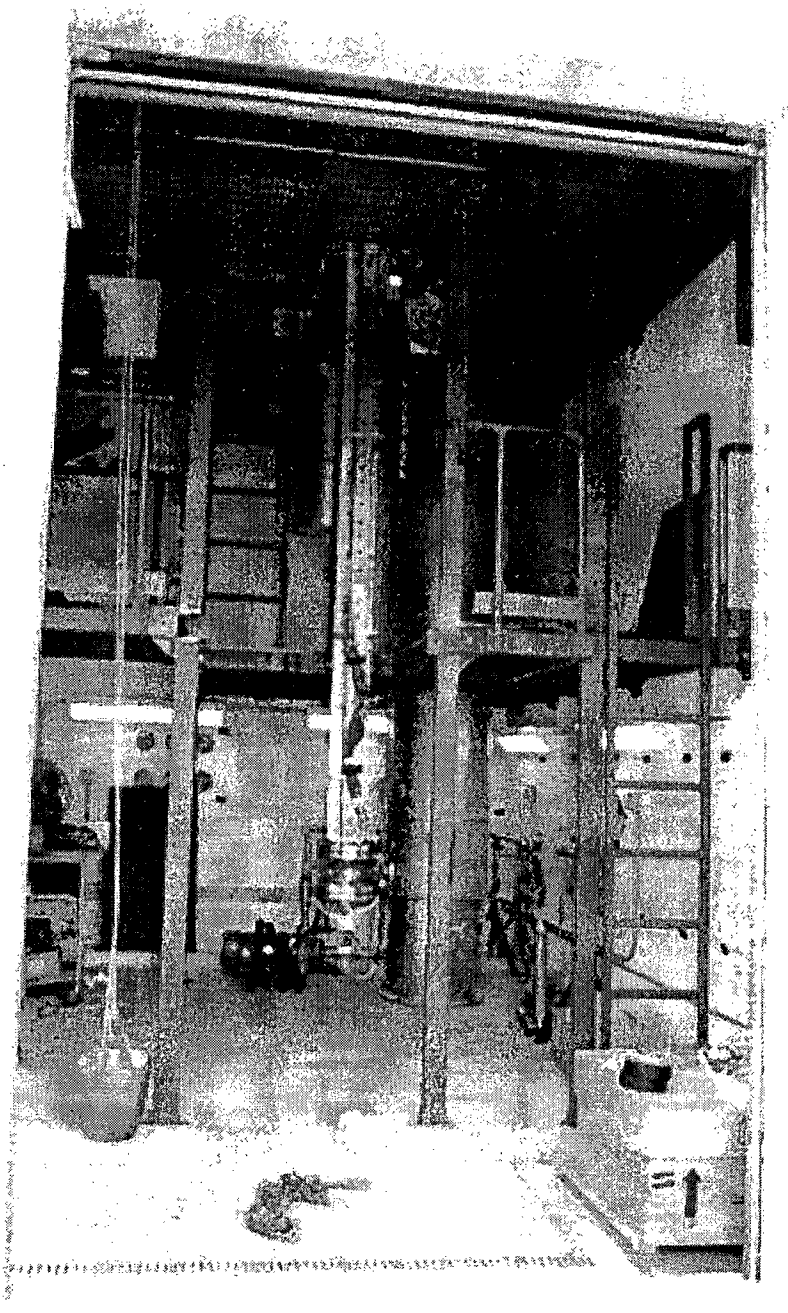

Photograph C.15 Inside View of the RBHT Test Facility Through the Roll-up Door Showing the Test Section, Water Injection Tank, Circulating Pump, and the Mezzanine Structure.

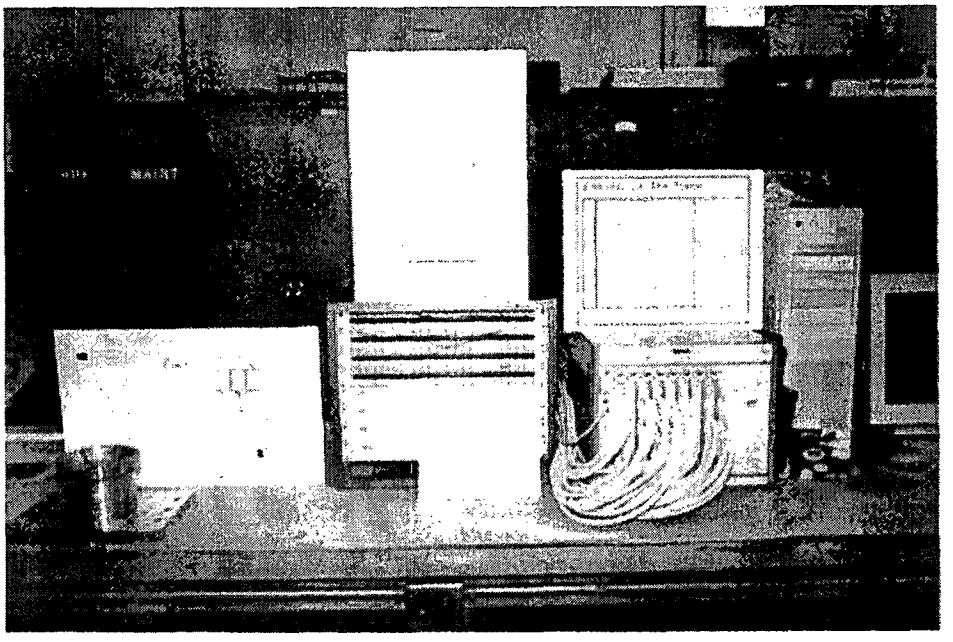

Photograph C.16 Data Acquisition Components: VXI Mainframe and Terminal Panels.

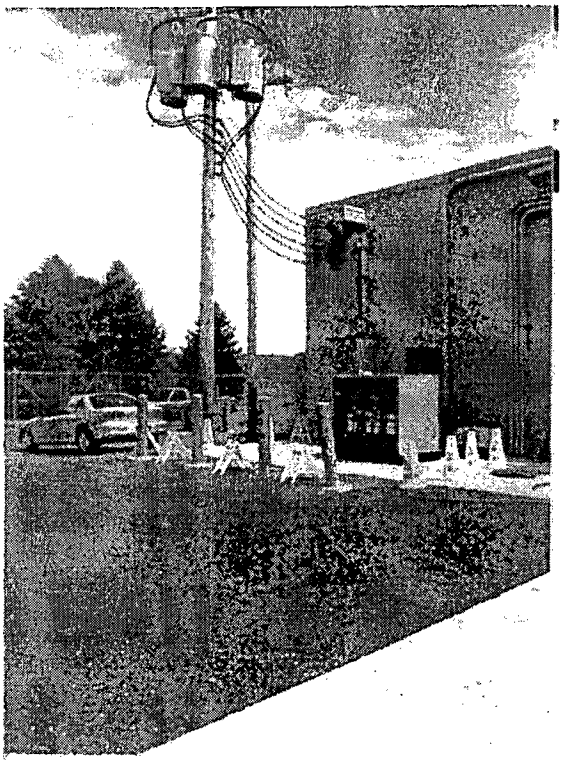

Photograph C.17 Electric AC Power Supply Showing the High Voltage Transformers, the Main Breaker, and the Phase Shift Transformer.

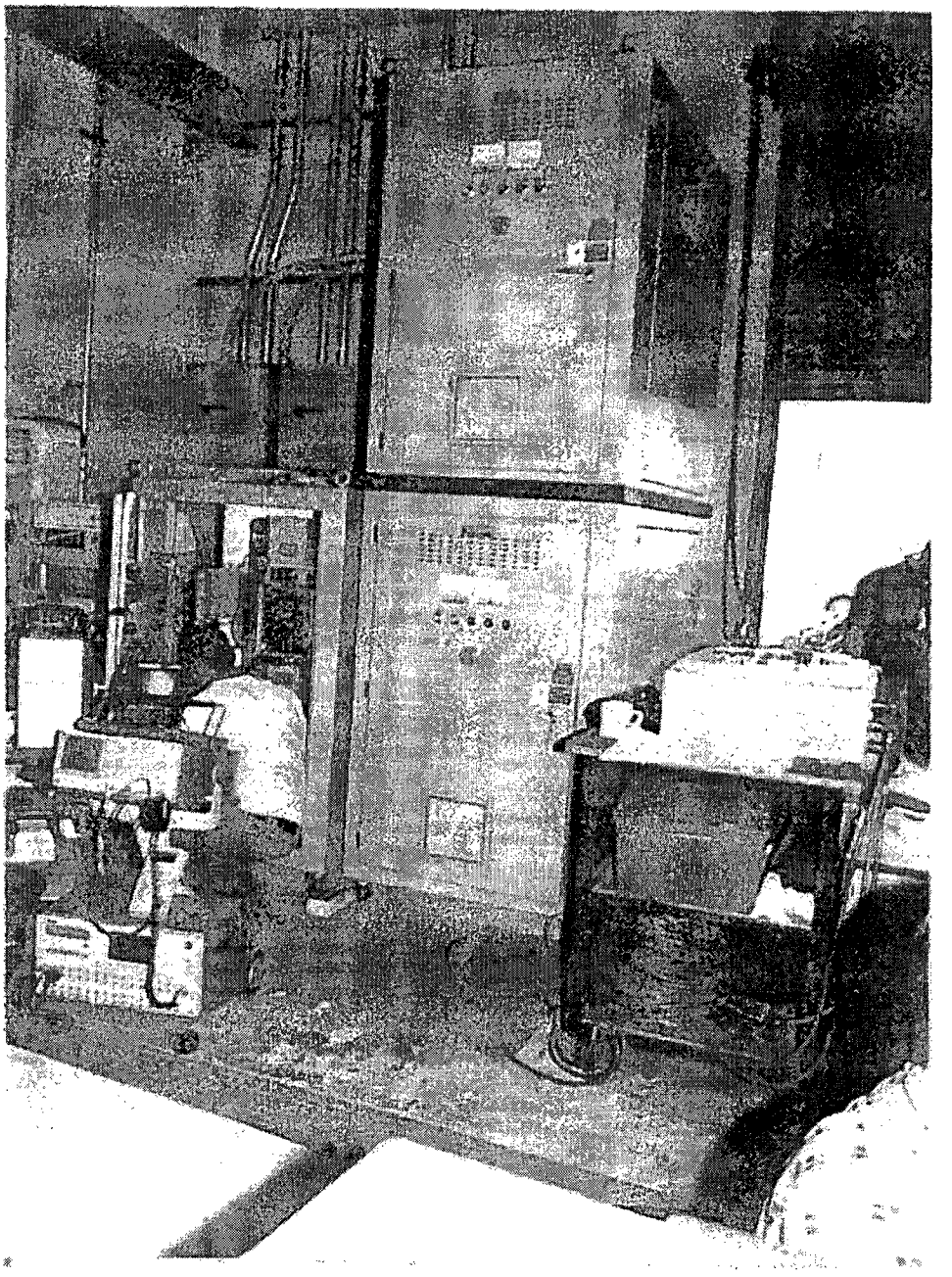

Photograph C.18 DC Power Supply Units Rated at 60 Volts DC, 12000 Amps and 750 KW.

APPENDIX D. EXPERIMENTAL VERIFICATION OF THE PERFORMANCE OF A DROPLET INJECTION SYSTEM FOR USE IN A ROD BUNDLE TEST FACILITY

IMECE 2001
Session 2-13-4

A. J. Ireland, E. Rosal, L. E. Hochreiter,
F. B. Cheung

Pennsylvania State University
Department of Mechanical and Nuclear Engineering
University Park, PA 16802

ABSTRACT

A droplet injection system has been developed for use in a rod bundle heat transfer test facility designed specifically for the study of dispersed flow film boiling during reflood transients in a nuclear reactor. Three different injectors having various pitch configurations and hole patterns were tested. The drop field produced by each was characterized using a laser-assisted size measurement technique. Appropriate mean diameter and drop size distributions that closely simulate the drop field encountered in a reactor bundle assembly under reflood conditions were obtained. The droplet injection system so developed can readily be employed in the rod bundle test facility to investigate the droplet heat transfer in the dispersed flow films boiling regime.

INTRODUCTION

A RBHT (Rod Bundle Heat Transfer) test facility has recently been constructed to investigate reflood heat transfer in electrically heated rod bundles which simulate nuclear fuel assemblies. The objective is to obtain basic two-phase flow and heat transfer data in the dispersed flow film boiling regimes where the peak fuel rod temperatures are calculated to occur for a postulated reactor design basis accident. The information and data required includes; the entrained liquid droplet sizes and velocity, vapor temperature, steam flow rate, and the interfacial heat and mass transfer.

The dispersed flow film boiling region is extremely complex since the dispersed droplets act as heat sinks and alter the vapor super-heat temperature such that the film boiling is a two-step process, that is heat is transferred to the continuous vapor phase from the heated walls, then heat is transferred to the entrained water droplets by interfacial heat and mass transfer[1-3]. As a result, the vapor temperature is a dependent parameter which is a function of both the wall heat transfer and the interfacial heat transfer. In addition to being a source of interfacial heat transfer, the entrained droplets can also affect the continuous vapor heat transfer from the heated wall by increasing the turbulence level in the flow, due to the additional interfacial drag in the flow, as well as acting as distributed heat sinks within the vapor flow.

Best estimate safety analysis computer codes are widely used to predict nuclear fuel rod

temperatures for postulated accidents. The most limiting accident is the Loss of Coolant Accident in which the calculated peak cladding temperatures for the reactor occur in the dispersed flow film boiling region[2]. These codes rely on models to accurately describe the physical processes in the dispersed two-phase flow heat transfer regime as described above. To date, the existing models have large uncertainties and do not capture all the physical phenomena which have been observed in various experiments. As a result the safety analysis calculations and associated method logics have large uncertainties and conservative calculations have to be performed to insure that the calculated peak cladding temperatures are within the licensing limits for the reactor[3].

One of the key features of the RBHT study is to provide improved data and analysis such that the analytical models which are used to represent the physical phenomena for the two-phase dispersed flow film boiling region can be improved such that the calculated uncertainty is reduced. The experimental approach in the RBHT work is to separate the different phenomena, as best as possible, such that it is easier to develop component models for the more complex dispersed flow film boiling region. Toward this end, a RBHT test facility has been constructed to study reflood heat transfer in rod bundles to obtain data for improving the heat transfer model for Best-Estimate computer codes. A series of steady state droplet injection tests are to be conducted with liquid injection into a steady steam flow in the bundle. The droplet injection tests simulate the dispersed flow film boiling region above the quench front and can be performed without the additional complexities of the quench front behavior. The purpose of the droplet injectors is to introduce into a rod bundle a narrow spectrum of droplet sizes in a controlled manner to study the effects of droplets on the dispersed flow film boiling heat transfer. In order to determine the effectiveness of the injection system, a method of testing the injectors was developed. The method involves forcing water through the injection tubes and analyzing, both qualitatively and quantitatively, the ability of the injector to produce droplets of uniform size. This is done with the use of a laser-illuminated digital camera system known as VisiSizer.

Steam cooling tests will be performed to obtain the single-phase convective heat transfer within the rod bundle and to examine the single phase behavior of the spacer grids on the downstream heat transfer. Once the single phase heat transfer tests are complete, droplets will be injected into the steam flow using the injectors which are being tested and presented in this paper. The injectors are designed to provide a narrow droplet size distribution and velocity distribution such that the data will be easier to analyze and characterize. The objective will be to inject droplets of similar size to that observed in forced reflood experiments. The injected droplets will evaporate, shatter on spacer grids, increase the turbulence in the flow and de-superheat the vapor such that the wall heat flux will increase. The droplets will be injected over a range of sizes and mass flow rates in to steam flow at different Reynolds numbers. Data will be obtained on the drop size and distributions are different axial positions to determine the droplet shattering effects as well as evaporation. A mass and energy balance will be performed on the test bundle to obtain the droplet evaporation and the total interfacial heat transfer.

This paper described the design of the droplet injection system and the resulting drop sizes that are to be simulated in the RBHT experiments.

ROD BUNDLE HEAT TRANSFER FACILITY

The droplet injections system will be implemented in the RBHT facility having a 7 x 7 rod bundle as shown in Figure 1. The rod bundle consists of full electrically powered heater rods with a

diameter of 9.5 mm and a pitch of 12.60 mm. The bundle has 45 heater rods and four unheated corner rods, which are used to support the bundle grids as well as carry various thermocouples leads.

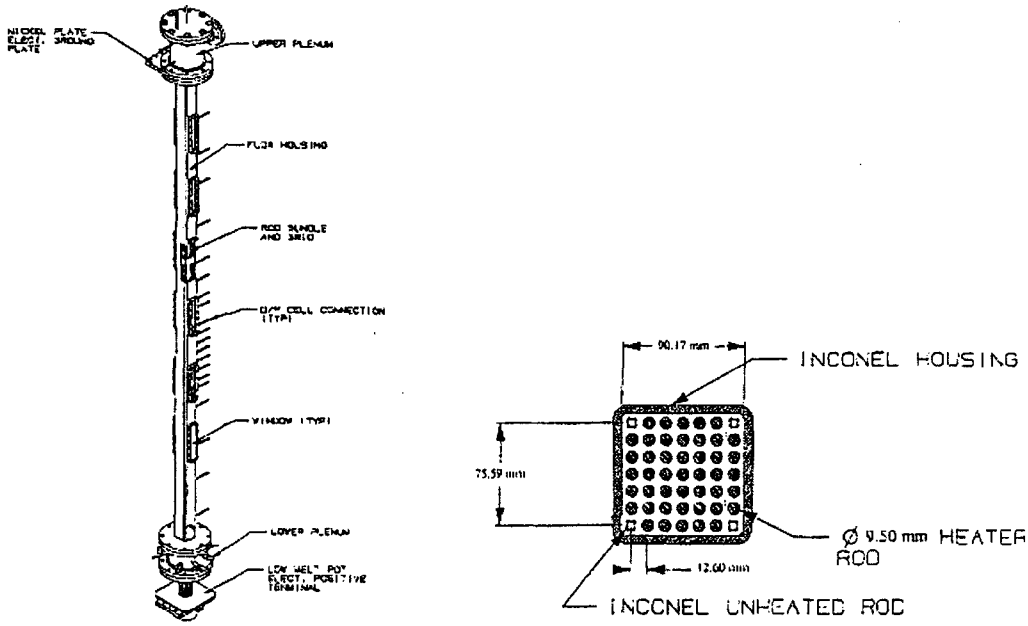

Figure 1 - An Overview and a Cross-section of the RBHT Rod Bundle

Six droplet injection tubes will be inserted into the bundle assembly as show in Figure 2, with the tube perpendicular to the heater rods. The tubes will penetrate both sides of the housing and will be supplied with water from both ends. The groupings of small holes in the tubes will be positioned such that droplets are injected into each of the 36 subchannels.

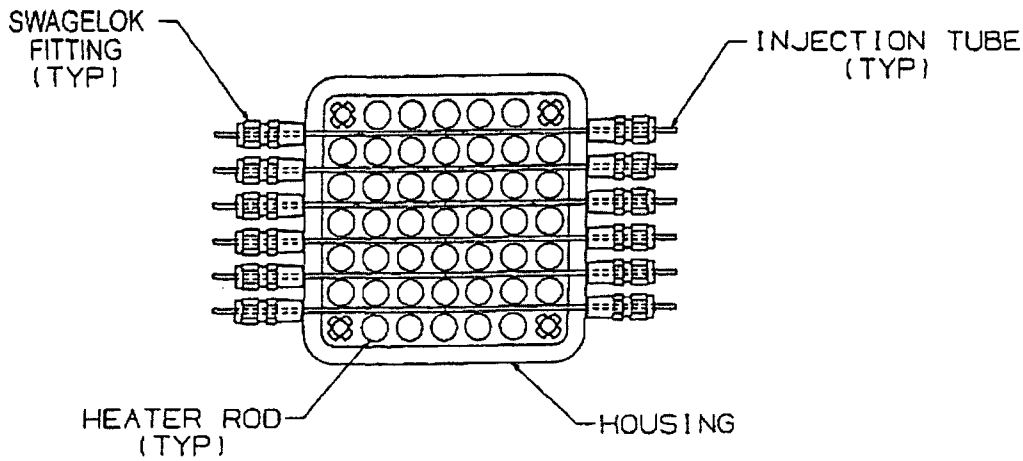

Figure 2 - A Schematic of the RBHT Droplet Injection System

The droplet injection system that was developed for use in the RBHT facility consists of small diameter tubes (2.36 mm) in which holes are drilled on one side. The holes can vary in size, pitch, and number. Three different injectors were employed in this study. Injector A incorporated 23 holes in a square pitch, as shown in Figure 3. The other two injectors, Injector B and Injector C, were both triangular pitch injectors with 22 and 23 holes, respectively. Injectors B and C are shown in Figures 4 and 5.

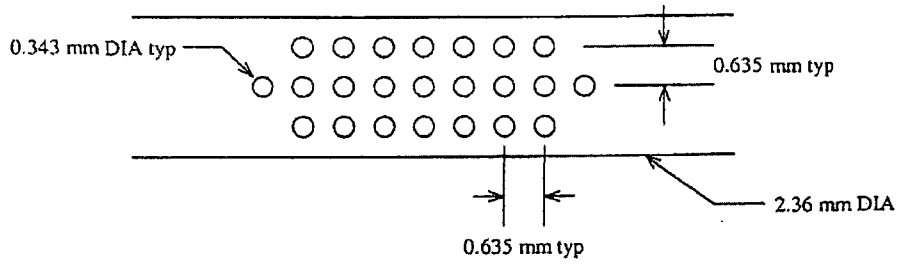

Figure 3. Hole Pattern and Pitch Configuration for Injector A (not to scale).

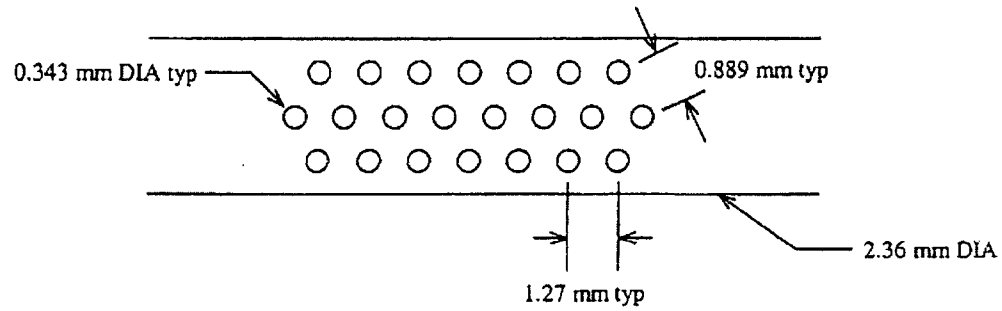

Figure 4. Hole Pattern and Pitch Configuration for Injector B (not to scale).

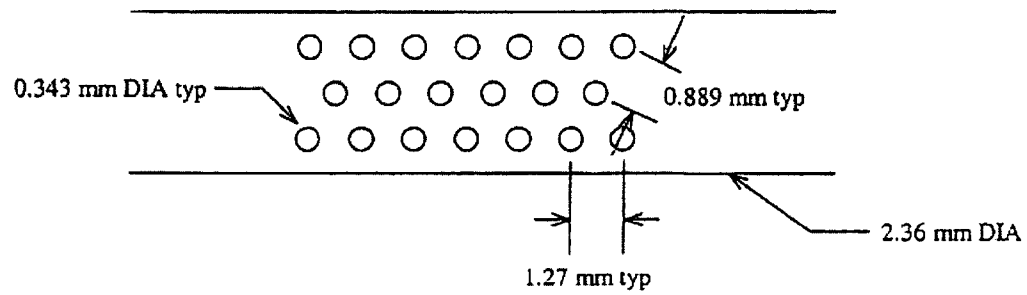

Figure 5. Hole Pattern and Pitch Configuration for Injector C (not to scale).

The droplet injectors were oriented in a horizontal manner, as they would be in the rod bundle, and water was pumped into the injector. The water exited the droplet holes as liquid jets which then broke up into a drop field who's size was characterized by the holes and spacing in the injector tube.

The method of analyzing the performance of the different droplet injection tubes involves the use of a system known as VisiSizer[4,5], which is capable of real-time analysis of droplet size and velocity distributions. The system consists of a high-resolution digital camera, infrared laser, data analysis software, and associated computer and control equipment.

The camera, a Kodak Megaplus™ digital camera, has a resolution of over 1.0 megapixels. The laser system incorporates an infrared beam of wavelength 805 nm and is capable of pulsing at frequencies up to 1000 Hz. The laser can also pulse twice during a single camera frame to produce a double image used in determining velocity information. The beam of the laser is scattered with an opaque sheet of plastic to produce uniform background lighting for imaging. The system captures high-resolution images of the injection streams and analyzes the images at a rate of about 7 frames per second, identifying droplets as dark images in front of the laser-illuminated scattering sheet. The diameter of each droplet is determined automatically by referencing the number of dark pixels in the droplet image to the pixel area of a calibration circle. A general setup of the system is shown in Figure 6.

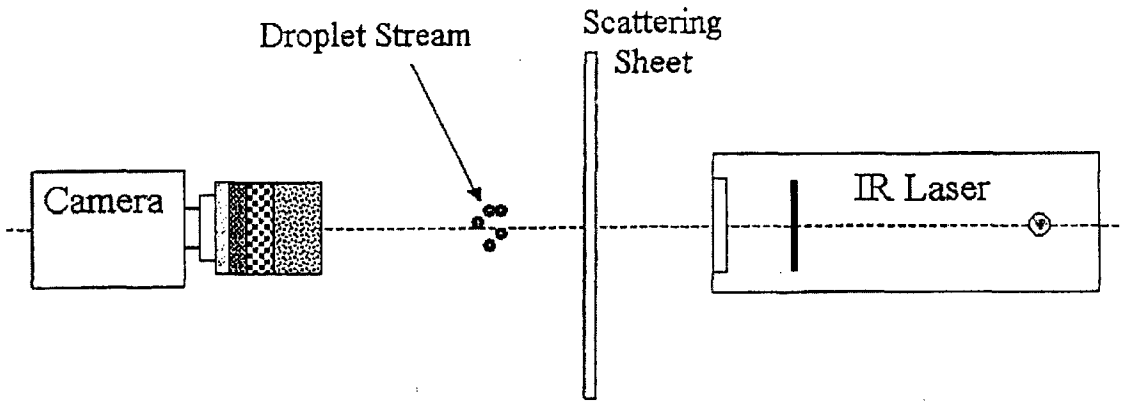

Figure 6. General Setup of the VisiSizer System for Drop Size and Velocity Measurement

A variety of user-defined parameters control the counting of the droplets, including focus rejection and sphericity criteria. Focus rejection is determined by considering the sharpness of a droplet image, done by quantifying the intensity gradient at the out edge of the droplet[5]. In addition to this, the droplet analysis duration can be controlled by elapsed time, number of frames, or number of droplets counted. The software also calculates real-time statistics such as mean and sauter-mean diameters as well as displays the diameter distribution and, if applicable, the velocity distribution. Velocity is determined by double-pulsing the laser to capture the motion of a droplet. Analysis of the velocity is done automatically using criteria such as angle of motion, velocity range, and size matching. The VisiSizer System has been thoroughly tested to characterize the system uncertainties and biases and is highly reliable and simple to set up and calibrate.

RESULTS AND DISCUSSION

Liquid jet breakup and drop formation were studied in the injection systems using the VisiSizer system. Qualitative and quantitative data for the drop size distribution were obtained. Images of the injector were taken with the digital camera to show the details of the breakup of the water jets and droplet diameter distributions were taken about 0.127 m above the point of injection at a liquid volumetric flowrate of about 10 cm^3/sec.

The results show that the Injector A, with the square pitch, does not provide uniform water jets. The streams from the injectors combine and cause much larger jets to emerge, as show in Figure 7. The result is large droplets shown in Figure 8 and a size distribution which is spread over a wide range of drop sizes as shown in Figure 9. The distribution shows clearly the result of the combined streams seen in Figure 7. The mean diameter for the droplets from Injector A is 1.6 mm. This was not the desired droplet size spectrum for use in the RBHT facility.

Injectors B and C behave in a very different way, as can be seen in Figures 10 through 15. Both injectors were able to produce streams that did not combine (or combined very little) and created a much more uniform distribution of size as seen qualitatively in Injectors B and C are 0.619 mm and 0.711 mm respectively. The mean diameters from these two injectors support the assumption that droplets formed from the injectors are about twice the size of the holes from which they are ejected.

Drop formation from an orifice has been discussed by Wallis (6) and is similar to bubble formation. The radius of a bubble formed by blowing through a small orifice at low flow rates was given by Kutateladze and Strukovich[7] as

$$R_b = 1.0\left[\frac{\sigma R_o}{g(\rho_f - \rho_8}\right]^{1/3} \tag{1}$$

where R_o is the radius of the orifice, g the gravitational acceleration, σ the surface tension, ρ_f the liquid density, and ρ_g the gas density. The above expression was obtained from experimental data. As the gas velocity is increased, individual bubbles are no longer formed and the gas leaves the orifice as a jet which then breaks into individual bubbles further down stream of the orifice[7]. The condition given for the formation of the gas jet is

$$v_g > \frac{1.25\left[g\sigma(\rho_f - \rho)\right]^{1/4}}{\sqrt{\rho_g}}\left[\frac{\sigma}{g(\rho_f - \rho_g)R_o^2}\right]^{1/2} \tag{2}$$

where v_g is the gas velocity through the orifice, of size R_o.

A similar analogy can be made for liquid droplets formed from orifices. As the liquid velocity through the orifice is increased, liquid jets issue from the orifice as seen in Figure 10 which then break into individual droplets which have a diameter of approximately

$$D_d \cong 1.9\, D_o \tag{3}$$

If the jet velocity would be increased further, the large relative velocity of the liquid jet (relative to

its surroundings) leads to severe instability and the liquid is atomized into very fine droplets. The drop size for the flow through an orifice of size 0.343 mm diameter should be approximately 0.650 mm as given by Wallis. The much larger size seen is due to the merging of the liquid stream such that the drop size is not indicative of the orifice opening in the injector tube.

The drop sizes for the different injectors, predicted by Equation 3, is shown on the distribution plots in Figures 9, 12, and 15. As Figures 12 and 15 indicate, the drop size from Equation 3 represents approximately the mean size of the drip distribution; however, there is still a significant spread of the drop diameters.

Note that during a reflood transient, the entrained droplets not only provide a major source of interfacial heat transfer, but also may enhance the turbulence level in the vapor flow, thus directly affecting the wall heat transfer. Thus in the droplet injection experiments to be performed in the RBHT facility, it is important to simulate the mean drop size and the drop distribution. In view of this, the drop field produced by Injector A is not acceptable not only because of the fact that the mean drop size is much too large, but also due to the peculiar drop size distribution. As can be seen from Figure 9, there are two unequal peaks in the drop field that does not simulate the drop field observed in the bundle of a reactor assembly. On the other hand, the drop fields produced by Injectors B and C are much better approximations to the actual one.

The droplet size distributions from Injectors B and C can be compared with the drop size distributions taken from the FLECHT-SEASET[8] series of tests for reflood conditions in a 17x17 rod bundle assembly. Droplet images were captured using high-speed black-and-white motion picture film taken through the housing windows for some test runs. An example of the droplet distribution obtained can be seen in Figure 16.

It can be seen from Figure 15 and 16 that the distributions are very similar in that they have a maximum that occurs between 0.6 and 0.8 mm and have similar distributions except that the FLECHT-SEASET distribution has a longer tail at larger drop sizes.

The drop distributions in Figures 15 and 16 can be normalized on their peak frequency values and compared. Figure 17 shows the comparison of the two normalized distributions. As this figure indicates, the droplet injector will provide a more uniform distribution of drops over the range from1.75 D_0 to 2.25 D_0 with the ideal value being about 1.9 D_0. The FLECHT-SEASET distribution shows that a wider range of drops exist for the true reflood process.

CONCLUSIONS

The drop field produced by the injector tubes developed in this study can be used in the RBHT facility to investigate the effects of liquid droplets on the steam flow and the resulting dispersed flow film boiling heat transfer in a rod bundle under reflood conditions. By performing experiments over a range of liquid flows and vapor flows, and using the measurements on the RBHT facility[9], the amount of evaporation can be measured such that the interfacial heat transfer can be calculated. Also, the laser illuminated camera system can be used at different elevations to obtain the drop size, velocities, and distributions. This data can lead to determining the interfacial heat transfer and the effects of droplet shattering caused by the spacer grids. In addition, the droplet injection experiments can also be modeled using COBRA-TF[10], in which the drops can be simulated as a source of liquid.

ACKNOWLEDGEMENTS

This work was supported by the U.S. Nuclear Regulatory Commission under Contract No. NRC-04-98-041.

REFERENCES

1. Clare, A. J., et al., "Droplet Dynamics and Heat Transfer in Dispersed Two-Phase Flow," CONF-8410331, pp 51-62, 1985.

2. Hochreiter, L. E., et al., "Application of PWR LOCA Margin with the Revised Appendix K Rule," Nuclear Engineering and Design, Vol. 132, pp 437-447, 1992.

3. Andreani, M. and G. Yadigaroglu, "Prediction Methods for Dispersed Flow Film Boiling," Int. J. Multiphase Flow, Vol. 20, pp. 1-51, 1994.

4. Oxford Lasers, "HSI1000 Fast Illumination System," Operation Manual, Issue 2, Rev. 1, Oxford Lasers, Ltd., 1997.

5. Todd, Donald R., "Characterization of the VisiSizer Particle/Drop Sizing System," MS Thesis, Pennsylvania State University, Aug. 1999.

6. Wallis, G. B., "One Dimensional Two-Phase Flow," McGraw Hill Book Co., pg 376, 1969.

7. Kutateladge, S. S., and M. A.Styrikovich, "Hydraulics of Gas-Liquid Systems," Moscow, Wright Field Trans. F-TS-9814/V, 1958.

8. Lee, N., et. Al., "PWR FLECHT SEASET Unblocked Bundle, Forced and Gravity Reflood Task Data Evaluation and Analysis Report," NUREG/CR-2256, Feb. 1982.

9. Hochreiter, L. E., et. Al., "Dispersed Flow Heat Transfer Under Reflood Conditions in a 49 Rod Bundle: Test Plan and Design - Results from Tasks 1-1 0," NRC-04-98-041 Contract Report 1, Sept. 1998.

10. Park, C. Y., Hochreiter, L. E., Kelly, J. M., and Kohrt, R. J., "Analysis of FLECHT- SEASET 163 Rod Bundle Data using COBRA-TF," NUREG-CR-4166, Jan. 1986.

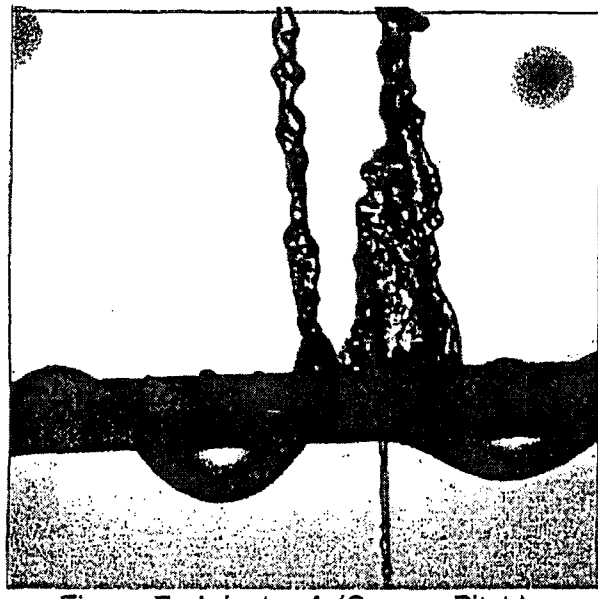

Figure 7. Injector A (Square Pitch)

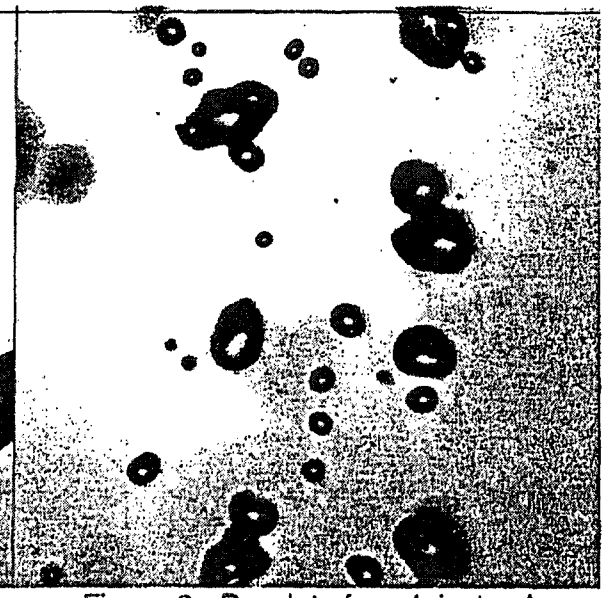

Figure 8. Droplets from Injector A.

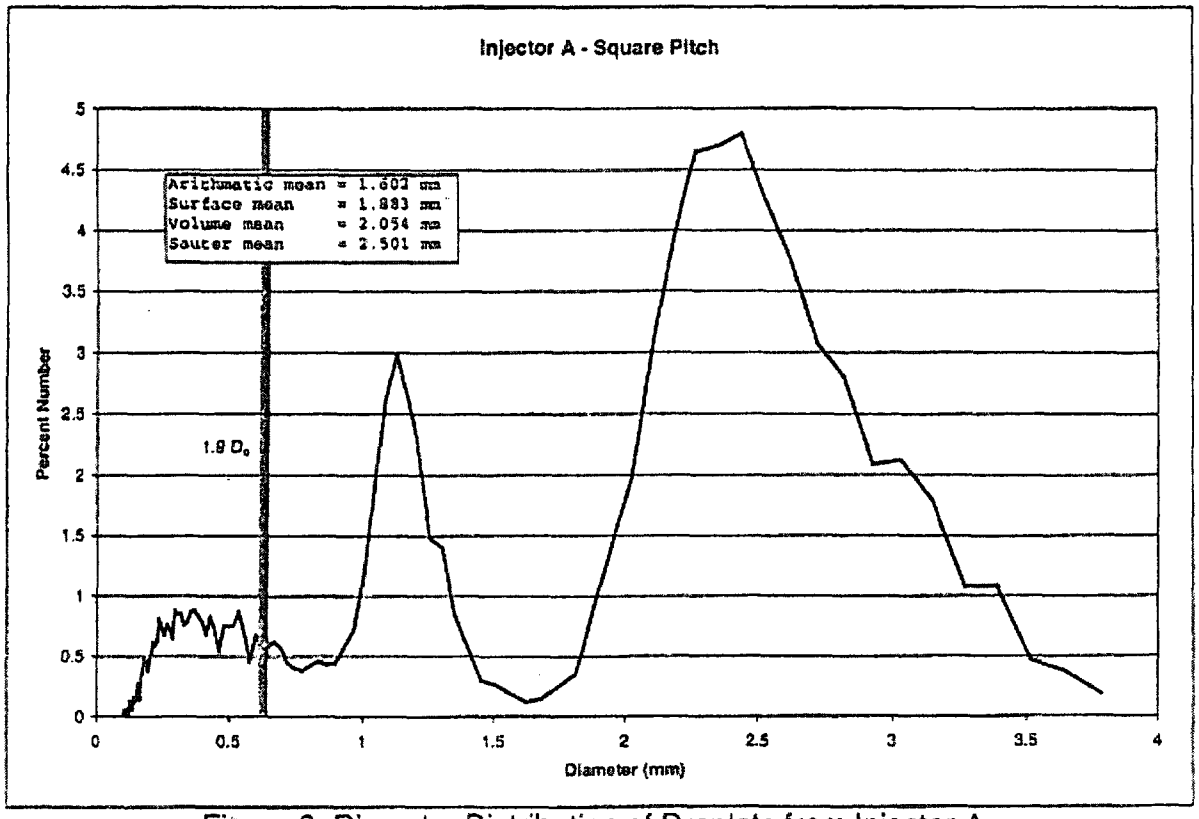

Figure 9. Diameter Distribution of Droplets from Injector A.

Figure 10. Injector B (Triangular Pitch)

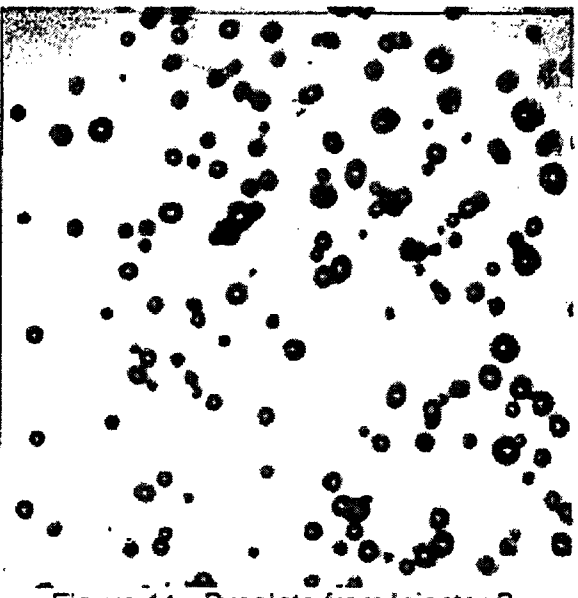

Figure 11. Droplets from Injector B.

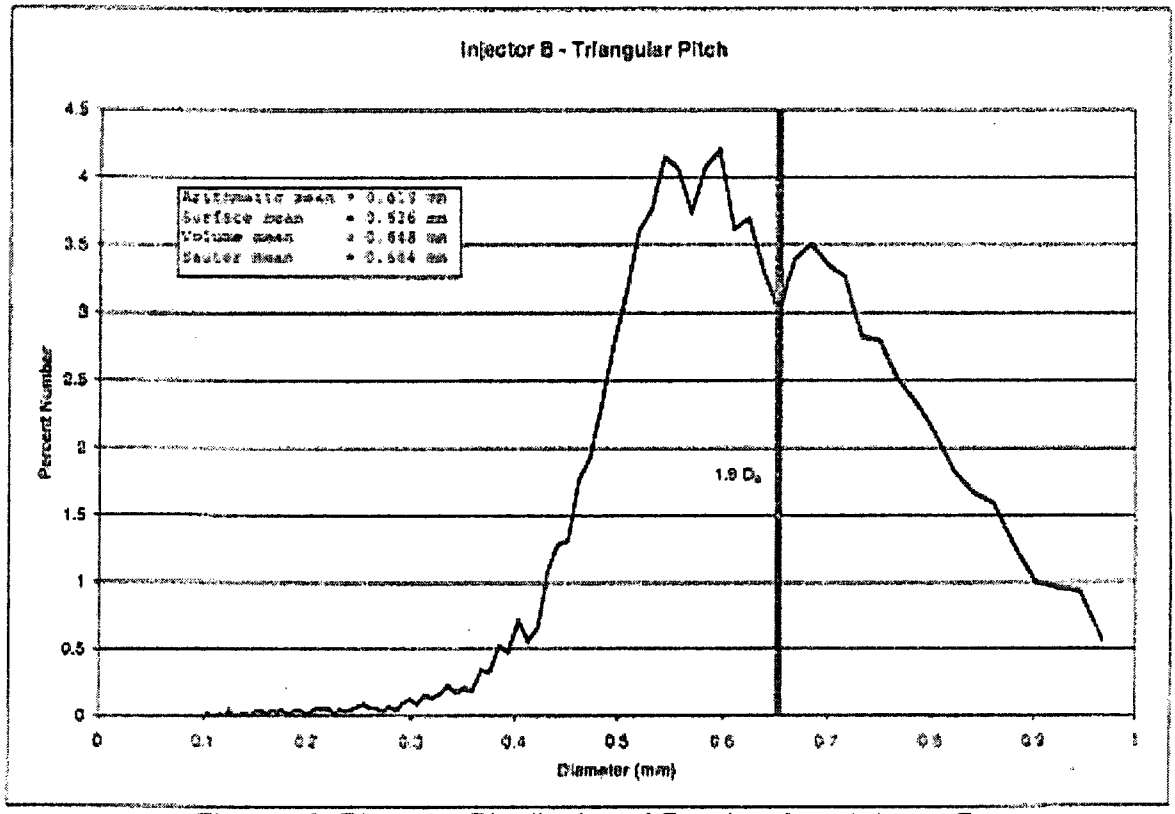

Figure 12. Diameter Distribution of Droplets from Injector B.

Figure 13. Injector C (Triangular Pitch)

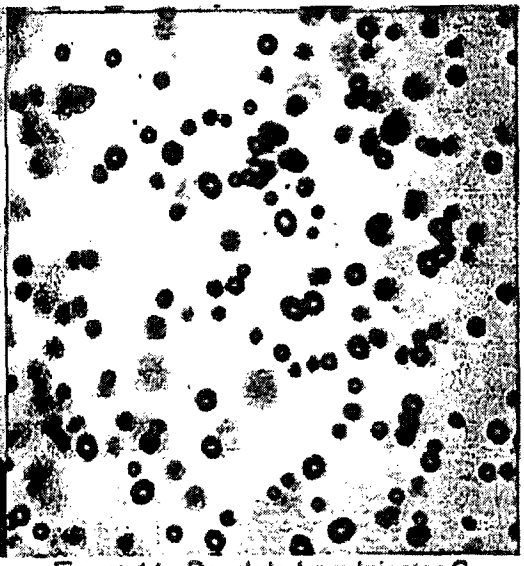

Figure 14. Droplets from Injector C.

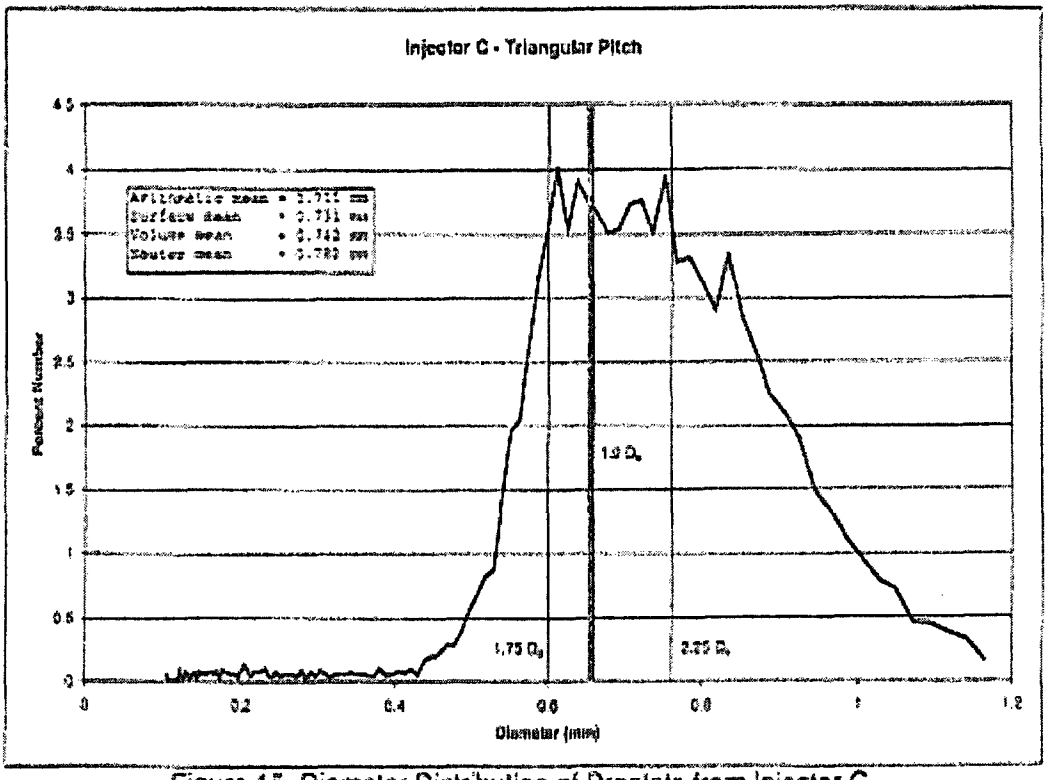

Figure 15. Diameter Distribution of Droplets from Injector C.

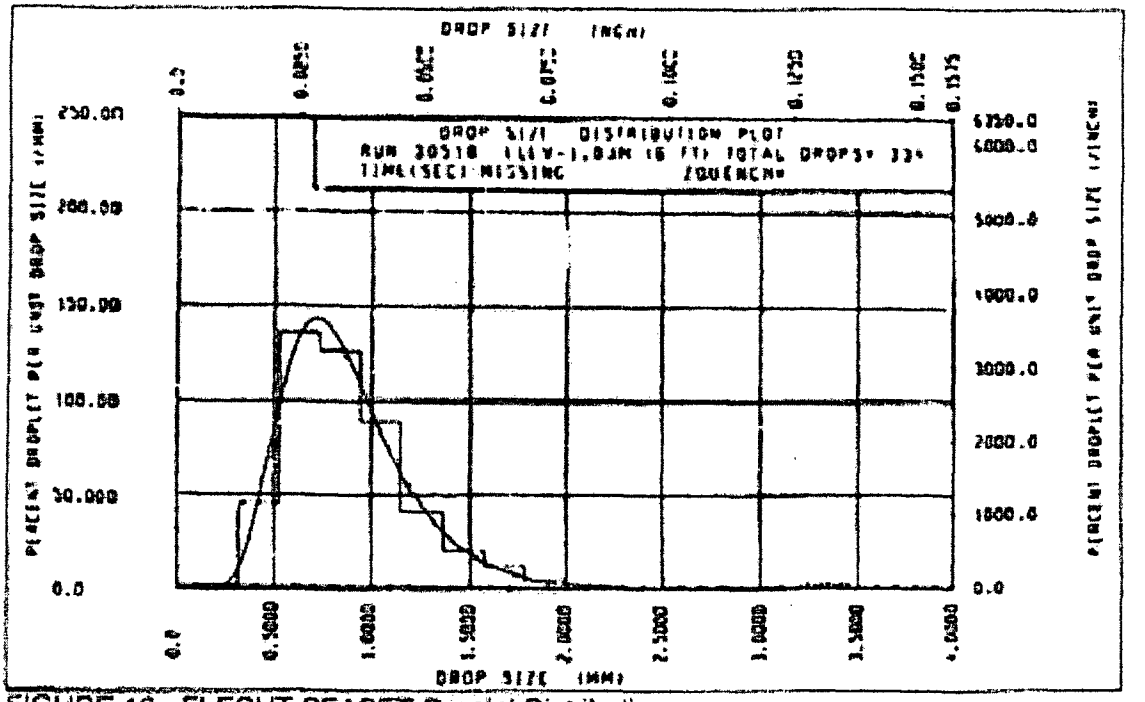

FIGURE 16 - FLECHT SEASET Droplet Distribution

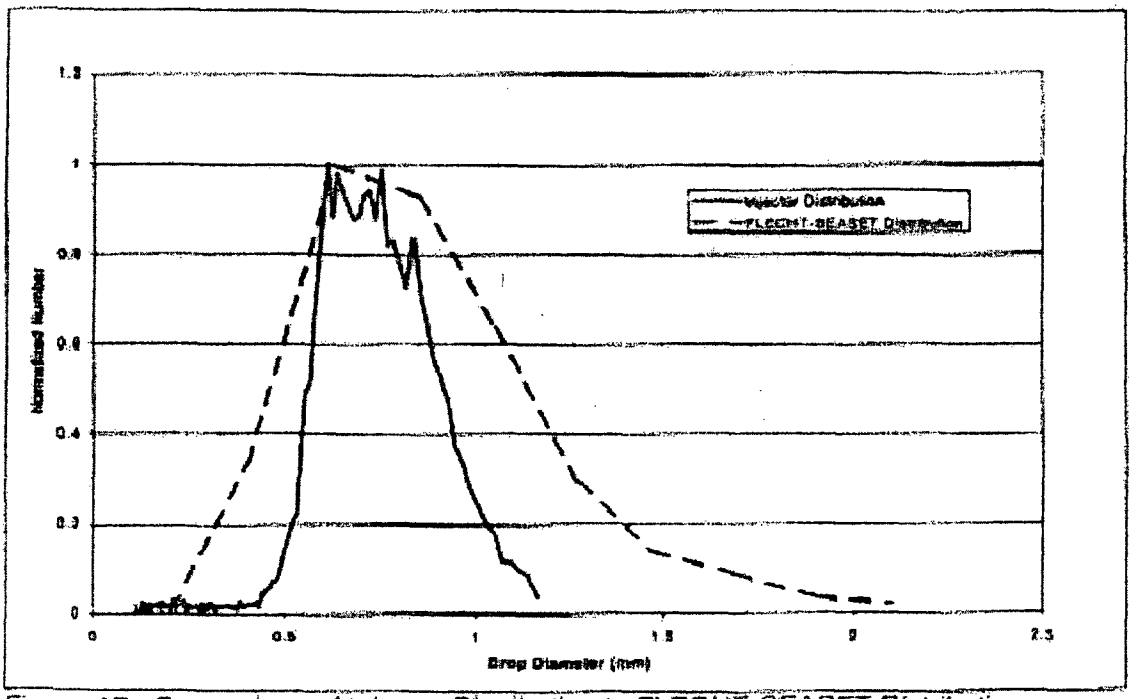

Figure 17. Comparison of Injector Distribution to FLECHT-SEASET Distribution.

APPENDIX E. DETAILED ENGINEERING DRAWINGS FOR THE FLOW HOUSING AND ROD BUNDLE INSTRUMENTATION

E.1 Flow Housing detailed mechanical drawing. Drawing E114244

E.2 Test Section detailed schematic showing the DP cell elevations. Drawing E118338

E.3 Test Section detailed schematic showing the Spacer Grid Instrumentation. Drawing E118340

E.4 Test Section detailed schematic showing the Traverse Steam Probe Rake and Flow Housing Wall Thermocouple locations. Drawing E118341

E.5 Overview schematic showing all the Test Section Instrumentation. Drawing E115073

NOTE: Electronic images of these drawings are included in the CD listed in Appendix G.

APPENDIX F. INSTRUMENTATION ERROR ANALYSIS

The instrumentation error associated with the data from RBHT test series can be derived either from equipment manufacturers' specifications or system calibration data. Component calibrations are performed to verify that the manufacturers' specifications are met, and these manufacturers' specifications are used to compute the error estimate for the data path. System calibrations are performed when component calibrations are not expedient or when an accuracy improvement could be accomplished with a system calibration. The system calibration data are used to compute an estimate of error for the system response, and calibration data points. The total system error from a system calibration is a function of both system response error and calibration data error.

In all cases of error estimate, the standard deviation has been computed and presented as the most probable error. The manufacturer-specified error is the maximum possible error. The standard deviation error is calculated from the maximum error by the following:

$$\rho^2 = \sum_{i=1}^{n}\left(\frac{E_i^2}{n}\right) \tag{F-1}$$

where

ρ	data path standard deviation
E_i	component i maximum error
n	number of sources of error

When a system calibration is performed, the standard deviation from the calibration data and that from the calibration equipment can be combined by the following equation to produce the best estimate of error:

$$\rho = \sqrt{E_d^2 + E_c^2} \tag{F-2}$$

where

E_d	calibration data standard deviation
E_c	calibration equipment standard deviation

The calibration data standard deviation is a measure of the error involved in fitting the calibration data. That is,

$$E_d = \left(\frac{\sum_{i=1}^{n}\left(Y_i - Y_f\right)^2}{n}\right)^{1/2} \tag{F-3}$$

where

Y_i	calibration point
Y_f	predicted output from the calibration curve

n number of calibration points

The calibration equipment standard deviation is a measure of the absolute error of the calibration point. If the calibration point in the above equation is calculated from an equation of the form

$$Y = x_1 \cdot x_2 \cdot x_3 \tag{F-4}$$

then

$$\left(\frac{\sigma_y}{y}\right)^2 = \sum_{i=1}^{n}\left(\frac{\sigma_{x_i}}{x_i}\right)^2 \tag{F-5}$$

and

$$E_c = \sqrt{\sigma_y^2} \tag{F-6}$$

The data path has been broken down into three parts called sensor, conditioner, and readout. The sensor is the device whose electrical output is proportional to a physical quantity (temperature, pressure, flow, power). The conditioner is a device which matches the electrical output of the sensor to the input requirements of the readout device. The readout device measures and records the electrical value of the signal from the conditioner. This recorded electrical value is subsequently used to compute the physical quantity it represents. The errors due to the transmission wire errors are very small (±0.001 percent) in comparison to the element errors and are considered negligible.

The error values for sensor, conditioning, and readout are the manufacturers' specifications in engineering units. These numbers are used to compute the most probable error, as previously described. Where systems calibrations are performed, the equipment calibration data provide the standard deviation and maximum error as computed from the calibration data points in fitting the points to a first-order polynomial. The calibration point standard deviation is computed using the method described above. The calibration point maximum error occurs simultaneously in each component of the calibration equation. The overall system standard deviation may then be calculated using equation F-2.

The calculated Total Probable errors using equation F-2 for each instrumentation channel are shown in the following tables:

Table F.1 Temperature measurements including the heater rods, grid fluid, grid walls, support rods, steam probe rakes, flow housing walls, flow housing insulation, vessel and piping walls, and quartz windows thermocouples.

Table F.2 Differential pressure cells (DP's), static pressure transducers (P's), and vessel liquid label transducers.

Table F.3 Inlet Mass and exhaust steam flows transmitters (FM).

Table F.1 Temperature Measurements

		INSTRUMENT			DATA ACQUISITION SYSTEM					TOTAL
	INPUT SENSOR	RANGE	ERROR ± 1.11°C		SCP	AUTO-RANGED ± 0.02% TEMPERATURE RANGE	REF JCTN MEAS	ISO REF GRADIENT	TEMP RANGE FOR ERROR NUMBERS	TOTAL PROBABLE ERROR
CHANNEL NO.	TYPE K TC	°C	± °C		± °C	± °C	± °C	± °C	°C	± °C
1-96, 98-183, 185-248, 311-313	HEATER RODS	10 - 1371 °C	1.11		0.20	0.08	0.01	0.20	0 TO 375	1.15
					0.25	0.16	0.01	0.20	375 TO 600	1.17
					0.40	0.27	0.01	0.20	600 TO 1371	1.23
249-278, 278-279	GRID WALL & FLUID	10 - 1371 °C	1.11		0.20	0.08	0.01	0.20	0 TO 375	1.15
					0.25	0.16	0.01	0.20	375 TO 600	1.17
					0.40	0.27	0.01	0.20	600 TO 1371	1.23
280 THRU 295	SUPPORT RODS	10 - 1371 °C	1.11		0.20	0.08	0.01	0.20	0 TO 375	1.15
					0.25	0.16	0.01	0.20	375 TO 600	1.17
					0.40	0.27	0.01	0.20	600 TO 1371	1.23
296-310, 314-334, 489-495	ST. PROBE RAKES	10 - 1371 °C	1.11		0.20	0.08	0.01	0.20	0 TO 375	1.15
					0.25	0.16	0.01	0.20	375 TO 600	1.17
					0.40	0.27	0.01	0.20	600 TO 1371	1.23
335 THRU 359, & 496	FLOW HOUSING WALL	10 - 1371 °C	1.11		0.20	0.08	0.01	0.20	0 TO 375	1.15
					0.25	0.16	0.01	0.20	375 TO 600	1.17
					0.40	0.27	0.01	0.20	600 TO 1371	1.23
97, 184, 277, 490	INSULATION	10 - 1371 °C	1.11		0.20	0.08	0.01	0.20	0 TO 375	1.15
385 THRU 388	L. PLEN. FL & WALL	10 - 1371 °C	1.11		0.20	0.08	0.01	0.20	0 TO 375	1.15
389, 391, 392	U. PLEN. FL & WALL	10 - 1371 °C	1.11		0.20	0.08	0.01	0.20	0 TO 375	1.15
399, 401	SUPPLY TANK FLUID	10 - 1371 °C	1.11		0.20	0.08	0.01	0.20	0 TO 375	1.15
407 THRU 410	SUP LINE FL. & WALL	10 - 1371 °C	1.11		0.20	0.08	0.01	0.20	0 TO 375	1.15
418 THRU 424	(SM, LG) CARRYOVER TANKS FL & WALL	10 - 1371 °C	1.11		0.20	0.08	0.01	0.20	0 TO 375	1.15
395, 404, 435, 436, 437	PRESS. OSC. DAMP TANK FL & WALL	10 - 1371 °C	1.11		0.20	0.08	0.01	0.20	0 TO 375	1.15
440 THRU 443	EXHAUST LINE	10 - 1371 °C	1.11		0.20	0.08	0.01	0.20	0 TO 375	1.15
360, 361	ROD BUNDLE INLET	10 - 1371 °C	1.11		0.20	0.08	0.01	0.20	0 TO 375	1.15
414-415	STM SUP FL & WALL	10 - 1371 °C	1.11		0.20	0.08	0.01	0.20	0 TO 375	1.15
429, 431-432	STEAM SEP	10 - 1371 °C	1.11		0.20	0.08	0.01	0.20	0 TO 375	1.15
445-457	QUARTZ WINDOWS	10 - 1371 °C	1.11		0.20	0.08	0.01	0.200	0 TO 375	1.15
		10 - 1371 °C			0.25	0.160	0.01	0.200	375 TO 600	1.17

CHANNEL NO.	THERMISTOR TYPE 5000	°C	± °C		± °C	± °C	± °C	± °C	°C	± °C
497-512	TERM PKL REF THERMISTORS	-10 - 65 °C	0.01						-10 TO 65	

Table F.2 Pressure Measurements

		INSTRUMENT			DAS					TOTAL
	INPUT SENSOR	SPAN CALIBRATION	ACCURACY ± 0.075% SPAN (1)	TOTAL PERFORMANCE ± 0.15% SPAN (2)	DCP LINEARITY ± 0.01% VOLTAGE RANGE	AUTO-RANGING ± 0.02% VOLTAGE RANGE	DCP OFFSET ERROR	NOISE	VOLTAGE RANGE FOR ERROR ANALYSIS	TOTAL PROBABLE ERROR
CHANNEL NO.	(DP) DIFFERENTIAL PRESSURE	mm H_2O	± mm H_2O	± mm H_2O	± mm H_2O	± mm H_2O	± mm H_2O	Linear H_2O	± Volts	± mm H_2O
367, 370, 373, 374, 376, 379, 380	FLOW HOUSING	0 TO 76.2 mm H20	0.05	0.11	0.003	0.005	0.005	0.025	0.25	0.13
368, 372, 377, 378	FLOW HOUSING	0 TO 101.6 mm H20	0.08	0.15	0.003	0.007	0.007	0.025	0.25	0.17
371	FLOW HOUSING	0 TO 127 mm H20	0.10	0.19	0.004	0.009	0.007	0.025	0.25	0.21
366	FLOW HOUSING	0 TO 152.4 mm H20	0.11	0.23	0.005	0.011	0.008	0.025	0.25	0.25
365	FLOW HOUSING	0 TO 177.8 mm H20	0.13	0.27	0.006	0.013	0.009	0.025	0.25	0.30
378, 381	FLOW HOUSING	0 TO 203.2 mm H20	0.15	0.30	0.007	0.015	0.010	0.025	0.25	0.34
385A	FLOW HOUSING	0 TO 279.4 mm H20	0.21	0.42	0.009	0.019	0.013	0.025	0.25	0.47
384, 385, 382	FLOW HOUSING	0 TO 304.8 mm H20	0.23	0.46	0.010	0.021	0.014	0.025	0.25	0.51
383, 383	FLOW HOUSING	0 TO 330.2 mm H20	0.25	0.50	0.011	0.023	0.015	0.025	0.25	0.55
382	FLOW HOUSING	0 TO 3657.6 mm H20	2.74	5.49	0.123	0.247	0.159	0.194	0.25	6.14
360	UPPER PLENUM	0 TO 311.15 mm H20	0.23	0.47	0.011	0.021	0.015	0.025	0.25	0.52
426	U PLEN - ACC DP	0 TO 127 mm H20	0.10	0.19	0.004	0.009	0.007	0.025	0.25	0.21
402	UP DP	0 TO 152.578 mm H20	0.12	0.23	0.005	0.011	0.008	0.025	0.25	0.25
433	ACC-DOC PIPE DP	0 TO 8382 mm H20	4.26	8.53	0.214	0.429	0.282	0.197	0.25	10.68
405	SUP TNK LVL	0 TO 3022.6 mm H20	2.27	4.53	0.102	0.204	0.133	0.294	0.25	5.05
408	LO CT LVL	0 TO 1676.8 mm H20	1.16	2.36	0.058	0.116	0.077	0.025	0.25	2.64
427	DM CT LVL	0 TO 685.28 mm H20	0.67	1.34	0.033	0.067	0.044	0.025	0.25	1.50
404	ST SEP DR TK LVL	0 TO 1663.7 mm H20	1.25	2.50	0.063	0.125	0.082	0.025	0.25	2.79

CHANNEL NO.	(P) PRESSURE TRANSDUCER	kPa	± kPa	± kPa	± kPa	± kPa	± kPa	± kPa	± Volts	± kPa
399, 410, 428, 447	UP SEP PR	0 TO 413.7 kPa	0.21	0.62	0.014	0.028	0.004	0.014	0.25	0.69
409	SUP TNK PRESS	0 TO 689.5 kPa	0.03	1.38	0.038	0.113	0.017	0.038	1.00	0.71
411	SUP LINE PRESS	0 TO 344.7 kPa	0.26	0.52	0.023	0.047	0.007	0.021	0.25	1.49
430	ST SUP-ACC DP	0 TO 34.5 kPa	0.03	0.05	0.053	0.106	0.039	0.038	1.00	1.16
					0.013	0.027	0.004	0.011	0.25	0.68
					0.047	0.095	0.014	0.030	1.00	0.69
					0.001	0.003	0.003	0.001	0.25	0.06
					0.005	0.009	0.001	0.003	1.00	0.06

(1) Includes: Repeatability, and Stability
(2) Includes: Accuracy, Temperature, and Line Pressure effects

Table F.3 Flow Measurements

		INSTRUMENT			DATA ACQUISITION SYSTEM					TOTAL
	INPUT SENSOR	SPAN CALIBRATION	ACCURACY ± 0.15% SPAN (1)		SCP LINEARITY ± 0.01% VOLTAGE RANGE	AUTO-RANGING ± 0.02% VOLTAGE RANGE	SCP OFFSET ERROR	NOISE	VOLTAGE RANGE FOR ERROR NUMBERS	TOTAL PROBABLE ERROR
CHANNEL NO.	LINEAR FLOW TRANSDUCER	g/sec	± g/sec		± g/sec	± g/sec	± g/sec	± g/sec	± Volts	± g/sec
412	SUPPLY LINE FM	0 TO 1247 g/sec	0.00187		0.125	0.050	0.045	0.030	0.05	0.139
					0.150	0.060	0.054	0.036	0.06	0.167
413	DROP INJ FM	0 TO 45 g/sec	0.00068		0.005	0.002	0.002	0.001	0.05	0.005
					0.006	0.002	0.002	0.001	0.06	0.006

		INSTRUMENT			DATA ACQUISITION SYSTEM					TOTAL
	INPUT SENSOR	SPAN CALIBRATION	ACCURACY ± 1.5% SPAN	PERFORMANCE ± 1.15% SPAN (2)	SCP LINEARITY ± 0.01% VOLTAGE RANGE	AUTO-RANGING ± 0.02% VOLTAGE RANGE	SCP OFFSET ERROR	NOISE	VOLTAGE RANGE FOR ERROR NUMBERS	TOTAL PROBABLE ERROR
CHANNEL NO.	VC LINEAR FLOW TRANSDUCER	ft³/min	± ft³/min	± ft³/min	± ft³/min	± ft³/min	± ft³/min	± ft³/min	± Volts	± ft³/min
411	STM SUPPLY FM	0 TO 7.1 m³/min	0.006	0.012	0.000	0.000	0.000	0.000	0.05	0.006
					0.001	0.000	0.000	0.000	0.06	0.006
445	EDI PIPE FM	0 TO 13.7 m³/min	0.172	0.032	0.000	0.000	0.000	0.000	0.05	0.172
					0.002	0.000	0.001	0.000	1.00	0.172

(1) Includes effects of Repeatability, Linearity, and Hysteresis.
(2) Includes effects of Repeatability, Stability, Ambient Temperature, EMI/RFI, Mode Noise Rejection, and the Power Supply.

Table F.4 Position Measurements

		INSTRUMENT			DATA ACQUISITION SYSTEM					TOTAL
	INPUT SENSOR	SPAN CALIBRATION	ACCURACY ± LIN SPAN		SCP LINEARITY ± 0.01% VOLTAGE RANGE	AUTO-RANGING ± 0.02% VOLTAGE RANGE (NOTE 5)	SCP OFFSET ERROR (NOTE 5)	NOISE SEE NOTE 5	VOLTAGE RANGE FOR ERROR NUMBERS	TOTAL PROBABLE ERROR
CHANNEL NO.	POSITION TRANSDUCER	mm	± mm		± mm	± mm	± mm	± mm	± Volts	± mm
401-410	RAKE POSITION	0 TO 88.9 mm	0.889		0.533	0.356	0.001	0.003	0.05	0.89
					0.610	0.534	0.004	0.003	1.00	0.89

Table F.5 Power Supply Measurements

		INSTRUMENT			DATA ACQUISITION SYSTEM					TOTAL
	INPUT SENSOR	SPAN (CALIBRATION)	ISOLATOR ACCURACY ± 0.1% SPAN		SCP LINEARITY ± 0.01% VOLTAGE RANGE	AUTO-RANGING ± 0.02% VOLTAGE RANGE	SCP OFFSET ERROR	NOISE	VOLTAGE RANGE FOR ERROR NUMBERS	TOTAL PROBABLE ERROR
CHANNEL NO.	VOLTAGE TRANSDUCER	Volts	± V		± mV	± mV	± uV	± mV	± Volts	± mV
397	ELECTRICAL SYSTEM	0 TO 10 Volts	0.01		0.27	0.47	107.69	310.49	0.38	10.69
					1.69	2.70	419.47	883.03	1.00	10.49

		INSTRUMENT			DATA ACQUISITION SYSTEM					TOTAL
	INPUT SENSOR	SPAN (CALIBRATION)	SHUNT ACCURACY ± 0.1% SPAN	ISOLATOR ACCURACY ± 0.1% SPAN	SCP LINEARITY ± 0.01% VOLTAGE RANGE	AUTO-RANGING ± 0.02 % VOLTAGE RANGE	SCP OFFSET ERROR	NOISE	VOLTAGE RANGE FOR ERROR NUMBERS	TOTAL PROBABLE ERROR
CHANNEL NO.	CURRENT TRANSDUCER	Amps	± A	± A	± A	± A	± A	± A	± Volts	± A
398	ELECTRICAL SYSTEM	0 TO 10000 Amps	10	10	0.43	1.66	6.16	0.47	0.25	21.25
					1.62	4.69	0.83	1.39	1.00	21.39

		INSTRUMENT			DATA ACQUISITION SYSTEM					TOTAL
	INPUT SENSOR	SPAN (CALIBRATION)	GAS VOLTS ACCURACY ± 0.1% SPAN	GAS AMPS ACCURACY ± 0.1% SPAN						TOTAL PROBABLE ERROR
CHANNEL NO.	DERIVED POWER (VA)	Watts	± W	± W						± W
397 * 398	ELECTRICAL SYSTEM	0 TO 750 Watts	750	1500						1290.35

APPENDIX G. RBHT TEST FACILITY COMPONENTS ENGINEERING DRAWINGS LIST

DRAWING NUMBER	TITLE
D115346	Drawing Tree
E115348 & L115345	Building Arrangement
D114345	Test Facility Schematic
E115073	Test Section Instrumentation
D114369	Steam Separator Drain Tank
D1144371	Small Carryover Tank
E114370	Large Carryover Tank
E115016	Steam Separator Tank
D114369	Steam Separator Drain Tank
D115347	Skirt, Steam Separator Tank
E115002	Water Supply Tank
E114343	Pressure Oscillation Damping Tank
E115815	Mezzanine Framework
D115587	Water Inlet Piping
D115597	Exhaust Line Piping
D115640	Steam By-pass Line
R114288 & L114287	Flow Housing Assembly
E114243	Housing Assembly
E114244	Weldment, Test Section
C114245	Pressure Gasket
C114246	Window Flange
C114247	Window

C114248	Window Stud Fixture
D114249	Flange Mod. Bottom
D114279	Flange Mod. Top
C114255	Cushion Gasket
B114306	Belleville Washer
E114346	Window Test Fixture
E114281 & L114280	Upper Plenum Assembly
C114282	Flange Mod.
E114289	Ground Plate
D114290	Housing Extension
D114291	Exhaust Baffle
E114292	Lower Plenum Assembly
D114293	Lower Plenum Flow Baffle
D114294	Seal Plate, Lower Plenum
C114295	Seal Sleeve Retaining Plate
C114296	Seal Sleeve
D114297	G10 Isolation Plate
C114298	Low Melt Reservoir
D114299	Reservoir Connector Plate
D114366	Seal Sleeve Extractor
E115073	Test Section Instrumentation
D118339	Droplet Injection System
E118338	Flow Housing Differential Pressure Instrumentation
E118340	Heater Rod Bundle Grid Temperature Instrumentation
D118337	Automatic Traverse Mechanism

C115132	Drain Tube
D114301	Unheated Rod
E114302	Heater Rod
D115075	Steam Probe Rake Assembly
D115076	Steam Probe Rake Tube
C115077	Steam Probe Rake Mounting
C118336	Traversing Steam Probe
D115261 & L115260	Grid Assembly
D115262	Outer Grid "A"
D115263	Outer Grid "B"
D115264	Outer Grid "C"
D115265	Outer Grid "D"
D115266	Inner Grid "A"
D115267	Inner Grid "B"
D115268	Inner Grid "C"
D115269	Inner Grid "D"

APPENDIX H. THERMOPHYSICAL PROPERTIES OF ONE BORON NITRIDE SAMPLE AND THREE ROD SAMPLES

TPRL

THERMOPHYSICAL PROPERTIES RESEARCH LABORATORY, INC.

TPRL 2237

Thermophysical Properties of One Boron Nitride Sample and Three Rod Samples

A Report to Penn State University

by

J. Gembarovic, H. Groot, J. Ferrier and D.L. Taylor

August 1999

TPRL, Inc.
2595 Yeager Road
West Lafayette, IN 47906
Phone: 765-463-1581
Fax: 765-463-5235
WWW.TPRL.COM

TPRL 2237

Thermophysical Properties of One Boron Nitride Sample and Three Rod Samples

A Report to Penn State University

by

J. Gembarovic, H. Groot, J. Ferrier and D.L. Taylor

August 1999

TABLE OF CONTENTS

Thermophysical Properties of One Boron Nitride Sample and Three Rod Samples

INTRODUCTION

A sample of AXOS Grade Boron Nitride sample (identified as BN) was submitted for thermophysical property testing. Three rod samples, identified as 0-12, 36-48, and 72-84, were also submitted for the hemispherical total emissivity measurement. Thermal diffusivity (α) was measured using the laser flash technique. Bulk density (d) values were calculated from the sample's geometries and masses. Specific heat (C_p) was measured using differential scanning calorimeters and thermal conductivity (λ) values were calculated as a product of the above quantities, i.e. $\lambda = \alpha C_p d$. Thermal expansion was measured using a dual push-rod dilatometer. Hemispherical total emissivity (ϵ_H) was measured using the heat balance method.

Thermal diffusivity is determined using the laser flash diffusivity method. In the flash method, the front face of a small disc-shaped sample is subjected to a short laser burst and the resulting rear face temperature rise is recorded and analyzed. A highly developed apparatus exists at TPRL and we have been involved in an extensive program to evaluate the technique and broaden its uses. The apparatus consists of a Korad K2 laser, a high vacuum system including a bell jar with windows for viewing the sample, a tantalum or stainless steel tube heater surrounding a sample holding assembly, a thermocouple or an i.r. detector, appropriate biasing circuits, amplifiers, A/D converters, crystal clocks and a microcomputer based digital data acquisition system capable of accurately taking data in the 40 microsecond and longer time domain. The computer controls the experiment, collects the data, calculates the results and compares the raw data with the theoretical model.

Specific heat is measured using a standard Perkin-Elmer Model DSC-2 Differential Scanning Calorimeter with sapphire as the reference material. The standard and sample were subjected to the same heat flux as a blank and the differential powers required to heat the sample and standard at the same rate were determined using the digital data acquisition system. From the masses of the sapphire standard and sample, the differential power, and the known specific heat of sapphire, the specific heat of the sample is computed. The experimental data are visually displayed as the experiment progresses. All measured quantities are directly traceable to NIST standards. A Netzsch model 404 differential scanning calorimeter (DSC) is used to measure specific heats from 323 to 1673°K.

A dual push-rod dilatometer (Theta Dilatronics II), is used to measure linear thermal expansion

from 100 to 1800K. The differential expansion between the sample and a known standard reference material is measured as a function of temperature. The expansion of the sample is computed from this differential expansion and the expansion of the standard. The measurements are made under computer control and linear expansion is calculated at preselected temperature intervals. The expansion can be monitored with the graphics terminal during the measurement process. Six standard reference materials for expansion were obtained from NBS and these include materials with low, moderate and large expansions. For the purposes of calibration and checkout, one NBS standard is measured against another NBS standard.

The mean CTE at a temperature T is calculated by dividing the change in length in the sample by the change in the temperature, i.e.

$$\alpha_{mean} = \frac{L_T - L_0}{T - T_0}$$

with T_0 being the reference temperature (normally 20°C or 70°F).

The hemispherical total emissivity is measured using a heat balance method (ASTM 835.04.06). The sample, in the form of a long rod or strip, is mounted between two electrodes. This assembly is contained in a high vacuum system equipped with long vertical optical windows. The sample is heated directly by passing DC current through it. The power supplies are highly regulated and the selected equilibrium temperatures are easily attained.

The sample's ends may be notched to compensate for heat losses to the end clamps. The power dissipated over a small central region of the specimen is determined as the voltage times current (VI) and the temperature (T) of the central region of the specimen is measured. When measurements are made at relativity low temperatures, the samples are surrounded by a liquid nitrogen cooled copper shield, the interior of which is painted black. Using the Stefan-Boltzmann equation, the power generated in the central region is equated to the radiative heat transfer to the surroundings and the hemispherical total emissivity (ϵ_H) calculated:

$$\epsilon_H = \frac{VI}{PL\ \sigma\ (T^4 - T_o^4)}$$

where P is the perimeter, L is the distance between voltage probes, σ is the Stefan-Boltzmann constant and T_a is the is the temperature of the surroundings.

RESULTS AND DISCUSSION

Thermal diffusivity Boron Nitride (BN) sample geometry, mass and bulk density value at room temperature are given in Table 1. Specific heat results for the sample are given in Table 2 and are plotted in Figure 1. Specific heat values increase with increasing temperature in the usual fashion for ceramics.

Thermal diffusivity results are given in Table 3 and Figure 2. Thermal conductivity values are calculated in Table 4 and the results are plotted in Figure 3. Density values were assumed to be constant in the calculations, in accordance with usual practice.

The thermal expansion results for the BN sample are plotted in Figure 4 and listed in Table 5. The mean CTE was calculated from the data and the results are given in Figure 5 and Table 6. The density as a function of temperature was calculated from the thermal expansion (we have assumed that the sample is isotropic and its thermal expansion in all three directions is the same) and the results are shown in Figure 6 and listed in Table 7.

Hemispherical total emissivity results for the three rod samples are given in Table 8 and Figure 7. The samples were measured in heating and cooling cycle . Sample 72-84 has the highest emissivity and the differences between heating (H) and cooling (C) part are relatively smallest. Sample 0-12 has relatively lowest emissivity values (only about 2/3 of 72-84 value at 550 °C for the heating part) and the cooling part, which remains relatively high, shows that irreversible changes of the sample surface take place within the measured temperature range.

TABLE 1

Sample Dimensions, Masses and Density Values

Sample (No.)	Thickness (cm)	Diameter (cm)	Mass (gm)	Density ($gms\ cm^{-3}$)
BN	0.2154	1.3044	0.55204	1.918

TABLE 2

Specific Heat Results

Sample Description	Temperature (C)	Specific Heat (W-s/gm-K)
BN	23.0	0.8530
	50.0	0.9220
	100.0	1.0340
	150.0	1.1350
	200.0	1.2260
	250.0	1.3050
	300.0	1.3770
	350.0	1.4410
	400.0	1.5000
	450.0	1.5510
	500.0	1.5940
	550.0	1.6370
	600.0	1.6700
	650.0	1.7020
	700.0	1.7310
	750.0	1.7590
	800.0	1.7860
	850.0	1.8090
	900.0	1.8300
	950.0	1.8510
	1000.0	1.8690
	1050.0	1.8880
	1100.0	1.9030

TABLE 3

Thermal Diffusivity Results

Sample Description	Temperature (C)	Diffusivity (cm^2 sec^{-1})
BN	23.0	0.78294
BN	100.0	0.50900
BN	200.0	0.37924
BN	300.0	0.29111
BN	400.0	0.24651
BN	500.0	0.21795
BN	600.0	0.19102
BN	700.0	0.16955
BN	800.0	0.15035
BN	900.0	0.13588
BN	1000.0	0.12716
BN	1100.0	0.11805

TABLE 4

Thermal Conductivity Calculations

Sample (No.)	Temp. (C)	Density (gm cm^{-3})	Specific Heat (W-s-$gm^{-1}K^{-1}$)	Diffusivity (cm^2 sec^{-1})	Conduct. (W-cm^{-1} K^{-1})	Conduct. (BTU *)	Temp (F)
BN	23.0	1.918	0.8530	0.78294	1.28083	888.65	73.4
	100.0	1.918	1.0340	0.50900	1.00937	700.31	212.0
	200.0	1.918	1.2260	0.37924	0.89170	618.67	392.0
	300.0	1.918	1.3770	0.29111	0.76879	533.39	572.0
	400.0	1.918	1.5000	0.24651	0.70914	492.01	752.0
	500.0	1.918	1.5940	0.21795	0.66628	462.27	932.0
	600.0	1.918	1.6700	0.19102	0.61180	424.47	1112.0
	700.0	1.918	1.7310	0.16955	0.56287	390.53	1292.0
	800.0	1.918	1.7860	0.15035	0.51498	357.29	1472.0
	900.0	1.918	1.8300	0.13588	0.47688	330.86	1652.0
	1000.0	1.918	1.8690	0.12716	0.45581	316.25	1832.0
	1100.0	1.918	1.9030	0.11805	0.43085	298.93	2012.0

* (BTU in hr^{-1} ft^{-2} F^{-1})

Table 5

Thermal Expansion Results

Temp. (F)	BN (in/in)
70.0	0.000000
90.0	-.000007
100.0	-.000012
110.1	-.000020
120.0	-.000030
130.0	-.000039
140.0	-.000049
150.1	-.000059
160.0	-.000069
170.0	-.000079
180.0	-.000087
190.0	-.000094
200.0	-.000102
210.1	-.000111
220.0	-.000120
230.1	-.000130
240.0	-.000140
250.0	-.000149
260.0	-.000159
270.0	-.000165
280.0	-.000172
290.0	-.000178
300.0	-.000184
310.0	-.000192
320.0	-.000198
330.0	-.000205
340.2	-.000212
350.0	-.000219
360.0	-.000224
370.0	-.000228
380.1	-.000232
390.0	-.000234
400.0	-.000235
410.0	-.000236
420.0	-.000237

Table 5 (cont.)

Thermal Expansion Results

Temp. (F)	BN (in/in)
430.1	-.000237
440.0	-.000237
450.0	-.000236
460.0	-.000233
470.0	-.000230
480.0	-.000228
490.0	-.000225
500.1	-.000222
510.0	-.000220
520.0	-.000216
530.0	-.000212
540.0	-.000206
550.0	-.000200
560.0	-.000193
570.1	-.000183
580.0	-.000173
590.0	-.000157
600.1	-.000142
610.0	-.000125
620.0	-.000113
630.0	-.000103
640.0	-.000091
650.0	-.000077
660.0	-.000062
670.0	-.000033
680.0	0.000009
690.0	0.000039
700.1	0.000077
710.0	0.000102
720.0	0.000133
730.0	0.000163
740.0	0.000182
750.0	0.000196
760.0	0.000243
771.9	0.000281

Table 5 (cont.)

Thermal Expansion Results

Temp. (F)	BN (in/in)
780.0	0.000311
790.1	0.000376
800.0	0.000396
810.0	0.000407
820.0	0.000418
830.0	0.000430
840.0	0.000441
850.0	0.000454
860.0	0.000464
870.0	0.000470
880.0	0.000472
890.0	0.000471
900.0	0.000472
910.1	0.000471
920.0	0.000473
930.0	0.000430
940.0	0.000428
950.0	0.000429
960.0	0.000433
970.0	0.000487
980.0	0.000498
990.0	0.000521
1000.0	0.000565
1010.0	0.000614
1020.0	0.000661
1030.0	0.000708
1040.0	0.000756
1050.0	0.000804
1060.0	0.000851
1070.0	0.000899
1080.0	0.000948
1090.1	0.000997
1100.0	0.001045
1110.0	0.001092
1120.0	0.001141

Table 5 (cont.)

Thermal Expansion Results

Temp. (F)	EN (in/in)
1130.0	0.001188
1140.0	0.001236
1150.1	0.001284
1160.0	0.001332
1170.0	0.001381
1180.1	0.001430
1190.0	0.001479
1200.0	0.001528
1210.0	0.001576
1220.0	0.001626
1230.0	0.001674
1240.0	0.001723
1250.0	0.001772
1260.0	0.001820
1270.0	0.001869
1280.0	0.001918
1290.0	0.001967
1300.0	0.002016
1310.0	0.002065
1320.0	0.002114
1330.0	0.002164
1340.0	0.002212
1350.0	0.002267
1360.0	0.002322
1370.1	0.002377
1380.0	0.002432
1390.0	0.002488
1400.0	0.002544
1410.0	0.002599
1420.0	0.002654
1430.0	0.002709
1440.0	0.002761
1450.0	0.002813
1460.0	0.002864
1470.0	0.002916

Table 5 (cont.)

Thermal Expansion Results

Temp. (F)	BN (in/in)
1480.0	0.002968
1490.0	0.003020
1500.0	0.003071
1510.1	0.003123
1520.0	0.003174
1530.1	0.003227
1540.0	0.003279
1550.0	0.003332
1560.0	0.003384
1570.0	0.003437
1580.0	0.003490
1590.0	0.003542
1600.0	0.003593
1610.0	0.003645
1620.0	0.003698
1630.0	0.003750
1640.0	0.003803
1650.0	0.003856
1660.0	0.003908
1670.0	0.003962
1680.0	0.004014
1690.0	0.004067
1700.0	0.004119
1710.1	0.004173
1720.0	0.004226
1730.0	0.004279
1740.0	0.004332
1750.0	0.004386
1760.0	0.004439
1770.0	0.004492
1780.0	0.004546
1790.0	0.004599
1800.0	0.004652
1810.0	0.004706
1820.0	0.004760

Table 5 (cont.)

Thermal Expansion Results

Temp. (F)	BN (in/in)
1830.0	0.004813
1840.1	0.004868
1850.0	0.004922
1860.0	0.004977
1870.0	0.005030
1880.1	0.005083
1890.0	0.005138
1900.0	0.005194
1910.0	0.005248
1920.0	0.005302
1930.0	0.005359
1940.0	0.005414
1950.0	0.005469
1960.0	0.005524
1970.0	0.005579
1980.1	0.005633
1990.0	0.005686
2000.0	0.005741

Table 6

Mean Coefficient of Expansion

Temperature (F)	BN (micro in/in F)
200.0	-0.788092
210.0	-0.792864
220.0	-0.801010
230.0	-0.809621
240.0	-0.821503
250.0	-0.827904
260.0	-0.834822
270.0	-0.824328
280.0	-0.817458
290.0	-0.809436
300.0	-0.800619
310.0	-0.797999
320.0	-0.790565
330.0	-0.786720
340.0	-0.784413
350.0	-0.783764
360.0	-0.771687
370.0	-0.761137
380.0	-0.748095
390.0	-0.731874
400.0	-0.713439
410.0	-0.694134
420.0	-0.675810
430.0	-0.658661
440.0	-0.641407
450.0	-0.619795
460.0	-0.597606
470.0	-0.575923
480.0	-0.555561
490.0	-0.535728
500.0	-0.516936
510.0	-0.498883
520.0	-0.479825
530.0	-0.460487
540.0	-0.439040

Table 6 (cont.)

Mean Coefficient of Expansion

Temperature (F)	BN (micro in/in F)
550.0	-0.417173
560.0	-0.393945
570.0	-0.365356
580.0	-0.339984
590.0	-0.301524
600.0	-0.268769
610.0	-0.230657
620.0	-0.205255
630.0	-0.183171
640.0	-0.159022
650.0	-0.133492
660.0	-0.105407
670.0	-0.055747
680.0	0.014413
690.0	0.063317
700.0	0.122062
710.0	0.159972
720.0	0.204191
730.0	0.246995
740.0	0.271130
750.0	0.288726
760.0	0.351524
770.0	0.392538
780.0	0.438233
790.0	0.521316
800.0	0.542999
810.0	0.550659
820.0	0.556648
830.0	0.565160
840.0	0.572248
850.0	0.582417
860.0	0.586821
870.0	0.586895
880.0	0.582234
890.0	0.574603

Table 6 (cont.)

Mean Coefficient of Expansion

Temperature (F)	BN (micro in/in F)
900.0	0.568362
910.0	0.561005
920.0	0.556269
930.0	0.499535
940.0	0.492379
950.0	0.487253
960.0	0.486329
970.0	0.540837
980.0	0.547101
990.0	0.566110
1000.0	0.607569
1010.0	0.652955
1020.0	0.695510
1030.0	0.737610
1040.0	0.779613
1050.0	0.820159
1060.0	0.859779
1070.0	0.899142
1080.0	0.938909
1090.0	0.976780
1100.0	1.014010
1110.0	1.050400
1120.0	1.086784
1130.0	1.120913
1140.0	1.154846
1150.0	1.188924
1160.0	1.221713
1170.0	1.255138
1180.0	1.288214
1190.0	1.320270
1200.0	1.351875
1210.0	1.382682
1220.0	1.413650
1230.0	1.443237
1240.0	1.472635

Table 6 (cont.)

Mean Coefficient of Expansion

Temperature (F)	BN (micro in/in F)
1250.0	1.501374
1260.0	1.529806
1270.0	1.557755
1280.0	1.585220
1290.0	1.612363
1300.0	1.639413
1310.0	1.665640
1320.0	1.691638
1330.0	1.717315
1340.0	1.742071
1350.0	1.771108
1360.0	1.800229
1370.0	1.828393
1380.0	1.856477
1390.0	1.884910
1400.0	1.912725
1410.0	1.939469
1420.0	1.965787
1430.0	1.991790
1440.0	2.015028
1450.0	2.038211
1460.0	2.060707
1470.0	2.082955
1480.0	2.105083
1490.0	2.126539
1500.0	2.147513
1510.0	2.168813
1520.0	2.189194
1530.0	2.210117
1540.0	2.230587
1550.0	2.251157
1560.0	2.270980
1570.0	2.291503
1580.0	2.311257
1590.0	2.330100

Table 6 (cont.)

Mean Coefficient of Expansion

Temperature (F)	BN (micro in/in F)
1600.0	2.348580
1610.0	2.366878
1620.0	2.385597
1630.0	2.404099
1640.0	2.422299
1650.0	2.440183
1660.0	2.458020
1670.0	2.475815
1680.0	2.493312
1690.0	2.510603
1700.0	2.527068
1710.0	2.544075
1720.0	2.561302
1730.0	2.577913
1740.0	2.594142
1750.0	2.610920
1760.0	2.626725
1770.0	2.642242
1780.0	2.658219
1790.0	2.673736
1800.0	2.689040
1810.0	2.704705
1820.0	2.719784
1830.0	2.734959
1840.0	2.750023
1850.0	2.764937
1860.0	2.780317
1870.0	2.794589
1880.0	2.808226
1890.0	2.823061
1900.0	2.838242
1910.0	2.852241
1920.0	2.866132
1930.0	2.880931
1940.0	2.895353

Table 6 (cont.)

Mean Coefficient of Expansion

Temperature (F)	BM (micro in/in F)
1950.0	2.908752
1960.0	2.922494
1970.0	2.936096
1980.0	2.949221
1990.0	2.961660
2000.0	2.974405

TABLE 7

Density Results

Sample Description	Temperature (C)	Density ($gm\ cm^{-3}$)
BN	23.0	1.918
	100.0	1.918
	200.0	1.918
	300.0	1.919
	400.0	1.919
	500.0	1.919
	600.0	1.919
	700.0	1.917
	800.0	1.916
	900.0	1.915
	1000.0	1.915
	1100.0	1.912
	1200.0	1.909

TABLE 8

HEMISPHERICAL TOTAL EMISSIVITY

SAMPLE NO.	TEMP (C)	TEMP (F)	EMISSIVITY
0-12H	510	950	0.482
	619	1146	0.483
	728	1343	0.501
	816	1501	0.526
	872	1602	0.549
	929	1705	0.582
	992	1817	0.632
	1033	1891	0.672
	1048	1918	0.693
	1083	1981	0.719
0-12C	1083	1981	0.719
	866	1590	0.668
	734	1353	0.642
	552	1025	0.634
36-48H	543	1010	0.631
	588	1091	0.645
	669	1236	0.654
	722	1331	0.663
	786	1447	0.678
	842	1547	0.675
	868	1595	0.685
	907	1665	0.699
	950	1741	0.725
	997	1826	0.736
	1026	1878	0.751
	1054	1930	0.768
36-48C	1054	1930	0.768
	933	1711	0.739
	932	1710	0.741
	835	1535	0.713
	735	1355	0.685
	600	1112	0.655
72-84H	550	1022	0.749
	610	1129	0.755
	663	1225	0.763
	713	1316	0.777
	762	1404	0.790
	843	1550	0.808
	930	1706	0.829
	964	1767	0.841
	1031	1888	0.860
	1078	1972	0.881
72-84C	910	1670	0.818
	735	1355	0.783

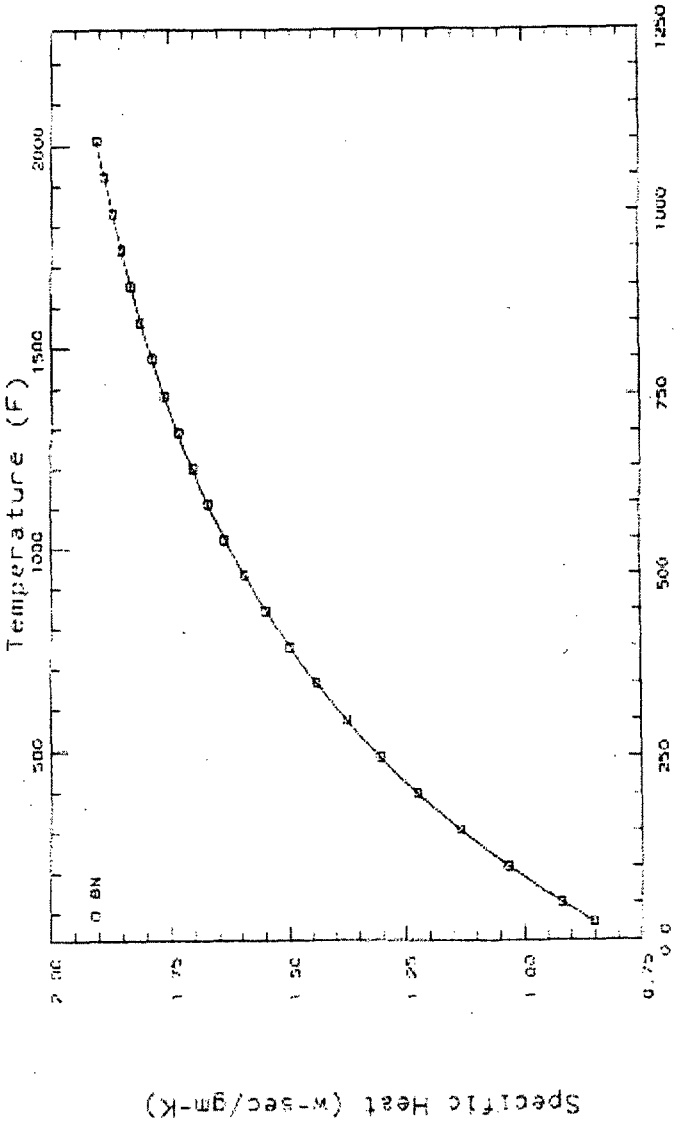

Figure 1 Specific Heat

Specific Heat (w-sec/gm-K)

Figure 2 Thermal Diffusivity

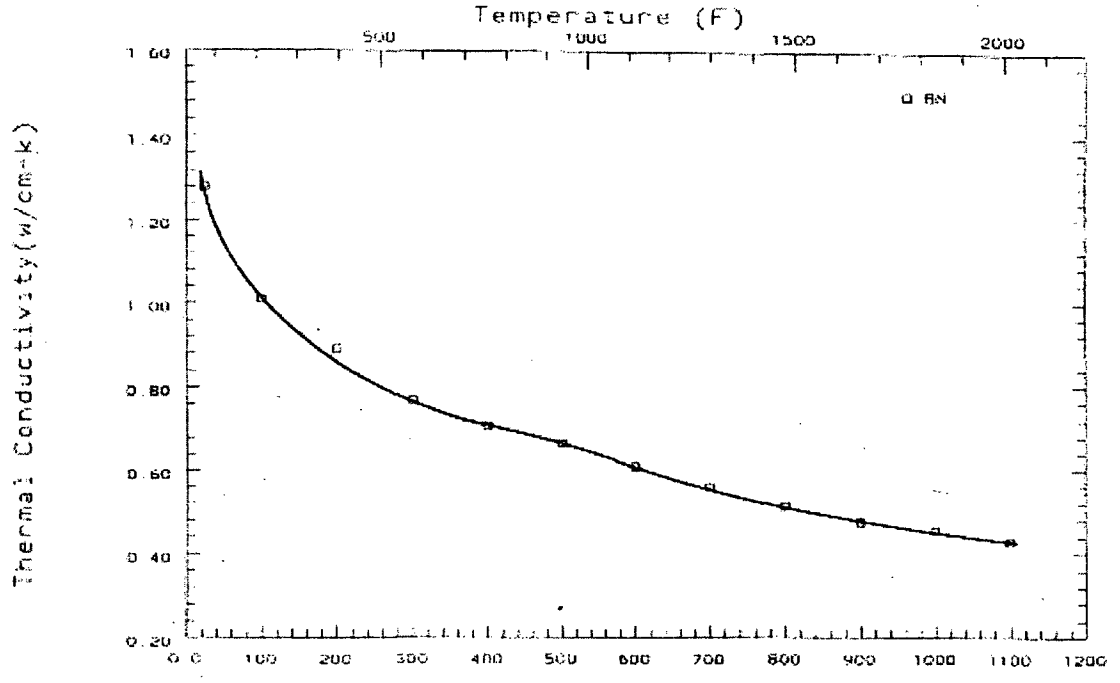

Figure 3 Thermal Conductivity

Figure 4 Thermal Expansion

Figure 5 Mean CTE

Figure 6 Density vs. Temperature

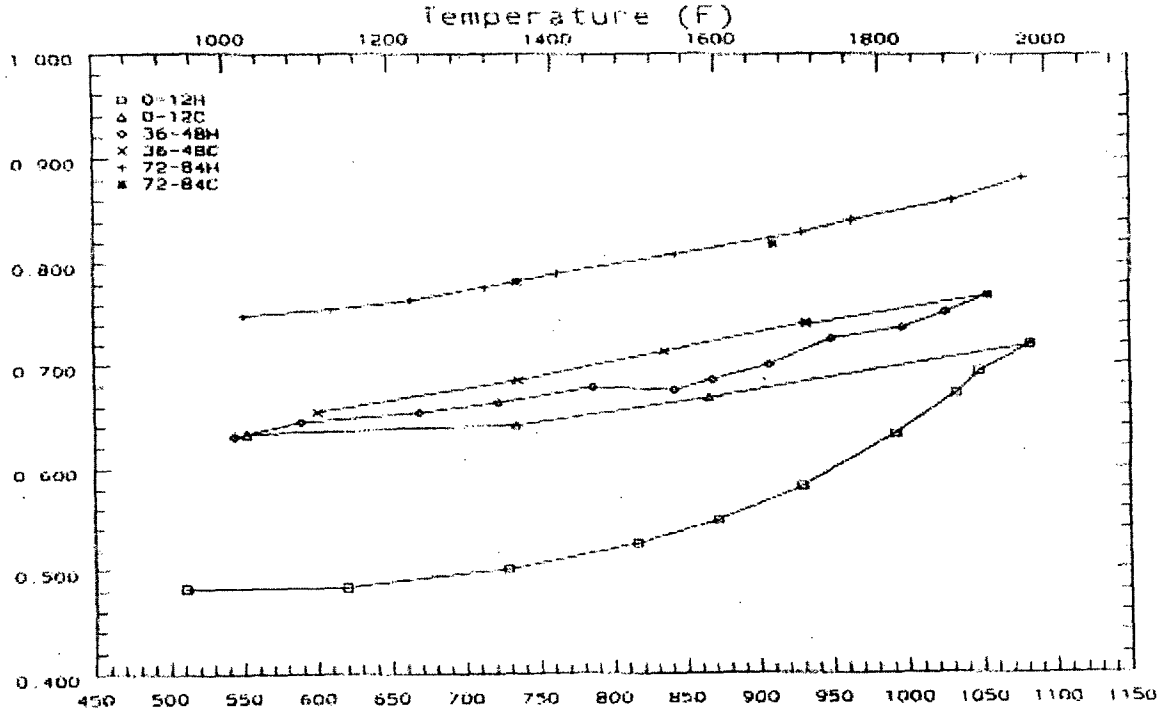

Figure 7 Hemispherical Total Emissivity

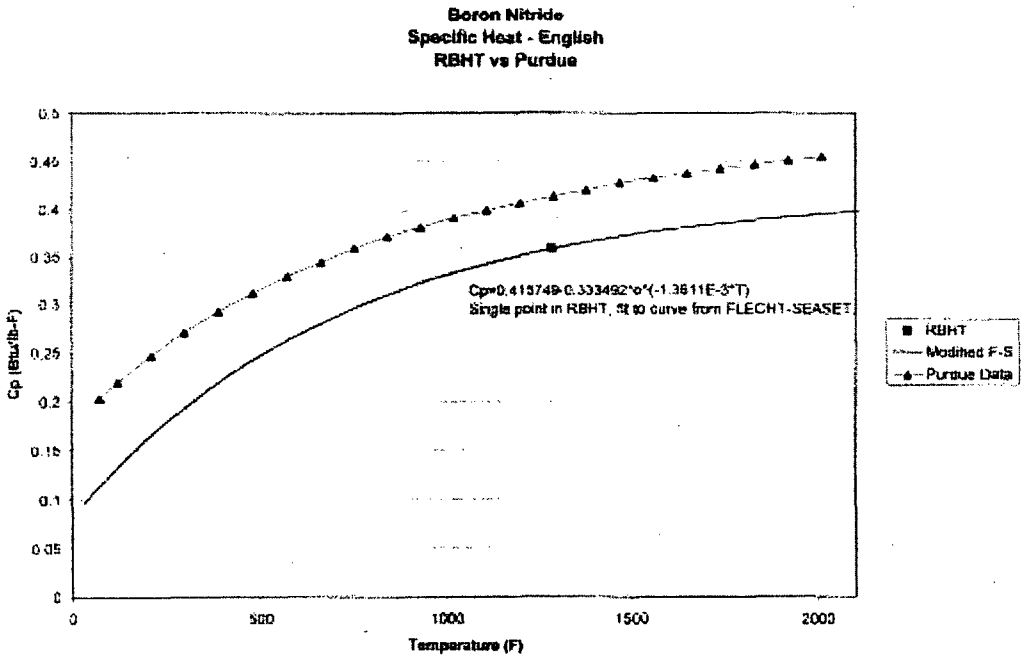
Boron Nitride
Specific Heat - English
RBHT vs Purdue
Cp (Btu/lb-F)
Temperature (F)
0
0.05
0.1
0.15
0.2
0.25
0.3
0.35
0.4
0.45
0.5
0
500
1000
1500
2000
Cp=0.415749-0.333492*e^(-1.3611E-3*T)
Single point in RBHT, fit to curve from FLECHT-SEASET
RBHT
Modified F-S
Purdue Data

Boron Nitride
Specific Heat - SI
RBHT vs Purdue

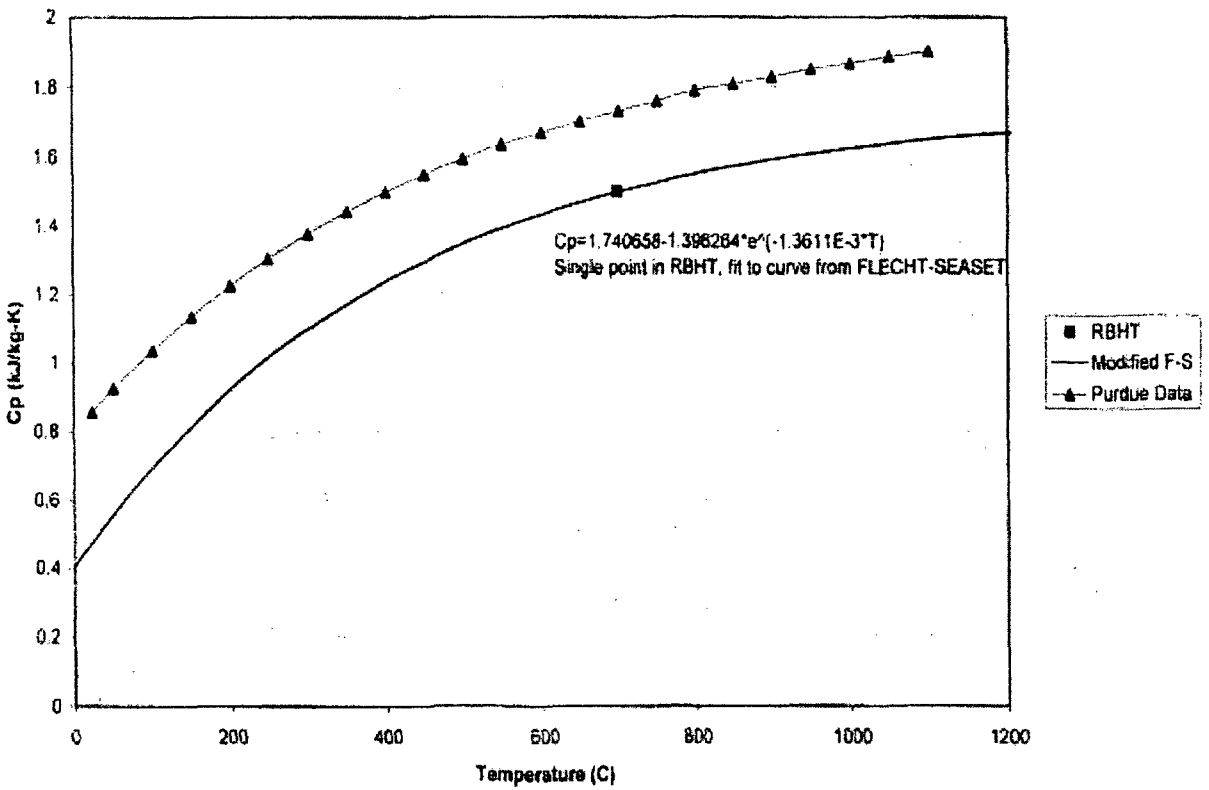

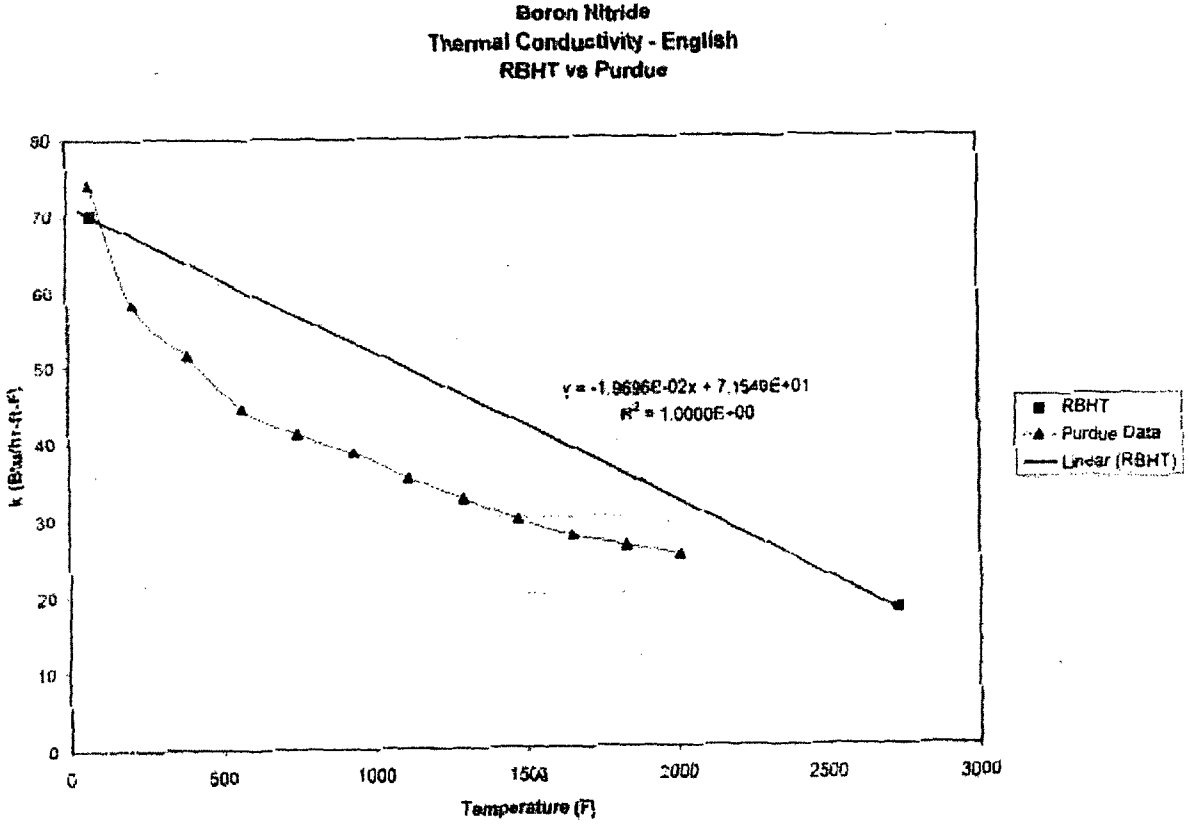
Boron Nitride
Thermal Conductivity - English
RBHT vs Purdue
k (Btu/hr-ft-F)
Temperature (F)
y = -1.9696E-02x + 7.1549E+01
R² = 1.0000E+00
RBHT
Purdue Data
Linear (RBHT)
0
10
20
30
40
50
60
70
80
0
500
1000
1500
2000
2500
3000

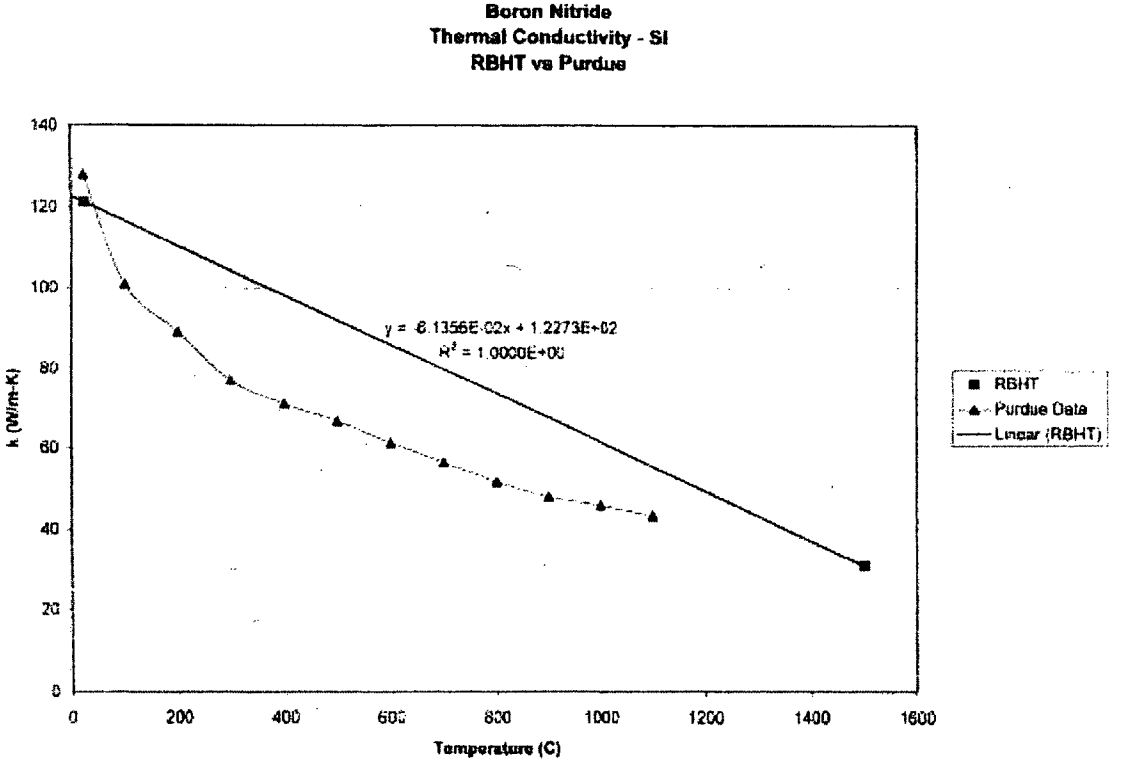
Boron Nitride
Thermal Conductivity - SI
RBHT vs Purdue
y = -8.1356E-02x + 1.2273E+02
R² = 1.0000E+00
k (W/m-K)
Temperature (C)
0
20
40
60
80
100
120
140
0
200
400
600
800
1000
1200
1400
1600
RBHT
Purdue Data
Linear (RBHT)

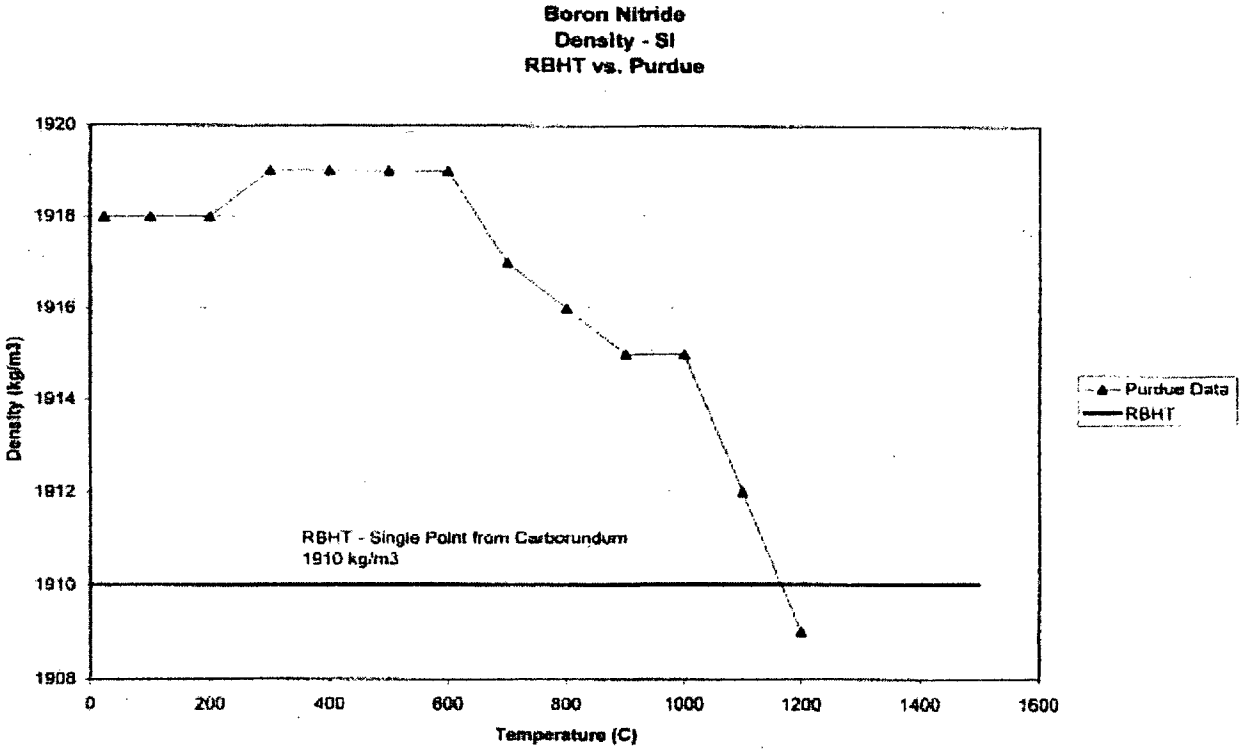
Boron Nitride
Density - SI
RBHT vs. Purdue
Density (kg/m3)
1920
1918
1916
1914
1912
1910
1908
0
200
400
600
800
1000
1200
1400
1600
Temperature (C)
RBHT - Single Point from Carborundum
1910 kg/m3
Purdue Data
RBHT

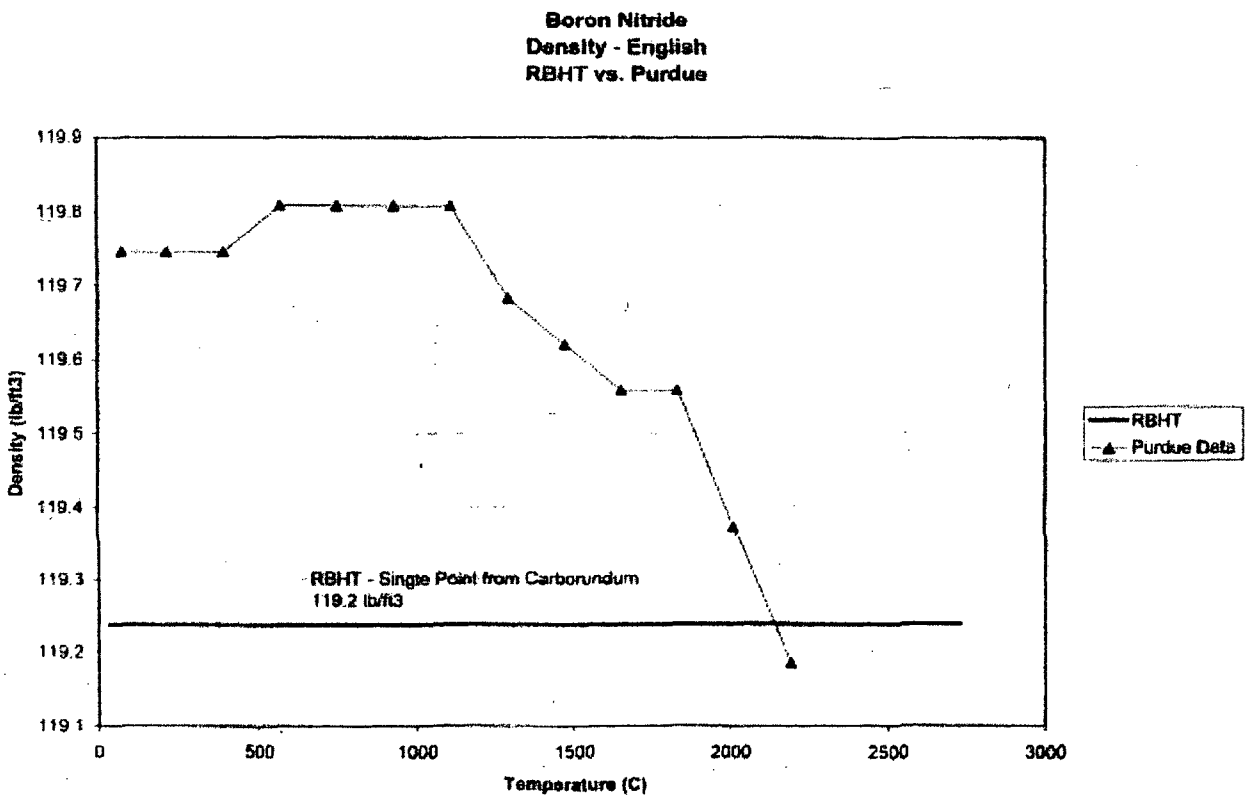
Boron Nitride
Density - English
RBHT vs. Purdue
119.9
119.8
119.7
119.6
119.5
119.4
119.3
119.2
119.1
Density (lb/ft3)
RBHT - Single Point from Carborundum
119.2 lb/ft3
0
500
1000
1500
2000
2500
3000
Temperature (C)
RBHT
Purdue Data

NRC FORM 335
(9-2004)
NRCMD 3.7

U.S. NUCLEAR REGULATORY COMMISSION

BIBLIOGRAPHIC DATA SHEET

(See instructions on the reverse)

1. REPORT NUMBER
(Assigned by NRC, Add Vol., Supp., Rev., and Addendum Numbers, if any.)

NUREG/CR-6976

2. TITLE AND SUBTITLE

Rod Bundle Heat Transfer Test Facility Description

3. DATE REPORT PUBLISHED

MONTH	YEAR
July	2010

4. FIN OR GRANT NUMBER

W6855

5. AUTHOR(S)

E.R. Rosal, T.F. Lin, I.S. McClellan, R.C. Brewer

6. TYPE OF REPORT

Technical

7. PERIOD COVERED *(Inclusive Dates)*

Nov 1997 - Feb 2003

8. PERFORMING ORGANIZATION - NAME AND ADDRESS *(If NRC, provide Division, Office or Region, U.S. Nuclear Regulatory Commission, and mailing address; if contractor, provide name and mailing address.)*

The Pennsylvania State University
University Park, PA 16802

9. SPONSORING ORGANIZATION - NAME AND ADDRESS *(If NRC, type "Same as above"; if contractor, provide NRC Division, Office or Region, U.S. Nuclear Regulatory Commission, and mailing address.)*

Division of Systems Analysis
Office of Nuclear Regulatory Research
U.S. Nuclear Regulatory Commission
Washington, DC 20555-0001

10. SUPPLEMENTARY NOTES

K.Tien, NRC Project Manager

11. ABSTRACT *(200 words or less)*

This report describes the Rod Bundle Heat Transfer (RBHT) Test Facility which is designed to conduct systematic separate effects tests under well-controlled laboratory conditions in order to generate fundamental rod bundle heat transfer data from single phase cooling tests, low flow boiling tests, steam flow tests with and without droplets injection, inverted annular film boiling tests, and dispersed flow film boiling tests in rod bundles. The facility is capable of operating in steady state forced and variable reflood modes covering a wide range of flow and heat transfer conditions at pressures from 0.134 to 0.402 MPa (20 to 60 psia). The RBHT Test Facility is a unique facility which will provide new data for the fundamental development of best-estimate computer codes to enhance our understanding of the complex two-phase phenomena, which are modeled for the reflood transient.

12. KEY WORDS/DESCRIPTORS *(List words or phrases that will assist researchers in locating the report.)*

dispersed flow film boiling, heat transfer enhancement, mixing vane, quench front progression, reactor safety, reactor systems codes, reflood heat transfer, rod bundle, spacer grid, thermal hydraulics

13. AVAILABILITY STATEMENT

unlimited

14. SECURITY CLASSIFICATION

(This Page)
unclassified

(This Report)
unclassified

15. NUMBER OF PAGES

16. PRICE

Federal Recycling Program

UNITED STATES
NUCLEAR REGULATORY COMMISSION
WASHINGTON, DC 20555-0001

OFFICIAL BUSINESS